ROTORCRAFT AEROELASTIC STABILITY

Army-NASA Research 1967-1987

Robert A. Ormiston
Chief, Rotorcraft Dynamics Division
Aeroflightdynamics Directorate
U.S. Army Aviation Research & Technology Activity

and

William G. Warmbrodt
Chief, Rotary Wing Aeromechanics Branch
NASA Ames Research Center

Moffett Field, California

and

Dewey H. Hodges
Professor

and

David A. Peters
Professor

Georgia Institute of Technology
Atlanta, Georgia

SUMMARY

Theoretical and experimental developments in the aeroelastic and aeromechanical stability of helicopters and tilt-rotor aircraft are addressed. Included are the underlying nonlinear structural mechanics of slender rotating beams, necessary for accurate modeling of elastic cantilever rotor blades, and the development of dynamic inflow, an unsteady aerodynamic theory for low-frequency aeroelastic stability applications. Analytical treatment of isolated rotor stability in hover and forward flight, coupled rotor-fuselage stability in hover and forward flight, and analysis of tilt-rotor dynamic stability are considered. Results of parametric investigations of system behavior are presented, and correlations between theoretical results

Paper presented at the NASA/Army Rotorcraft Technology Conference, NASA Ames Research Center, March 17-19, 1987.

and experimental data from small- and large-scale wind-tunnel and flight testing are discussed.

1. INTRODUCTION

Aeroelastic stability, like other rotorcraft technologies, is a broad and complex subject. Extensive research has been conducted during the last 20 years prompted by the emergence of new technical challenges, as well as the establishment of Army research organizations and the NASA-Army agreement for cooperative research. Therefore, it is appropriate to survey the accomplishments during this period. The scope, depth, and technical sophistication of the work to be discussed have greatly increased. We now have an established and sound foundation and an active research program. The purpose of this survey is to present a comprehensive overview of Army-NASA research in rotorcraft aeroelastic stability accomplished over the past 20 years, to assess and summarize the major contributions of government research, and to identify needs and opportunities for future research and development.

It is of interest to define the state of the art in rotorcraft aeroelastic stability before 1970 as a background for this survey. Such a description should serve to highlight how far technology in this area has progressed. An outline of the key technology areas for this description is given in table 1. Before 1970, several research compound helicopters had extended rotorcraft flight-test experience to high-speed, high-advance ratio conditions. Examples of blade-stability problems were encountered at high advance ratios. However, as emphasis on high-speed rotorcraft shifted away from compound helicopters and toward the tilt rotor, these problems were not vigorously pursued. For conventional articulated- or teetering-rotor helicopters operating at moderate flight speeds, aeroelastic stability was not a significant concern. Although experience with the XV-3 tilt rotor had exposed significant potential for aeroelastic stability problems, only limited research was devoted to these problems.

The rotorcraft situation changed rather substantially as 1970 approached. Interest in the hingeless rotor intensified during the late 1960's, but vehicle development programs, including the AH-56A, began to expose the aeroelastic complexities of such systems. The hingeless-rotor YUH-61A UTTAS prototype did exhibit acceptable aeromechanical stability characteristics but was not selected for production. Even more advanced but structurally complex configurations such as the bearingless rotor were being explored. With the advent of the XV-15 program, the uncertainties about tilt-rotor aeroelastic stability took on much more urgency.

In terms of rotor-blade stability, the pre-1970 era dealt primarily with bending-torsion flutter, including wake-excited flutter. In the post-1970 era, these phenomena, together with the unique properties of hingeless- and bearingless-rotor configurations, opened up a new class of problems in aeroelastic instability. These problems were associated with the poorly understood structural dynamics

of cantilevered rotor blades. With the availability of Floquet theory, research in the post-1970 period also began to deal with the long standing problem of forward-flight aeroelastic stability.

For rotating-beam structural dynamics, the metal bladed-articulated rotors of the pre-1970 period could be quite adequately handled with the equations of linear beam theory and isotropic material properties. With the advent of hingeless and bearingless rotors and composite materials, rotor-blade structural dynamics became a complex nonlinear problem.

Unsteady aerodynamics theory for rotor-blade flutter in the pre-1970 period was relatively standard, based on two-dimensional Theodorsen and Loewy theories. In the post-1970 period, efforts were made to extend aerodynamic theory to include three-dimensional effects, dynamic inflow for simplified low-frequency aeroelastic stability, transonic tip aerodynamics, and dynamic stall effects.

In coupled rotor-body dynamics, the pre-1970 era dealt mainly with classical ground resonance of articulated rotors. The post-1970 period of hingeless rotors brought with it the complexity of aeromechanical instability, both on the ground and in flight, with greatly increased complexity owing to the importance of aerodynamics. In sum, the post-1970 era presented a very significant expansion of technical issues facing the aeroelastician.

The objectives of research and development on rotorcraft aeroelastic stability are to ultimately meet the needs of the rotorcraft user. For the user, either military or civilian, this means improving rotorcraft capability—for example, performance, speed, maneuverability, payload-range, and reliability—as well as reducing acquisition, operating, and maintenance costs. With respect to aeroelastic stability, this translates into reducing development cost and risk for improved rotorcraft and enabling the designer to exploit new technology with minimal risk of unforeseen aeroelastic instabilities. Without a firm technology base for aeroelastic stability, the designer may be forced to adopt a more conservative design of lower performance, or excessive testing may be required during development, thereby adversely affecting cost and schedule. Even more serious, an unexpected instability encountered during flight testing could seriously disrupt the schedule, cause major cost overruns, or even jeopardize the program.

The success of research and development to meet the objectives outlined above depends in part on the effectiveness of the approach employed. The success of the Army-NASA efforts in this field can be attributed in part to an approach that includes (1) developing a thorough understanding of the structural dynamics, aerodynamics, and aeroelastic stability characteristics of a wide variety of rotorcraft components and systems; (2) developing and validating improved theoretical analysis methods to predict stability; and (3) developing design approaches and concepts that eliminate or minimize the potential for aeroelastic instability.

Understanding dynamic phenomena can be achieved through parametric analytical studies or exploratory experimental investigations. Since understanding a dynamic system is often synonymous with being able to represent it mathematically, the derivation of analytical models, comparing them against measured data, and carefully studying and reconciling the results is a valuable part of the process. For complex physical systems, breaking the system down into a series of simpler problems is often essential to get to the core of the problem. Ultimately a thorough understanding of aeroelastic stability phenomena is essential to avoid problems in new designs and to mimimize design compromises necessary to avoid instability.

Development of theoretical prediction methods is a key part of aeroelastic stability research. These methods permit the researcher to apply general knowledge in a precise way and ultimately equip the designer with concrete design tools. Developing analysis methods involves basic research in the subdisciplines of aeroelastic stability: materials, solid mechanics, numerical analysis, and further subspecialties. Validation of prediction methods is also essential. Developing analyses and computer programs in a rigorous way is a very exacting process, but success can never be determined nor is a program of much value unless it can be adequately validated. Done properly, validation can be as demanding as development of the theoretical analysis.

To be fully effective, experimental tests must be carefully planned to take into account the specific objectives of the validation. The experiment should be designed to eliminate phenomena not germane to the correlation; moreover, the physical properties of the model must be accurately determined. Careful planning will insure that proper interpretation of the correlation between theoretical and experimental results can be made.

Finally, satisfying research objectives also involves identifying means to forestall potential aeroelastic instability, whether through proper design practices, alternative design approaches to avoid problems, or generating concepts that may eliminate such instabilities.

This survey is intended to cover aeroelastic stability research in a broad sense, from the development of analysis methods to their effect on the development of flight vehicles. The material is organized in the following manner. Analysis methods are treated first in section 2, focusing on the development of equations for the prediction of rotorcraft aeroelastic stability. Included is a detailed discussion of underlying theory of kinematics and solid mechanics for rotating elastic beams, unsteady aerodynamics pertinent to rotorcraft aeroelastic stability (including dynamic inflow), and a limited treatment of solution methods used in aeroelastic stability analysis. The analysis methods section includes results of experimental investigations to validate basic theories for beam structural dynamics, unsteady aerodynamics, and solution methods. Experimental investigations or correlations of aeroelastic stability are not included.

In section 3, information about the aeroelastic stability characteristics and behavior of rotorcraft is surveyed. This includes results of parametric analytical investigations, experimental testing, and correlations to validate prediction

methods. The material is organized in order of increasing complexity of the physical system, beginning with stability of a single flapping blade up to fully coupled rotor-body dynamic systems. Section 4 surveys the experience gained in the design or development of specific rotorcraft systems from the point of view of how aeroelastic stability technology affected the development or yielded insights during design and testing of these systems. The organization of sections 2-4 necessarily leads to some overlap or duplication, for some research efforts naturally span two or even more of these sections. Finally, the results of the work surveyed are summarized, and the contributions of Army-NASA research in this field are assessed. Recommendations for future research are also provided.

A few comments are in order regarding this survey. It was intended that Army-NASA research contributions be emphasized in the material discussed herein. In order to provide perspective and technical continuity, selected non-government research and development efforts have been included where deemed appropriate. While it is hoped that all relevant government contributions have been accounted for, this survey is not complete for the field of aeroelastic stability as a whole. Furthermore, since the volume of work in the field is considerable, the treatment in the survey is necessarily limited in depth and the reader should refer to the references for more detail.

Mention is also in order regarding the distinctions between government and non-government research. For the purposes of this paper Army-NASA contributions include research and development conducted by the four directorates of the U.S. Army Aviation Research and Technology Activity (the Aeroflightdynamics Directorate (AFDD), the Propulsion Directorate, the Aerostructures Directorate, and the Aviation Applied Technology Directorate (AATD)); the NASA Ames, Langley and Lewis Research Centers; and academic or industry research supported by these government organizations. In the case of the Aeroflightdynamics Directorate this includes a number of investigations sponsored jointly with the Army Research Office. The material included herein but not derived from government or government sponsored efforts is denoted by an asterisk entry in the reference list.

2. ANALYSIS METHODS

This section deals with the development of analysis methods for calculating the aeroelastic and aeromechanical stability characteristics of rotorcraft including formulation of equations of motion to model aeroelastic stability behavior. This involves research in fundamental solid mechanics, structural dynamics, materials properties, rigid-body dynamics, and unsteady aerodynamics. This section also deals with the development of mathematical methods to solve the aeroelastic stability equations.

STRUCTURAL DYNAMICS

Rotorcraft structural dynamics encompasses the mechanics of both rigid and flexible bodies generally used to model the structural, inertial, and mechanical characteristics of a rotorcraft or its components. The equations are useful for various rotorcraft applications, but here we focus on their use in aeroelastic stability analysis. This section will address the evolutionary development of rotorcraft equations, primarily the equations of motion for rotating elastic beams used in modeling the rotor blades and equations for coupled rotor-body systems including both helicopters and tilt-rotor aircraft.

It is a given among rotorcraft researchers that because of the complexity of the flow fields, an adequate description of rotary wing aerodynamics is well beyond the current state of the art. Because the mechanics of rotating structures is considerably less difficult than the aerodynamic problem, it is sometimes assumed that rotorcraft structural dynamics is an exact science. However this is not the case and the material presented below will describe the issues that researchers are dealing with.

Rigid-Blade Equations

Early rotor-blade and rotorcraft analyses usually treated both hinged and cantilever elastic blades as hinged, rigid blades for the purposes of aeroelastic or aeromechanical stability. In the case of articulated rotor blades this is appropriate for many problems. For cantilever hingeless rotor blades, the hinged, rigid blade represents a greater degree of approximation. Nevertheless, when the blade bending flexibility is simulated with a rotational spring placed at the hinge, the resulting equations may be adequate for many applications. The equations are easier to derive, and the solutions can be computed much more economically. The approximate hinged-rigid-blade model has been widely used and served as a very effective means to initiate more refined analyses of elastic cantilever blades. The rigid-blade equations are also valuable when insight into dynamic behavior is sought.

In contrast to structural dynamics of elastic rotor blades, the equations of motion describing the mechanics of hinged-rigid blade models are well defined, even though the algebra can become very involved when many degrees of freedom are included. The principal issue in deriving approximate hinged-rigid-blade equations is the selection of the hinge geometry that will best simulate the elastic blade. The development of the hinged-rigid-blade models, their relative accuracy in representing elastic blades, and the results of aeroelastic stability investigations based on such approaches will be covered under Flap-Lag Stability in section 3.

Development of Elastic-Blade Equations

The fundamental basis for rotor-blade equations of motion, and one of the key topics in rotorcraft aeroelastic analysis, is the structural dynamics of rotating

elastic beams. Over the last 20 years, extensive Army and NASA efforts have been devoted to the development of suitable equations to describe the elastic bending and torsion of rotating cantilever beams. Much of this effort has been directed toward the analysis of advanced hingeless and bearingless rotor blades. Although these mechanically simple configurations offer considerable benefit for rotorcraft, they also present a significant challenge for the structural dynamicist. The lack of hinges results in moderately large bending and torsional deformations of cantilever blades during rotorcraft operation. From a structural dynamics point of view these moderately large deformations give rise to geometrically nonlinear structural and inertial terms in beam equations, even when the material properties are linear and the strains are small.

In contrast to hingeless rotor blades, articulated rotor blades could usually be treated quite adequately with linear equations. Since the middle 1950's, the standard equations for this class of problems were the classic Houbolt and Brooks equations for combined flapwise bending, chordwise bending and torsion of twisted, nonuniform rotor blades (ref. 1). Although these equations are linear, they contain the geometrical stiffening, owing to centrifugal force, normally considered a nonlinear effect. These equations were the starting point for much of the subsequent development of nonlinear equations for elastic rotor blades.

The following sections will deal with nonlinear equations for elastic beams undergoing moderate deformations, the nonlinear kinematics of deformed beams, nonlinear torsion of pretwisted beams under axial tension, advanced theories for beams undergoing large rotation and small strains, bearingless rotor blades, finite-element formulations, and treatment of composite materials in rotor-blade equations.

Moderate deformation blade equations- As noted above, the accepted standard for elastic-blade equations was the work of Houbolt and Brooks (ref. 1). One of the first attempts at a complete derivation of equations suitable for aereolastic analysis of both articulated and cantilever blades was the work of Arcidiacono, who developed nonlinear equations for combined flapwise bending, chordwise bending, and torsion motions of an elastic blade (ref. 2). The final modal equations were linearized for small motions and included a quasi-steady aerodynamic formulation as well.

The Aeroflightdynamics Directorate initiated research on development of nonlinear elastic-blade equations in order to treat aeroelastic stability of hingeless rotor blades. Early AFDD research considered the restricted problem of coupled flap and lead-lag elastic bending of torsionally rigid cantilever rotor blades. Ormiston and Hodges developed elastic-blade flap-lag equations to extend analysis capabilities beyond the rigid-blade equations (refs. 3,4). Their derivation was based on Hamilton's principle because of its suitability for complex problems, especially when the nonconservative aerodynamic forces are included. It also helps in correctly formulating the internal forces based on strain energy. The resulting flap-lag equations differed little from the Houbolt-Brooks equations except for a kinematical variable for axial displacement of the blade, based on nonlinear strain-displacement relations. The axial variable was eliminated from the equations by assuming the blades to be inextensible. This assumption neglects axial elastic

deformation of the blade and expresses axial displacement in terms of lateral displacements; this is the well-known kinematical foreshortening of the beam axis caused by bending. Points on the beam axis move radially as the blade bends, resulting in both steady-state and perturbation centrifugal forces and Coriolis forces. These effects are needed to capture essential nonlinear features of hingeless rotor flap-lag stability. Galerkin's method was used to reduce the partial differential equations to ordinary differential equations in terms of elastic bending modes.

Friedmann and Tong also developed equations for analysis of flapwise and chordwise bending of elastic cantilever rotor blades (ref. 5). Blade-pitch motion was treated as rigid-body rotation about the blade-root pitch axis and was restrained by a root spring that represented pitch-link flexibility. Aerodynamic and mass center chordwise offsets from the pitch axis were included. These equations accounted for axial foreshortening of the blade but did not include linear flap-lag structural coupling or distributed elastic torsion deformation along the length of the blade. Quasi-steady aerodynamic forces were included and these equations were used to study aeroelastic stability.

One of the most important features of an elastic cantilever beam is the nonlinear coupling between torsion and combined flapwise and chordwise bending. A schematic illustration of the nonlinear torsion produced by simultaneous flapwise and chordwise bending is given in figure 1. This coupling has a very powerful effect on hingeless rotor blade aeroelastic stability, the precise effects being very sensitive to the detailed structural and geometric properties of the blade. This problem has stimulated much research on beam theory and rotor-blade equations.

Hodges utilized Hamilton's principle to derive nonlinear equations for coupled bending and torsion of an elastic rotor blade (ref. 6). The nonlinear kinematical basis is an extended version of the formulation by Novozhilov (ref. 7). Hodges also introduced the idea of an ordering scheme to deal with the numerous higher-order terms that arise when geometric nonlinearities associated with moderate deformations are included in the equation formulation. The purpose of the ordering scheme was to simplify the equations by discarding higher-order terms in a reasonably consistent manner. There are minor inconsistencies in the kinematical equations of reference 6 associated with finite rotation and nonlinear beam kinematics that will be further addressed below. Hodges also developed a quasi-steady aerodynamic formulation and applied the equations to a modal analysis of aeroelastic stability of uniform cantilever rotor blades that clearly illustrated the significant influence of the nonlinear bending-torsion coupling terms.

One of the early AFDD objectives was to derive a system of nonlinear equations for cantilever rotor blades that would take the place of the Houbolt and Brooks equations. In a significant work, which has since become a standard in the field, and a starting point for many subsequent investigations, Hodges and Dowell derived the dynamic equations of motion governing coupled bending and torsion of twisted nonuniform rotor blades subject to arbitrarily applied loads (ref. 8). Hodges and Dowell used essentially the same ordering scheme as that of Hodges (ref. 6). Both Hamilton's principle and a Newtonian approach were used in the derivation of the

structural and inertial terms in the equations of motion. As discussed in reference 8, the Newtonian approach does not necessarily yield a symmetric structural operator and although the equations from the two methods are not identical, one set can be obtained from the other simply by taking linear combinations of the individual equations. The ordering scheme was carefully applied to insure self-adjoint structural and inertial operators. Both Hamilton's principle and the Newtonian method rely on a nonlinear strain-displacement relation that when used in conjunction with a linear constitutive law, permits the strain energy and force and moment resultants to be expressed in terms of blade-deformation variables.

The kinematical formulation of the Hodges-Dowell equations is based essentially on Green strain components, although Almansi strain components play an intermediate role in the formulation. The strain components were derived from a blade-displacement field that was in turn based on a deformed blade coordinate transformation developed by Peters (appendix, in ref. 8). This transformation, based on reference 9, allowed the inconsistencies in the equations of reference 6 to be rectified. In this formulation the torsional kinematical variable is defined as the integral of the torsional component of the curvature vector, a definition that has been used by only a few other investigators. The final results are given in the form of partial differential equations, accurate to second order, that include the effects of precone and cross-section chordwise offsets. These equations have been the basis for a number of refinements that will be discussed below, as well as for numerous investigations of hingeless rotor blade aeroelastic stability. Dowell applied these equations to derive modal equations for blades with radially varying properties in reference 10.

One of the principal contributions of the Hodges-Dowell elastic-blade equations was the nonlinear structural operator that properly represented the nonlinear bending-torsion coupling needed for cantilever blade aeroelasticity. To evaluate the accuracy of the theory, Dowell and Traybar conducted a series of laboratory experiments on static deformation and vibration of uniform elastic cantilever beams with large deflections (refs. 11,12). The Princeton beam data have since come to be regarded as a benchmark for evaluating nonlinear beam theories. In the experimental setup shown in figure 2, a 20-in. aluminum cantilever beam with unequal bending stiffnesses is loaded at the tip with a concentrated mass. As the load angle θ of the beam is varied, the weight of the tip mass generates combined flatwise and edgewise loading that in turn produces a torsional deformation owing entirely to geometrically nonlinear effects. A comparison of the experimental data with the Hodges-Dowell theory presented in reference 13 and in figures 3 and 4 validates the nonlinear theory for moderate deformations. However, for load conditions in which the bending deformations exceeded the assumptions of the second-order theory, the correlation was poor. In figure 4, bending deformations as a function of the tip mass show how the Hodges-Dowell theory breaks down when the bending deflections become excessive; the flatwise deflection caused by a 5-lb load is 35% of the length of the 20-in. beam.

Nonlinear structural behavior also has a strong effect on beam-bending frequencies. The fundamental flatwise frequency of the beam when loaded in the edgewise

direction, $\theta = 0°$, is compared with both linear and nonlinear theory in figure 5. The correlation with nonlinear theory is excellent in comparison with a linear theory since the static edgewise bending does not exceed moderate deformations. Closer examination of the correlation as the frequency approached zero prompted further study of the theory in connection with lateral buckling of slender beams. Hodges and Peters (ref. 14) found inconsistencies in classic theories of lateral buckling and developed an improved formula that matched the experimental data shown in figure 5. In a different comparison for bending frequencies shown in figure 6, moderate deformation theory is again shown to be inaccurate when large deformations are encountered.

Hodges and Ormiston modified the Hodges-Dowell equations to include variable flap-lag structural coupling and quasi-steady aerodynamics, and applied the equations to investigate hovering rotor-blade aeroelastic stability (ref. 15). The Hodges-Dowell equations were further extended by Hodges to include additional configuration parameters such as twist, droop, torque and hub offset, and a root pitch bearing with pitch-link elastic restraint (ref. 16). Galerkin's method was used to generate modal equations for radially uniform blades without chordwise offsets, including quasi-steady aerodynamic terms for the hover flight condition. The equations were very long and complicated partly because of the choice of variables and coordinate systems and partly because of the explicit appearance of the numerous configuration parameters. This complexity was one stimulus for later development of a finite-element approach so that all the parameters could be put into the analysis in generic form. The analysis was used by Hodges and Ormiston to study the stability of hingeless rotors with pitch-link flexibility (ref. 17).

The adequacy of the structural dynamics equations for rotating cantilever blades was examined by performing in-vacuum vibration experiments on a model rotor blade having uniform mass and stiffness properties (ref. 18). The equations derived by Hodges in reference 16 were checked by comparison with the experimentally measured vibration frequencies, as shown in figure 7.

The elastic-blade equations developed by Friedmann and Tong (ref. 5) were refined by Friedmann to treat moderately large deformations, and therefore, include nonlinear bending-torsion coupling in the structural operator as in the Hodges-Dowell equations (refs. 19,20). The resulting equations included distributed blade torsion in addition to rigid-body blade root pitch motion, linear flap-lag structural coupling, precone, and cross-section chordwise offsets. More refined equations including blade droop and aerodynamics for forward flight conditions were used for forward flight stability investigations by Friedmann and Reyna-Allende (ref. 21).

In a subsequent development, Rosen and Friedmann undertook an extensive re-derivation of the nonlinear equations for moderate deformation of elastic rotor blades based on the assumption of small strains and finite rotations (refs. 22,23). Only the structural operator was presented in the form of explicit partial differential equations; the inertial terms were left in general form. The equations were derived using both the Newtonian method and the principle of virtual work and improved on the previously developed equations in references 20 and 21.

The blade model was cantilevered at the rotor hub, with precone, pretwist, a symmetrical cross section, and chordwise offsets of the elastic axis, mass center, and tension axis. However, several aspects of the development were unusual, particularly in regard to the absence of warp in the formulation and the absence of certain well known terms in the torsion equation, as will be discussed below.

The Rosen-Friedmann equations were extended for application to rotor-blade aeroelastic stability analysis by including a more complete derivation of the inertial terms by Shamie and Friedmann (ref. 24). They also included a derivation of quasi-steady aerodynamic terms appropriate for the forward flight condition. The equations were transformed into modal equations by using Galerkin's method and linearized for use in studies of rotor aeroelastic stability in forward flight. The same equations were also used by Friedmann and Kottapalli for further applications studies (ref. 25).

Results obtained from an enhanced version of the Rosen-Friedmann equations were also compared with the Princeton beam data in reference 26 and typical results of that comparison are included in figures 3 and 4. The accuracy of the theory is confirmed by the data and is an improvement over that of the Hodges-Dowell equations. As pointed out by Hodges in reference 27, the two sets of equations for this problem are equivalent except that Rosen and Friedmann retained several third-order terms that become important for configurations in which the ratio of the edgewise to flatwise stiffness is large compared to unity.

Another derivation of the nonlinear elastic-blade equations was carried out by Kaza and Kvaternik who developed equations for elastic flap bending, lead-lag bending, and torsion in forward flight (ref. 28). Kvaternik et al. also developed flap-lag equations for arbitrarily large precone (ref. 29). The Kaza and Kvaternik equations in reference 28 are similar to the Hodges-Dowell equations (ref. 8), except for the following differences. Kaza and Kvaternik proposed two sets of equations, each with a distinct kinematical variable for torsional rotation. With the appropriate changes of kinematical variable, these two sets of equations and those of Hodges and Dowell can be shown to be essentially equivalent. Rather than use an ordering scheme as did Hodges and Dowell, Kaza and Kvaternik simply restricted the nonlinearities in the equations to second degree. Finally, Hodges and Dowell used the axial displacement as a kinematical variable whereas Kaza and Kvaternik used a kinematical variable defined as the integral of the axial strain (analogous to the torsional kinematical variable of Hodges and Dowell). These differences will be discussed below in connection with finite rotation.

Crespo da Silva derived hingeless-rotor-blade equations based on Hamilton's principle and solved them by the Galerkin method (ref. 30). An ordering scheme was used in which terms of one order higher in the ordering parameter are retained; thus the equations are valid to third order. The purpose of this work was to evaluate the influence of those higher-order terms in the equations. It is found that for stiff-inplane configurations having low torsional rigidity the influence of higher-order terms can be important. A typical example from Crespo da Silva et al. (refs. 31,32), is shown in figure 8, where the dashed lines show blade lead-lag

damping and frequency from second-order theory (e.g., ref. 15) and the solid lines give results with third-order terms retained.

Finite rotation- To adequately model helicopter blades in general and hingeless rotor blades in particular, the elastic deflections must be treated as moderately large and the resulting equations of motion will therefore be nonlinear. The previous section described the development of such equations. To derive these equations, it is necessary to first specify the geometry of the beam both in its undeformed state and in its deformed state at some particular instant in time. For typical beam theories, this involves expressing the position of a generic point on the elastic axis and the orientation of a coordinate frame attached at that point to adequately specify the location of every point in the beam. It is common practice in the helicopter rotor-blade literature to evaluate the transformation matrix between the deformed and undeformed states using a Euler-like sequence of three successive rotations. For linear mathematical models undergoing small rotations, the order of rotation does not affect the final form of the transformation matrix. However, in nonlinear analysis involving moderately large deformations, the final form of the transformation matrix, and subsequently the derived equations of motion, will depend on the rotation sequence. When rotations cannot be treated as small linear deformations they are termed finite rotations. The subject of nonlinear beam kinematics involving finite rotation is complex and sometimes controversial (e.g., Kaza and Kvaternik, ref. 33, regarding the correctness of various derivations of elastic-blade equations) and has attracted the attention of a number of researchers.

The kinematical basis of the Hodges-Dowell elastic blade equations (ref. 8) was derived from rigorous representation of nonlinear beam kinematics based in part on Peters' derivation of the deformed-blade transformation matrix (ref. 9). A similar set of kinematical relations was derived by Kvaternik and Kaza (ref. 34) and Kaza and Kvaternik (ref. 28), and led to the differences between the Kaza-Kvaternik equations and the Hodges-Dowell equations. These differences were addressed by Hodges et al. as part of a general treatment of nonlinear beam kinematics (ref. 35). One purpose of that work was to show that the sequence of rotational transformations used in defining the orientation of the cross section of a beam during deformation is immaterial. The kinematics of large-deformation geometry for a Euler-Bernoulli beam was developed, including the transformation matrix relating the local principal axes in the deformed state to space-fixed Cartesian axes, the components of angular velocity and virtual rotation vectors, the torsion, and the components of bending curvature. Nonlinear expressions were developed to relate the orientation of the deformed beam cross section, torsion, local components of bending curvature, angular velocity, and virtual rotation to deformation variables. These expressions were developed in an exact manner in terms of a quasi-coordinate in the space domain for the torsion variable. The entire formulation was shown to be independent of the sequence of the three rotations used to describe the orientation of the deformed-beam cross section. For more common cases in the literature in which one of the three rotation angles is used as the torsion variable, the resulting equations depend on the choice of the three angles. Differences in the equations, however, were demonstrated to be in form only since the torsion variables in such cases represent different rotations.

Following the general treatment of nonlinear beam kinematics of reference 35, additional work along the same line was carried out by Alkire (ref. 36). In this work the relationships between the twist variables associated with different rotation sequences, as well as corresponding forms of the transformation matrix, were studied, and the earlier work was extended to examine the role of blade built-in pretwist for sequences other than flap-lag-pitch and lag-flap-pitch. In addition to reiterating many of the conclusions of reference 35, Alkire developed a procedure for evaluating the transformation matrix that eliminated the Euler-like sequences altogether. The resulting form of the transformation matrix was unaffected by rotation sequence. This method, upon further analysis, turned out to be a variant of the Rodrigues formulation as shown by Hodges (ref. 37).

Another rather unusual approach was presented by Jonnalagadda and Pierce (ref. 38), and discussed by Hodges et al. (ref. 39). This approach, instead of using one of the orientation angles as the torsional variable, used the average of the two angles used by Kaza and Kvaternik (ref. 28). In the special case of moderate rotation, their method is equivalent to the Rodrigues formulation.

A survey of standard methods of representing finite rotation of rigid body kinematics in relation to nonlinear beam kinematics was presented by Hodges in reference 37. Orientation angles, Euler parameters, and Rodrigues parameters were reviewed and compared. These standard methods of representing finite rotations were applied to general kinematical relations for a large rotation beam theory. The resulting kinematical expressions were compared for both the standard methods and some additional methods found in the literature, such as quasi-coordinates and linear combinations of projection angles. The method of Rodrigues parameters is unique for both its simplicity and generality when applied to beam kinematics. Especially for large rotations, as might be encountered in the flexbeam portion of a bearingless rotor blade, the Rodrigues formulation was shown to be superior to all other methods.

Tension-torsion coupling- In the development of elastic-blade equations, the tension force and tension-torsion coupling have attracted considerable attention. This research expanded to encompass problems of constitutive laws and beam extensional vibrations.

Although the beam equations developed by Rosen and Friedmann (refs. 22,23) were similar to those previously developed, they omitted two well-known terms in the torsion equation that are present in work all the way back to that of Houbolt and Brooks (ref. 1). Previous analyses contain (1) a pretwist moment term owing to combined pretwist and tension and (2) a tension-torsion stiffness term that increases effective torsional stiffness owing to tension. Furthermore, these terms are present in the older analyses even for the limiting case of a beam with circular cross section, although the pretwist moment seems inconsistent since pretwist of a circular beam is arbitrary. Previous investigators had made use of a curvilinear coordinate system, which arises because of pretwist; unfortunately, a constitutive law appropriate for that type of coordinate system had not been used. The equations of Rosen and Friedmann were carefully derived based both on an orthogonal coordinate system and, in reference 22, on the same curvilinear coordinate system used by

previous investigators, except with an appropriate constitutive law. They concluded that the pretwist moment would not have been present, had previous investigators used an appropriate constitutive law, and that the tension-torsion stiffness term should be negligibly small for rotor blades. Although their derivation was carried out correctly, they assumed warping to be unimportant.

Hodges showed that when the analysis is done correctly and includes warping, both of these terms are present; but the form of the first term is different from that found in older works (ref. 40). In the limiting case of a beam with circular cross section, which does not warp, the pretwist moment vanishes, as expected. More significantly, however, for thin cross sections (like those of rotor blades) and with warping included, the pretwist moment reduces to a term very similar to that of Houbolt and Brooks and previous work as well. This problem was discussed further by Rosen (ref. 41) and Hodges (ref. 42). Later work by Rosen (ref. 43), based on an analysis essentially identical to that of Hodges (ref. 40), included warp and exhibited good agreement with experimental results for the pretwist moment of pretwisted strips.

The above discussion addressed the pretwist moment term. Friedmann and Rosen discarded the tension-torsion stiffness term, the one showing increased torsional rigidity owing to tension, based on an order-of-magnitude analysis. This term is present in Hodges's equations unaltered from the classic form. Petersen analyzed beam tension-torsion coupling and obtained a different form for this term, one in which the effective torsional stiffness increases because of tension for warping beams but does not increase for nonwarping beams (such as beams of circular cross section) (ref. 44). Why Petersen's analysis turned out this way was unknown at first. In an attempt to reconcile the analyses of Hodges and Petersen it was found that the main difference between their approaches was the constitutive law. Hodges had used the classic strain energy approach based on Green strain, whereas Petersen had used a strain energy based on Almansi strain. Hodges later showed that a rigorous small-strain analysis would qualitatively confirm Petersen's conclusion regarding the tension-torsion stiffness term (ref. 45).

The influence of the strain-energy function (or constitutive law) had been encountered before. Hodges found disagreements in the technical community concerning the extensional vibration of rotating beams (ref. 46). Depending on the strain-energy definition used (whether based on Green, Hencky, or Almansi strain), one could find significant differences in the trends of extensional frequency versus angular speed. Thus, it was concluded that without experiments or knowledge of second-order material constants, it would be impossible to determine the correct trend. The reason is that the different strain definitions contain terms of higher order in elongations. Use of Hooke's law implies linearity between some definition of stress and some definition of strain. The choice of stress and strain definitions is essentially arbitrary. The different choices imply different relationships between physical stress and strain, thus resulting in different predicted behavior. For Green strain the predicted extensional frequency will increase with rotor angular speed, whereas for the Hencky logarithmic strain, extensional frequency will

decrease with rotor angular speed. This is further discussed in Venkatesan and Nagaraj (refs. 47,48), Hodges (ref. 49), and Kvaternik and Kaza (ref. 34).

It was now clear that a similar situation existed for torsion in the presence of axial stress. The main reason for the differences between the equations of Petersen (ref. 44) and those of Hodges (ref. 40) is the form of the constitutive equation. In joint experimental and theoretical work, Degener et al. (ref. 50) have shown that the effective torsional stiffness of a circular-cross-section, nonwarping, rubber beam under large axial elongation actually decreases and is best predicted by the Hencky strain-energy function (fig. 9). A classical analysis based on Green strain energy is completely inadequate, and even the well-known neo-Hookean material strain energy function only performs fairly well. A strain-energy function closely associated with Petersen's formulation also performs well.

In other closely related work, Kaza and Kielb examined the effects of warping and pretwist on torsional vibrations of rotating beams (ref. 51). They found, based on an analysis similar to that of the older works (such as that of Houbolt and Brooks) that warping, pretwist, and tension increased the torsional stiffness of beams.

Advanced beam theories- Most of the effort in the development of elastic-blade equations, represented by the contributions of Hodges and Dowell (ref. 8), Kaza and Kvaternik (ref. 28), and Rosen and Friedmann (ref. 23), used a geometric nonlinear analysis based on the assumption that structural deformations were limited to moderate rotations. Although adequate for many applications in rotor-blade aeroelastic stability, this assumption has limitations. For example, bearingless-rotor flexbeams undergo combined bending and torsion deformations that produce large rotations, exceeding the moderate rotation of conventional analyses. Furthermore, the moderate rotation theories may be valid for a certain range of beam configuration parameters and then break down for other configurations. One example is the case of a thin beam for which the ratio of bending stiffnesses is small in some sense. Ideally, the magnitude of parameters in the equations for general-purpose analyses should not influence the structure of the equations themselves. Such an ideal is evidently not present in the ordering schemes of references 8 and 23 or in any arbitrary a priori restriction to second-degree nonlinearity, as in reference 28. Furthermore Stephens et al. showed that inconsistencies are virtually unavoidable in ordering schemes based on displacements and rotations when the magnitude of the torsion rigidity is small compared with the bending stiffnesses (ref. 52). Another shortcoming in the moderate rotation equations in references 8, 23, and 28 is that the effects of pretwist are not treated rigorously.

To address these problems, Hodges developed a more general system of nonlinear bending-torsion equations for pretwisted beams undergoing small strains and large rotations (ref. 53). Hodges abandoned the common assumption of moderate rotations. To avoid some of the limitations of previous analyses, Hodges modeled the kinematics of a slender beam without resorting to an ordering scheme for rotations or to arbitrary restrictions on degree of nonlinearity allowed in expressions involving displacement. The transformations used Tait-Bryan orientation angles although a parallel development based on Rodrigues parameters was included in an

appendix to reference 53. The kinematic relations that describe the orientation of the cross section during deformation were simplified by systematically ignoring the extensional strain compared with unity in those relationships. Open-cross-section effects such as warping rigidity and dynamics were ignored, but other influences of warp were retained. The beam cross section was not allowed to deform in its own plane and the stress-strain relation was assumed to be isotropic. Various means of implementation were discussed, including a finite-element formulation. This beam formulation was used as the basis for the GRASP finite-element, coupled rotor-body aeromechanical stability analysis that will be discussed below.

To evaluate the validity of this theory, particularly for the case of large deformations, Hodges (ref. 53) compared results for static deformations with the Princeton beam data from references 11 and 12. These comparisons are also included together with the earlier theories in figure 3 and show excellent agreement. Furthermore, the large-rotation theory also shows excellent agreement with the data in figure 6 for beam-bending natural frequencies.

Although Hodges's large-rotation equations in reference 53 represented a significant advance, they also contained limitations that stimulated further developments. First, these equations are restricted to beams to which the Euler-Bernoulli hypothesis applies. This restriction may be violated for composite rotor blades. Second, the treatment of tension-torsion coupling is somewhat weak. As in Hodges (ref. 40), the Green strain components were used and simplified based on heuristic geometrical arguments to a form valid for small strains and large rotations. In particular, the nonlinear term in the axial strain expression responsible for the tension-torsion coupling is difficult to identify based on geometrical arguments alone. Also, the derivations from Rosen and Friedmann (ref. 22) and Hodges (refs. 40,53) are very complex as a result of the curvilinear coordinate system. The derivation and simplification of the strain-displacement relations is so lengthy and tedious that the details are not included in reference 53.

To remedy these limitations, Hodges initiated development of a new definition of strain displacement relation for a beam based on the idea of engineering strain. The motivation was primarily that calculation of Green strain produces many superfluous terms that need to be removed by some process for small elongations and shears. The reason for this is that the Green strain principal values contain terms of the order of elongations squared. This gives rise to terms in the final strain expression which are of the order of "strain" squared in addition to the true strain. The Jaumann-Biot-Cauchy "engineering" strain tensor has principal values that are linear in elongation. Hodges (ref. 45) and Danielson and Hodges (ref. 54) present this new strain definition, starting with the engineering-strain definition and rigorously decomposing the finite rotation field. This work does not invoke the Euler-Bernoulli hypothesis in the kinematics and adds initial curvature to the description of the reference state of the beam. Most significantly, the algebra of dealing with the curvilinear coordinate system is greatly simplified with this formulation in comparison with previous ones.

These developments provide the basis for new advanced beam theories for small strains and finite rotations. The representation of finite rotation can be by any

method one desires. For large rotations Rodrigues parameters make the most sense. For moderate rotations a variant of the Rodrigues formulation, often called the finite-rotation vector, is preferred. This is the approach recommended for analytical schemes in which a polynomial expression is desirable for the strain components, such as a perturbation scheme.

A complete theory based on this kinematical formulation has yet to be developed. The initial curvature of the elastic axis and effects associated with open cross sections should also be incorporated. In order to be a practical tool for rotor-blade analysis, a modeling approach for anisotropic materials must somehow be included. This problem is not yet fully solved, but several investigators have begun to work, as discussed below, in connection with composite blade modeling.

Bearingless rotor analysis- This section will discuss Army-NASA research to develop analysis methods for bearingless-rotor systems, a specialized but important subclass of elastic blades. The bearingless rotor offers benefits for advanced rotorcraft development and simplifies rotor hubs by eliminating blade-pitch-change bearings, and thereby reducing weight, complexity, and maintenance, and increasing reliability and productivity. Although the physical structure is simplified, the bearingless rotor requires more sophisticated structural and aeroelastic analysis of the rotor hub and blades. The bearingless-rotor design is based on replacing blade-root hinges and bearings with a flexbeam sufficiently flexible in torsion to accommodate all blade-pitch-control motion provided by the pitch change bearing of articulated and hingeless rotors.

The bearingless rotor blade configuration is one of the most challenging problems for the rotorcraft structural dynamicist. Although the hingeless rotor blade is already complex, the bearingless rotor presents potentially more difficult problems because of the flexbeam and the blade-feathering mechanism. Basically, to accommodate blade motion and feathering, the flexbeam undergoes complex combined bending and torsion deformations that may be significantly larger than for a hingeless rotor blade. The elastic twist needed to accommodate blade feathering may be of the order of 15°-20°. At the same time, the flexbeam must carry the full centrifugal tension load of the blade. The pitch-control mechanism introduces a second load path for blade-root shears and moments and makes the system structurally redundant. Multiple flexbeams introduce additional structural complexities.

Combinations of flexbeam and pitch-control systems lead to a variety of bearingless-rotor types; the principal ones are depicted in figure 10. The most direct is a simple torque tube pinned at the hub and either pinned or cantilevered at the blade root. The cantilever pitch configuration is physically simple but structural interaction of the pitch arm, flexbeam, and elastic flexbeam generates complex aeroelastic coupling. The structural interaction may be reduced by a torque tube and snubber configuration. The snubber, located at the inboard end of a torque tube fixed to the blade root and enclosing the flexbeam, constrains translation of the torque tube. Given the unique structural characteristics, it is clear that conventional elastic-blade equations for hingeless rotor blades are not satisfactory for bearingless-rotor analysis. The purpose of this section is to describe the

development of analyses especially tailored to the unique requirements of bearingless rotors.

The first serious development of an aeroelastic analysis for bearingless rotors was due to Bielawa (ref. 55). The differential equations of motion were derived for the bending and torsional deformations of a nonlinearly twisted rotor blade operating in a steady flight condition including aeroelastic characteristics germane to composite bearingless rotors. The differential equations were formulated in terms of uncoupled vibratory modes with exact coupling effects owing to finite, time-variable blade pitch and with approximate second-order effects owing to twist. Also presented were derivations of the fully coupled inertia and aerodynamic load distributions, automatic pitch-change coupling effects, structural redundancy characteristics of the composite bearingless-rotor flexbeam-torque tube pitch-control system, and a description of the linearized equations appropriate for eigensolution analyses. These equations were used as the basis for the G400 code and aeroelastic investigations reported in reference 56.

Subsequently, Hodges developed a simplified analysis for coupled rotor-body stability of rotorcraft with bearingless-rotor blades. FLAIR (flexbeam air resonance) was intended for efficient application as a preliminary design tool and treated the blade as a rigid body, thereby avoiding the complexity of an elastic blade formulation (refs. 57,58). The objective was an analysis that possessed the simplicity of a rigid-blade model but included a relatively detailed treatment of the flexbeam and pitch-control system. The analysis was based on modeling the rotor blade as a rigid body attached to the hub by an elastic beam for the flexbeam portion of a bearingless-rotor blade. The flexbeam deflections were treated exactly for a Euler-Bernoulli beam segment, using the Kirchhoff-Love equations, which are valid for large rotations. An iterative structural analysis including geometric nonlinearities, solved by a shooting algorithm for two-point boundary-value problems, yielded the equilibrium deflected shape of the flexbeam. A numerical perturbation scheme was then used to obtain the stiffness matrix for the tip of the flexbeam. No ordering scheme was used. The flexbeam degrees of freedom were the three rotations and three translations of the outboard end of the flexbeam. The rigid-blade inertial, gravity, and quasi-steady aerodynamic equations were derived for arbitrarily large deflections and analytically linearized about equilibrium. The linear flexbeam and blade equations were developed as part of the coupled rotor-body analysis described later in this section under Helicopter Rotor-Body Equations. The treatment of the bearingless rotor in FLAIR was sufficiently flexible to permit analysis of all of the principal configurations in figure 10. The principal limitation of FLAIR was the lack of an elastic blade to capture the intermodal coupling characteristics typical of many bearingless-rotor blade instabilities.

Another bearingless-rotor analysis was developed by Sivaneri and Chopra, based on a finite-element approach for the isolated rotor blade including treatment of dual-flexbeam configurations (ref. 59).

The most recent development in bearingless rotor blade analysis is the GRASP code, a finite-element analysis developed by Hodges et al. to treat coupled rotor-body stability of a rotorcraft in hover (ref. 60). GRASP (General Rotorcraft

Aeromechanical Stability Program) is an advanced analysis system capable of modeling rotorcraft structures in a very general manner, including rotor-body coupling. In this sense it is not uniquely designed to handle bearingless-rotor blades; it simply has the capability to handle arbitrarily complex bearingless-rotor configurations along with numerous other rotor types as well. In fact, a general finite-element analysis provides the only realistic means to address the potential complexity of bearingless rotors. The elements and constraints in GRASP permit the modeling of large rotation elastic beams, rigid-body masses, and mechanical joints capable of translation and large rotation. The analysis includes quasi-steady aerodynamic formulation and dynamic inflow. A more complete description of the features of GRASP is given the following subsection and later in this section under Helicopter Rotor-Body Equations.

Finite element formulations- The previous sections described development of elastic-blade equations aimed at treating the fundamental nonlinear behavior of cantilever rotor blades. Applications to stability analysis typically use a modal approach to spatially discretize and solve the elastic-blade partial differential equations. A Galerkin approach is commonly used to generate ordinary differential equations in terms of a number of bending and torsion modes of the blade. There are a number of limitations to this approach and inevitably the use of finite-element methods is desirable. A considerable part of rotorcraft structural mechanics research effort has begun to focus in this direction.

Some of the limitations of the modal methods stem from complexities of deriving nonlinear equations for rotating beams. These equations can be extremely long and complicated. The problem is made worse by the explicit appearance of many structural and geometric configuration parameters that play an important role in the aeroelastic stability of hingeless rotor blades. For bearingless rotors, the redundant load paths present further difficulty. In addition to their complexity and lack of generality, the modal equations cannot accurately represent rotor blades having large or discontinuous radial variations in mass or in structural and geometric properties. With these difficulties as a stimulus, Army-NASA researchers began to investigate the application of finite-element methods to the problems of rotating slender beams undergoing nonlinear axial, bending, and torsional deformations.

In one of the first applications, Hohenemser and Yin studied a simple stability problem involving flap bending of rotor blades mounted on flexible supports (ref. 61). Strictly speaking, their approach utilized the transfer matrix technique, not a true finite element method, but one in common use in the rotorcraft field. Friedmann and Straub developed a weighted residual Galerkin-type finite-element method to study the aeroelastic stability of flap-lag motions of a hingeless rotor blade in the hovering flight condition (ref. 62). This method was also applied in references 63 and 64 to formulate the finite-element equations for flap-lag-torsion of hingeless rotor blades in forward flight and to investigate flap-lag stability characteristics in forward flight.

The method is based on the partial differential equations of equilibrium, which are discretized directly, using a local weighted residual Galerkin method. Each

element has eight nodal degrees of freedom representing flap and lag bending displacements and slopes at the ends of the element. The later analyses that treat torsion have three torsional degrees of freedom, one at each end of the element and one in the middle. Blade bending is discretized using conventional shape functions for beam bending based on cubic Hermite polynomials. Torsion is discretized using a quadratic function resulting in the additional internal nodal degree of freedom. The axial displacement has no degrees of freedom associated directly with it because the blade is assumed to be inextensional. The element matrices obtained in this procedure are dependent on the nonlinear equilibrium position. The element matrices are assembled using a conventional direct stiffness method. After assembly, a normal-mode transformation is used to reduce the number of nodal degrees of freedom.

In another investigation, Celi and Friedmann (ref. 65), treat the aeroelastic stability of swept-tip rotor blades using a Galerkin finite-element technique (ref. 62) including a special element for the structural, inertial, and aerodynamic terms of the swept tip. The element equations were based on the Shamie and Friedmann formulation (ref. 24).

Another approach to finite-element formulations for rotor blade aeroelasticity is based on a conventional local Rayleigh-Ritz finite-element method. Sivaneri and Chopra studied the problem of hingeless rotor blade flap-lag-torsion in hover and solved the nonlinear equilibrium equations using the finite-element analysis directly (ref. 66). A normal-mode method is used for the linearized flutter analysis. Chopra and Sivaneri (ref. 67) and Sivaneri and Chopra (ref. 59) extended this work with a more elaborate fifteen-degree-of-freedom beam finite element applied to analyze the hover stability of bearingless-rotor blades including multi-flexbeam configurations. There are two reasons for the additional degrees of freedom: (1) it is necessary to include the axial displacement explicitly in order to treat structures with multiple load paths such as bearingless rotor blades; and (2) it is necessary to have a more accurate interpolation of axial displacement so that inaccuracies in determining the effective bending stiffness, owing to a form of membrane locking, do not occur.

Early work at the Aeroflightdynamics Directorate was aimed at development of a finite-element analysis with ample modeling flexibility to deal with realistic bearingless-rotor-blade configurations. The work described above was based on discretization of the equations for a rotating blade having a specified orientation. That is, the finite-element equations were not sufficiently general to allow assembly of elements together at arbitrary angles to one another. An approach general enough to allow coupling of rotating blade elements together in such a manner still did not exist.

Furthermore, rotating beam finite elements are subject to a form of membrane locking that can generate serious errors, especially in portions of the structure where the geometric stiffness must be determined from the strain instead of from the integration of the loading, such as in a redundant load path (see ref. 59). One way to circumvent this problem is to introduce generalized coordinates associated with higher-order polynomials. Since redundant load paths are typical of bearingless-

rotor systems, early work at the Aeroflightdynamics Directorate was aimed at development of a variable-order finite element.

Hodges investigated the vibration and response of nonuniform rotating beams with discontinuities in mass and bending stiffness (ref. 68). The direct analytical method of Ritz was used by Hodges to generate finite elements with shape functions of arbitrary order (ref. 69). Free vibration and forced-response results were presented to establish the capabilities of the method. Results for planar bending of a rotating beam indicated excellent convergence to exact solutions, even at points of discontinuity and near boundaries. The development of this variable-order finite-element method continued to progress toward incorporation into conventional finite-element codes. Hodges and Rutkowski (ref. 70) and Hodges (ref. 71) provided details on development of shape functions and modified the work reported in reference 69 to a true finite-element form so that the generalized coordinates were actual displacements and slopes at ends of the element. In addition to the usual nodal displacements at the ends of the element, an arbitrary number of additional internal generalized coordinates were used.

Hodges extended the AFDD efforts in rotor-blade finite-element analysis to the implementation of a variable-order finite element based on the large rotation-beam theory (ref. 53). This element was the basis for the aeroelastic beam element developed for the GRASP analysis that will be discussed in more detail in this section under Helicopter Rotor-Body Equations.

The aeroelastic beam element developed for GRASP represents a slender-beam element without shear deformation that is subject to elastic, inertial, gravitational, and aerodynamic forces. The element is derived on the basis of small strains and large rotations (limited to 90° because of use of orientation angles to define finite rotation kinematics inside the element). The element degrees of freedom include a reference frame, structural nodes at the ends of the beam, an air node, and internal degrees of freedom for increased accuracy of beam-deformation calculations. The main element properties include mass, inertias, pretwist, axial, bending, and torsion stiffness, structural damping, and airfoil aerodynamic properties, including chordwise aerodynamic center offsets. The GRASP element is not intended to accommodate composite material properties.

One finding from Hodges et al. (ref. 35), which should be mentioned at this point for the benefit of ongoing finite-element development work, is that the torsional kinematical variable used by Hodges and Dowell (ref. 8), although suitable for integration and modal methods of solution, may not be suitable in a general-purpose finite-element context. This applies both to this variable, defined as the integral of the torsional component of the curvature vector, and to analogous axial displacement variables, defined as integrals of axial strain. The presence of integrals in the kinematical relations can introduce undesirable couplings into a finite-element analysis. The work by Hodges uses an angle, which is suitable for finite element work; use of Rodrigues parameters would also be suitable (ref. 53).

Composites- Most modern rotor blades are constructed from composite materials. The initial impetus for the use of composites was the very significant

improvement in fatigue life and damage tolerance of the blades and, later, the benefits afforded by the ability to incorporate more refined aerodynamics into planform and airfoil section geometries. For advanced rotor blades, composite materials provide opportunities for structural simplicity of hingeless and bearingless designs, and structural couplings to improve the aeroelastic stability of these configurations. Most structural models described above have been limited to isotropic material properties. Rotor blades and flexbeam structures are built up from composite materials, and cannot be regarded as isotropic. There may be coupling between extension, bending, and shear deformation; warping effects may be much more significant. These complexities generally invalidate the Euler-Bernoulli beam assumptions that plane beam cross sections remain plane and perpendicular to the elastic axis.

Work in this area can be classed in two distinct areas: (1) the development of modeling approaches so that the three-dimensional constitutive law for general anisotropic elasticity can be reduced to a simple one-dimensional form for the beam problem; and (2) the use of a specialized, simple model for the blade cross section in order to assess the stability of rotor blades for various values of ply orientation and other geometric parameters.

Work in the first category focuses on the determination of the shear center location and warp functions. Cross-section properties can then be evaluated for use in the one-dimensional beam theory, which has been developed with appropriate kinematics and material constants. Determination of the shear center location and warp functions can either be from use of a two-dimensional finite-element model of the blade cross section or analytically from simplified physical models for the cross section. Fundamental work by Rehfield and Murthy was aimed at representing nonclassic effects of composites on beam structural behavior (ref. 72). These effects are related to transverse shear, bending-related warping, and torsion-related warping. Bauchau developed an anisotropic beam theory in which out-of-plane cross-section warping is determined from a finite-element solution of a Laplace-type equation over the cross section (ref. 73). The solution is expressed in terms of an arbitrary number of so-called eigenwarpings. In practice, only a few eigenwarpings are needed.

More recently, Kosmatka developed a method for analyzing highly swept curved blades constructed of anisotropic composite materials (ref. 74). A finite-element model of the cross section yields both in-plane and out-of-plane warping functions and the shear center location. This method is applicable to rotor blades as well. Kim and Lee have developed a similar approach, although not as general (ref. 75). A considerably simpler approach was developed by Rehfield, in which a general cross section is approximated as a multi-celled box beam whose shear center location and warp function can be determined analytically (ref. 76). The Rehfield and Bauchau methods both yield results of comparable accuracy for box beams (ref. 77). None of these methods has yet been developed and validated to the degree necessary for general-purpose analysis of rotor-blade cross sections.

Work in the second category has been chiefly that of Chopra and his co-workers. Hong and Chopra developed a composite beam finite-element anlaysis for

flap-lag-torsion stability of a hingeless rotor blade in hover (ref. 78). The blade was treated as a single-cell-dominated shell beam composed of an arbitrary layup of composite plies. Stiffness coupling terms caused by bending-torsion and tension-torsion couplings were correlated with different composite ply layups. The results show that such couplings can have a significant effect on the stability.

Coupled Rotorcraft Equations

Equations for isolated rotor blades have been discussed in previous sections; this section deals with coupled rotorcraft equations where the isolated blade equations are combined with equations of other blades or rotorcraft components such as fuselages, support systems, or nacelle-pylon-wing components. The most important coupling is that between the rotating and fixed system; this coupling is one of the central features of rotorcraft dynamics. Other important coupled systems involve rotor feedback control systems, certain rotor types such as teetering or gimbal rotors that structurally couple rotor blades, or even the dynamic inflow model. This section is divided into two principal areas, helicopter coupled rotor-body systems and tilt-rotor systems.

Helicopter rotor-body equations- Rotor-body coupling is important in aeroelastic stability because of the strongly destabilizing mechanical coupling that occurs for some rotorcraft configurations; for example, the classic ground resonance treated by Coleman and Feingold (ref. 79). When both aerodynamic and aeroelastic considerations are involved, this phenomenon is often termed aeromechanical stability. The principal issue in coupled rotor-body equations of motion is the fact that rotor-blade equations are written in a rotating frame of reference whereas fuselage equations are written in a nonrotating frame of reference. When arbitrarily large rigid-body motions of an elastically deforming fuselage are considered, this becomes a formidable problem in dynamics.

For most problems in aeroelastic stability, only small motions are involved and the problem is relatively straightforward. The use of a coordinate transformation from the blade-fixed rotating system to the body-fixed nonrotating coordinate system has long been used in deriving equations for rotorcraft analysis. Hohenemser and Yin developed a formal version of this technique known as multiblade coordinates that has since gained wide acceptance in the rotorcraft technical community (ref. 80). The multiblade transformation changes blade equations from a rotating frame of reference to a nonrotating frame of reference and also combines the equations for a given degree of freedom of k individual blades into a system of equations for the corresponding multiblade degrees of freedom for a rotor having k blades. It is particularly useful for formulating equations of coupled rotor-body systems, for simplifying the periodic-coefficient equations of motion of rotor blades in forward flight, and for providing rotor degrees of freedom that better lend themselves to physical interpretation of analysis results than individual blade degrees of freedom.

Within the scope of this survey, important work on coupled rotor-body aeromechanical stability of hingeless rotorcraft in hover was carried out by Cardinale

using a simplified modal representtion for the blade together with coupled fuselage and control gyro equations (ref. 81). Hammond developed equations of motion, using the Coleman and Feingold physical model, to represent rotorcraft configurations having one of the blade dampers inoperative (ref. 82). In general, these equations have periodic coefficients, and Hammond used Floquet theory to solve them. Johnston and Cassarino developed a system of coupled rotor-body equations, based on a modal analysis of coupled flap-lag-torsion dynamics for an elastic blade (ref. 83). The equations were linearized for aeroelastic stability analysis in hover and forward flight. The latter equations were approximated by the constant-coefficient form of the multiblade coordinate equations. A more restricted example of coupled rotor-blade equations is the two-bladed teetering-rotor problem treated by Shamie and Friedmann (ref. 84). Hohenemser and Yin developed coupled equations for a rotor and elastic supports, using a finite-element formulation (ref. 61).

Johnson developed a very complete set of equations of motion for an analytical model of the aeroelastic behavior of a rotorcraft operating in a wind tunnel or in free flight (ref. 85). A unified development is presented for a wide class of rotors, helicopters, and operating conditions. The rotor model includes coupled flap-lag bending and blade torsion degrees of freedom, and is applicable to articulated, hingeless, gimballed, and teetering rotors with an arbitrary number of blades. The aerodynamic model is valid for both high and low inflow, and for axial and forward flight. The rotor rotational speed dynamics, including engine inertia and damping, and the perturbation inflow dynamics are included. A normal-mode representation of the wind-tunnel test module, strut, and balance system is used. The aeroelastic analysis for the rotorcraft in flight is applicable to a general two-rotor aircraft, including single main-rotor and tandem helicopter configurations, and side-by-side or tilting proprotor aircraft configurations. The aircraft motion is represented by the six rigid-body degrees of freedom and the elastic free-vibration modes of the airframe. The aircraft model includes rotor-fuselage-tail aerodynamic interference, a transmission and engine dynamics model, and the pilot's controls. A constant-coefficient approximation for forward flight and a quasi-static approximation for the low-frequency dynamics are also described. The coupled rotorcraft or support dynamics are represented by a set of linear differential equations, from which the stability and aeroelastic response may be determined.

A simplified system of equations for air-ground resonance of hingeless rotors in hover was developed by Ormiston for application to parametric investigations reported in reference 86. The equations of motion treat a simplified model of a hingeless-rotor helicopter having spring-restrained, hinged-rigid blades with flap-lag motion (ref. 87). Kinematic aeroelastic couplings were included to represent the effects of blade torsion and typical couplings of hingeless blades.

Hodges developed a coupled rotor-body analysis for aeromechanical stability of bearingless-rotor helicopters in hover, axial flight, and ground contact. A detailed derivation of the equations of motion for FLAIR (flexbeam air resonance) is given in references 57 and 58. Treatment of the bearingless blade was described earlier in this section. The fuselage is treated as a rigid body and the landing gear as simple spring elements. The equations are limited to hover and axial flight

and include four rigid-body degrees of freedom for the fuselage pitch and roll angular motion, and longitudinal and lateral translations.

The analysis was based on the set of generalized forces owing to inertia, gravity, body springs and dampers (for the aircraft in ground contact), quasi-steady aerodynamics, and the flexbeam structure. All of these generalized forces (except those caused by flexbeam structural loads) were written exactly, for arbitrarily large deflections, and analytically linearized about equilibrium. The linearized perturbation forces and moments associated with the flexbeam structure, the pitch-control links, body springs and dampers, and inertial, gravitational, and aerodynamic loadings, when combined, yielded a system of constant-coefficient, linear, homogeneous, ordinary differential equations in the nonrotating reference system. Only the cyclic multiblade rotor modes were retained. Solutions were obtained by standard eigenanalysis. Results of stability investigations will be discussed below. The FLAIR analysis was used to support the design development of the Boeing Vertol Bearingless Main Rotor (refs. 88-90), and it has been extended and used in support of the ITR/FRR bearingless rotor preliminary design as reported by Hooper (ref. 91).

Warmbrodt and Friedmann also developed equations of motion for coupling rotor-fuselage and rotor-support systems (refs. 92,93). An aerodynamic formulation is included for hover and forward flight. The equations are written in partial differential equation form and are applicable to the aeroelastic stability problem. The importance of an ordering scheme for deriving a consistent set of nonlinear coupled rotor-body equations is emphasized.

Following earlier work (ref. 85), Johnson extended the general rotorcraft analysis to a more comprehensive analysis known as CAMRAD (refs. 94-96). Intended for application to both rotorcraft dynamic response and stability, this comprehensive analysis is intended for calculating performance, loads, noise, vibration, gust response, flight dynamics, handling qualities, and aeroelastic stability. The equations applicable for aeroelastic stability are similar to those developed in reference 85.

A coupled rotor-fuselage analysis for application to multi-rotor hybrid heavy-lift vehicles was developed by Venkatesan and Friedmann (refs. 97,98). These equations represent the blades as spring-restrained, flap-lag hinged-rigid blades and the fixed system as rigid bodies attached to a flexible supporting structure. The aerodynamic formulation is derived for hover and forward flight.

The GRASP analysis developed by Hodges et al. (ref. 60) is a major development for coupled rotorcraft systems. GRASP (General Rotorcraft Aeromechanical Stability Program) is a hybrid of a finite-element program and a spacecraft-oriented multibody program. GRASP differs from standard finite-element programs by incorporating multiple levels of substructures which can translate or rotate relative to other substructures without small-angle approximations. This capability facilitates the modeling of rotorcraft structures, including the rotating-nonrotating interface and details of the blade-root kinematics for various rotor types. GRASP treats aeroelastic effects, including dynamic inflow (treated later in this section) and non-

linear aerodynamic coefficients. The aeroelastic beam element of GRASP was described in more detail earlier in this section under Finite-Element Formulation. The analysis includes the equations of equilibrium for the hover flight condition and calculates linearized perturbation equations for stability analyses. To illustrate how a problem is defined using the hierarchical substructuring of the GRASP system, a simple coupled rotor-body problem was chosen for modeling. This example is illustrated in figure 11 (from ref. 60). Three blades are combined to form a rotor subsystem which is in turn combined with the air mass and fuselage rigid-body elements to form the complete coupled rotor-body system.

Tilt rotor analysis methods- Analysis of tilting proprotor dynamics has historically drawn from rotorcraft technology. Tilt-rotor aeroelastic stability analysis is fundamentally similar to coupled rotor-body helicopter dynamics; the differences in analysis are mainly a matter of detail, primarily the complexity of the physical system and the many degrees of freedom needed to insure a reasonably complete dynamic analysis. In general, tilt-rotor analysis must include coupled wing bending and torsion, pylon pitch and yaw, rotor-blade flap bending, lead-lag bending and torsion, as well as rotor speed and rigid-body airframe degrees of freedom. Although the rotors operate in axial flow conditions when in the hover and airplane modes, forward flight operation in the helicopter mode and the intermediate nacelle tilt conversion mode introduce the same periodic coefficient effects into the equations of motion as experienced by the helicopter. Some of the differences between helicopter and tilt-rotor analysis include larger rotor speed variations, larger collective pitch range and blade twist, high inflow aerodynamics, and different rotor-airframe wake interference effects.

Before the period addressed in this survey, government researchers contributed to the development and understanding of theories of propeller-nacelle whirl flutter, using simplified methods to understand the mechanisms and predict the relevant phenomena. Typical analyses were developed by Reed and Bland, Houbolt and Reed, and Reed; this work will be discussed in section 3 under Tilt-Rotor Aircraft Stability. These methods treated the propeller blades as rigidly attached to a hub mounted on a nacelle free to pivot in pitch and yaw. Aerodynamic forces for the axial flow condition typically were derived from simple quasi-steady strip theory. Such an approach, although generally sufficient for classical propeller whirl flutter, is not adequate for tilt-rotor aircraft configurations. Additional requirements for such analyses were addressed independently in the works of Kvaternik and Johnson.

Kvaternik developed a proprotor aeroelastic stability analysis including wing, nacelle, and rotor-blade degrees of freedom (ref. 99). All elements were modeled as rigid bodies with spring-restrained hinges where appropriate. The nacelle included pitch and yaw degrees of freedom and the rotor blades were hinged for flap motions. The effectiveness of this analysis in predicting proprotor whirl flutter was verified by extensive comparisons with model test data described by Kvaternik and Kohn (ref. 100). This analysis was the basis for later extensions that included provisions for a gimbaled hub with offset coning hinges, blade lead-lag motion, a modal representation of the airframe structure, full span free-free or semispan

cantilevered configurations, and rigid-body aircraft degrees of freedom. Nonthrusting-, windmilling-, and cruise-mode flight conditions were included. This analysis was named PASTA (Proporotor Aeroelastic Stability Analysis) and was later used in support of V-22 aeroelastic model testing in the NASA Langley Transonic Dynamics Tunnel.

Johnson developed a series of tilt-rotor aeroelastic stability analyses later incorporated in the comprehensive CAMRAD analysis for rotorcraft performance, loads, stability and control, aeroelastic stability, and acoustics. CAMRAD contains the capability to predict the linear stability characteristics of tilt-rotor configurations in various flight conditions (ref. 94). The initial development of the tilt-rotor equations, reported in reference 101, treated a semispan configuration consisting of a cantilever wing, nacelle, and proprotor and modeled uncoupled flap and lead-lag bending of elastic rotor blades, and elastic beam and chord bending and torsion of the wing. Quasi-steady aerodynamic forces were included and equations for rotors having two or more blades were developed. For the two-bladed configurations the equations included periodic coefficients; for rotors having three or more blades, the use of the multiblade transformation yielded equations with constant coefficients. The equations in reference 101 were used by Johnson to correlate with full-scale experimental test data of two semispan wing-nacelle-proprotor models.

Johnson extended his analysis in reference 102 by refining the rotor modeling to include coupled elastic flap and lead-lag bending modes, rigid pitch motion of the blades to reflect pitch control system flexibility, blade elastic torsion, gimbal tilt, and rotor speed perturbations. The aerodynamic model treated high and low inflow, axial and nonaxial flight. The effects of compressibility and static stall on the airfoil coefficients were included. The rotor model included gimbal undersling, torque offset, precone, droop, sweep, and feather axis offset. Blade section center of gravity, aerodynamic center, and tension axis offsets from the elastic axis were included. In reference 103, Johnson added an engine-transmission-governor model including an interconnect shaft between the two rotors, refined the method for treating kinematic pitch-bending coupling of the blade, and extended the rotor aerodynamics model to include reverse flow. In reference 85, Johnson continued development of rotorcraft aeroelastic analysis, generalizing a system of coupled rotor-body equations to treat multirotor helicopters (single main rotor and tail rotor, twin rotor tandem) and symmetric tilt-rotor vehicles in both free flight or in wind tunnel or ground contact conditions. For tilt rotors, this analysis was advanced over previous work because it included complete rigid-body aircraft degrees of freedom and two complete proprotors. Linearized small-perturbation equations were developed for aeroelastic stability analysis.

Finally, this analytical model was used as the basis for the CAMRAD comprehensive rotorcraft analysis for use in predicting performance loads, stability and control, and acoustics characteristics in addition to aeroelastic stability (ref. 94). Johnson used these analyses for a number of research investigations of tilt-rotor aeroelastic stability that will be discussed below. Johnson used XV-15 wind-tunnel and flight-test data for comparison with the CAMRAD analysis to assess its adequacy to predict tilt-rotor aircraft performance, loads, and stability

(ref. 104). Generally the aeroelastic stability prediction capability was judged to be good; however, additional capabilities were considered desirable for future configurations such as bearingless rotors.

In summary, the development of aeroelastic stability analysis capability described herein has had and will continue to have a significant effect on the successful development of the revolutionary tilt-rotor aircraft concept.

UNSTEADY AERODYNAMICS

This section will treat developments in rotor unsteady aerodynamics applicable to rotorcraft aeroelastic stability.

Unsteady aerodynamics of rotor blades is considerably more complex than that of fixed wings for which flutter analysis for three-dimensional, unsteady, compressible flow is reasonably well developed. For the rotor blade, many aeroelastic stability problems may be successfully treated with two-dimensional quasi-steady aerodynamics; however, there is also a need to treat unsteady, compressible flow, dynamic stall, and varying free-stream velocity, as well as three-dimensional effects of returning wake sheets and variable sweep angle. In view of these complications, progress in advanced unsteady aerodynamics for rotary wing applications has been slow, and researchers and designers alike have had to rely on approximate simplified methods.

Most rotary-wing aerodynamics research has been directed toward rotor performance, loads, vibrations, and stability and control. For these applications, rotor aerodynamics generally is divided into two parts: rotor-blade airfoil section airloads and rotor-wake-induced inflow. The rotor-blade section airloads are calculated using approximate or empirical methods such as linear steady or unsteady thin-airfoil theory, or from airfoil aerodynamic coefficients tabulated as a function of angle of attack and Mach number. Empirical corrections are applied to account for blade sweep, compressibility, static and dynamic stall, and blade-vortex interaction effects. The wake-induced velocity is needed to define the local blade-section angle of attack from which blade-section airloads are calculated. Various momentum and discrete vortex-wake theories have been developed for the rotor-induced inflow. The formulations for airfoil airloads and wake-induced velocity are solved together with the blade dynamic response equations either by numerical integration in the time domain, or by iteratively calculating the response coefficients in the frequency domain.

In general, this approach provides the rotor transient or steady-state periodic airloads that can be used to calculate rotor performance, loads, vibrations, and vehicle stability and control. However, these methods do not yield direct information on rotor aeroelastic stability characteristics. It is sometimes possible to use direct numerical integration of the rotor loads equations to determine stability, but it is more desirable to solve linear differential equations by means of eigenanalysis to obtain stability characteristics directly.

In general, rotor-blade flutter analysis employing unsteady aerodynamic theory is carried out using methods adopted from fixed-wing flutter analysis. Fixed-wing unsteady aerodynamic theory, in contrast to the typical rotorcraft approach described above, generally relates the airfoil airloads directly to the motion of the airfoil—combining airfoil-section airloads and wake-induced inflow in a single analytical model. The unsteady aerodynamic theory is generally formulated in the frequency domain—harmonic airloads expressed in terms of harmonic airfoil motions. Aeroelastic stability equations therefore assume airfoil motion to be harmonic and solutions that satisfy this assumption therefore determine the neutral stability condition.

If a time-domain aerodynamic theory is available, it is preferable to use a standard eigenanalysis solution yielding both damping and frequency for conditions of arbitrary stability. The latter approach is typically used for quasi-steady theory but is more difficult for sophisticated unsteady aerodynamics.

The scope of this section will cover a variety of unsteady aerodynamic developments, including two-dimensional linear and nonlinear unsteady aerodynamic theory; finite state models; three-dimensional unsteady aerodynamic theory; and dynamic inflow, a simplified three-dimensional unsteady actuator disc rotor wake model.

Two-Dimensional Unsteady Aerodynamics

As noted above, rotary-wing aeroelastic stability has borrowed from methods developed for fixed-wing flutter analysis. Classical Theodorsen unsteady aerodynamic theory is applicable for rotor-blade bending-torsion flutter and is commonly applied in quasi-steady form (ref. 105). Loewy's theory, which extends Theodorsen theory to the hovering rotor problem, approximately represents the effects of wake vorticity of previous blade passages (ref. 106). Greenberg's theory is commonly applied to account for the effects of varying free-stream velocity of rotor-blade airfoil sections caused by forward flight or inplane motion of the blade (ref. 107). These theories formed a basis for government research activities addressed in this survey.

One area addressed by government researchers is the application of these two-dimensional, unsteady aerodynamic theories to rotor-blade problems. The elastic motion of a fixed-wing configuration is clearly defined, but a rotor blade undergoing moderately large deformations in elastic bending and torsion and pitch rotations is kinematically more complex and requires special attention. Relating the rotor-blade motion variables to the airfoil-motion variables of two-dimensional unsteady aerodynamic theory was addressed by Johnson (ref. 108), Kaza and Kvaternik (ref. 109), Friedmann and Yuan (ref. 110), and Peters (ref. 111). These works indicate that a failure to properly include the aerodynamic theory in the aeroelastic analysis can lead to erroneous stability predictions.

Recent efforts have also been made to transform rotor unsteady aerodynamic theories from the frequency domain to the time-domain. Frequency-domain formulations are not convenient to use for aeroelastic stability analysis and,

except for neutral stability conditions, provide only an approximation to unsteady aerodynamics for transient motion. Dinyavari and Friedmann developed approximate time-domain models for Loewy and Greenberg unsteady aerodynamic theories (ref. 112). The finite-state models were obtained by using Pade approximants of the appropriate lift deficiency functions contained in the Loewy and Greenberg theories. The approximation did not, however, capture the oscillatory behavior of the Loewy lift-deficiency function that represents the effects of wake vorticity shed by previous revolutions of the rotor blades.

The Greenberg finite-state model was applied to predict aeroelastic stability of a rotor blade in hover and forward flight (ref. 113). Friedmann and Venkatesan also formulated another technique for approximating the Loewy lift-deficiency function (refs. 114-116). This method, derived from linear control system theory and termed the Bode plot method, involves curve fitting an approximate function for the Bode plot of the lift-deficiency function. This model may be incorporated in rotor aeroelastic equations and solved by eigenanalysis techniques to yield frequency and damping characteristics. Although these methods are not yet in common use by rotorcraft analysts, they are an important step in beginning to take advantage of analysis capabilities that are in use in the fixed-wing field.

Two-dimensional linear unsteady aerodynamic theory, even without nonlinear stall behavior, is a valuable and powerful tool for predicting rotor aeroelastic stability in the hover flight condition, but there are serious theoretical limitations for forward flight applications. As advance ratio increases, reverse flow and localized high-lift conditions produce time-varying nonlinear stall effects. Recent research aimed at aeroelastic stability analysis applications has begun to focus on nonlinear aerodynamics problems.

Ormiston and Bousman used quasi-steady stall analysis for application to flap-lag stability in hover (ref. 117). It was shown that the static nonlinearities in the airfoil lift and drag coefficients versus angle of attack, when included in a linearized aeroelastic analysis, were sufficient to adequately account for differences observed between measured blade-lead-lag damping and predictions based on unstalled airfoil theory.

Rogers has recently made progress in adapting nonlinear dynamic stall models to aeroelastic stability analysis in forward flight (ref. 118). Dynamic stall models have been developed for use in rotor airloads analysis, that is, in predicting rotor blade dynamic response and the associated unsteady blade airloads in forward flight, primarily in steady-state, trimmed flight conditions. These are usually empirical models in either the time domain or frequency domain and they rely on experimental data obtained from oscillating airfoil testing. Tran and Petot developed a time domain model consisting of differential equations relating the unsteady aerodynamic coefficients to airfoil motion variables (ref. 119). The parameters in these equations are functions of mean angle of attack of the airfoil and are derived from airfoil test data. However the formulation is valid for arbitrary motion rather than just simple harmonic motion. Rogers and Peters used the Tran-Petot nonlinear stall model to analyze the flapping stability of a rotor blade in forward flight

(ref. 118). The model was used to numerically calculate a nonlinear periodic equilibrium solution for rotor-blade response in forward flight.

Thereafter the nonlinear equations were analytically linearized for small-perturbation motions about the periodic equilibrium solution. The resulting periodic coefficient, linear differential equations were solved by Floquet theory to yield frequency and damping of the blade flapping motion.

Peters extended the Tran-Petot dynamic stall model with the objective of developing a unified model for unsteady aerodynamic lift of a two-dimensional airfoil section for use in rotor-blade aeroelastic stability analysis (ref. 111). The model is unified in the sense that it explicitly distinguishes between airfoil pitch and plunge motion and includes unsteady velocity, reverse flow, and large angles of attack. The model also reduces to Greenberg theory at small angles of attack and further reduces to Theodorsen theory for steady velocity.

Three-Dimensional Unsteady Aerodynamics

There is much to be done for three-dimensional unsteady aerodynamics applicable to rotor-blade aeroelastic stability. An important early work in the field by Miller developed an analytical formulation for unsteady airloading (ref. 120). Substantial contributions have been made at ONERA by Dat (ref. 121), and more recently by Runyan and Tai (ref. 122). The problem, even in linear form, is a difficult one that has not attracted sufficient attention by rotorcraft researchers. Nevertheless, a rational, three-dimensional linear unsteady aerodynamic theory applicable to forward flight would be very useful for basic aeroelastic stability analyses in forward flight.

Much of the problem of three-dimensional unsteady aerodynamics of rotors lies in the complexity of the rotor configuration. In the case of fixed-wing unsteady aerodynamics, the extension from the two-dimensional airfoil problem to the three-dimensional problem involves the spanwise variations in airloads distribution and (implicitly) the associated shed and trailed vorticity convected from the wing by the free-stream velocity in an undeformed planar sheet.

Linear potential-flow theory has been used to develop rigorous unsteady lifting-surface aerodynamic theories (e.g., vortex doublet lattice). For the three-dimensional rotor blade, there are also the effects of the helical wake configuration, the effects of unsteady variations in free-stream velocity and direction, and the effects of other blades on the rotor. For the purposes of aeroelastic stability, the wake geometry may be assumed undeformed, and the perturbation unsteady aerodynamics may be obtained from linear theory.

Dat has developed linear three-dimensional unsteady lifting-line and lifting-surface theories for rotor blades, using an integral equation formulation based on the acceleration potential including linear compressibility effects. The theory has been applied to aeroelastic stability analysis of proprotor blades in axial flight as reported by Dat (ref. 123).

A similar theory has been developed by Runyan and Tai (refs. 122,124). They developed a lifting-surface theory for a helicopter rotor blade in forward flight utilizing the concept of the linearized acceleration potential and a doublet lattice procedure. The method was applied to rotor blade forced-response airload calculations. Results are also calculated for the rotor-blade airload response to an oscillatory blade-pitch excitation. Although the theory was not applied to an aeroelastic stability analysis, it would be suitable for such investigations.

Dynamic Inflow

Background- Dynamic inflow is a simplified model for the unsteady induced inflow of a rotor. It treats the inflow but not the airloads part of unsteady aerodynamic theory. When used with quasi-steady airfoil theory, it provides a convenient, inexpensive, unsteady aerodynamic model that is useful for a number of rotor and coupled rotor-body low-frequency aeroelastic stability problems. In some respects, it may be thought of as a low-frequency approximation for a linear, three-dimensional, unsteady aerodynamic theory for a rotor blade. Dynamic inflow represents the rotor as an actuator disk, in effect ignoring the higher frequency influence of the airfoil shed wake while including the effect of the trailing wake. In contrast with the relatively limited unsteady aerodynamic research efforts discussed above, dynamic inflow theory has been the focus of considerable study. This section will review the significant accomplishments in this area, and also indicate the effect of this work on rotorcraft aeroelastic stability analysis.

By 1971, it had already been established, although it was not widely recognized, that the induced inflow of a rotor responds in a dynamic fashion to changes in rotor lift. Amer recognized that the roll damping of a helicopter was significantly affected by the induced-flow gradients from the asymmetric lift associated with the rolling motion (ref. 125). Sissingh was able to quantify this phenomenon through a set of equations that related the induced-flow gradient to the lift gradient (ref. 126). Curtiss and Shupe showed that the Sissingh theory could be placed in the form of a lift-deficiency function, involving an equivalent Lock number (ref. 127).

Although these theories are only quasi-steady representations which assume that inflow responds instantly to changes in thrust, it is important to recognize that the induced inflow response to rotor loads can involve significant time delays. In fact, Carpenter and Fridovich had performed experiments on the thrust and inflow response of a helicopter rotor to step inputs in collective pitch and had found time constants of the order of the apparent mass of an impermeable disk (ref. 128). Furthermore, Loewy's theory, a two-dimensional approximation to unsteady rotor aerodynamics, had been shown to yield a lift deficiency that exactly matches the Sissingh result at zero frequency, but that approached unity as frequency increases (ref. 106). Yet, despite this rather extensive knowledge based on the low-frequency behavior of the unsteady aerodynamics of rotors, no general theory existed that could model these aerodynamics in hover, in axial flight, and in forward flight. Furthermore, there was no comprehensive set of data to compare with prospective

theories. Government-sponsored research changed this situation beginning in the early 1970's.

Initial interest in rotor inflow resulted from an Aeroflightdynamics Directorate experimental investigation of the response characteristics of hingeless rotors at high advance ratios. This work was carried out on a 7.5-ft-diam rotor model in the AFDD 7- by 10-Foot Wind Tunnel (fig. 12) under a contract with Lockheed California Company. The objective was to obtain a comprehensive set of data to define the static and dynamic response characteristics of typical hingeless rotors to support applications, including vehicle feedback control systems for stability augmentation, gust alleviation, and vibration reduction. The tests involved a simplifed four-bladed rotor having untwisted blades of very high lead-lag bending and torsional stiffness to emphasize the basic flapping response dynamics. The model was operated at sufficiently low lift and tip speeds that stall and compressibility effects were largely avoided. This series of tests is described by Kuczynski and Sissingh (refs. 129,130), Kuczynski (ref. 131), and London et al. (ref. 132).

Very low thrust testing in hover and forward flight up to advance ratios of 1.75 for high flap stiffness (p = 1.33 - 2.33) is described in reference 129. Rotor thrust, roll, and pitch moments were measured in response to steady-state collective, cyclic, and shaft-angle inputs. In reference 130, harmonic excitation of the cyclic control was introduced to determine the rotor thrust, pitch, and roll moment frequency response functions in hover and forward flight, up to $\mu = 1.44$. Steady-state testing was carried out for lower flap stiffness (p = 1.17) and advance ratios from $\mu = 0.07$ to 0.44. In reference 131, the blade-root bending stiffness was reduced to achieve blade-flap frequencies (p = 1.125 to 1.28) more representative of typical hingeless rotors. For these tests both the cyclic controls and rotor shaft were harmonically excited for the frequency-response tests. The last series of tests (ref. 132), was intended to gather data for moderate and high rotor thrust levels at low to moderate advance ratios. Advance ratios included $\mu = 0$ to 0.5 and collective pitch ranged from 0° to 20°. Again, static and harmonic cyclic and shaft motion excitations were applied.

Static inflow model- One objective of these 7.5-ft model investigations was to verify a rotor-response analysis based on linear quasi-steady aerodynamics to predict the flapping response of a rotor blade in high-advance-ratio forward flight for low-lift conditions without stall or compressibility. Measured data from static control response derivatives (thrust and hub moment coefficients, C_T, C_L, C_M, with respect to collective and cyclic pitch, θ_o, θ_s, θ_c) were compared to a rotor-blade flapping response analysis including several elastic flap bending modes, linear quasi-steady aerodynamics with reversed-flow effects, and a harmonic balance solution procedure retaining an arbitrary number of harmonics (ref. 133). Comparisons of data and theory revealed very substantial quantitative and qualitative differences, especially at low advance ratios. Those differences could not be explained in terms of any known modeling errors and led to consideration of the effects of induced inflow.

The results of these investigations were reported by Ormiston and Peters (ref. 134). First, the steady-state momentum theory inflow models of Sissingh, Curtiss, and Shupe were formulated in terms of matrix equations to relate perturbations in the inflow gradients to perturbations in the thrust, roll moment, and pitch moment of the rotor. These perturbation inflow gradients characterized in a relatively simple way the complex nonuniform induced-velocity field of a lifting rotor. They represent a time- and space-averaged measure of the mean, lateral, and longitudinal gradients of the rotor-induced inflow distribution. This inflow model takes the form of a diagonal matrix of coupling coefficients, the L matrix, that was easily combined with the rotor-blade response analysis of reference 133. In hover

$$\begin{Bmatrix} d\lambda_0 \\ d\lambda_s \\ d\lambda_c \end{Bmatrix} = \frac{1}{2\nu}[L] \begin{Bmatrix} dC_T \\ -dC_L \\ -dC_M \end{Bmatrix}_{aero} \quad \text{where} \quad [L] = \begin{bmatrix} 1/2 & 0 & 0 \\ 0 & -2 & 0 \\ 0 & 0 & -2 \end{bmatrix} \tag{1}$$

and where ν is the mean induced inflow of the rotor.

This model was then incorporated in the flapping response analysis described in reference 134. As shown in figure 13, it brought the theoretical predictions and experimental data into excellent agreement for the hover condition. The effect of the inflow on the rotor moment response derivatives is simply a result of the fact that a perturbation thrust is accompanied by a like perturbation in inflow. For example, increased blade pitch increases rotor thrust which increases inflow, reducing the angle of attack, and thereby reducing a part of the original thrust increase. This effect reduces the rotor thrust derivative. The same effect occurs for rotor pitch and roll moments. Since the sensitivity of inflow perturbations is inversely proportional to the mean rotor inflow, the effect illustrated in figure 13 is much more pronounced at low rotor thrust than at high rotor thrust. The momentum theory concept works well in hover where the distribution of inflow perturbations corresponds closely to the distribution of rotor-blade lift perturbations. This situation does not hold in forward flight and the simple diagonal L-matrix was not nearly as successful in correlating with the experimental data. This led to the search for a more general L-matrix that would include off-diagonal coupling between inflow and loads.

Simple vortex models postulated in reference 134 were more successful than momentum theory but the best result was a numerical empirical model for the L-matrix generated by a parameter identification process to provide the best fit for the measured rotor derivatives. Figure 14 shows the measured rotor control derivatives in forward flight compared with the two different inflow models: momentum theory and the empirical model. As noted above, momentum theory is not satisfactory for forward flight, whereas the empirical model gives good results, confirming the utility of the general L-matrix form of the inflow model. It may be seen that the

effects of inflow are most pronounced at low advance ratios. Again it is noted that these results are for the nonlifting rotor condition.

To illustrate the effect of thrust and advance ratio on the sensitivity of rotor derivatives to the steady-state perturbation inflow model, figure 15 shows a typical hub-moment derivative calculation with and without the inflow. The mean inflow ν is a measure of the rotor thrust. In hover, the hub-moment derivative vanishes for zero thrust ($\nu = 0$). In forward flight the effect of inflow decreases with advance ratio.

Dynamic inflow model- Although an understanding of the effects of induced inflow on rotor response was not one of the original objectives of the Lockheed experimental program, the results were significant for hingeless rotors with large control derivatives and their important role in vehicle response and handling qualities. The effect of induced inflow on articulated rotor control characteristics received little attention because articulated rotor hub moments are small to begin with. Beyond the effects on stability and control, the effects of inflow were the subject of considerable speculation regarding air and ground resonance stability. It was theorized that air and ground resonance stability of hingeless rotors benefited substantially from the high rotor flap-damping characteristic of hingeless-rotor blades. It was further speculated that loss of rotor damping at low rotor lift (analogous to reductions of hub-moment derivatives) might therefore degrade the ground resonance stability of hingeless-rotor helicopters. Because ground resonance is a dynamic phenomenon, it was also postulated that such a reduction in rotor flap damping at low rotor thrust might not occur for unsteady motions at the ground-resonance frequencies. Therefore, it was of interest to determine the transient response characteristics of the perturbation inflow mode.

At this point Peters developed a formulation to model the transient response of the static inflow model (ref. 135). He assumed that the inflow perturbations would respond with a first-order time lag to perturbations in the rotor airloads. This is equivalent to postulating an apparent mass for the air, where the inertia of the air mass prevents the static perturbation inflow from establishing itself instantaneously in response to rotor airload perturbations. Combining the static inflow model with the apparent mass terms, Peters set forth the inflow model now known as dynamic inflow theory.

$$\begin{bmatrix} K_m & 0 & 0 \\ 0 & -K_I & 0 \\ 0 & 0 & -K_I \end{bmatrix} \begin{Bmatrix} d\dot{\lambda}_o \\ d\dot{\lambda}_s \\ d\dot{\lambda}_c \end{Bmatrix} + V [L]^{-1} \begin{Bmatrix} d\lambda_o \\ d\lambda_s \\ d\lambda_o \end{Bmatrix} = \begin{Bmatrix} dC_T \\ -dC_L \\ -dC_m \end{Bmatrix}_{aero} \tag{2}$$

The apparent mass K_m and apparent inertia K_I were taken from potential flow solutions for impermeable disks. This formulation for the apparent inertia terms

was a generalization of the approach used by Carpenter and Fridovich (ref. 128) to model the unsteady uniform inflow for a rotor with unsteady thrust response. In equation (2), a mass-flow parameter, V, allows the L-matrix to be applied for combinations of thrust (ν), climb (λ), and forward flight (μ)

$$V = \frac{\mu^2 + (\lambda + \nu)(\lambda + 2\nu)}{\sqrt{\mu^2 + (\lambda + \nu)^2}} \tag{3}$$

Peters also developed a complex lift-deficiency function (for roll and pitch) that included the time-delay effects. That function involves a reduced frequency based on the steady inflow velocity. This established the strong relationship between dynamic inflow theory and other theories of unsteady aerodynamics.

The Peters dynamic inflow model was first correlated with experimental data obtained by Hohenemser and Crews. Here the blade pitch of a small two-bladed hovering rotor model was harmonically excited in the rotating system. The resulting blade flapping was measured over a wide range of frequencies. Crews et al. (ref. 136) compared the results calculated using the dynamic inflow theory with measured data as shown in figure 16 and confirmed the excellent representation provided by the very simple dynamic inflow formulation although they used time-constants chosen to give a best fit with the data instead of the K_M and K_I values of Peters.

More extensive correlations were carried out by Peters, with the 7.5-ft-diam Lockheed model-rotor data further confirming the success of the dynamic inflow theory in representing the perturbation wake effects over a wide frequency range in hover and forward flight (ref. 135). Typical hover results presented in figure 17, are based on the measured data from references 130 and 131; they show that the contribution of static inflow alone is adequate at low frequencies but actually worsens the correlation at higher frequencies. At higher frequencies, predictions without any perturbation inflow are better than including static inflow alone. Adding the apparent mass effects to static inflow corrects the prediction at higher frequencies without appreciably influencing the results at low frequencies. The full dynamic inflow model thus provides a very satisfactory result over the full range of frequencies. Similar results are observed in forward flight as shown in figure 18; here the static inflow is based on the empirical inflow model.

In addition to the investigations based on the 7.5-ft model-rotor data, Hohenemser and his associates carried out extensive experimental studies of dynamic inflow under AFDD support. Although the original intent was to study rotor-blade flapping response to stochastic excitation, it was evident that the results of basic frequency response tests did not agree with theory, as noted previously. Hohenemser and Crews presented results in both hover and forward flight for the flapping response to harmonic blade pitch excitation of a 16-in.-diam torsionally rigid, two-bladed model rotor (ref. 137). Progressing and regressing cyclic pitch excitation was accomplished by a unique variable-frequency pitch-control mechanism in the rotating system that avoided free-play problems of conventional swashplate, actuators, and pitch-link mechanisms in the nonrotating system. This mechanism also

permitted excitation of progressing and regressing blade flapping over a wide frequency range. Test data were obtained in hover and advance ratios up to 0.8, for low to moderate values of collective pitch. A description of the two-bladed model and initial test results were also reported by Hohenemser and Crews (ref. 138).

As discussed above, these data were compared with dynamic inflow theory in reference 136. Hohenemser and Crews obtained additional data for a four-bladed rotor model in hover and forward flight, including hot-wire measurements of the unsteady downwash in the hover condition (ref. 139). Since the solidity of the four-bladed rotor was larger than that of the two-bladed rotor, the effects of dynamic inflow were also larger. Further measurements of unsteady downwash were obtained in reference 140.

Hohenemser and his associates also introduced the use of formal parameter identification theory to determine the inflow gains and time-constants associated with the dynamic inflow mode (refs. 141-147). These techniques were based on measurements of transient response obtained from the small-scale rotor model following modifications to the cyclic pitch excitation system. The identified coefficients for the inflow model were in very close agreement with momentum theory in hover. Identification of forward flight inflow parameters was not as successful as in hover, a result of the inability to excite collective modes.

Refined theory- The next significant refinement of dynamic inflow was the development of a rigorous aerodynamic formulation for the steady-state forward flight perturbation inflow model, the L-matrix. Although the empirical model was accurate and quite satisfactory for the rotor in edgewise flow and low rotor lift, it did not extend to very low advance ratios and, therefore, could not transition continuously to hover. Furthermore, it lacked a rigorous theoretical basis and suffered numerical singularities at certain advance ratios.

For these reasons researchers began to pursue more satisfactory alternatives. For a simplified aerodynamic formulation, such as dynamic inflow, an actuator disk theory was considered an appropriate basis on which to develop a more rigorous formulation. Following early NASA research (e.g., ref. 148) on actuator disk vortex theory models, Ormiston represented the rotor loading as a series of azimuthal and radial distributions of bound circulation (ref. 149). The Biot-Savart law was used to determine induced inflow influence coefficients associated with each circulation function. With a sufficient number of circulation functions, the L-matrix could be determined. This approach was not carried to completion and the solution to the problem awaited the efforts of other investigators. Mangler had previously calculated the induced flow for an actuator disk representation of a rotor (ref. 150). He used the potential-flow solution discovered by Kinner, who represented the aerodynamic loading of a circular disk by a complete series of radial and azimuthal pressure functions. Joglekar and Loewy, extended the Mangler work and evaluated the induced inflow for additional pressure functions. (ref. 151).

Using Joglekar and Loewy's work as a basis, Pitt and Peters successfully developed a rigorous, elegant, and practical L-matrix for dynamic inflow theory (refs. 152-154). They found that the Kinner potential functions would yield the

matrix coefficients analytically in closed form as a function of advance ratio and disk angle of attack. These coefficients were applicable for any advance ratio and at any disk angle of attack. Furthermore they extended the Kinner theory to the unsteady case and showed that under the assumption that velocities are mutually in phase, the exact potential-flow theory takes on a form identical to the dynamic-inflow theory of equation (2). The apparent-mass terms depend on the spanwise lift distribution but agree with those for an impermeable disk for the simplest distributions. The L-matrix is the closed-form static inflow result and is insensitive to the details of lift distribution. The Pitt-Peters dynamic inflow theory is given by

$$\begin{bmatrix} \frac{128}{75\pi} & 0 & 0 \\ 0 & \frac{-16}{45\pi} & 0 \\ 0 & 0 & \frac{-16}{45\pi} \end{bmatrix} \begin{Bmatrix} \dot{\lambda}_o \\ \dot{\lambda}_s \\ \dot{\lambda}_c \end{Bmatrix} + V \begin{bmatrix} 1/2 & 0 & \frac{15\pi}{64}\sqrt{\frac{1-\sin\alpha}{1+\sin\alpha}} \\ 0 & -\frac{4}{1+\sin\alpha} & 0 \\ \frac{15\pi}{64}\sqrt{\frac{1-\sin\alpha}{1+\sin\alpha}} & 0 & -\frac{4}{1+\sin\alpha} \end{bmatrix} \begin{Bmatrix} d\lambda_o \\ d\lambda_s \\ d\lambda_c \end{Bmatrix} = \begin{Bmatrix} dC_T \\ -dC_L \\ -dC_M \end{Bmatrix}_{aero}$$

where V is given by equation (3) and α is the wake angle of attack at the rotor disk. In hover ($\alpha = 90°$), the theory reduces identically to momentum theory and in edgewise flow ($\alpha = 0°$) it takes on a structure very similar to that of the empirical model. At intermediate disk angles, the L-matrix of equation (4) agrees with results extracted from a prescribed-wake discrete vortex element analysis.

The Pitt-Peters dynamic inflow model was exensively compared with experimental data by Gaonkar and Peters (ref. 155) using the original data of references 129-131, including data not used in the previous correlations. Figure 19 shows typical comparisons for static derivatives and although the Pitt-Peters does not agree quite as well as the empirical model, it represents the major physical effects very well. Figure 20 gives a typical correlation of unsteady data for rotor response in forward flight.

Effects of dynamic inflow on rotorcraft stability- As described above, dynamic inflow is a relatively simple model of the unsteady aerodynamics of the rotor wake that is suprisingly effective and accurate in representing the static and low-frequency dynamic inflow response phenomena. Since the theory is expressed in a time-domain differential-equation form it is a simple matter to incorporate it into rotorcraft stability analyses. A number of these investigations have provided further understanding of the nature of dynamic inflow in addition to demonstrating improvements in prediction accuracy available by including dynamic inflow effects. It may be noted that using such an approach constitutes an approximation for the more rigorous finite-blade (as opposed to an actuator disk), three-dimensional unsteady aerodynamic theories discussed in previous sections. In effect, dynamic inflow theory in conjunction with quasi-steady aerodynamics for the rotor blade airloads represents a low-frequency approximation to Loewy theory.

As noted, dynamic inflow theory is easily incorporated in rotorcraft dynamic analysis. Ormiston studied the effect on rotor flap dynamics; flap damping was greatly affected at low rotor thrust and the effect varied significantly between the regressing, collective, and progressing modes (ref. 156). The dynamic inflow model introduces additional degrees of freedom, leading to inflow modes similar to augmented states found in other finite-state unsteady aerodynamic theories. Peters and Gaonkar found similar results for rotor flap-lag stability in forward flight (ref. 157). Although dynamic inflow mainly influences the rotor-blade flap modes, coupling between blade flap and lead-lag motions results in a secondary effect of dynamic inflow on lead-lag damping. It was found as a result that the rotor regressing lead-lag mode was significantly influenced by dynamic inflow.

In another investigation, Bousman encountered significant discrepancies between theory and small-scale model experimental data for damping of coupled rotor-body roll and pitch-mode damping at low rotor thrust conditions (ref. 158). It was postulated that these low measured damping levels were attributable to the effects of dynamic inflow for reasons similar to rotor-response results shown above. Gaonkar et al. performed coupled rotor-body stability analyses including dynamic inflow and confirmed the hypothesis (ref. 159). In addition, the effects of dynamic inflow also accounted for anomalies in regressing lead-lag damping of ground- and air-resonance modes noted in Bousman's results. Subsequently, Johnson (refs. 160,161) presented predictions of coupled rotor-body frequencies with and without dynamic inflow and compared them with Bousman's data as shown in figures 21(a) and 21(b).

For rotor speeds above 400 rpm, predictions of regressing inplane mode frequency (ζ_R) without dynamic inflow correlate well with data in figure 21(a). Correlation of predicted body-roll-mode frequency (Φ) is fair but predictions of body pitch (θ) and flap regressing (β_R) modes are poor. However, when dynamic inflow is included (fig. 21(b)), all of the calculated frequencies agree with the experimental data. Of particular interest is the branch labeled λ. The analysis identified this as a coupled inflow and flap regressing mode dominated by the inflow degrees of freedom. These important results show that in effect, the inflow model completely changes the character of the coupled rotor-body dynamics for this configuration. Thus, one would not expect to be able to predict rotor-body dynamics without dynamic inflow.

Several additional works on dynamic inflow might be noted. Gaonkar et al. (ref. 162) and Nagabhushanam and Gaonkar (ref. 163) investigated the properties of extended dynamic inflow models, including a 5×5 L-matrix in place of the 3×3 L-matrix described above. The 5×5 L-matrix model included second-harmonic cyclic inflow degrees of freedom and associated second-harmonic components of the rotor airload distribution. It was found that if the number of inflow degrees of freedom exceeded the number of blades in the rotor, inconsistent results for rotor dynamic characteristics would be obtained. Later work indicated that the inconsistency was due to an incorrect assumption regarding the radial distribution of lift for the second-harmonic airload.

More recent developments include the extension of dynamic inflow theory into a higher frequency range. The original work of Pitt and Peters allowed for an arbitrary number of harmonics of induced flow, although only two were used. As shown by Gaonkar and Peters in reference 164, it now appears that by including additional harmonics, the theory of dynamic inflow will automatically include a three-dimensional version of Loewy theory (for hover and forward flight) which implicitly includes a near-wake approximation to the Theodorsen function. Correlations with data showed that the new theory is superior to former unsteady theories for all cases considered.

Significant progress has been made in development, validation, and application of rotor dynamic inflow theory. It offers an efficient and effective tool for expanding capabilities in analyzing rotorcraft aeroelastic stability.

SOLUTION METHODS

This section addresses Army-NASA contributions to the development of methods for solving rotorcraft aeroelastic stability equations. The following material deals with automated equation derivation, solution of the dynamic equilibrium equations, and stability solutions using both Floquet theory and perturbation methods.

Automated Symbolic Manipulation

A relatively recent development in rotorcraft aeroelastic stability is the application of symbolic manipulation programs to derive rotorcraft equations of motion. Because of the complexity of the equations of motion for even a moderately sophisticated rotorcraft model, derivation of the equations by hand is a tedious, time-consuming, and error-prone process. With this stimulus some very promising work has been carried out to automate the derivation of rotorcraft equations of motion. Nagabhushanam et al. described a self-contained FORTRAN IV symbolic processor, HESL (Helicopter Equations for Stability and Loads) that is capable of both deriving and solving rotorcraft stability equations (ref. 165). In contrast to general-purpose manipulations such as FORMAC or MACSYMA, HESL is specifically designed for rotorcraft applications. This processor derives state equations for a given ordering scheme, including energy expressions, generalized aerodynamic forces, the Lagrangian formulation, linear perturbation equations, and the multiblade coordinate transformation. It also carries out the subsequent numerical computations to determine system stability. A flowchart for these processes is shown in figure 22. This processor was used by Reddy (ref. 166), Reddy and Warmbrodt (ref. 167), and Reddy (ref. 168) to treat the flap-lag-torsion stability of an elastic blade, including dynamic inflow, in hover and forward flight. The numerical results, compared with previously published results, indicated the powerful capability represented by this approach. Typical results shown in figure 23 (from ref. 166,293) for flap-lag-torsion stability of an elastic hingeless rotor blade in hover are compared with results obtained using the Hodges-Dowell equations

(ref. 8). The lead-lag damping versus collective pitch shows small differences that Reddy (ref. 166), was able to relate to terms in the structural and aerodynamic operators of references 8 and 28.

A similar approach using MACSYMA was described by Crespo da Silva and Hodges, who investigated computerized symbolic manipulation to develop the equations of rotor-blade stability in forward flight and solved them using a multiple time-scales perturbation analysis (ref. 169). The derivation and the solution were both part of a single operation involving MACSYMA. Also, the equations used by Crespo da Silva and Hodges were derived by symbolic manipulation, and portions of the computer program used to solve the equations were output from MACSYMA (ref. 31).

Solution for Dynamic Equilibrium

In general, many rotorcraft aeroelastic stability problems are governed by nonlinear equations. However, for many important cases, it is desirable to determine the stability characteristics from linear perturbation equations of motion about a steady-state equilibrium solution of the nonlinear equations. In the hover condition, the nonlinear equilibrium solution is generally constant and the linear perturbation equations are constant-coefficient, ordinary differential equations. In the forward flight condition, the nonlinear equilibrium solution is generally periodic in time (dynamic equilibrium) and the linear perturbation equations have periodic coefficients. In either case, standard eigenanalysis or Floquet analysis techniques are available to determine stability characteristics. The solution for the steady-state dynamic equilibrium solution is not as straightforward.

There are actually two tasks involved in the determination of the dynamic equilibrium solution. First, even if the rotor collective and cyclic pitch controls are known, there is the problem of finding the periodic solution to a set of nonlinear differential equations with periodic coefficients. This is complicated by the fact that the periodic solution may not be stable. The second problem is that the blade controls are generally not known a priori. Instead, the analyst is supplied with a set of trim constraint equations (e.g., six components of force and moment equilibrium) that must be satisfied. Therefore, the second response problem is to find the unknown controls (an inverse problem), as well as the periodic response associated with the unknown controls such that the vehicle satisfies the trim constraints. Over the past 10 years, considerable government-funded work has been directed at these important issues. This work has resulted in a number of solution strategies for both the periodic solution (response) and the trim-control solution.

The periodic response problem is reviewed first. For the hover case, this is a static response which can be solved by Newton-Raphson or other nonlinear equation solvers; for example, as in references 6 and 15. In forward flight, however, the problem is dynamic response. The most fundamental solution strategy is that of simple time-marching. Gaonkar et al. showed that Hamming's modified predictor-corrector is among the most cost-effective marching algorithms (ref. 170). However, recent work by Panda and Chopra has also shown that finite elements in time can also be competitive, provided they are correctly formulated in a bilinear-operator

notation (ref. 171). The problem with time-marching of any kind, however, is that it becomes cumbersome as damping decreases; and it is not feasible at all for unstable systems. This is because time-marching will not converge to an unstable equilibrium. Therefore, other methods have been developed for the periodic-response problem that can generally be divided into two categories.

The first category is that of transition-matrix methods. These rely on the transition matrix, or an approximation to it, over one period of motion in order to iterate on the periodic equilibrium. For linear problems, convergence is assured provided there are no neutrally stable eigenvalues with integer-multiple frequencies. For nonlinear problems, the system is assumed linear in each iteration. Such methods have proven very robust in terms of finding the solution. The method of Schrage and Peters finds the eigenvalues and periodic eigenvectors of the approximate transition matrix and uses modal expansion to determine the response (ref. 172). The methods of Friedmann and Shamie (ref. 173), Friedmann and Kottapalli (ref. 174), and Panda and Chopra (ref. 171) use the transition matrix in a convolution integral to generate the linearized response in each iteration. A similar method, called periodic shooting, used by O'Malley et al. in reference 175, gives numerically identical results but without the need for convolution or expensive eigenanalysis. A good review of transition-matrix methods is given by Friedmann (ref. 176).

The second category of methods for the periodic-response problem is that of harmonic balance techniques. These place the equations in the frequency domain before solving and, as with transition-matrix methods, they assume a linear solution within each iteration (ref. 177). The robustness of these methods depends critically on the extent to which nonlinearities are linearized and placed on the left-hand side of the equations. Strategies that include only inertial terms on the left-hand side often fail; and strategies that linearize all terms are very robust.

Methods of trim solution will now be addressed. Trim strategies can generally be divided into three categories. The first category is that of algebraic trim equations which must be solved along with the response. In some cases, these are from simplified equtions and can be solved in closed form (ref. 178). In other cases, these equations come naturally from a full harmonic balance and must be solved iteratively. A second category of solution strategies is Newton-Raphson iteration. Here, no explicit equations are developed, but controls are adjusted based on numerically determined improvements in the constraint conditions. This has been the most widely used method for large, production analysis codes: O'Malley et al. (ref. 175) and Johnson (ref. 94). However, the method is not robust and often fails to converge. To combat this, analysis codes often apply the iteration only to a simplified set of rotor equations. Thus, the system is often not truly trimmed. The third category of strategies is that of auto-pilot equations (ref. 179). Here, a controller is designed to continuously monitor equilibrium conditions and update the pilot controls accordingly. Gains and time-constants are critical; and sometimes an adaptive controller is needed.

The government-sponsored research referenced above has not only developed the techniques listed, but it has also applied them to a large class of rotor

problems. These applications have led to the conclusions listed above and have identified natural matches between methods. For example, the automatic pilot is ideally suited to time-marching techniques (ref. 179), and the Newton-Raphson technique for controls is ideally suited for combination with periodic shooting (ref. 180). Furthermore, each of these two combinations has a set of problems (depending on damping and order) for which it is optimal. Algebraic equilibrium equations are naturally amenable to the harmonic-balance method, and these are useful in problems of rotor-body coupling or when the aerodynamics are in the frequency domain. Thus, the government-sponsored research in response and trim has developed to the point that the new methods can be applied to practical problems.

Stability Analysis

In the hover condition for constant-coefficient equations of motion, stability is normally determined from the characteristic roots obtained from standard eigenanalysis techniques. Hodges presents a simplified algorithm for determining stability when it is not necessary to evaluate all of the eigenvalues of a system of linear equations (ref. 181). This method is computationally advantageous for cases in which stability must be determined for a large number of system parameter values as might be the case in constructing stability boundaries.

In the forward flight condition, and in hover with unsymmetric or two-bladed rotors, the linear stability equations have periodic coefficients. Many investigators have pursued solutions for this important problem in rotorcraft dynamics. Although supported in part by the results of previous investigators, Peters and Hohenemser carried out the first extensive application of multivariable Floquet theory to problems of rotorcraft aeroelastic stability, primarily the flapping stability of a single rigid blade in forward flight (ref. 182). Peters generated the Floquet transition matrix by numerical integration of the equations of motion for one period, and then determined the corresponding eigenvalues and eigenvectors. Following publication of this work, many investigators began to apply Floquet theory to rotorcraft aerelastic stability problems. Some of the subsequent work was intended to reduce the computational cost of generating the Floquet transition matrix. Friedmann and Silverthorn applied an approximate method developed by Hsu, a generalization of the rectangular ripple method, to substantially reduce the computational time for Floquet analysis (ref. 183). Hammond developed a refined version of the numerical integration technique of Peters that required only a single-pass integration of the equations for one period, rather than n integrations for an n-order system (ref. 82). Both these methods are also described by Friedmann et al. (ref. 184). Further discussion of this subject is contained in Gaonkar et al. (ref. 170) and Friedmann (ref. 176).

Perturbation Methods

Perturbation methods have been applied to a number of problems in rotorcraft dynamics and are the object of continuing research. Use of perturbation methods has

typically fallen into two categories. First there is the use of perturbation methods in the space domain to approximate vibration frequencies, mode shapes, and buckling behavior of rotating beams. The significance of this work is mainly in the results. Peters was able to derive approximate, closed-form solutions to the free-vibration frequencies and mode shapes for uncoupled flap, lag, and torsion of rotating, elastic cantilever blades (ref. 185). Hodges later extended this work to include blades clamped off the axis of rotation (ref. 186). This work was also extended by Peters and Hodges to obtain simple, closed-form expressions for the inplane buckling of rotating beams (ref. 187).

The second category is the use of perturbation methods in the time-domain to obtain information about the response and stability. Tong (ref. 188) and Friedmann and Tong (ref. 189) used perturbation methods to study nonlinear flap-lag dynamics of rigid and elastic blades in hover and forward flight. Johnson used perturbation methods to study the flapping stability of rigid blades in forward flight (refs. 190-193). Crespo da Silva and Hodges also investigated the application of perturbation techniques to rotor-blade stability in forward flight (ref. 169). The significance of this latter work is that it has the potential to bypass Floquet theory, making use instead of analytical techniques such as the method of multiple time-scales. Such methods tend to become intractable by traditional manual approaches. However, when coupled with powerful, general-purpose symbolic manipulation programs such as MACSYMA it becomes a practical tool. This method is yet to be fully developed for general rotor-blade analysis, however.

3. INVESTIGATIONS OF AEROELASTIC STABILITY CHARACTERISTICS

The previous section described the development of methods to analyze and predict the aeroelastic stability of a variety of rotorcraft configurations in various operating conditions. Although methods in themselves tell little about rotorcraft behavior and stability characteristics, they may be used to generate such information. In this section, the results of Army-NASA investigations to study and identify such behavior and stability characteristics will be described. Such investigations may involve parametric analyses using the prediction methods described in the previous section, experimental testing to explore rotorcraft stability characteristics, or correlations of theoretical predictions and experimental data to check underlying assumptions and validate the theory. All of this is important because advancing rotorcraft technology is a difficult process, and it requires a thorough understanding of the fundamental physical behavior of rotorcraft aeroelastic stability, whether obtained through analysis or experiment, and it requires a high level of confidence in theoretical prediction capability that can only be achieved by careful checking of theory against experimental measurements.

In this section the material is divided into somewhat arbitrary categories, isolated blade-flapping stability, isolated blade flap-lag stablity, isolated blade flap-lag-torsion stability, coupled rotor-body stability, bearingless-rotor stability, tilt-rotor aircraft stability, and an analysis correlation effort undertaken in

connection with the ITR/FRR Project. In the section on flap-lag stability, material on the development of analysis methods for rigid-hinged blades has been included here instead of in section 2. In addition, the material on coupled rotor-body, bearingless rotor, and tilt-rotor aircraft stability is arranged differently from that in section 2.

FLAPPING STABILITY

The flapping stability of a rotor blade in forward flight is a basic problem of rotorcraft dynamics because it is one of the simplest systems on which to represent the effects of periodically varying aerodynamic damping and stiffness. Many investigators have addressed this problem, both to study methods of solving periodic-coefficient differential equations and to understand the stability characteristics of rotor blades described by such equations. Peters and Hohenemser significantly advanced this work both in their introduction of Floquet theory to solve periodic-coefficient equations and in clearly describing the complex forward flight behavior of a rigid blade with a flapping hinge (ref. 182). These results illustrated the existence of parameter regions (such as Lock number and advance ratio) where the characteristic roots exhibit natural frequencies of half or integer multiples of rotor speed, 0.5 or 1 per rev, that remain constant for an extended range of parameter values. This only occurs for constant-coefficient systems when the frequency is zero. Peters and Hohenemser presented numerous plots of damping contours in the Lock number-advance ratio plane illustrating the effects of pitch-flap coupling, flap hinge spring stiffness, and hub-moment feedback. A typical result shows regions of an 0.5 and 1 per rev natural frequency and the high advance ratio stability boundary (fig. 24).

Yin and Hohenemser studied the same stability problem after transforming the equations into multiblade coordinate form (ref. 194,195). They found that neglecting the periodic terms in these equations, a constant-coefficient approximation yielded results of acceptable accuracy for the low-frequency modes up to advance ratios of about 0.8. Hohenemser and Yin extended this work to include the effects of blade torsion and flap-bending flexibility on stability in forward flight (ref. 196). The effect of blade flexibility, in comparison with a rigid hinged-blade model, was shown to reduce flap-mode damping in forward flight, especially at higher advance ratios.

Johnson applied the perturbation method of multiple time-scales to the rigid flapping-blade problem in forward flight (refs. 190-193), confirming and clarifying some details of the results of Peters and Hohenemser. He developed approximate analytical expressions for the eigenvalues quite accurate for advance ratios up to about 0.5. Johnson also gave a comprehensive and detailed review of the many earlier studies of this problem before the work of Peters and Hohenemser (ref. 193). He also presented a thorough discussion of the dynamic behavior of the flapping blade in forward flight.

Biggers also investigated the accuracy of constant-coefficient approximations for this problem (ref. 197). Beginning with the forward-flight, blade-flapping equations in multiblade coordinate form, he showed that constant-coefficient approximation of these equations was reasonably accurate for moderate advance ratios up to about 0.5. This was considerably better than would be obtained for a constant-coefficient approximation of the isolated blade-flapping equations written in the rotating reference frame. Typical results of Biggers compare the variation of the flap-mode frequency with advance ratio for a constant-coefficient approximation of the multiblade flapping equations with exact Floquet analysis results (fig. 25).

Rogers studied blade-flapping stability in forward flight to examine dynamic stall effects; this work was discussed earlier in section 2. Finally, Crespo da Silva and Hodges used a computerized symbolic processor to perform a perturbation analysis of rigid, hinged, flapping-blade stability (ref. 169).

FLAP-LAG STABILITY

Analysis of rotor blade flap-lag degrees of freedom enables the researcher to investigate the most basic characteristics of cantilever rotor blades, including both hingeless and bearingless configurations. For articulated rotor blades, flap-lag dynamics are generally not important unless aeroelastic couplings are introduced in the blade-pitch control system. Although flap-lag analyses of hingeless rotor blades omit the important torsion effects and are, therefore, not generally of practical use, they do permit the underlying structural, inertial, and aerodynamic coupling of flap and lead-lag motions to be investigated with more clarity. Some of the earliest work in this field was carried out by Young who drew attention to nonlinear flap-lag coupling, generating some controversy in the process (ref. 198). Hohenemser and Heaton then studied the same problem and concluded that the effects of the nonlinearities could be adequately accounted for by linearizing the flap-lag equations for small-perturbation motions (ref. 199). At this point government researchers began to investigate these problems.

Hover Analytical Investigations

For investigations of flap-lag stability in the hover conditions, results of rigid-blade analyses are treated separately from results of elastic-blade analyses.

Rigid blade analyses- In keeping with increased interest in hingeless rotors, and a lack of information about such systems, Ormiston and Hodges initiated a study of flap-lag stability to gain a general understanding of their basic aeroelastic stability characteristics (ref. 3). They used the rigid-hinged-blade analysis of Hohenemser and Heaton (ref. 199) as a starting point. The flap-lag equations are fundamentally nonlinear, and a proper formulation for stability analysis requires linearization to derive small-perturbation equations of motion. Standard eigen-analysis then yields the characteristic roots that define stability of the small-

perturbation motions. Hohenemser and Heaton applied such a procedure, thereby improving on Young's original flap-lag analysis. In reference 3, Ormiston and Hodges refined the analysis of Hohenemser and Heaton, correcting an error in the linearization procedure of reference 199, and investigated the stability characteristics of hingeless rotor blades for a wide range of parameters. These investigations used the simplified, rigid blade with discrete spring-restrained hinges to represent the bending flexibility of a cantilever elastic blade as originally proposed by Young (ref. 200). This approach simplified the equations of motion and clarified the mechanisms that determined flap-lag stabiity.

Ormiston and Hodges extended this concept to provide a more complete representation of hingeless rotor blades, by introducing a double spring system to distinguish between the flexibility contained in the hub inboard of the pitch bearing and the flexibility contained in the blade outboard of the pitch bearing (fig. 26(a)). Thus the rigid-hinged blade model shown in figure 26(b) included two sets of flap and lead hinge springs, one set fixed inboard of the pitch bearing and a second set outboard of the pitch bearing and rotating with the blade as pitch angle changes. The parameter R, generally varying between 0 and 1, defined the hub-to-blade distribution of flexibility. When all of the bending flexibility is located in the hub and none in the blade, there is no structural flap-lag coupling and R = 0. When the flexibility is in the blade and not in the hub, R = 1, and the structural flap-lag coupling is roughly proportional to blade pitch angle. Combinations of hub and blade flexibility are represented by intermediate values of R according to a simple formula. Curtiss has also proposed additional versions of this hub and blade hinge spring model (ref. 201).

It should also be noted that for the rigid-blade model, the sequence of rotations of the rigid blade is defined by the chosen arrangement of physical hinges; in reference 3, a lag-flap sequence was chosen. This means that the flap hinge is radially outboard of the lead-lag hinge and moves with the blade during lead-lag motion. The kinematics of the flap-lag hinge sequence are slightly different and lead to small differences in the aeroelastic stability characteristics comnpared with the lag-flap hinge sequence, as will be addressed below. The effect of hinge sequence is much more pronounced when a discrete hinge is also included to represent torsion of an elastic blade.

The basic flap-lag stability characteristics of the rigid blade in hover were investigated in reference 3 and are illustrated in figure 27. For rotor blades having a flap hinge spring ($p > 1.0$), a flap-lag instability can occur when the lead-lag natural frequency is close to the flap frequency and when the flap frequency is near $(4/3)^{1/2}$. The nonlinear inertial and aerodynamic moments produce flap-lag coupling terms in the linearized perturbation equations that vary in proportion to blade-pitch angle. Thus the regions of instability in figure 27 expand as blade pitch increases. The simplified flap-lag equations were used by Ormiston and Hodges to develop several closed-form expressions to describe flap-lag stability characteristics and stability boundaries.

The results of Ormiston and Hodges showed the strong influence of flap-lag elastic coupling; for example, as the structural coupling parameter R increases,

the region of flap-lag stability in figure 27 shifts to higher lead-lag frequencies until it ceases to exist for practical configurations. Other results delineated the differences between stiff- and soft-inplane blade configurations (fig. 28). Soft-inplane configurations are generally stable, independent of structural flap-lag coupling, whereas stiff-inplane configurations typically exhibit flap-lag instability at some intermediate level of flap-lag structural coupling.

Flap-lag instabilities described are typically relatively weak; a small amount of structural damping is often sufficient to stabilize the blade. Blade-pitch couplings, however, may cause very large changes in flap-lag stability. Ormiston and Hodges included the effects of kinematic pitch-lag coupling with results shown in figure 29. For soft-inplane configurations, positive pitch-lag coupling (pitch up with lead) is destabilizing for all values of flap-lag structural coupling. The behavior of the stiff-inplane configuration is considerably more complex; depending on the flap-lag structural coupling, both positive and negative pitch-lag coupling may be destabilizing. Reference 3 also included blade precone, and it was found that although precone could be either stabilizing or destabilizing, its effect was not large for torsionally rigid blades. Ormiston attempted to identify aeroelastic couplings that would augment lead-lag damping to help control coupled rotor-body instabilities such as air and ground resonance (ref. 202). A combination pitch-lag and flap-lag elastic coupling was most effective in increasing the damping of the isolated blade at zero pitch.

Peters used the flap-lag equations of Ormiston and Hodges to derive approximate but useful closed-form analytical expressions for the lead-lag damping as a function of the various configuration parameters (ref. 203). He was also able to show that minimum stability occurs when the blade-tip motion moves along a straight line bisecting the blade chord and the direction of mean airflow velocity, the axis of minimum damping.

The rigid-blade flap-lag results of Ormiston and Hodges served to identify many of the basic characteristics of hingeless-rotor-blade aeroelastic stability, the nature of destabilizing aerodynamic and inertial flap-lag coupling, the important role of flap-lag structural coupling, the essential differences between soft- and stiff-inplane configurations, and how the important effects of pitch-lag coupling depend on flap-lag structural coupling and lead-lag natural frequency. Much of this behavior has been reflected in numerous subsequent works that have included blade elastic bending, torsion, forward flight aerodynamics, and rotor-body coupling.

As noted above, when a continuous elastic blade is modeled in an approximate way by using a spring-hinged rigid blade, the order of rotations about the discrete flap and lead-lag hinges will influence the geometric orientation of the blade in space. The influence of the flap and lead-lag hinge sequence on the stability of the system was investigated by Kaza and Kvaternik who compared the results obtained for the flap-lag sequence with results (fig. 27) obtained with the lag-flap sequence (ref. 204). The change in hinge sequence introduces a small effective pitch-lag coupling that alters the stability boundaries for low flap stiffness configurations as shown in figure 30.

As originally formulated by Young the rotor-blade flap-lag equations are nonlinear (ref. 198). However, it has been shown that the nonlinear aerodynamic and inertial terms are relatively weak and that the linearized solutions discussed above are usually satisfactory. Tong studied nonlinear flap-lag stability of the hinged rigid blade in references 188 and 205 and determined the regions of linear instability that would produce stable or unstable limit cycles, as shown in figure 31. He was also able to estimate limit cycle amplitudes of stable limit cycles using perturbation methods.

Elastic blade analyses- In addition to studying the flap-lag stability of the simplified rigid, spring-hinged representation of the elastic cantilever blade, Ormiston and Hodges also treated a uniform elastic blade, using a modal analysis method, and showed that with proper treatment of nonlinear aerodynamic and inertial coupling in the elastic blade equations, the two representations exhibit very similar behavior (ref. 3). Additional results were reported in reference 4.

Other investigators also studied the flap-lag stability of elastic blades in hover. In reference 5, Friedmann developed and solved the elastic-blade flap-lag equations, achieving results similar to those in reference 4, although flap-lag structural coupling was not included. In references 206 and 207, Friedmann examined the effects of mode shape on flap-lag stability and showed that the rigid blade with appropriate hinge offset would agree closely with elastic blade stability boundaries, as shown in figure 32. In references 206 and 208 Friedmann found that the effects of precone had a strong effect on flap-lag stability, although this was later found to be due to an extraneous term in the equations (ref. 209). Friedmann and Tong (ref. 189) also studied the nonlinear flap-lag stability of an elastic blade, using perturbation methods, again identifying regions where linear instabilities result in stable limit cycles; White also studied flap-lag stability of elastic blades in hover, using a collocation method of solution (ref. 210). His results, including the effects of flap-lag structural coupling, correspond to those in reference 4.

Further investigations of elastic blade flap-lag stability were carried out by Straub and Friedmann, using the finite-element method (refs. 62,64). Typical results in figure 33 show a comparison of flap-lag stability boundaries for the finite-element method, and a conventional modal method for a uniform elastic blade in hover. These results show the basic effect that flap-lag structural coupling shifts the region of flap-lag instability to increasingly stiff-inplane configurations as R increases from 0 to 1. Reddy compared elastic and rigid-blade models for flap-lag stability and also included the effects of dynamic inflow (ref. 166,168).

Effects of unsteady aerodynamics- Only limited investigation of the effects of unsteady aerodynamics on flap-lag stability have been carried out. Since flap-lag instability occurs at a low frequency, unsteady aerodynamics has not been considered important. Kunz (ref. 211) used Theodorsen and Loewy unsteady aerodynamic theories to calculate flap-lag stability of the rigid, spring-restrained hinged-blade model of a four-bladed rotor and showed moderately large effects, especially with Loewy theory, at larger blade-pitch angles, as shown in figure 34. More recently,

Dinyavari and Friedmann used a finite-state representation of Greenberg's unsteady aerodynamic theory to calculate flap-lag stability of the rigid-hinged blade model (ref. 113). Results shown in figure 35 indicate a moderate effect, roughly consistent with results of Kunz using Theodorsen unsteady aerodynamics.

Forward Flight Analytical Investigations

Early work on flap-lag stability of hingeless rotor blades in forward flight included the original work of Young (ref. 198). Tong and Friedmann also studied nonlinear flap-lag stability in hover and forward flight using perturbation techniques (refs. 188,189,207,208). In reference 189 they concluded that for moderate advance ratios the periodic coefficients in forward flight would not have a large effect on flap-lag stability unless the lead-lag frequency is near 0.5 or 1.0 per rev.

The analysis of flap-lag stability in forward flight only received serious attention after the utility of Floquet theory had been widely recognized. This afforded a practical means of dealing with linear periodic-coefficient equations of motion. However, the nonlinear properties of the flap-lag equations with reverse flow introduced some additional problems such as determining a periodic steady-state solution, satisfying the trim condition of the rotor, and obtaining linearized equations. Early investigations of flap-lag stability in forward flight were conducted by Friedmann and Silverthorn, using an elastic-blade model and a modal solution method (refs. 212-214). An approximate method was used to treat the reversed-flow region and a simplified trim procedure was used, based on the hover trim solution. Nevertheless, stability results were sensitive to several system parameters, including reversed flow, mode shapes, and flap-lag structural coupling. Typical results shown in figure 36 illustrate the effect of reverse flow on lead-lag damping.

An extensive investigation of hingeless rotor blade flap-lag stability in forward flight was conducted by Peters in (ref. 215). This study was based on the hinged, rigid-blade model having reverse flow and including contributions to the periodic coefficients arising from the steady-state blade response and cyclic pitch associated with specific forward flight trim conditions. Figure 37 illustrates the importance of different trim conditions on the variation of lead-lag damping with advance ratio. Figure 38 illustrates one of the unusual properties of periodic-coefficient systems. For configurations with lead-lag natural frequencies close to 1 or 0.5 per rev, instabilities may occur that exhibit the integer or half-integer frequencies characteristic of periodic-coefficient systems. For the flap-lag problem, these regions of parametric instability are quite restricted. Other configurations exhibit "conventional" instabilities; that is, the frequencies may take on any value.

Figure 39 summarizes the effects of flap-lag structural coupling on forward flight flap-lag stability and, as discussed previously, the stiff-inplane configuration is more sensitive to these effects than the soft-inplane configuration. These results illustrate the basic flap-lag stability behavior of soft- and stiff-inplane

rotor blades in forward flight. Peters also presented results showing the effects of pitch-flap and pitch-lag kinematic couplings on stability.

Kaza and Kvaternik (ref. 204) studied flap-lag stability of the rigid-hinged blade in forward flight, including approximating the periodic-coefficient equations with the constant-coefficient set obtained by transforming the blade equations in the rotating system to multiblade coordinate equations in the fixed system, and dropping periodic-coefficient terms, as Biggers did in reference 197 and as is shown in figure 25. The results, shown in figure 40 for the same case considered by Peters (fig. 39), illustrate that the collective and regressing lead-lag modes from the constant-coefficient equations are quite adequate up to relatively high advance ratios. A similar study was carried out by Gaonkar and Peters (ref. 216). Gaonkar and Peters investigated the effects of dynamic inflow on hinged-rigid blade flap-lag stability in forward flight (ref. 157). Lead-lag damping of stiff- and soft-inplane configurations is illustrated in figure 41; depending on the particular configuration parameters and the advance ratio, this unsteady aerodynamic effect may significantly alter the stability.

In reference 173, Friedmann and Shamie revisited the elastic-blade flap-lag stability problem in forward flight by considering more representative trim conditions and including the periodic equilibrium solution in the linearized stability equations. Their results, an example of which is shown in figure 42, confirmed the findings of Peters about the sensitivity of stability to the details of the trim solution. In a related work, Shamie and Friedmann studied the problem of flap-lag stability of a two-bladed teetering rotor in forward flight and compared the results with those of a single isolated blade (ref. 217).

Finite-element techniques have also been applied to the elastic-blade flap-lag problem in forward flight; typical results of Straub and Friedmann (refs. 63,64) are shown in figure 43. Here, both the first and second lead-lag mode damping are presented for a trimmed flight condition. Finally, Reddy and Warmbrodt calculated flap-lag stability of an elastic blade in forward flight, using modal equations and retaining two bending modes for each bending direction (ref. 218). The results, shown in figure 44 for soft- and stiff-inplane blades with and without flap-lag structural coupling, are for trimmed flight conditions and may be compared with rigid-blade results in figure 39. These results were developed using a symbolic processor to generate and solve the equations.

Flap-Lag Experiments in Hover and Forward Flight

A series of experiments using small-scale model rotors was conducted at the Aeroflightdynamics Directorate specifically to verify the results of analytical investigations of the flap-lag stability of simplified rigid-hinged-blade models in hover and forward flight. The flap-lag system does not represent a practical configuration since typical rotor systems generally exhibit varying degrees of pitch control and blade torsional flexibility. However, from a research point of view, the restricted flap-lag experiment greatly simplifies the process of correlating and interpreting analytical and experimental results. These experiments were designed

to minimize as many sources of error and uncertainty as possible in order to provide a clear test of the essential features of the flap-lag stability analysis. To this end the blades were designed to be as rigid as possible in bending and torsion. Flexures placed at the blade root to represent spring-restrained hinges were used to eliminate, as much as possible, the nonlinear damping of hinges and bearings. The hub-support system was designed to be sufficiently stiff to maintain a fixed hub, isolated-blade condition.

The experimental technique consisted of initiating transient lead-lag motions and measuring the decay rate to determine damping of the lead-lag mode. Figure 45 illustrates the hover test stand experimental apparatus and figure 46 the layout of the hub flexures used to simulate flap and lead-lag hinges. The straight flexures represented simple flap and lead-lag hinge springs; the skewed flexures provided, in addition, kinematic pitch-flap and pitch-lag aeroelastic couplings. Both the straight and skewed flexures could provide flap-lag structural coupling if they are rotated in pitch with the blade. Hover tests were performed using a two-bladed 5.5-ft-diam rotor.

The typical results in figure 47 are from Ormiston and Bousman (refs. 117,219, 220); they show the variation of lead-lag damping with blade-pitch angle for two different blade and hub configurations. The experimental results in figure 47(a) confirm the destabilizing effects of flap-lag aerodynamic and inertial coupling predicted by linear analysis. In addition, however, at high pitch angles the linear analysis fails to predict the abrupt onset of instability. This was subsequently determined to be due to airfoil stall that with suitable modification to the analysis, could be reasonably well predicted. The results in figure 47(b) illustrate a stiff-inplane configuration where the effects of stall were stabilizing. Another experimental investigation was aimed at confirming the effectiveness of aeroelastic couplings postulated by Ormiston (ref. 202) to enhance lead-lag damping of hingeless rotor blades. Results of Bousman et al. (ref. 221) shown in figure 48 illustrate how combined flap-lag structural coupling and pitch-lag coupling significantly increase the rotor-blade lead-lag damping.

Another flap-lag stability experiment to investigate intermediate values of flap-lag structural coupling ($R \approx 0.5$), using blades with distributed bending flexibility, was conducted by Curtiss and Putman at Princeton University (ref. 222), using the apparatus and rotor hub described above. Test results agreed well with analysis, even though the rigid-hinged-blade analysis was used to model the elastic blade.

Although a considerable amount of analytical research has been conducted on forward flight flap-lag stability, relatively little experimental research has been carried out. An extensive experimental study of flap-lag stability in forward flight was conducted at the Aeroflightdynamics Directorate and reported by Gaonkar et al. (ref. 223). A 5.5-ft-diam three-bladed model rotor (fig. 49) similar to that used for hover experiments described above, was tested up to a moderately high (0.55) advance ratio. In order to simplify operation and minimize nonlinear lead-lag damping of pitch bearings, the model did not have a swashplate. Collective pitch was changed manually and the rotor was trimmed to minimize steady-state blade

flapping by varying the angle of attack of the rotor shaft. The results in figure 50 show the variation in lead-lag damping with advance ratio for several shaft angles at 0° and 3° collective pitch. Agreement between data and theory is very good except for the high shaft angle condition at 3° collective pitch. The inclusion of airfoil stall improved the correlation for this case but degraded correlation for the other cases. The detailed mechanisms of the stall influence are not yet clear since the rotor is operating at moderate lift levels; however, large angles of attack do exist for some regions of the rotor disc.

These experiments have done much to help our understanding of the dynamic behavior of hingeless rotor blades and have provided a large body of high-quality rotor-stability data that is useful for confirming theoretical predictions.

FLAP-LAG-TORSION STABILITY

Flap-lag-torsion stability of cantilever rotor blades represents one of the important problems in rotorcraft aeroelastic stability. The effects of torsion generally tend to overpower the effects of coupled flap-lag structural dynamics. When blade torsion is coupled with flap and lead-lag bending, practical problems in aeroelastic stability of hingeless and bearingless rotor blades may be addressed. Articulated rotor blades are not strongly influenced by the structural bending-torsion coupling so important for cantilever rotor blades. Articulated rotor blades generally experience flap bending-torsion flutter, a result of unsteady aerodynamics and chordwise offsets of the airfoil mass, elastic, and aerodynamic centers (cf. ref. 224). Much of the research on cantilever blade flap-lag-torsion stability has focused on the effects of nonlinear bending-torsion structural coupling, as will be illustrated below. However, the chordwise aerodynamic offset couplings are also important for cantilever rotor blades and they, too, will be addressed.

Hover Analytical Investigations

Before aeroelastic analysis of cantilever rotor blades that are fully elastic in bending and torsion, a simpler problem was addressed by Friedmann and Tong (ref. 5). They studied the stability of cantilever blades flexible in flap and lead-lag bending and with rigid body root pitch motion restrained by pitch-link flexibility. Results also presented in references 207 and 208 by Friedmann show the strong effect of root pitch motion stability as shown in figure 51.

With the development by Hodges and Dowell (ref. 6,8) of the general nonlinear equations applicable to combined bending and torsion of elastic cantilever rotor blades as described above, means were available to investigate the dynamic stability characteristics of hingeless rotor blades. Many studies were devoted to analysis of simple blades having radially uniform properties to help facilitate understanding of the essential dynamic phenomena. Several early studies of this kind were carried out by Hodges (ref. 6) and by Hodges and Ormiston (refs. 15,17,225). Typical basic

results are shown in figure 52 (from ref. 225) where stability boundaries are plotted as a function of the torsion natural frequency, a measure of torsional rigidity.

These results illustrate how the introduction of blade-torsion flexibility progressively alters the stability of the simpler flap-lag bending problem. It may be seen that the effects of torsion are significant for some configurations even at quite high torsion frequencies. Also presented are results of calculations that include the bending-torsion structural coupling but omit torsion dynamics. In this case the bending-torsion coupling generates effective pitch-lag and pitch-flap aeroelastic couplings that control stability in a manner consistent with the results of the simple rigid-hinged blade flap-lag analyses discussed above. Only for very flexible blades does torsion dynamics significantly alter flap-lag-torsion stability, because most of the effect of torsion flexibility is due to structural coupling.

Because the torsion structural coupling is so powerful, small amounts of blade precone or droop, usually introduced to reduce steady blade stresses, can have a large effect on stability. Figure 53 illustrates the influence of precone for configurations with (R = 1.0) and without (R = 0) structural flap-lag coupling (ref. 15). At low rotor thrust, the steady blade bending counteracting the built-in precone produces a destabilizing pitch-lag coupling effect that causes a "precone instability." As thrust increases and the blade equilibrium deflection coincides with the precone orientation, the destabilizing coupling is removed, and stability returns. At higher rotor thrust, other instabilities may occur, especially for stiff-inplane configurations without flap-lag structural coupling. The effects of droop can be similar to precone. Droop is a built-in flap rotation of the blade outboard of the pitch bearing, whereas for precone the pitch bearing axis has the same built-in flap rotation as the blade and hence remains in alignment with it. The similarity between the effects of precone and droop is determined by the ratio of pitch-link stiffness to blade-torsional rigidity, f. Results in figure 54 (from ref. 17) compare the effects of precone and droop on flap-lag-torsion stability boundaries and show that depending on the value of f, precone and droop have identical or very different effects on the flap-lag-torsion stability boundaries.

In reference 226, Johnson presented results of a flap-lag-torsion stability analysis for comparison with the results of reference 15 in order to validate the analysis of reference 85. Good qualitative agreement was found.

Friedmann extended earlier results by investigating flap-lag-torsion stability of blades with elastic torsion, using improved equations (ref. 19). These equations retained root pitch motion and added flap-lag structural coupling and airfoil chordwise offsets. Results in figure 55 (from ref. 20) show the effect of aerodynamic center offsets on stability and divergence boundaries. Friedmann also showed that structural damping is moderately effective in eliminating the precone instability.

Reddy investigated flap-lag-torsion stability of elastic blades in hover, including the effects of dynamic inflow (refs. 166,168). His results were obtained using computerized symbolic manipulation to derive and solve modal equations for

elastic blades. This permitted an easy means of examining the influence of small terms in the equations of motion. Figure 56 illustrates the effects of dynamic inflow on lead-lag damping at a moderate collective pitch angle.

To deal with practical rotor-blade configurations, especially bearingless-rotor blades, more advanced structural analysis methods are needed and researchers have begun to address this area. Chopra and Sivaneri (ref. 66,67) applied finite-element methods to the elastic-blade flap-lag-torsion problem (fig. 57) and demonstrated close agreement with earlier modal-analysis results from reference 15. More advanced work by Hong and Chopra treated hingeless rotor blades constructed of composite materials (ref. 78). Using a finite-element method, they showed how aeroelastic tailoring of the spar ply layup configuration could stabilize or destabilize the lead-lag mode damping. A root locus plot shown in figure 58 illustrates these results.

There have been other applications of flap-lag-torsion aeroelastic stability analysis, including circulation control rotors by Chopra and Johnson (ref. 227) and constant-lift and free-tip rotors by Chopra (ref. 228).

Effects of Unsteady Aerodynamics

The effect of unsteady aerodynamics on flap-lag-torsion stability in hover has also been investigated. Pierce and White examined the effect of compressibility on flap-pitch flutter owing to Theodorsen and Loewy aerodynamics (ref. 229). Friedmann and Yuan (ref. 110) studied the influence of different unsteady aerodynamic theories on flap-lag-torsion stability, as shown in figure 59. These theories included classical incompressible unsteady aerodynamic theory such as Theodorsen and Loewy, compressible theories such as Possio, Jones, and Rao, in comparison with conventional quasi-steady theory. In some cases the influence of unsteady aerodynamics is small; in other cases it may be significant.

Flap-Lag-Torsion Hover Experiments

A number of experiments on flap-lag-torsion stability of hingeless rotors in the hub fixed condition have been conducted in order to validate analysis of cantilever rotor-blade stability. Sharpe (ref. 230) tested a 5.5-ft-diam two-bladed model rotor intended specifically to validate the theoretical analyses of references 16 and 17. The cantilever blades were designed to be uniform in mass and stiffness and with no chordwise offsets of aerodynamic or mass centers. Blade-root-to-hub attachments were designed to provide variations in precone, droop, and pitch restraint stiffness. An illustration of the model is given in figure 60. Typical lead-lag damping measurements are shown together with theoretical predictions in figure 61. The comparisons with theory reveal that the analysis is quite accurate at low pitch angles, whereas there are significant differences at higher blade pitch angles. These differences are attributed in part to airfoil stall effects magnified by the low test Reynolds number. Figure 62 demonstrates that the variations of

damping with precone and droop are accurately predicted for $\theta_o = 2°$ where airfoil stall effects are not present.

Another experimental investigation of flap-lag-torsion stability was conducted in the NASA Ames 40- by 80-Foot Wind Tunnel with a full-scale, four-bladed BO-105 soft-inplane hingeless rotor. Because of the size of the rotor test apparatus, the rotor-blade stability results were considered representative of a fixed hub condition. Warmbrodt and Peterson compared measured regressing lead-lag damping against the CAMRAD theory for varying numbers of elastic blade modes with and without dynamic inflow (refs. 59,231-233). The results shown in figure 63 illustrate that correlation is improved with the addition of additional modes and dynamic inflow.

Forward Flight Flap-Lag-Torsion Analysis

In the late 1960's, before development of strong interest in aeroelastic stability characteristics of hingeless rotor blades, an investigation of articulated-rotor instability at high speeds was sponsored by the Aviation Applied Technology Directorate. This study involved prediction and correlation with experimental data of articulated-rotor bending-torsion flutter (ref. 234); stall flutter (ref. 235); torsional divergence (ref. 236); and flapping and flap-lag stability (ref. 237). The predictions were obtained from stability analyses based on the equations derived by Arcidiacono in reference 2 which were also included as a part of the AATD-sponsored investigation. The bending-torsion flutter analysis used a classic fixed-wing approach; for the rotor in forward flight, a fixed azimuth approximation was used, holding aerodynamic properties constant corresponding to the particular azimuth being analyzed. The torsional divergence analysis was based on a similar assumption. Results emphasized the importance of airfoil aerodynamic center chordwise offset from the cross-section center of mass. Subsequent experimental investigations of Niebanck and Bain confirmed that the fixed azimuth assumption is very conservative (ref. 238). The flap-lag analysis of articulated-rotor blades, based on forced and transient response calculations, did not produce any unstable behavior in forward flight.

For the experimental investigation of reference 238, a 9-ft-diam, dynamically scaled, articulated-rotor model with several unbalanced chordwise center of mass positions was tested at speeds up to 300 knots and at advance ratios up to 1.0. A variety of unstable blade responses were encountered, including stall flutter, advancing-blade flutter, retreating-blade divergence, and flapping instability. The experimental results were compared with the analyses described above.

With the availability of Floquet theory and the increasing experience obtained from fully coupled flap-lag-torsion stability analysis in hover, government-sponsored researchers began to turn attention to the forward flight analysis of cantilever rotor blades. These studies were marked by progressive refinements in the analyses as the equations were improved and restrictive assumptions removed. Nevertheless it must be noted that this is a problem of considerable complexity. It involves determining the nonlinear trim state of a system of many degrees of freedom (if multiple modes for blade bending or torsion deflection are retained) in response

to unsteady excitation, obtaining linearized system equations, and performing a Floquet analysis. Some early results of Friedmann and Reyna-Allende (ref. 21) are shown in figure 64 for flap, lead-lag, and torsion-mode damping versus advance ratio. More refined results of Shamie and Friedmann (ref. 24) were based on equations derived from reference 22; the results are shown in figure 65. Differences in the results shown in figures 64 and 65 were attributed to the differences in the equations used in the two analyses. In general, the results of these two studies showed similar trends. Further investigation using multiple modes for bending and torsion deflections and improved solution procedures was carried out by Friedmann and Kottapalli in (ref. 174). Typical results for soft- and stiff-inplane configurations for both propulsive and moment trim conditions are shown in figure 66. These results again confirmed the general findings that stiff-inplane configurations are less stable than soft-inplane blades.

Reddy and Warmbrodt (ref. 168,218) also studied the flap-lag-torsion problem in forward flight and identified the effects of dynamic inflow and elastic coupling for soft- and stiff-inplane cantilever rotor blades as shown in figures 67(a) and 67(b). These results are in good agreement with those in figure 66, even though the blade parameters are not identical. The results of this investigation are unique in that they provide a clear and relatively complete picture of the aeroelastic stability behavior of hingeless rotor blades in forward flight. Furthermore, these results have been compared with work of earlier investigators, allowing some judgments to be made about the validity of the results when, as in the case of flap-lag-torsion stability of hingeless rotor blades in forward flight, appropriate experimental data are not available for correlation purposes.

COUPLED ROTOR-BODY STABILITY

An important class of rotorcraft stability problems arises from mechanical coupling between the rotor-system degrees of freedom and motions of the fuselage. This coupling gives rise to the classic ground resonance of articulated-rotor systems studied extensively by Coleman and Feingold (ref. 79) and others beginning in the early 1940's. With the emerging interest in hingeless rotors in the 1960's, mechanical instability began to receive renewed attention for configurations having lead-lag natural frequencies below rotor speed (soft-inplane). In the case of hingeless rotors, the strong rotor-body coupling generated by the cantilever blades significantly increased the complexity of the mechanical instability and created the potential for air resonance, as well as ground resonance. The work of Cardinale and his co-workers on the XH-51A Matched Stiffness Rotor helicopter (ref. 81), and of Lytwyn and Miao on the BO-105 (ref. 239) illustrate early efforts in aeromechanical stability. For stiff-inplane configurations, mechanical instability is not of practical concern; however the effects of rotor-body coupling may aggravate aeroelastic instabilities arising from blade or control-system characteristics. During the last 20 years, a significant amount of government-sponsored research on coupled rotor-body stability has been carried out, including analytical investigations and large- and small-scale experiments. This section will address coupled rotor-body

stability problems of conventional articulated and hingeless rotor helicopters. Rotor-body stability bearingless rotor and tilt rotor systems is discussed later in separate sections.

Analytical Investigations in Hover and Forward Flight

Under AFDD sponsorship, Hohenemser and Yin investigated the stability and response of coupled rotor-body systems with feedback controls in order to understand fundamental rotor-stability characteristics and identify means to reduce gust response in high-speed forward flight. Hohenemser and Yin studied the whirl dynamics of a flapping rotor coupled to a body with pitch and roll angular freedom and found that whirl instability could occur for some configurations at high advance ratio (ref. 196). In reference 240 they studied feedback control systems designed to improve response characteristics and gust response of hingeless rotors operating at high advance ratios without inducing aeroelastic instablities. Further studies of this type were conducted in references 241 and 242. Finally, Hohenemser and Yin investigated the stability of a flapping rotor on flexible supports using a finite-element formulation (ref. 61). Results showed how higher flap-bending modes could couple with support dynamics and influence stability of the coupled rotor-body system.

One important problem in the area of classic mechanical instability is the case of a rotor with one lag-damper inoperative. This asymmetric rotor problem gives rise to periodic coefficients in the equations of motion, even in the hover condition. Hammond treated this problem using both Floquet theory eigenanalysis and direct numerical integration (ref. 82). Typical results are shown in figure 68; they illustrate how the modal dynamic behavior increases in complexity and how the system can be destabilized as a result of losing one damper.

As noted above, hingeless rotorcraft mechanical instability is more complex than classical ground resonance. Early analyses of hingeless-rotor air and ground resonance were carried out in support of full-scale rotorcraft development programs; for example, the BO-105, XH-51, WG-13, and YUH-61A. However, there did not exist a clear understanding of the role of hingeless-rotor configuration parameters in determining aeromechanical stability. Aerodynamic damping acting through the hingeless-rotor flapwise hub moments was thought to counter air and ground resonance. The unsteady wake effects were not understood. Very little work had been done to study blade aeroelastic couplings; consequently, designers had little information to help make important design decisions.

In order to address these issues, government-sponsored analytical and experimental research was undertaken by the Army and NASA to develop a better understanding of this topic and thus help to design rotorcraft free of such instabilities. Ormiston carried out an extensive parametric investigation of hingeless-rotorcraft air and ground resonance using a simplified model consisting of a rigid-body fuselage and rigid-spring-restrained blades with flap-lag degrees of freedom (refs. 86, 87,243). Initial results were presented in reference 243. Typical results are shown in figures 69 and 70 (from ref. 86); they show the effects of rotor

aerodynamics and collective pitch on ground- and air-resonance stability boundaries for a wide range of configurations. The results indicate that hingeless-rotor aerodynamic damping is stabilizing for air resonance but that as flap stiffness increases, stability decreases (contrary to what might be expected).

The effectiveness of aeroelastic couplings to alleviate air-resonance instability was also investigated, as shown in figure 71. Although blade aeroelastic coupling can be very effective in many cases, it is difficult to alleviate mechanical instability over a wide range of operating conditions for a fixed set of configuration parameters. The results of this study revealed that aeromechanical instability of soft-inplane hingeless-rotor helicopters is indeed a very complex subject, even for the simplified physical model employed in the analysis. In another study, Ormiston explored in depth the detailed properties of the coupled rotor-body dynamic modes and how they influenced air resonance behavior (ref. 87).

Other investigators have studied the effects of dynamic inflow on hingeless-rotor air resonance. Since the aerodynamic damping resulting from cantilever blade-flap stiffness exerts a powerful influence on hingeless rotor dynamics, it would be expected that dynamic inflow might have a potentially significant effect on air resonance stability. Gaonkar et al. (ref. 159) extended the aeromechanical stability investigation of Ormiston to include dynamic inflow; a typical result is shown in figure 72. In this example air resonance was stabilized; in other results the opposite was shown to occur. Nagabhushanam and Gaonkar extended the rotor-body hover analysis to forward flight and studied the effects on stability of dynamic inflow models and trim methods, for soft- and stiff-inplane configurations (ref. 163). A typical result in figure 73 shows how strongly the trim condition influences coupled rotor-body stability in forward flight. In reference 244, Johnson also analyzed the aeromechanical stability of a soft-inplane helicopter in forward flight, using the equations developed in reference 85. Another approach receiving renewed attention is the use of feedback control to stabilize air resonance instability. Straub and Warmbrodt showed promising results using a relatively basic approach, with cyclic lag and body angular rate feedback to control cyclic pitch (ref. 245).

Venkatesan and Friedmann also studied coupled rotor-body stability of a multi-rotor hybrid airship (ref. 98,246).

Rotor-Body Experiments in Hover and Forward Flight

One of the first experimental investigations of rotor-body aeromechanical stability was conducted by Burkham and Miao at Boeing Vertol, using a 1/14th-scale, Froude-scaled model of the BO-105 helicopter (ref. 247). An important series of experiments was conducted at the Aeroflightdynamics Directorate by Bousman (refs. 158,248,249) to confirm analytical results obtained in reference 86 for hingeless-rotor aeromechanical stability. The resulting data, obtained for the hover condition using a 5.5-ft-diam model, are noteworthy for both quantity and quality and have been used in numerous aeroelastic correlations. Several rotor and body configurations were tested over a range of rotor speed and collective pitch for

different fuselage restraints and blade aeroelastic couplings. Frequency and damping were obtained for all measurable fuselage and blade modes. As in previous AFDD experiments, rigid-hinged blades with flap and lead-lag flexures were used. In addition a simulated in-vacuum condition was tested, using non-airfoil shaped stub blades.

Figure 74 shows the in-vacuum rotor configuration mounted on a motor-transmission gimbal frame structure that represented a fuselage with pitch and roll degrees of freedom. Frequency and damping results versus rotor speed for this model are shown in figure 75 (from ref. 249). Comparison with Hodges' FLAIR analysis (ref. 57) shows excellent correlation for the frequencies of four rotor and body modes and excellent correlation for lead-lag damping of the regressing lead-lag mode. This would be expected for a clean mechanical model without aerodynamic effects. These results confirmed that the physical model, configuration definition, test, and data analysis procedures were sufficiently refined to produce very high quality data.

The airfoil-blade rotor configuration, mounted on an improved fuselage frame having flex pivots in place of ball-type gimbal bearings, is shown in figure 76. In figure 77, a sampling of regressing lead-lag mode damping results from reference 158 exhibits very low data scatter and agrees well with predictions of the FLAIR theory. These results clearly confirmed trends predicted by earlier analyses for the basic effects of rotor speed that reduce damping at body pitch and roll frequency coalescences, the destabilizing effect of collective pitch, and the influence of aeroelastic couplings where damping is dependent on configuration. Systematic discrepancies between theory and measured results for some configurations indicate that not all phenomena are accurately accounted for; likely candidates were postulated to be unsteady aerodynamics, and possibly, blade flexibility.

Bousman's experimental results also led to new insights about the role of unsteady aerodynamics in low-frequency coupled rotor-body dynamics. The effects of dynamic inflow on coupled rotor-body modal frequencies were discussed above in section 2. The measured damping data also provided confirmation of suspected sources of discrepancies in body-pitch and roll-mode damping, as shown in figure 78 by calculations by Johnson with and without dynamic inflow (refs. 160,161). The effects of dynamic inflow on lead-lag regressing mode damping are shown in figure 79, where dynamic inflow marginally improves the agreement between analysis and data. Interestingly, Johnson's predicted lead-lag regressing-mode damping with dynamic inflow does not agree with the data as well as Bousman's prediction without dynamic inflow in reference 158, using Hodges's FLAIR analysis. This indicates that the prediction of aeromechanical stability may be rather sensitive to small details of the analysis. Friedmann and Venkatesan also correlated analyses with Bousman's data (refs. 250,251). They also confirmed the favorable effects of dynamic inflow on the correlation, and furthermore, in reference 250, their predictions of regressing lead-lag damping correlated well with data at high rotor-blade collective pitch angles where correlation was rather poor for the FLAIR analyses.

Other coupled rotor-body experiments have been carried out; Yeager et al. tested a hingeless-rotor research model in the Langley Transonics Dynamics Tunnel

for hover and forward flight conditions (refs. 252,253). Good correlation was achieved with predictions by the CAMRAD analysis.

BEARINGLESS-ROTOR STABILITY

The bearingless-rotor configuration, a refinement of the basic hingeless rotor, has been the subject of much development activity by the helicopter technical community and the focus of a significant amount of government research. The isolated bearingless-rotor blade encompasses all of the basic flap-lag-torsion aeroelastic stability characteristics of hingeless blades described above, as well as additional complications of the flexbeam and pitch control mechanisms. Because of the wide variations in different bearingless rotor configurations and the more pronounced effects of higher blade-bending modes, bearingless-rotor stability characteristics can be more difficult to understand or to generalize than those for hingeless rotor blades.

Since most of the applications have been soft-inplane configurations, many bearingless-rotor investigations have also treated air and ground resonance and thus included coupled rotor-body dynamics. It is, therefore, appropriate to survey both isolated rotor blade as well as coupled rotor-body studies, as a single topic in this section.

Bearingless-Rotor Stability Analysis

Bielawa carried out one of the first analytical investigations of bearingless-rotor aeroelastic stability using the G400 analysis described above to evaluate the stability of candidate full-scale bearingless rotors for application to the RSRA aircraft. Hover stability results were presented in reference 56 for soft- and stiff-inplane isolated (fixed hub) rotor-blade configurations having snubbed torque tubes. Instabilities were evident at high collective pitch angles, and these were aggravated by airfoil stall effects. The first three flap-bending modes, the first two edgewise-bending modes, and the torsion mode were highly coupled and led to very complex behavior.

Development of FLAIR by Hodges (described earlier in section under Helicopter Equation) was initiated to support the full-scale Bearingless Main Rotor (BMR) developed and flight tested on a BO-105 helicopter by Boeing Vertol under Army AATD sponsorship. The BMR development program is described in more detail in a later section. The simplified FLAIR analysis considered the blades to be rigid in bending and torsion, attached to a uniform stiffness flexbeam modeled by exact nonlinear bending-torsion equations for a continuous flexible beam. The rotor was attached to a rigid-body fuselage having pitch and roll degrees of freedom. Quasi-steady aerodynamic theory was used for the hover condition only. The FLAIR analysis was used by Hodges in reference 186 to identify the configuration parameters that would maximize the air and ground resonance stability of the BMR configuration

(ref. 58). The Boeing Vertol BMR configuration corresponds to Case II in figure 10. Parameters such as flexbeam and blade precone, droop, sweep, and flexbeam pre-pitch were studied. Air resonance was easily stabilized over a reasonable rotor speed range; however, ground resonance was more difficult. The FLAIR analysis was also checked by Hodges (ref. 88) against model-scale BMR experimental measurements of air and ground resonance stability reported in reference 254. Typical results are shown in figure 80 for two different BMR configurations; there is generally good agreement between FLAIR and the measured data.

Sivaneri and Chopra developed a finite-element, bearingless-rotor blade analysis capable of modeling a twin flexbeam configuration (refs. 59,67). They compared the accuracy of a simplified approach using a single flexbeam to represent a dual flexbeam configuration, an approach that they found to be inaccurate in some cases.

Bearingless-Rotor Experimental Investigations

Considerable experience in testing bearingless rotors has been gained through government research and development activities, including development of prototype systems. Only a part of this has been focused to meet specific research objectives; therefore, there is a need for continuous experimental investigations in this area.

A moderate amount of experimental testing data has been accumulated through development testing of prototype rotorcraft systems. These developments are discussed in section 4. The Boeing Vertol Bearingless Main Rotor (BMR) program was particularly noteworthy for the amount of test data obtained (refs. 89,90). Extensive test data for the 1/5.86-Froude-scaled BMR model was reported by Chen et al. (ref. 254). An interesting correlation of model data, full-scale flight-test data, the FLAIR analysis, and the Boeing Vertol C-45 rigid-blade analysis for a hover air resonance condition of the BO-105/BMR is shown in figure 81. Following the BMR flight-test program, extensive experimental testing of the full-scale BMR rotor was conducted in the 40- by 80-Foot Wind Tunnel as described in section 4. Typical experimental results from reference 255 are shown in figure 82 together with predictions from a Boeing Vertol code. The rotor apparatus used for the wind-tunnel testing provided a nearly hub-fixed condition for the rotor, therefore, the results represent isolated rotor-blade stability.

A series of experimental investigations using a small-scale bearingless-rotor model was carried out at AFDD by Dawson with the specific intent of verifying the FLAIR analysis and of investigating bearingless-rotor stability characteristics in general (ref. 256). This model was designed to accommodate variations of a wide variety of flexbeam and control-system geometric parameters to permit testing a wide variety of bearingless-rotor types. These features are illustrated in the exploded view of the hub, flexbeam, pitch control torque tube, and pitch links (fig. 83). The model was tested in both two- and three-bladed versions. Typical results from reference 256 for lead-lag damping versus blade-pitch angle are shown in figure 84 at two different rotor speeds and for two different pitch-control configurations. The correlation with the FLAIR analysis is reasonably good; however, instances of flutter involving unsteady aerodynamics not treated by FLAIR were also

encountered. Further experimental investigation by Bousman and Dawson of the flutter results identified several distinct types of flutter that may be experienced by bearingless rotors (ref. 257).

Finally, a considerable amount of small-scale experimental data has been obtained by Weller and Peterson for the air resonance characteristics of an advanced bearingless rotor in hover and forward flight (refs. 258-260). These results are more fully described in section 4. In addition, small-scale experimental studies in connection with the ITR/FRR Project were conducted in hover and forward flight, as noted in section 4. The Boeing Vertol ITR bearingless-rotor model testing was reported by Mychalowycz (ref. 261).

TILT-ROTOR AIRCRAFT STABILITY

In the early 1960's, considerable attention was given to the problem of rotor-pylon stability of tilt-rotor aircraft. Before the emergence of the tilt-rotor, research had been performed in efforts to understand the problem of classical propeller whirl-flutter instability where nacelle pitch and yaw motions are coupled through gyroscopic effects of a spinning rigid propeller. Reed and Bland (ref. 262) and Houbolt and Reed (ref. 263) investigated both classical propeller whirl flutter and static divergence, using rigid-rotor models. A comprehenseive review of propeller whirl flutter by Reed can be found in reference 264.

Actual tilting proprotor stability analyses were subsequently found to be considerably more complicated than classical propeller whirl flutter. The importance of rotor flapping for tilting proprotor configurations was first investigated by Young and Lytwyn (ref. 265). Using a representation including yaw and pitch motion of a rigid nacelle and with rigid flapping for each blade, it was shown that a forward whirl instability was possible but would be self-limiting because of nonlinear aerodynamics. Most importantly, it was found that increased blade flexibility reduced the pitch and yaw stiffness requirements for proprotor whirl flutter, thereby allowing weight reductions for the pylon mounting in tilt-rotor aircraft.

During development and testing of the Army Bell XV-3 tilt-rotor aircraft, further investigations of proprotor whirl flutter were carried out by Hall (ref. 266) and Edenborough (ref. 267); they provided additional understanding of rotor-pylon dynamics. Two potentially unstable modes were identified for an XV-3-type tilt-rotor aircraft: a pylon mode at a frequency near the natural frequency of the pylon, with little rotor flapping, requiring little damping for stabilization; and a rotor mode at much lower frequency, with large rotor flapping, requiring substantial damping for stabilization.

Coupled Rotor, Pylon, and Rigid-Body Dynamics

In the early 1970's, following initiation of the XV-15 program, the government increased efforts to improve analysis capabilities and understanding of tilt-

proprotor aircraft stability. Up to this time, no dynamic analysis of a full rotor-pylon-wing-airframe system had not been undertaken. Kvaternik developed the analysis of reference 99 to better understand wing-rotor dynamics using a linear analysis of an idealized proprotor in cruise-mode flight with rigid, spring-restrained flapping blades. This analysis was used to predict the aeroelastic stability of a small-scale model of the Bell Model 266 tested in the Langley Transonic Dynamics Tunnel. Figure 85 shows a comparison of experimental and analytical results for two configurations of the model, with and without aerodynamics. The analysis of reference 99, together with an extensive small-scale-model test program conducted in the Langley Transonic Dynamics Tunnel with Grumman (ref. 100), was used by Kvaternik and Kohn to investigate the applicability of a simple mathematical model to predict whirl flutter for both backward and forward whirl modes. The model is shown in figure 86. The study showed the ability to predict dynamic stability from such a simple mathematical model using linear aerodynamics for both types of rotor-pylon instabilities. Additional descriptions of these investigations are reported in references 268 and 269.

In support of the development testing of the XV-15 tilt-rotor aircraft, Johnson used a sophisticated analysis for predicting tilt-rotor aeroelastic stability behavior. The initial analysis (ref. 101) treated rotor-blade flap and lag elastic bending and wing beam bending, chord bending, and torsion, and was used to study the sensitivity of analytical predictions to various elements of the theoretical model. This analysis was also used for comparisons with results of two full-scale semispan prop-rotor-wing models tested in the NASA Ames 40- by 80-Foot Wind Tunnel. The Boeing Vertol soft-inplane proprotor configuration tested in the wind tunnel is shown in figure 87; measured results for damping of the wing vertical bending mode for a Boeing Vertol soft-inplane configuration are compared with analytical predictions in figure 88. Johnson also discussed these results in reference 270.

Johnson further investigated the sensitivity of tilt-proprotor stability to details of the analytical model (ref. 271). That investigation used an extended version of the equations of reference 101, including coupling of rotor-blade flap-lag bending deflections, blade torsion, additional blade-bending modes, rotor rotational speed perturbations, and wing aerodynamic forces. Typical results (fig. 89) indicate the importance of blade-pitch and blade-lag motion on wing bending-mode damping. In reference 103 Johnson investigated the influence of the rotor shaft (rotational) degree of freedom. When rotor shaft angular rotation is unlocked from the wing tip rotation (which accompanies wing tip vertical deflections), rotor aerodynamic damping no longer damps wing vertical bending motion, resulting in a pronounced destabilizing effect. He also showed that interconnect shaft dynamics were important in coupled rotor-wing antisymmetric modes, as shown by the typical results in figure 90. Johnson also investigated the importance of pitch-lag coupling on proprotor stability (ref. 272). Proprotors have built-in blade precone for relieving high steady blade-flap bending moments in hover. However, in the cruise mode, with reduced rpm and significantly reduced thrust, the elastic bending decreases the blade coning. The resulting negative pitch-lag coupling then becomes destabilizing. This coupling can be reduced using increased control-system

stiffness or by introducing blade droop. This work also investigated the effects of lift divergence at high speed where compressibility effects reduce aeroelastic stability, as shown in figure 91.

In preliminary studies for the XV-15 aircraft, a soft-inplane proprotor was investigated analytically and experimentally by Alexander et al. (ref. 273). Unlike a stiff-inplane rotor system, a soft-inplane system can experience air resonance at low speed when the regressing lead-lag motion coalesces with the wing vertical bending mode. Once again, the rotor rotation degree of freedom is very important; otherwise the wing mode is incorrectly predicted to be highly damped. The results of this study showed excellent damping predictions compared with full-scale 40- by 80-Foot Wind Tunnel data for the full-scale semispan Boeing Vertol rotor-nacelle-wing model.

Subsequent to the XV-15 wind-tunnel and flight-test program, Johnson (ref. 104) assessed the capability to predict performance, loads, and stability of the XV-15 aircraft, using the CAMRAD comprehensive analysis of reference 94. The conclusions from that study for tilting proprotor dynamics recognize the established confidence in predicting whirl flutter for the configurations that have been built and tested. However, new configurations with expanded flight capabilities will require new treatment and analyses to overcome current shortcomings.

A good indication of the capabilities for predicting proprotor whirl stability is provided in figure 92, which shows test results obtained for a V-22 Osprey model tested in the NASA Langley Transonic Dynamics Tunnel (refs. 274-276). Measured damping data for several test configurations are compared with predictions by CAMRAD, PASTA, and a Bell analysis DYN4. Although some preliminary adjustment in the input parameters of the analyses is usually necessary, the agreement between test and analysis is reasonably good.

Methodology Assessment

It is a given that theoretical prediction methods for rotorcraft aeroelastic stability require validation of some sort to be accepted as trustworthy. There are many ways of doing this. Three typical approaches are to check the predictions with (1) a known closed-form analytical solution to a theoretical problem, (2) results from other validated programs, and (3) experimental data.

A useful way to validate individual computer programs and at the same time assess the analytical state of the art in a given technical field is to analyze the same problem with several programs and compare the results. This has value for hypothetical problems (comparing only computer results), but it is obviously more desirable to analyze a problem for which experimental data are also available. Such an exercise is particularly useful in the rotorcraft dynamics technical community, especially given the many independent computer programs used within the industry. Validation for these codes is often minimal or limited to a narrow range of vehicle or rotor configurations. Taken collectively, the comparisons serve to calibrate the prediction methods for specific applications and identify areas where additional

research effort might have a high payoff. The results often provide the clues or information useful in upgrading individual codes.

A methodology assessment of this type was conducted by the Aeroflightdynamics Directorate in connection with the ITR/FRR Project in June 1983 (ref. 277). Aeroelastic stability predictions were compared with a variety of carefully selected experimental data encompassing simple and complex rotor blades; isolated rotor and coupled rotor-body configurations; and small- and large-scale rotors operating in hover, wind-tunnel, and flight-test conditions. A total of eight different prediction codes from industry, universities, and government laboratories were included in the comparisons. The results were very useful, and a few are included herein to illustrate some of what was learned.

The first case is for the elastic hingeless-rotor-blade model discussed in section 3. Data for lead-lag damping in the hover condition (ref. 230) are used to compare with predictions for two cases, one without built-in blade droop and the other with -5° droop. Predicted results without droop (fig. 93(a)) are relatively good for most of the analyses except at higher pitch angles where airfoil stall occurs. The situation changes completely for the droop configuration, shown in figure 93(b). Now the correlation is poor and there is a wide spread among the predictions. The only difference in the two cases was a "small change" in rotor geometry. Since the bending-torsion behavior of cantilever elastic blades is very sensitive to the precone and droop, it may be concluded that the basic structural dynamics was not adequately modeled. One benefit of such comparisons is the insight and stimulus to correct such discrepancies by identifying the sources of error in the program. Although such a problem had not been previously suspected, the G400 analysis was revised to correct the undiscovered problems in the analytical treatment of the blade structural deformations. The revised G400 results included in figure 93 were a substantial improvement over the original calculations.

Another example is regressing lead-lag mode damping of the coupled rotor-body dynamic system of Bousman described previously. Figure 94 shows experimental data at $\theta = 9°$ (ref. 158) compared with the predicted results of various analyses. Again, there is a considerable scatter in the predictions, even though the general trends are reasonably well represented. Given that only quasi-steady aerodynamic theory and hinged-rigid blade dynamics are included, it would be expected that the predictions would be in much closer agreement.

In order to determine the sources of differences between the various predictions it is necessary to compare the equations directly at some level or to compare predictions for a simplified problem in stages until the differences are accounted for.

4. EFFECT OF AEROELASTIC STABILITY CHARACTERISTICS ON ROTORCRAFT SYSTEMS

Previous sections have addressed the development of analysis methods for aeroelastic stability and investigations of the different types of aeroelastic stability

phenomena exhibited by rotor blades and coupled rotor-body systems. This section will describe the effect of aeroelastic stability considerations on the design of specific rotorcraft systems. Insights provided by development and testing experience will also be addressed. The purpose is to identify the government research that contributed to the development of these systems, such as helping to insure freedom from instability, resolving unexpected occurrences of aeroelastic instability, or supporting research on a particular class of rotor systems to overcome inherent aeroelastic stability limitations.

HINGELESS ROTORS

During the 1960's considerable interest arose in the hingeless rotor as a natural step in the evolution of a simpler, lighter, and more reliable helicopter rotor. Much of the early interest was sparked by the Lockheed CL-475 and XH-51A gyro-controlled, rigid-rotor vehicles, the MBB BO-105, and the Westland WG-13 Lynx. Hingeless rotors offer a number of advantages such as elimination of heavy, bulky, and unreliable hinges and bearings of articulated rotors and the potential to eliminate lead-lag dampers used to prevent ground resonance. The many possible configurations and associated design variables complicate the subject of hingeless-rotor aeroelastic stability, and the potential for instability makes it central to the design of a successful system.

AH-56A Cheyenne

The U.S. Army Lockheed AH-56A Cheyenne was a high-speed compound helicopter designed as an advanced aerial fire support system. The gyro-controlled stiff-inplane hingeless rotor was derived from the highly successful Lockheed XH-51 demonstrator aircraft that was flown as both a pure and compound helicopter. The hingeless rotor, combined with a mechanical gyro feedback control system, provided high maneuverability and low gust response. The stiff-inplane rotor precluded the need for lag dampers to suppress ground or air resonance instability. However, during flight testing the AH-56A revealed several aeroelastic instabilities not encountered with the XH-51, a result of differences in design details of the scaled-up AH-56A configuration. Furthermore, the hingeless rotor was a significant departure from conventional articulated rotor configurations, and the complex behavior of stiff-inplane hingeless rotors was not adequately understood at the time. As a result, this experience stimulated a wide range of basic research into the aeroelastic stability of hingeless-rotor systems and indeed much of AFDD research grew out of AH-56A development experiences. Following the conclusion of the AH-56A program, the U.S. Army Aviation Systems Command and the Aeroflightdynamics Directorate sponsored a Lockheed effort to document the experience obtained regarding dynamics phenomena of this aircraft. This information is contained in reports by Donham and Cardinale (ref. 278) and Johnston and Connor (ref. 279). Additional sources for this and other information are Johnston and Cook (ref. 280), Anderson (ref. 281), and Anderson and Johnston (ref. 282).

During early development of the AH-56A, two problems received most attention. The 1P-2P phenomenon (ref. 278) occurred at low rotor speed in the presence of high rotor hub moments as might occur in ground contact, where nonlinear blade-feathering moments resulting from combined flap and lead-lag bending were fed back into the control gyro in such a way as to produce a coupled rotor-gyro instability. The second problem, termed 1/2 P-Hop (refs. 279,282), involved coupling of the lead-lag regressing mode, vehicle roll mode, collective rotor flapping, and vehicle vertical translation near the regressing inplane frequency of about 0.5 per rev. This phenomenon occurred in high-speed flight and led to loss of an aircraft.

Because of the high advance ratio and proximity to a half-integer frequency, the 1/2 P-Hop stimulated interest in the use of Floquet theory to treat periodic-coefficient systems. To further study the problem, the AH-56A was installed in the 40- by 80-Foot Wind Tunnel at Ames for further testing under controlled conditions (fig. 95). Early in the test, while at a moderate-speed, high-thrust condition a rotor pitch-up divergence occurred that destroyed the test vehicle. This instability was attributed to aerodynamic stall-feathering moments overpowering and destabilizing the normal gyro feedback generated by rotor flapping. Following this incident, the Advanced Mechanical Control System (AMCS) was developed, using direct flap feedback from the blades instead of indirect feathering moments. This eliminated the source of both the 1P-2P and moment stall instabilities. A final problem of the reactionless mode instability was encountered during a low-speed, high-gross-weight condition (refs. 279,281). This was essentially an isolated-blade flap-lag-torsion instability of the type discusssed previously.

During the AH-56A Cheyenne development, government researchers worked closely with Lockheed engineers to attempt to understand the new phenomena being encountered and to devise means to eliminate the problems. This program was instrumental in revealing the complexity of stiff-inplane hingeless-rotor aeroelastic stability and the necessity of a firm technology base on which to launch a major development program. Government research subsequently confirmed the complexity of hingeless-rotor aeroelastic stability characteristics and provided key information to guide further rotor system developments.

Bell Flexhinge Rotor

The two-bladed teetering rotor has long been synonymous with Bell Helicopter Textron but in recent years the company has developed several production hingeless-rotor helicopters and has flight tested a prototype bearingless rotor. These accomplishments were preceded by an active research and development effort, much of it in cooperation with or sponsored by the government. While much of this research addressed flying qualities, rotor loads, and vibration characteristics, aeroelastic stability played a prominent role in the later stages of development. Early Bell hingeless rotors from the first Model 47 flown in 1957 to the Model 609 flexbeam rotor tested on the UH-1 under Army sponsorship in 1972 (ref. 283) were stiff-inplane configurations. The chief drawbacks of these rotors were excessive chordwise blade stresses in high-speed and maneuvering flight.

To resolve these problems, Bell evolved a soft-inplane version of the Model 609 rotor, using elastomeric lag hinges and dampers, and demonstrated greatly reduced chordwise bending moments in flight tests. The dampers insured air and ground resonance stability. Bell initiated further investigations of the aeromechanical stability of soft-inplane rotors using a small-scale research and development rotor, the Model 652, having capabilities to vary the aeroelastic coupling parameters. In cooperation with the U.S. Army Aerostructures Directorate and NASA Langley, the Model 652 rotor was extensively tested for aeromechanical stability in the Transonic Dynamics Tunnel, as reported by White and Weller (ref. 284). They investigated effects of elastomeric damping, kinematic pitch-lag coupling, pitch-flap coupling, flap-lag coupling, and hub stiffness. They also analytically investigated ground resonance using combinations of rotor blade pitch-lag and flap-lag coupling that Ormiston found effective for increasing lead-lag damping of a fixed-hub rotor (ref. 202). However, for coupled rotor-body configurations including pylon flexibility, they were unable to stabilize both the pylon and ground-resonance mode with a single combination of couplings.

Bell completed development of a refined version of a soft-inplane hingeless rotor, the Model 654, using elastomeric dampers to insure ground and air resonance stability, and conducted successful flight testing of a Model 206L aircraft (ref. 285). Bell used a similar approach to insure stability of the Flexhinge Rotor, subject of a predesign study for candidate rotor systems for the Rotor Systems Research Aircraft (ref. 286).

BEARINGLESS ROTORS

The hingeless-rotor concept is based on simplifying the rotor hub by eliminating blade flap and lead-lag hinges and carefully designing the structure to permit necessary blade-motion response without incurring excessive bending stresses. The bearingless rotor simply extends this idea and eliminates the blade-pitch-change bearing as well, substituting a flexbeam of sufficient torsional flexibility to accommodate the required pitch-change motion of the blade. Elimination of the rotor-hub bearings significantly reduces weight, complexity, and maintenance, thereby increasing helicopter productivity and reliability. However, aeroelastic complexity of the bearingless rotor introduces new unknowns in the development of advanced rotorcraft.

XH-51A Matched-Stiffness Rotors

The XH-51A Matched Stiffness Rotor program was conducted by Lockheed California Company under sponsorship of the Aviation Applied Technology Directorate to improve the gyro-controlled rigid-rotor design proved by the basic XH-51A aircraft. The basic gyro control system was designed to sense rotor-flapping motion caused by external disturbances and to feed back appropriate cyclic pitch to counter the flapping response. The mechanical system for sensing blade-flapping moments also

sensed blade-pitch moments that could potentially contaminate the feedback signal. Hence any reduction of blade-torsion moments was desirable. The nonlinear torsion moments, which result from combined flap and lead-lag bending, vanish for rotor blades with equal flap and lead-lag bending stiffnesses; therefore, the so-called matched-stiffness blade promised to eliminate a principal source of gyro-control contamination and permit a reduction in the size of the gyro. When the lead-lag stiffness was reduced to match the flap stiffness, the rotor also became soft-inplane, and therefore susceptible to ground and air resonance. The study of these phenomena became the principal focus of the program.

While the design for a matched stiffness configuration was being formulated, it was also decided to incorporate another feature: replacement of the feather bearings with a flexbeam, thus converting the hingeless rotor to a bearingless rotor. No auxiliary damping was used in the design of the rotor. As reported by Cardinale (ref. 81) and Donham et al. (ref. 287) the XH-51A Matched Stiffness Rotor system did not exhibit a sufficiently wide stable range of rotor speed to operate safely throughout the flight envelope. Nevertheless, the ground and air resonance boundaries were extensively documented for ground-contact conditions and for hover and low-speed flight, and a number of configuration changes were evaluated and correlated with theoretical analyses. The program provided valuable experience that aided later bearingless-rotor development programs such as that of the Boeing Vertol Bearingless Main Rotor.

Composite Bearingless-Rotor Design Studies

Increasing interest in bearingless rotors, together with the development of the Army-NASA Rotor Systems Research Aircraft (RSRA) for flight testing advanced rotor systems, resulted in government sponsorship of several preliminary design studies of candidate rotor systems. These studies emphasized the application of composite materials to the bearingless-rotor concept and gave special consideration to the requirements for adequate levels of aeroelastic stability. These studies were discussed by Swindlehurst in reference 288.

One of the first studies of the bearingless rotor for eliminating all hinges and bearings through the use of composite materials was initiated at UTRC in 1968. In the Composite Bearingless Rotor (CBR) concept, two flexbeam members crossed at the center of the rotor form the spars of a four-bladed rotor. The early UTRC work led to Army and NASA support for analytical and design studies including composite materials investigations, small-scale model testing, development and correlation of stability analysis with test data, and preliminary design layouts of a full-scale rotor. Results of this work were reported by Bielawa et al. (ref. 56). Both two- and four-bladed stiff-inplane configurations with pinned-pinned torque tube and cantilever torque tube pitch-control systems were wind-tunnel tested in the fixed hub condition. The G400 program developed by Bielawa (ref. 55) was used for this investigation. Principal aeroelastic test results and correlations with analysis involved blade-bending moment response and stresses. The results also verified the analysis, in that all experimental cases observed to be stable were also predicted

to be stable. Experimental results did indicate a tendency for the cantilver torque tube configuration to exhibit adverse pitch coupling resulting from torque-tube flapwise motion under some operating conditions.

The full-scale Composite Bearingless Rotor design used a four-bladed 62-ft-diam rotor sized for an S-61 class aircraft. Two torque tube configurations were designed, a cantilever torque tube and a snubbed torque tube to eliminate the potential for adverse couplings owing to flapwise motion of the torque tube observed in the model tests. An aeroelastic stability analysis of the full-scale snubbed torque tube configuration was carried out using the G400 analysis for both stiff- and soft-inplane versions of the design and showed both configurations to be stable for the conditions analyzed.

Another government-funded design study was undertaken by Boeing Vertol to evaluate the feasibility of a four-bladed Composite Structures Rotor (CSR) for installation and testing on the NASA-Army RSRA (ref. 289). The CSR design was roughly similar to the BMR configuration, having twin flexbeams, a torque shaft between the flexbeams, and no auxiliary elastomeric damping. Design of 53-ft-diam and 60-ft-diam rotors were studied and air and ground resonance analyses performed using the equivalent-hinged, rigid-blade C-45 analysis. This exercise revealed the difficulty of analyzing a complex elastic system, such as the bearingless rotor, with a discrete, equivalent-hinged analysis.

Although the flexbeam designs for the 53-ft and 60-ft rotors were the same, the different blade lengths led to different locations for the equivalent flap and lead-lag hinge, such that the C-45 flap and lead-lag hinge sequences for the two designs were different. For the 53-ft-diam rotor, the sequence was flap-lag-pitch; for the 60-ft-diam rotor, the sequence was lag-flap-pitch. This difference was sufficient to cause moderately large differences in the stability of the two rotors. For the 60-ft rotor, it was necessary to reduce the chordwise frequency to insure aeromechanical stability.

Boeing Vertol Bearingless Main Rotor

The Applied Technology Directorate sponsored a very successful Boeing Vertol program to develop and flight test the Bearingless Main Rotor (BMR) on the BO-105 aircraft; the purpose was to demonstrate concept feasibility with emphasis on aeroelastic stability. The principal objectives of the project were to demonstrate that acceptable aeroelastic stability, structural loads, and flying qualities could be achieved with such a rotor. The rotor design concept was an outgrowth of Boeing's YUH-61A stiff-inplane bearingless tail rotor. The four-bladed BMR was designed to replace the BO-105 hingeless rotor; the existing hub and inboard portions of the blade were removed and replaced with a bearingless hub, dual fiberglass flexbeams and a torque tube cantilevered to the blade and pinned at the hub (fig. 96). The basic dynamic properties of the BO-105 rotor were retained, with moderate flapwise stiffness, soft-inplane chordwise stiffness, and no auxiliary lead-lag dampers. The results of the design effort were reported by Harris et al. (ref. 290).

Marginal air and ground resonance characteristics of the XH-51A Matched Stiffness Rotor and a desire to avoid the use of lag dampers served to focus considerable attention on aeroelastic stability in the early phases of the BMR program. Extensive small-scale-model testing was conducted to check theoretical stability predictions. Test results (refs. 254,290) confirmed a reasonably wide rotor speed range of stable operation, generally in agreement with the predicted characteristics. The Boeing Vertol predictions were obtained from the C-45 analysis of a simplified spring-restrained hinged-rigid blade. With careful exercise of engineering judgment in the selection of effective hinge configuration parameters for the bearingless rotor, reasonably accurate predictions of stability could be made. The need for a more rigorous approach to better support the BMR design was recognized, however, and led to the development of the FLAIR analysis by Hodges, as described in section 2. In an effort to determine the most effective aeroelastic couplings to prevent air and ground resonance instability, parametric studies were conducted using the C-45 and FLAIR analyses; FLAIR results are published in reference 58. Both analysis and model test results indicated that a combination of flap-lag structural coupling from blade negative-droop outboard of the flexbeam were most effective for aeroelastic stability. Aeroelastic stability characteristics determined during flight testing of the BMR on the BO-105 aircraft were reported by Dixon (ref. 90), Staley and Reed (ref. 291), and Staley et al. (ref. 89).

Extensive ground and air resonance tests were conducted in a variety of ground contact and flight conditions. Initial ground testing revealed lower than expected stability, and led to minor modifications of the skid landing gear to raise the body frequency slightly. Air resonance damping was similar to theoretical and model test data. The BMR was slightly less stable than the baseline BO-105 hingeless rotor, and this was attributed in part to lower inherent structural damping of the BMR flexbeam-blade structure. Nevertheless, the BMR demonstrated a major advance in rotor-system technology and remains the only damperless, bearingless rotor successfully tested throughout the vehicle flight envelope.

Following flight testing, the BMR was installed in the 40- by 80-Foot Wind Tunnel at Ames to gather additional data on rotor stability characteristics as well as performance, loads, and flight-control characteristics outside the BO-105 aircraft flight envelope. The wind-tunnel testing also included modifications to vary the pitch-link stiffness and addition of elastomeric damper strips to increase flexbeam structural damping. The results of the wind-tunnel test, reported by Sheffler et al. (ref. 292) and Warmbrodt and McCloud (ref. 293), indicated that the relatively simple modification of adding elastomeric damping strips was very effective in increasing the lead-lag damping in all cases tested. Sheffler et al. subsequently reported on model testing of an advanced BMR II flat-strap configuration that was also stabilized with the use of elastomeric damping strips (ref. 294).

Bell Advanced Bearingless Rotor

Following the successful development of the Model 654 soft-inplane hingeless rotor and application of that technology to several production aircraft, Bell

initiated a program to design and test an advanced bearingless rotor. This effort produced the very successful Model 680 rotor system, which was flown on a Model 222 aircraft. As a part of that program, Bell sought to improve in-house analysis capabilities for predicting the aeroelastic stability of bearingless-rotor configurations.

In support of this work, NASA Ames sponsored a model-scale experimental program to obtain data for determining the adequacy of these prediction methods. The small-scale model was similar to the Model 680 configuration—a four-bladed, soft-inplane bearingless rotor with a single element flexbeam and a torque tube with a snubber and elastomeric damper. Blade coning, sweep, pitch flap and pitch lag couplings, and fuselage inertial properties could be changed to conduct parametric studies. The model was tested in hover and forward flight for both fixed hub and coupled rotor-body configurations. The testing and results were reported by Weller (refs. 258,259) and by Weller and Peterson (ref. 260). In general the Bell analytical predictions were in good agreement with the measured test data. It was also concluded that for this rotor configuration the effects of rotor geometric and structural design parameters on stability were not large, and that an auxiliary elastomeric damper was the best means of insuring acceptable mechanical stability.

Integrated Technology Rotor/Flight Research Rotor

The Integrated Technology Rotor/Flight Research Rotor (ITR/FRR) Project was undertaken by the Aeroflightdynamics and Aviation Applied Technology Directorates of the U.S. Army Aviation Research and Technology Activity, and NASA Ames, to advance rotor-system technology by combining advances in the structures, dynamics, materials, aerodynamics, and acoustics technical disciplines to design and demonstrate, through actual full-scale flight test, the benefits of an optimized rotor system. Although the project was not funded as far as the full-scale flight test phase, sufficient research and development was completed that it significantly influenced related and follow-on programs. The project consisted of several phases and efforts, undertaken primarily through industry contracts. A methodology assessment exercise was conducted to evaluate the adequacy of industry aeroelastic stability prediction capabilities, as described in section 3. Concept definition studies were undertaken by five helicopter industry contractors to examine the feasibility of various hub concepts for further consideration during preliminary design. Many of these hub concepts were bearingless-rotor configurations, and design features to generate aeroelastic couplings and to enhance aeroelastic stability were examined. Bousman et al. presented an overview of these studies in reference 295. An example of one damperless, bearingless-hub design examined by Bell Helicopter Textron is illustrated in figure 97.

Three contracts were awarded to conduct preliminary design of ITR/FRR rotors. A significant part of these studies included testing small-scale models to confirm the aeroelastic stability of the candidate designs. The Boeing Vertol design reported by Mychalowycz was a single-flexbeam bearingless rotor with a torque-tube pitch control system having an offset shear pin at the hub to introduce pitch-lag

aeroelastic coupling (ref. 261). Hooper used the FLAIR analysis to conduct parametric studies of the ITR hub coupling parameters to optimize the aeroelastic stability characteristics (ref. 91). Negative droop and an offset of the torque-tube shear pivot to introduce pitch-lag coupling were effective in inhibiting air and ground resonance instability. No auxiliary elastomeric damping was included. Bell Helicopter Textron designed a refinement of the Model 680 bearingless-rotor configuration and included a torque tube with snubber and elastomeric damper. The Sikorsky design was based on the elastic gimbal rotor design originally studied by Carlson and Miao (ref. 296).

The results of the ITR/FRR Project served to identify the technical readiness of several advanced rotor technologies. Regarding aeroelastic stability of bearingless rotors, a consensus on the feasibility of a damperless configuration was not reached. The definition of blade and flexbeam frequencies, and the identification of aeroelastic couplings to insure aeromechanical stability over a sufficient range of rotor speed and vehicle operating conditions, is a difficult design task; at the present time, most designers will opt for a lower-risk approach that incorporates auxiliary elastomeric lead-lag damping.

Related structural issues of flexbeam strength and flexibility are better understood, but more progress is needed. It is worth noting that the government-sponsored preliminary design studies prompted a parallel MDHC-funded program that culminated in successful flight testing of the HARP bearingless rotor on the Model 500 helicopter. In addition NASA will sponsor fabrication and testing of a large-scale version of the Boeing Vertol ITR in the NASA Ames 40- by 80-Foot Wind Tunnel.

TILT-ROTOR AIRCRAFT

The U.S. Army Bell XV-3 Convertiplane was designed in the early 1960's. It used a two-bladed, teetering-rotor system to partially decouple the gyroscopic rotor moments from the pylon, and the blades were designed with conventional negative pitch-flap coupling to reduce rotor flapping during low-speed maneuvers. Development of the XV-3 aircraft identified many of the dynamic problems of tilt-rotor aircraft, including proprotor whirl flutter, which occurred during full-scale wind-tunnel testing in the NASA Ames 40- by 80-Foot Wind Tunnel.

With the conclusion of the XV-3 program and the initiation of the Advanced Composite Aircraft Program leading to the development of the XV-15, considerable work was done to better understand the shortcomings of the XV-3 design and the importance of rotor elastic motions, rotor couplings, control system flexibility, drive train effects, and wing dynamics. Gaffey made an important contribution by investigating the use of positive pitch-flap coupling for improving flap-lag stability of stiff-inplane rotors in high inflow axial flight (ref. 297). Although the XV-3 used negative pitch-flap coupling to minimize flapping during maneuvers in the high-speed airplane mode, Gaffey showed that a possible coalescence of the flap and lead-lag frequencies of the rotor blade could lead to flap-lag instability. The use

of positive pitch-flap coupling prevents such a coalescence, thereby stabilizing flap-lag motion; Gaffey also showed that positive coupling was equally effective in controlling flapping motion.

XV-15 Tilt Rotor Research Aircraft

The XV-15 Tilt Rotor Research Aircraft was developed as a joint NASA-Army effort to demonstrate the solution of the key technical problems of this configuration (fig. 98). Substantial government efforts were devoted to developing the technology base needed to deal with aeroelastic stability issues of the tilt rotor. This work has been discussed in detail in sections 2 and 3. At the appropriate point, the government initiated a full-scale proof-of-concept aircraft program to complete the technology development process. Following a competitive preliminary design phase, Bell was selected to design and manufacture two XV-15 aircraft. Extensive government participation in this program contributed to its ultimate success. The following will describe some of the aeroelastic stability considerations relevant to the program.

The XV-15 proprotor design was the result of 15 years of technology development. The three-bladed proprotors use a gimbaled hub to minimize gyroscopic coupling between the rotor and the pylon. The blades are stiff inplane to avoid air and ground resonance, and are similar to hingeless helicopter rotor blades in many respects. Positive pitch-flap coupling of the blades was used to stabilize flap-lag motion and to minimize rotor flapping during maneuvers, based on Gaffey's findings described above. The blade flap frequency was chosen, in part, to minimize pylon stiffness requirements for proprotor whirl-flutter stability. Gaffey et al. (ref. 298) and Johnson (refs. 270,272,299) summarize much of the dynamics-related technology development during aircraft design.

The results of the dynamics testing of the XV-15 aircraft are reported by Marr et al. (ref. 300) and by Bilger et al. (ref. 301). The aeroelastic stability of the aircraft has been cleared to speeds up to 300 knots at altitude. At very high speeds (and at high altitude with the reduction in the speed of sound), lift divergence over a significant portion of the rotor is stabilizing for proprotor dynamics. XV-15 whirl-flutter stability was not a problem.

The successful development of the XV-15 aircraft was the culmination of efforts to demonstrate the ability to effectively control potential aeroelastic instability that hindered acceptance of the revolutionary tilt rotor concept. The NASA and Army contributions in research and the development of the basic technology, as well as management of the XV-15 aircraft program, were major accomplishments.

V-22 Osprey Aircraft

The V-22 Osprey tilt rotor being developed by the U.S. Marine Corps is tangible proof of the potential brought to fruition with the XV-3 and XV-15 research aircraft. The development of the V-22 is benefiting from significant support from NASA

and Army researchers and experimental facilities. Activities in the area of aeroelastic stability will be discussed below.

A detailed summary of the dynamic stability analysis and testing of the proposed V-22 tilting proprotor system is presented by Popelka et al. (ref. 302). An initial rotor design by the Bell-Boeing team used XV-15 technology with a three-bladed, stiff-inplane, gimballed hub rotor system. However, after initial testing in the Langley Transonics Dynamics Tunnel, aeroelastic stability characteristics were found to be poor. Because of the improved rotor blade airfoils with a higher lift-curve slope, rotor aerodynamics effects reduced the proprotor whirl-flutter stability boundary. Since the rotor precone angle was chosen for hover, destabilizing negative pitch-lag coupling was generated in the airplane mode. To reduce this coupling, lower the effective pitch flap coupling angle, and reduce the resultant aerodynamic moment transmitted to the rotor hub as well, a coning hinge was added to each blade. The result of this design modification was to markedly improve the whirl-flutter stability well beyond the operational envelope of the V-22 aircraft. This gimballed-coning hub required the modification of the Bell Helicopter dynamics prediction code and the codes of Kvaternik (ref. 99) and Johnson (ref. 94). This new hub configuration was also used in predicting the dynamic performance of a high-speed tilt-rotor design (ref. 303) using the modified analysis of reference 94.

Although a great deal has been learned about tilting proprotor dynamics, future designs will likely use more advanced hub configurations (benefiting from the use of composite materials and redundant load path designs) requiring new analyses. Higher airspeeds will require better understanding of the influence of compressible aerodynamics on proprotor stability. True optimization of the design process for rotor-pylon-wing aeroelastic stability has yet to be attempted. Also, the use of active controls has yet to be fully investigated for the potential of improving tilting proprotor stability characteristics.

OTHER ROTOR SYSTEMS

In addition to the rotor systems described in the previous sections, government research and development efforts have also addressed the aeroelastic stability of a number of other rotor configurations. These will be briefly described below.

The search for high-speed aircraft having vertical takeoff and landing capability has led to consideration of a number of configuration concepts. The compound helicopter has received much attention, and slowing, stopping, or stowing the rotor has been studied as a way of minimizing or eliminating the aerodynamic problems of operating rotors at high forward speeds. All of these concepts involve high advance ratio conditions. Watts et al. report results of 40- by 80-Foot Wind Tunnel tests of a Lockheed gyro-stabilized slowed-stopped hingeless rotor (ref. 304). Aeroelastic analysis and comparisons with test data were undertaken to determine the ability to predict coupled rotor-gyro stability under extreme operating conditions of low

rotor speed and very high advance ratios. Results showed that relatively simple aerodynamic theory was reasonably accurate for these conditions.

In the course of development of advanced bearingless-rotor systems, valuable experience has been gained from earlier development of bearingless helicopter tail rotors constructed from composite materials. The goverment has supported research and development on several such systems where aeroelastic stability required careful considerations in design. Maloney described the elastic pitch beam rotor developed by Kaman, a two-bladed teetering rotor using a fiberglass flexbeam for blade-pitch change motion, coning deflections, and chordwise bending (ref. 305). The rotor was designed for application to full-scale aircraft and was tested and demonstrated to have acceptable stability characteristics.

Boeing Vertol also gained bearingless rotor experience with a tail rotor application. In the course of development of the YUH-61A UTTAS aircraft prototype, a mechanically simple but structurally advanced four-bladed stiff-inplane fiberglass tail-rotor was introduced. This rotor used a cantilever torque tube configuration that permitted significant aeroelastic coupling of bending and torsion motions. During development testing a number of instabilities were encountered including stall flutter and high-amplitude lead-lag limit cycle motions. A stable configuration evolved through extensive trial and error testing and modifications. Because of the complex behavior of the bearingless rotor, analytical methods were of limited use in predicting or identifying solutions to observed instabilities. The extensive aeroelastic stability data obtained in this program were sufficiently valuable, however, that it was documented (under government sponsorship) by Edwards and Miao (ref. 306).

The Sikorsky ABC compound helicopter was developed under sponsorship of the U.S. Army. The two three-bladed coaxial, high-flap stiffness rotors form a unique stiff-inplane hingeless-rotor system. To confirm the general adequacy of the design, including aeroelastic stability, the flight rotors were tested in the 40- by 80-Foot Wind Tunnel (ref. 307); flight-test results were reported in reference 308. Without auxiliary dampers, the lead-lag damping of the blades was very low, but adequate stability was maintained throughout the flight envelope.

The constant-lift rotor (CLR) and free-tip rotor (FTR) designs use airfoil sections that are free to pivot on the spar of the rotor blade in order to maintain nearly uniform lift during forward flight and thereby minimize the vibratory response of helicopter rotor blades in forward flight. However, the additional degrees of freedom provide more opportunities for aeroelastic stability, and investigations of the flap-lag-torsion stability of these design were carried out by Chopra for the hover flight condition (refs. 309,310). With suitable selection of aeroelastic design parameters, it was possible to identify stable configurations.

5. CONCLUSION

The material presented herein shows the extensive involvement of the Army and NASA in rotorcraft aeroelastic stability research. In most of the areas addressed, significant technology advances have occurred as a result of this research. Some of these areas were essentially nonexistent 20 years ago. As a result, the technical community is in a much stronger position to deal with the risks of aeroelastic instability of new rotor systems. In this section, the key contributions of Army-NASA research will be summarized, followed by recommendations for future efforts.

SUMMARY OF ARMY-NASA RESEARCH CONTRIBUTIONS

1. A substantial capability for predicting helicopter and tilt-rotor aeroelastic stability now exists, capable of treating rotorcraft structural dynamics and aerodynamics in considerable detail. Hover flight conditions are relatively straightforward, and very substantial progress has been made in forward flight prediction capabilities. In addition to conventional articulated-rotor systems, hingeless-rotor stability analysis is now nearly routine, and bearingless rotors can be satisfactorily treated in many respects. Prediction capability resides in a number of different analyses, many of which have been extensively validated with experimental data.

2. A comprehensive understanding of the aeroelastic stability characteristics of hingeless rotorcraft now exists. This includes nonlinear bending-torsion coupling, structural flap-lag coupling, the influence of kinematic aeroelastic coupling, the effects of aerodynamics and rotor body coupling on aeromechanical stability, and the effects of dynamic inflow and dynamic stall on aeroelastic stability. The differences between soft- and stiff-inplane hingeless rotors have been identified, and this has contributed to shift emphasis away from stiff-inplane and toward soft-inplane configurations for new rotorcraft.

3. The technology base for tilt-rotor aeroelastic stability has expanded substantially. Validated prediction codes now exist to treat fully coupled systems, including rotor, pylon, wing, and fuselage dynamics. Parametric studies have contributed to a good general understanding of tilt-rotor systems including the effects of rotor-blade in-plane, pitch, and torsion motions, drive train coupling effects, and compressible airfoil aerodynamics.

4. An extensive experimental data base has been generated, for small-scale models and full-scale aircraft, for both helicopter and tilt-rotor configurations. The data are of high quality, much of them obtained from experiments specifically designed to acquire data for correlation with prediction methods.

5. A solid theoretical basis for the structural dynamics of nonlinear beams has been established. The subject has been investigated by numerous researchers, and the theory has been validated experimentally. The moderate deformation theory,

valid for small strain, has been extended from moderate rotation to large rotation deformations. Advanced nonlinear finite-element methods are being developed and characteristics of composite materials can now be treated for some simple cases.

6. Dynamic inflow theory is a substantial development that has found wide acceptance by rotorcraft aeroelasticians. It has been placed on a rigorous theoretical foundation and has been extensively validated with experimental data. Because of its accuracy, simplicity, and computational efficiency, it has been found useful in other disciplines such as rotorcraft flight dynamics. It is also amenable to refinement for application to higher-frequency aeroelastic phenomena.

7. Mathematical methods for solving rotorcraft aeroelastic stability equations have also advanced significantly. Floquet theory for periodic coefficient linear systems is now in common use and the rotating-to-fixed system transformation has been formalized as multiblade coordinates. Recent work has also demonstrated significant potential for the use of symbolic processors for automatic generation of the complex multi-degree-of-freedom rotorcraft equations of motion.

8. In addition to generic rotorcraft aeroelastic stability research, invaluable knowledge and progress have resulted from full-scale systems design, testing, and development of advanced rotorcraft and rotorcraft components. These efforts are the final proof of the contributions of aeroelastic stability research development. Full-scale development and flight test of aircraft such as the Bell XV-15 and the Boeing Vertol BMR have been particularly effective in demonstrating mastery of aeroelastic stability technology for critical dynamic phenomena.

RECOMMENDATIONS

Although the last 20 years have witnessed great progress in the technology of rotorcraft aeroelastic stability, not all of the problems have been solved. A great many pressing needs and attractive opportunities remain, and these should be vigorously pursued. As new rotorcraft systems evolve, continual emphasis will be required to address these new problems. The following general recommendations are offered for consideration.

1. It is usually taken for granted that aeroelasticians can apply Newton's second law without error and when the results of analysis are unsatisfactory the aerodynamic theory is often faulted. There is evidence that structural dynamics analysis is not yet adequately understood and that prediction of rotating-beam dynamics is not yet solved. More experimental data are needed. The most complex of all rotorcraft structures are rotor hubs, blades, and blade-to-hub attachments; they deserve more attention under the influence of pure inertial loading.

2. Vibration testing of rotating blades in vacuum should continue and be expanded to include more structurally complex blade and hub configurations, including nonuniform properties, typical bearingless configurations, and blade structures composed of composite materials. Careful experiments, correlated with analysis, may

reveal analysis deficiencies in solid mechanics, material properties, and structural damping effects.

3. The structural mechanics basis is now available for a large-rotation small-strain beam theory. Such development should be continued, and a modeling approach should be included for anisotropic materials. This will provide a capability to analyze fully the most complex structural rotor-blade flexbeam configurations now envisioned.

4. As the primary structural material for rotor blades, fiber-reinforced composites deserve the full attention of the aeroelastician. Capability of modeling and analyzing composite materials for rotorcraft applications needs to be substantially improved.

5. Finite-element methods are necessary for effective aeroelastic analysis of future rotorcraft. These methods need to be made more effective for dealing with rotating blades and for coupling rotating and nonrotating structures.

6. Computational efficiency of rotorcraft aeroelastic analysis needs to be improved. As the number of degrees of freedom increases, the solutions for nonlinear systems in forward flight have become more difficult. The trim and dynamic equilibrium solutions need to be improved and made more robust. Without practical solution methods, the benefits of improvements in structural and aerodynamic theory may not be realized.

7. Many of the analytical prediction methods developed have emphasized narrow research investigations. Prediction capability for a broad range of applications is needed. Prediction capability of research codes should be incorporated into comprehensive analyses (e.g., 2GCHAS) to make the technology more readily available to the designer.

8. More attention should be devoted to linear, three-dimensional unsteady aerodynamics theory for rotor-blade flutter analysis. In the age of computational fluid dynamics, numerically efficient methods are needed for rapid flutter analysis of rotor blades when stall and shocks are not present. New blade- and tip-shape configurations will depart from the traditional design practice of chordwise coincident elastic, aerodynamic, and mass centers, and thus will require more attention to deal with classical flutter.

9. At the same time, the most advanced unsteady aerodynamic research capabilities, focused on formulations for aeroelastic stability, should be directed at nonlinear problems of transonic flow and airfoil stall. In addition, a better understanding of the role of dynamic stall on rotor-blade flutter in forward flight is needed.

10. An excellent experimental data base has been obtained for small-scale, low-tip-speed hingeless and bearingless rotors and rotor-body systems. This data base should be expanded to include representative full-scale tip speeds and higher Reynolds numbers. Structural configurations should include examples of both simple

and complex blades. Emphasis should be on forward flight, but these models need to be fully tested in hover as well. Isolated rotors are best; the effects of rotor-body coupling are much more tractable analytically.

11. Rotor-blade flutter experiments should be conducted for configurations having significant chordwise offsets of aerodynamic, mass, and elastic centers to test new unsteady aerodynamic theories and gain experience with more advanced blade design concepts.

12. Full-scale rotor testing should be maintained to provide periodic exposure to the real world environment of aeroelastic stability.

13. Directed analysis assessment correlation exercises should be continued. These provide unique opportunities to address and correct unwarranted assumptions, derivation errors, coding errors, and other anomalies of individual analysis methods. To achieve maximum return, the causes of discrepant results need to be traced back to their source.

14. The tilt rotor is a key vehicle of the future. The technology base has grown enormously in the past 15 years, and it must continue to advance. Analyses tailored to the unique structural and aerodynamic features of the tilt rotor need to be pursued. Modeling compressible aerodynamics needs to be better understood and potential applications of active controls to improve stability characteristics should be pursued.

15. Research on the fundamental aeroelastic stability characteristics of bearingless rotors should continue. Notwithstanding the extensive results obtained to date, a sure formula for a damperless bearingless rotor has eluded the technical community. Research should continue in order to find a solution for this problem.

REFERENCES

1. Houbolt, John C.; and Brooks, George W.: Differential Equations of Motion for Combined Flapwise Bending, Chordwise Bending, and Torsion of Twisted Nonuniform Rotor Blades. NACA Report 1346, 1958.

2. Arcidiacono, P. J.: Steady Flight Differential Equations of Motion for a Flexible Helicopter Blade with Chordwise Mass Unbalance. USAAVLABS TR 68-18A, vol. 1, Feb. 1969.

3. Ormiston, R. A.; and Hodges, D. H.: Linear Flap-Lag Dynamics of Hingeless Helicopter Rotor Blades in Hover. J. Am. Helicopter Soc., vol. 17, no. 2, Apr. 1972, pp. 2-14.

4. Hodges, Dewey H.; and Ormiston, Robert A.: Nonlinear Equations for Bending of Rotating Beams with Applications to Linear Flap-Lag Stability of Hingeless Rotors. NASA TM X-2770, 1973.

5. Friedmann, P.; and Tong, P.: Dynamic Nonliner Elastic Stability of Helicopter Rotor Blades in Hover and in Forward Flight. NASA CR-114485. (Also TR 166-3, Massachusetts Institute of Technology, ASRL, Cambridge, Mass., May 1972.)

6. Hodges, Dewey Harper: Nonlinear Bending and Torsion of Rotating Beams with Application to Linear Stability of Hingeless Helicopter Rotors. Ph.D. thesis, Stanford University, Palo Alto, Calif., Dec. 1972.

7. Novozhilov, V. V.: Foundations of the Nonlinear Theory of Aeroelasticity. Translated ed., Graylock Press, Rochester, N.Y., 1953.*

8. Hodges, D. H.; and Dowell, E. H.: Nonlinear Equations of Motion for the Elastic Bending and Torsion of Twisted Nonuniform Rotor Blades. NASA TN D-7818, 1974.

9. Peters, David A.; and Ormiston, Robert A.: The Effects of Second Order Blade Bending on the Angle of Attack of Hingeless Rotor Blades. J. Am. Helicopter Soc., vol. 18, no. 4, Oct. 1973, pp. 45-48.

10. Dowell, E. H.: A Variational-Rayleigh-Ritz Modal Approach for Non-Uniform Twisted Rotor Blades Undergoing Large Bending and Torsional Motion. AMS Report No. 1193, Princeton University, Princeton, N.J., Nov. 1974.

*Research not derived from government or government-sponsored efforts.

11. Dowell, E. H.; and Traybar, J.: An Experimental Study of the Nonlinear Stiffness of a Rotor Blade Undergoing Flap, Lag, and Twist Deformations. AMS Report No. 1194, Princeton University, Princeton, N.J., 1975. (Also NASA CR-137968, 1975.)

12. Dowell, E. H.; and Traybar, J.: An Experimental Study of the Nonlinear Stiffness of a Rotor Blade Undergoing Flap, Lag, and Twist Deformations. AMS Report No. 1257, Princeton University, Princeton, N.J., 1975. (Also NASA CR-137969, 1975.)

13. Dowell, E. H.; Traybar, J.; and Hodges, D. H.: An Experimental Theoretical Correlation Study of Non-Linear Bending and Torsion Deformations of a Cantilever Beam. J. Sound and Vibration, vol. 50, no. 4, Feb. 22, 1977, pp. 533-544.

14. Hodges, Dewey H.; and Peters, David A.: On the Lateral Buckling of Uniform Slender Cantilever Beams. Int. J. Solids/Structures, vol. 11, no. 12, Dec. 1975, pp. 1269-1280.

15. Hodges, D. H.; and Ormiston, R. A.: Stability of Elastic Bending and Torsion of Uniform Cantilever Rotor Blades in Hover with Variable Structural Coupling. NASA TN D-8192, 1976.

16. Hodges, D. H.: Nonlinear Equations of Motion for Cantilever Rotor Blades in Hover with Pitch Link Flexibility, Twist, Precone, Droop, Sweep, Torque Offset, and Blade Root Offset. NASA TM X-73,112, 1976.

17. Hodges, Dewey H.; and Ormiston, Robert A.: Stability of Hingeless Rotor Blades in Hover with Pitch Link Flexibility. AIAA J., vol. 15, no. 4, Apr. 1977, pp. 475-482.

18. Srinivasan, A. V.; Cutts, D. G.; and Shu, H. T.: An Experimental Investigation of the Structural Dynamics of a Torsionally Soft Rotor in a Vacuum. NASA CR-177418, 1986.

19. Friedmann, Peretz: Influence of Structural Damping, Preconing, Offsets, and Large Deflections on the Flap-Lag-Torsional Stability of a Cantilevered Rotor Blade. AIAA Paper 75-780, Denver, Colo., 1975.

20. Friedmann, P.: Influence of Modeling and Blade Parameters on the Aeroelastic Stability of a Cantilevered Rotor. AIAA J., vol. 15, no. 2, Feb. 1977, pp. 149-158.

21. Friedmann, Peretz; and Reyna-Allende, M.: Aeroelastic Stability of Coupled Flap-Lag-Torsional Motion of Helicopter Rotor Blades in Forward Flight. AIAA Paper 77-455, San Diego, Calif., 1977.

22. Rosen, A.; and Friedmann, P.: Nonlinear Equations of Equilibrium for Elastic Helicopter or Wind Turbine Blades Undergoing Moderate Deformation. Report UCLA-ENG7718, U. California at Los Angeles, rev. June 1977. (Also NASA CR-159478, 1978.)

23. Rosen, Aviv; and Friedmann, Peretz P.: Nonlinear Equations of Equilibrium for Elastic Helicopter or Wind Turbine Blades Undergoing Moderate Deformation. NASA CR-159478, 1978.

24. Shamie, J.; and Friedmann, P.: Effect of Moderate Deflections on the Aeroelastic Stability of a Rotor Blade in Forward Flight. Paper No. 24, Proceedings of the 3rd European Rotorcraft and Powered Lift Aircraft Forum, Aix-en-Provence, France, Sept. 1977, pp. 24.1-24.37.

25. Friedmann, P. P.; and Kottapalli, S. B. R.: Rotor Blade Aeroelastic Stability and Response in Forward Flight. Paper No. 14, Proceedings of the 6th European Rotorcraft and Powered Lift Aircraft Forum, Sept. 1980, pp. 14.1-14.34.

26. Rosen, A.; and Friedmann, P.: The Nonlinear Behavior of Elastic Slender Straight Beams Undergoing Small Strains and Moderate Rotations. J. Appl. Mech., vol. 46, no. 1, Mar. 1979, pp. 161-168.

27. Hodges, Dewey H.: Discussion of The Nonlinear Behavior of Elastic Slender Straight Beams Undergoing Small Strains and Moderate Rotations. A. Rosen and P. Friedmann, eds. J. Appl. Mech., vol. 47, no. 3, Sept. 1980, p. 688.

28. Kaza, K. R.; and Kvaternik, R. G.: Nonlinear Aeroelastic Equations for Combined Flapwise Bending, Chordwise Bending, Torsion, and Extension of Twisted Nonuniform Rotor Blades in Forward Flight. NASA TM-74059, 1977.

29. Kvaternik, R. G.; White, W. F.; and Kaza, K. R.: Nonlinear Flap-Lag-Axial Equations of a Rotating Beam with Arbitrary Precone Angle. Proceedings of the AIAA SDM Conference, Bethesda, Md., Apr. 1978, pp. 214-227.

30. Crespo da Silva, M. R. M.: Flap-Lag Torsional Dynamic Modeling of Rotor Blades in Hover and in Forward Flight, Including the Effect of Cubic Nonlinearities. NASA CR-166194, 1981.

31. Crespo da Silva, Marcelo R. M.; and Hodges, Dewey H.: Nonlinear Flexure and Torsion of Rotating Beams with Application to Helicopter Rotor Blades. I. Formulation. Vertica, vol. 10, no. 2, 1986.

32. Crespo da Silva, Marcelo R. M.; and Hodges, Dewey H.: Nonlinear Flexure and Torsion of Rotating Beams with Application to Helicopter Rotor Blades. II. Results for Hover. Vertica, vol. 10, no. 2, 1986.

33. Kaza, K. R. V.; and Kvaternik, R. G.: A Critical Examination of the Flap-Lag Dynamics of Helicopter Rotor Blades in Hover and in Forward Flight. Paper No. 1034, 32nd Annual National V/STOL Forum of the American Helicopter Society, Washington, D.C., 1976.

34. Kvaternik, Raymond G.; and Kaza, Krishna R. V.: Nonlinear Curvature Expressions for Combined Flapwise Bending, Chordwise Bending, Torsion and Extension of Twisted Rotor Blades. NASA TM X-73997, 1976.

35. Hodges, D. H.; Ormiston, R. A.; and Peters, D. A.: On the Nonlinear Deformation Geometry of Euler-Bernoulli Beams. NASA TP-1566, 1980.

36. Alkire, K.: An Analysis of Rotor Blade Twist Variables Associated with Different Euler Sequences and Pretwist Treatments. NASA TM-84394, 1984.

37. Hodges, Dewey H.: Finite Rotation and Nonlinear Beam Kinematics. Vertica, vol. 11, no. 1/2, 1987, pp. 297-308.

38. Jonnalagadda, V. R. P.; and Pierce, G. Alvin: Nonlinear Deformation of Rotating Beams--An Alternative Method of Formulation. J. Am. Helicopter Soc., vol. 30, no. 2, Apr. 1985, pp. 68-70.*

39. Hodges, Dewey H.; Peters, David A.; Pierce, G. Alvin; and Jonnalagadda, V. R. P.: Comment on "Nonlinear Deformation of Rotating Beams--An Alternate Method of Formulation." Technical Note, J. Am. Helicopter Soc., July 1986.

40. Hodges, D. H.: Torsion of Pretwisted Beams Due to Axial Loading. J. Appl. Mech., vol. 47, no. 2, June 1980, pp. 393-397.

41. Rosen, Aviv: Discussion of "Torsion of Pretwisted Beams Due to Axial Loading." J. Appl. Mech., vol. 48, no. 3, Sept. 1981, pp. 697-780.*

42. Hodges, Dewey H.: Author's Closure to A. Rosen's Discussion of "Torsion of Pretwisted Beams Due to Axial Loading." J. Appl. Mech., vol. 48, no. 3, Sept. 1981, pp. 680-681.

43. Rosen, A.: Theoretical and Experimental Investigation of the Nonlinear Torsion and Extension of Initially Twisted Bars. J. Appl. Mech., vol. 50, no. 2, pp. 321-326, 1983.*

44. Petersen, D.: Interaction of Torsion and Tension in Beam Theory. Vertica, vol. 6, no. 4, 1982, pp. 311-325.*

45. Hodges, Dewey H.: Nonlinear Beam Kinematics for Small Strains and Finite Rotations. Vertica, vol. 11, no. 3, 1987, pp. 573-589.

46. Hodges, Dewey H: On the Extensional Vibrations of Rotating Bars. Int. J. Non-Linear Mech., vol. 12, no. 5, 1977, pp. 293-296.

47. Venkatesan, C.; and Nagaraj, V.T.: On the Axial Vibrations of Rotating Bars. J. Sound and Vibration, vol. 74, 1981, pp. 143-147.*

48. Venkatesan, C.; and Nagaraj, V.T.: Authors' Reply to Comments on "On the Axial Vibration of Rotating Bars" by D. H. Hodges. J. Sound and Vibration, vol. 87, no. 3, 1983, pp. 516-518.*

49. Hodges, Dewey H.: Comments on "On the Axial Vibration of Rotating Bars." J. Sound and Vib., vol. 87, no. 3, Apr. 8, 1983, pp. 513-515.

50. Degener, Manfred; Hodges, Dewey H; and Petersen, Dieter: Analytical and Experimental Study of Beam Torsional Stiffness with Large Elongation. To be published in J. Appl. Mech., 1987.

51. Kaza, K. R. V.; and Kielb, R. E.: Effects of Warping and Pretwist on Torsional Vibration of Rotating Beams. J. Appl. Mech., vol. 51, Dec. 1984, pp. 913-920.*

52. Stephens, Wendell B.; Hodges, Dewey H.; Avila, John H.; and Kung, Ru-Mei: Stability of Nonuniform Rotor Blades in Hover Using a Mixed Formulation. NASA TM-81226, 1980. (Also, AVRADCOM TR 80-A-10, Aug. 1980.)

53. Hodges, D. H.: Nonlinear Equations for Dynamics of Pretwisted Beams Undergoing Small Strains and Large Rotations. NASA TP-2470, 1985. (Also, AVSCOM TR 84-A-5, May 1985.)

54. Danielson, Donald A.; and Hodges, Dewey H.: Nonlinear Beam Kinematics by Decomposition of the Rotation Tensor. J. Appl. Mech., vol. 54, June 1987, pp. 258-262.

55. Bielawa, R. L.: Aeroelastic Analysis for Helicopter Rotor Blades with Time Variable, Nonlinear Structural Twist and Multiple Structural Redundancy--Mathematical Derivation and Program User's Manual. NASA CR-2638, 1976.

56. Bielawa, R. L.; Cheney, Jr.; M. C. and Novak, R. C.: Investigation of a Bearingless Helicopter Rotor Concept Having a Composite Primary Structure. NASA CR-2637, 1976.

57. Hodges, D. H.: Aeromechanical Stability of Helicopters with a Bearingless Main Rotor. Pt I: Equations of Motion. NASA TM-78459, 1978; Pt II: Computer Program. NASA TM-78460, 1978.

58. Hodges, D. H.: A Theoretical Technique for Analyzing Aeroelastic Stability of Bearingless Rotors. AIAA J., vol. 17, no. 4, Apr. 1979, pp. 400-407.

59. Sivaneri, N. T.; and Chopra, I.: Finite Element Analysis for Bearingless Rotor Blade Aeroelasticity. J. Am. Helicopter Soc., vol. 29, no. 2, Apr. 1984.

60. Hodges, Dewey H.; Hopkins, A. Stewart; Kunz, Donald L.; and Hinnant, Howard E.: Introduction to GRASP--General Rotorcraft Aeromechanical Stability Program--A Modern Approach to Rotorcraft Modeling. Proceedings of the 42nd Annual National Forum of the American Helicopter Society, Washington, D.C., 1986, pp. 739-756.

61. Hohenemser, K. H.; and Yin, S. K.: Finite Element Stability Analysis for Coupled Rotor and Support Systems. NASA CR-152024, 1977.

62. Friedmann, P. P.; and Straub, F.: Application of the Finite Element Method to Rotary-Wing Aeroelasticity. J. Am. Helicopter Soc., vol. 25, no. 1, Jan. 1980, pp. 36-44.

63. Straub, F. K.; and Friedmann, P. P.: A Galerkin Type Finite Element Method for Rotary-Wing Aeroelasticity in Hover and Forward Flight. Vertica, vol. 5, no. 1, 1981, pp. 75-98.

64. Straub, F. K.; and Friedmann, P. P.: Application of the Finite Element Method to Rotary Wing Aeroelasticity. NASA CR-165854, 1982.

65. Celi, R.; and Friedmann, P. P.: Aeroelastic Modeling of Swept Tip Rotor Blades Using Finite Elements. Proceedings of the 43rd Annual National Forum of the American Helicopter Society, St. Louis, Mo., 1987, pp. 257-269.

66. Sivaneri, N. T.; and Chopra, I.: Dynamic Stability of a Rotor Blade Using Finite Element Analysis. AIAA J., vol. 20, no. 5, May 1982, pp. 716-723.

67. Chopra, Interjit; and Sivaneri, Nithiam Ti: Aeroelastic Stability of Rotor Blades Using Finite Element Analysis. NASA CR-166389, 1982.

68. Hodges, Dewey H.: Vibration and Response of Nonuniform Rotating Beams with Discontinuities. J. Am. Helicopter Soc., vol. 24, no. 5, Oct. 1979, pp. 43-50.

69. Hodges, Dewey H.: Direct Solutions for Sturm-Liouville Systems with Discontinuous Coefficients. AIAA J., vol. 17, no. 8, Aug. 1979, pp. 924-926.

70. Hodges, Dewey H.; and Rutkowski, Michael J.: Free-Vibration Analysis of Rotating Beams by a Variable-Order Finite-Element Method. AIAA J., vol. 19, no. 11, Nov. 1981, pp. 1459-1466.

71. Hodges, Dewey H.: Orthogonal Polynomials as Variable-Order Finite Element Shape Functions. AIAA J., vol. 21, no. 5, May 1983, pp. 796-797.

72. Rehfield, L. W.; and Murthy, P. L. N.: Toward a New Engineering Theory of Bending: Fundamentals. AIAA J., vol. 20, no. 5, May 1982, pp. 693-699.*

73. Bauchau, O. A.: A Beam Theory for Anisotropic Materials. J. Appl. Mech., vol. 52, June 1985, pp. 416-422.*

74. Kosmatka, J.: Structural Dynamic Modeling of Nonisotropic Blades by the Finite Element Method. Ph.D. Dissertation, Mechanical, Aerospace, and Nuclear Engineering Department, University of California at Los Angeles, Los Angeles, Calif., Oct. 1986.*

75. Kim, Y. H.; and Lee, S. W.: A New Approach to Finite Element Modeling of Composite Helicopter Rotor Blades. Presented at the U.S. Army Research Office Workshop on Dynamics and Aeroelastic Stability Modeling of Rotor Systems, Georgia Institute of Technology, Atlanta, Ga., Dec. 1985.*

76. Rehfield, Lawrence W.: Design Analysis Methodology for Composite Rotor Blades. Seventh DOD/NASA Conference on Fibrous Composites in Structural Design, Denver, Colo., June 1985.*

77. Bauchau, O. A.: Composite Box Beam Analysis: Theory and Experiments. J. Reinforced Plastics and Composites, vol. 6, Jan. 1987, pp. 25-35.*

78. Hong, C.-H.; and Chopra, I.: Aeroelastic Stability Analysis of a Composite Rotor Blade. J. Am. Helicopter Soc., vol. 30, Apr. 1985, pp. 57-67.*

79. Coleman, Robert P.; and Feingold, Arnold M.: Theory of Self-Excited Mechanical Oscillation of Helicopter Rotors with Hinged Blades. NACA TR-1351, 1956.

80. Hohenemser, K. H.; and Yin, S. K.: Some Applications of the Method of Multiblade Coordinates. J. Am. Helicopter Soc., vol. 17, no. 3, July 1972, pp. 1-12.*

81. Cardinale, Salvatore V.: Soft In-Plane Matched-Stiffness/Flexure-Root-Blade Rotor System Summary Report. USAAVLABS TR 68-72, Aug. 1969.

82. Hammond, C. E.: An Application of Floquet Theory to the Prediction of Mechanical Instability. J. Am. Helicopter Soc., vol. 19, no. 4, Oct. 1974, pp. 14-23.

83. Johnston, R. A.; and Cassarino, S. J.: Aeroelastic Rotor Stability Analysis. USAAMRDL-TR-75-40, 1976.

84. Shamie, J.; and Friedmann, P.: Aeroelastic Stability of Complete Rotors with Application to a Teetering Rotor in Forward Flight. Paper No. 1031, 32nd Annual National V/STOL Forum of the American Helicopter Society, Washington, D.C., May 1976. (Also, J. Am. Helicopter Soc., Oct. 1977.)*

85. Johnson, Wayne: Aeroelastic Analysis for Rotorcraft in Flight or in a Wind Tunnel. NASA TN D-8515, 1977.

86. Ormiston, Robert A.: Aeromechanical Stability of Soft Inplane Hingeless Rotor Helicopters. Paper No. 25, 3rd European Rotorcraft and Powered Lift Aircraft Forum, Aix-en-Provence, France, Sept. 1977.

87. Ormiston, R. A.: Rotor-Fuselage Dynamic Coupling Characteristics of Helicopter Air and Ground Resonance. Proceedings of the AHS/NAI Conference, The Theoretical Basis of Helicopter Technology, Nanjing Aeronautical Institute, Nanjing, China, Nov. 1985.

88. Hodges, D. H.: An Aeromechanical Stability Analysis for Bearingless Rotor Helicopters. J. Am. Helicopter Soc., vol. 24, no. 1, Jan. 1979, pp. 2-9.

89. Staley, J. A.; Gabel, R.; and McDonald, H. I.: Full Scale Ground and Air Resonance Testing of the Army-Boeing Vertol Bearingless Main Rotor. Paper No. 79-23, Proceedings of the 35th Annual National Forum of the American Helicopter Society, May 1979.*

90. Dixon, P. C. G.: Design, Development, and Flight Demonstration of the Loads and Stability Characteristics of a Bearingless Main Rotor. USA AVRADCOM-TR-80-D-3, June 1980.

91. Hooper, W. Euan: Parametric Study of the Aeroelastic Stability of a Bearingless Rotor. NASA CP-2400, 1984.*

92. Warmbrodt, William; and Friedmann, Peretz: Formulation of the Aeroelastic Stability and Response ASD Problem of Coupled Rotor/Support Systems. AIAA Paper 79-0732, AIAA/ASME/ASCE/AHS 20th SDM Conference, St. Louis, Mo., 1979.

93. Warmbrodt, W.; and Friedmann, P.: Formulation of Coupled Rotor/Fuselage Equations of Motion. Vertica, vol. 3, no. 3, 1979, pp. 254-271.

94. Johnson, W.: A Comprehensive Analytical Model of Rotorcraft Aerodynamics and Dynamics. Pt I. Analysis Development. NASA TM-81182, 1980.

95. Johnson, Wayne: Development of a Comprehensive Analysis for Rotorcraft. I. Rotor Model and Wake Analysis. Vertica, vol. 5, no. 2, 1981, pp. 99-129.

96. Johnson, Wayne: Development of a Comprehensive Analysis for Rotorcraft. Pt II. Aircraft Model, Solution Procedure, and Applications. Vertica, vol. 5, no. 3, 1981, pp. 185-216.

97. Venkatesan, C.; and Friedmann, P. P.: Aeroelastic Effects in Multirotor Vehicles with Application to a Hybrid Heavy Lift System. Pt I. Formulation of Equations of Motion. NASA CR-3822, 1984.

98. Venkatesan, V.; and Friedmann, P. P.: Aeroelastic Effects in Multirotor Vehicles. Pt II. Methods of Solution and Results Illustrating Coupled Rotor/Body Aeromechanical Stability. NASA CR-4009, 1987.

99. Kvaternik, R. G.: Studies in Tilt Rotor VTOL Aircraft Aeroelasticity. NASA TM X-69496 and TM X-69497, 1973.

100. Kvaternik, R. G.; and Kohn, J. S.: An Experimental and Analytical Investigation of Proprotor Whirl Flutter. NASA TP 1047, 1977.

101. Johnson, W.: Dynamics of Tilting Proprotor Aircraft in Cruise Flight. NASA TN D-7677, 1974.

102. Johnson, W.: Analytical Model for Tilting Proprotor Aircraft Dynamics, Including Blade Torsion and Coupled Bending Modes, and Conversion Mode Operation. NASA TM X-62369, 1974.

103. Johnson, W.: The Influence of Engine/Transmission/Governor on Tilting Proprotor Aircraft Dynamics. NASA TM X-62455, 1975.

104. Johnson, W.: An Assessment of the Capability to Calculate Tilting Prop-Rotor Aircraft Performance, Loads, and Stability. NASA TP-2291, 1984.

105. Theodorsen, T.: General Theory of Aerodynamic Instability and the Mechanism of Flutter. NACA Report 496, 1949.

106. Loewy, R. G.: A Two Dimensional Approach to the Unsteady Aerodynamics of Rotary Wings. J. Aeronaut. Sci., vol. 24, no. 2, Feb. 1957, pp. 82-98.*

107. Greenberg, J. M.: Airfoil in Sinusoidal Motion in a Pulsating Stream. NACA TN-1326, 1947.

108. Johnson, W.: Application of Unsteady Airfoil Theory to Rotary Wings. J. Aircraft, vol. 17, no. 4, Apr. 1980, pp. 285-286.

109. Kaza, K. R. V.; and Kvaternik, R. G.: Application of Unsteady Airfoil Theory to Rotary Wings. J. Aircraft, vol. 18, no. 7, July 1981, pp. 604-605.

110. Friedmann, P.; and Yuan, C.: Effects of Modified Aerodynamic Strip Theories on Rotor Blade Aeroelastic Stability. AIAA J., vol. 15, no. 7, July 1977, pp. 932-940.

111. Peters, D. A.: Toward a Unified Model for Use in Rotor Blade Stability Analyses. J. Am. Helicopter Soc., vol. 30, July 1985, pp. 32-42.

112. Dinyavari, M. A. H.; and Friedmann, P. P.: Unsteady Aerodynamics in Time and Frequency Domains for Finite Time Arbitrary Motion of Rotary Wings in Hover and Forward Flight. AIAA Paper 84-0988, Proceedings AIAA/ASME/ASCE/AHS 25th SDM Conference, Palm Springs, Calif., May 1984, pp. 266-282.

113. Dinyavari, M. A. H.; and Friedmann, P. P.: Application of the Finite State Arbitrary Motion Aerodynamics to Rotor Blade Aeroelastic Response and Stability in Hover and Forward Flight. AIAA Paper 85-0763, Proceedings of AIAA/ASME/ASCE/AHS 26th SDM Conference, Orlando, Fla., Apr. 1985, pp. 522-535.

114. Friedmann, P. P.; and Venkatesan, C.: Finite State Modeling of Unsteady Aerodynamics and Its Application to a Rotor Dynamic Problem. Paper No. 72, Proceedings of the 11th European Rotorcraft Forum, London, Sept. 1985.

115. Venkatesan, C.; and Friedmann, P. P.: A New Approach to Finite State Modeling of Unsteady Aerodynamics. AIAA Paper 86-0865CP, Proceedings of AIAA/ASME/ASCE/AHS 27th SDM Conference, San Antonio, Tex., May 1986, pp. 178-191.

116. Friedmann, P. P.: Arbitrary Motion Unsteady Aerodynamics and Its Application to Rotary-wing Aeroelasticity. Proceedings of the 42nd Annual National Forum of the American Helicopter Society, Washington, D.C., June 1986, pp. 757-776.

117. Ormiston, R. A.; and Bousman, W. G.: A Study of Stall Induced Flap-Lag Instability of Hingeless Rotors. J. Am. Helicopter Soc., vol. 20, no. 1, Jan. 1975, pp. 20-30.

118. Rogers, J. P.: Application of an Analytic Stall Model to Time-History and Eigenvalue Analysis of Rotor Blades. J. Am. Helicopter Soc., vol. 29, Jan. 1984, pp. 25-33.*

119. Tran, C. T.; and Petot, D.: Semi-Empirical Model for the Dynamic Stall of Airfoils in View of the Application to the Calculation of Responses of a Helicopter Blade in Forward Flight. Vertica, vol. 5, no. 1, 1981, pp. 35-53.*

120. Miller, R. H.: Rotor Blade Harmonic Airloading. AIAA J., vol. 2, no. 7, July 1964, p. 1260.*

121. Dat, R.: La theorie de la surface portant appliquee a l'aile fixe et a l'helice. Rech. Aerospatiale No. 1973-4, Traduction ESRO-TT-90, 1974.*

122. Runyan, Harry L.; and Tai, Hsiang: Application of a Lifting Surface Theory for a Helicopter in Forward Flight. Vertica, vol. 10, no. 3/4, 1986, pp. 269-280.

123. Dat, R.: Development of Basic Methods Needed to Predict Helicopter Aeroelastic Behaviour. Vertica, vol. 8, no. 3, 1984, pp. 209-228.*

124. Tai, H.; and Runyan, Harry L.: Lifting Surface Theory for a Helicopter Rotor in Forward Flight. Second Decennial Specialists' Meeting on Rotorcraft Dynamics, AHS/NASA-Ames Research Center, Moffett Field, Calif., Nov. 1984.

125. Amer, K. B.: Theory of Helicopter Damping in Pitch or Roll and Comparison with Flight Measurements. NACA TN-2136, 1948.

126. Sissingh, G. J.: The Effect of Induced Velocity Variation on Helicopter Rotor Damping in Pitch or Roll. Aeronautical Research Council (Great Britain), Paper No. 101, Technical Note No. Aero. 2132, Nov. 1952.*

127. Curtiss, H. C., Jr.; and Shupe, N. K.: A Stability and Control Theory for Hingeless Rotors. 27th Annual National Forum of the American Helicopter Society, Washington, D.C., May 1971.*

128. Carpenter, P. J.; and Fridovich, B.: Effect of a Rapid Blade Pitch Increase on the Thrust and Induced Velocity Response of a Full Scale Helicopter Rotor. NASA TN-3044, 1953.

129. Kuczynski, W. A.; and Sissingh, C. J.: Research Program to Determine Rotor Response Characteristics at High Advance Ratios. NASA CR-114290, 1971.

130. Kuczynski, W. A.; and Sissingh, G. J.: Characteristics of Hingeless Rotors with Hub Moment Feedback Controls Including Experimental Rotor Frequency Response. NASA CR-114427 (Vol. I) and NASA CR-114428 (Vol. II), 1972.

131. Kuczynski, W. A.: Experimental Hingeless Rotor Characteristics at Full Scale First Flap Mode Frequencies. NASA CR-114519, 1972.

132. London, R. J.; Watts, G. A.; and Sissingh, G. J.: Experimental Hingeless Rotor Characteristics at Low Advance Ratio with Thrust. NASA CR-114684, 1973.

133. Peters, David A.; and Ormiston, Robert A.: Flapping Response Characteristics of Hingeless Rotor Blades by a Generalized Harmonic Balance Method. NASA TN D-7856, 1975.

134. Ormiston, Robert A.; and Peters, David A.: Hingeless Helicopter Rotor Response with Nonuniform Inflow and Elastic Blade Bending. J. Aircraft, vol. 9, no. 10, Oct. 1972, pp. 730-736.

135. Peters, David A.: Hingeless Rotor Frequency Response with Unsteady Inflow. Proceedings of the AHS/NASA Ames Specialists' Meeting on Rotorcraft Dynamics, NASA SP-352, 1974.

136. Crews, S. T.; Hohenemser, K. H.; and Ormiston, R. A.: An Unsteady Wake Model for a Hingless Rotor. J. Aircraft, vol. 10, no. 12, Dec. 1973, pp. 758-760.

137. Hohenemser, Kurt H.; and Crews, S. T.: Further Experiments with Progressing/ Regressing Rotor Flapping Modes. NASA CR-114711, 1973.

138. Hohenemser, Kurt H.; and Crews, S. T.: Model Tests on Unsteady Rotor Wake Effects. J. Aircraft, vol. 10, no. 1, Jan. 1973, pp. 58-60.

139. Hohenemser, K. H.; and Crews, S. T.: Experiments with a Four-Bladed Cyclic Pitch Stirring Model Rotor. NASA CR-137572, 1974.

140. Hohenemser, K. H.; and Crews, S. T.: Additional Experiments with a Four-Bladed Cyclic Pitch Stirring Model Rotor. NASA CR-137966, 1975.

141. Hohenemser, K. H.; Banerjee, D.: and Yin, S. K.: Methods Studies on System Identification from Transient Rotor Tests. NASA CR-137965, 1975.

142. Hohenemser, K. H.; Banerjee, D.; and Yin, S. K.: Rotor Dynamic State and Parameter Identification from Simulated Forward Flight Transients. NASA CR-137963, 1976.

143. Hohenemser, K. H.; Banerjee, D.; and Yin, S. K.: Rotor Dynamic State and Parameter Identification from Simulated Forward Flight Transients. NASA CR-137963, 1976.

144. Hohenemser, K. H.; and Crews, Sam T.: Unsteady Hovering Wake Parameters Identified from Dynamic Model Tests. NASA CR-152022, 1977.

145. Hohenemser, K. H.; and Banerjee, D.: Application of System Identification to Analytical Rotor Modeling from Simulated and Wind Tunnel Dynamic Test Data. NASA CR-152023, 1977.

146. Banerjee, D.; Crews, S. T.; Hohenemser, K. H.; and Yin, S. K.: Identification of State Variables and Dynamic Inflow from Rotor Model Dynamic Tests. J. Am. Helicopter Soc., vol. 22, no. 2, Apr. 1977, pp. 28-36.

147. Banerjee, D.; Crews, S. T.; and Hohenemser, K. H.: Parameter Identification Applied to Analytic Hingeless Rotor Modeling. J. Am. Helicopter Soc., vol. 24, no. 1, Jan. 1979, pp. 26-32.

148. Heyson, H. H.; and Katzoff, S.: Induced Velocities Near a Lifting Rotor with Non-Uniform Disk Loading. NASA TR-1319, 1957.

149. Ormiston, R. A.: An Actuator Disk Theory for Rotor Wake Induced Velocities. AGARD Specialists' Meeting on the Aerodynamics of Rotary Wings, Marseilles, France, AGARD CP-111, Sept. 1972, pp. 2-1 to 2-19.

150. Mangler, K. W.: Calculation of the Induced Velocity Field of a Rotor. Royal Aircraft Establishment Report No. 2247, London, Feb. 1948.*

151. Joglekar, M.; and Loewy, R.: An Actuator-Disk Analysis of Helicopter Wake Geometry and the Corresponding Blade Responses. USAAVLABS TR 69066, 1970.

152. Pitt, D. M.: Rotor Dynamic Inflow Derivatives and Time Constants from Various Inflow Models. Dissertation, Washington University, St. Louis, Mo., USATSARCOM TR 81-2, Dec. 1980.*

153. Pitt, D. M.; and Peters, D. A.: Theoretical Prediction of Dynamic Inflow Derivatives. Vertica, vol. 5, no. 1, Mar. 1981, pp. 21-34.*

154. Pitt, D. M.; and Peters, D. A.: Rotor Dynamic Inflow Derivatives and Time Constants from Various Inflow Models. Paper No. 55, 9th European Rotorcraft Forum, Stresa, Italy, Sept. 1983.*

155. Gaonkar, G.; and Peters, D.: Effectiveness of Current Dynamic-Inflow Models in Hover and in Forward Flight. J. Am. Helicopter Soc., vol. 31, Apr. 1986, pp. 47-57.*

156. Ormiston, R. A.: Application of Simplified Inflow Models to Rotorcraft Dynamic Analysis. J. Am. Helicopter Soc., vol. 21, no. 3, July 1976, pp. 34-39.

157. Peters, D. A.; and Gaonkar, G. H.: Theoretical Flap-Lag Damping with Various Dynamic Inflow Models. J. Am. Helicopter Soc., vol. 25, no. 3, July 1980, pp. 29-36.

158. Bousman, W. G.: An Experimental Investigation of the Effects of Aeroelastic Couplings on Aeromechanical Stability of a Hingeless Rotor Helicopter. J. Am. Helicopter Soc., vol. 26, no. 1, Jan. 1981, pp. 46-54.

159. Gaonkar, G. H.; Mitra, A. K.; Reddy, T. S. R.; and Peters, D. A.: Sensitivity of Helicopter Aeromechanical Stability to Dynamic Inflow. Vertica, vol. 6, no. 1, 1982, pp. 59-75.*

160. Johnson, Wayne: The Influence of Unsteady Aerodynamics on Hingeless Rotor Ground Resonance. NASA TM-81302, 1981. (Also USAAVRADCOM TR 81-B-16, July 1981.)*

161. Johnson, W.: Influence of Unsteady Aerodynamics on Hingeless Rotor Ground Resonance. J. Aircraft, vol. 29, no. 8, Aug. 1982, pp. 668-673.

162. Gaonkar, G. H.; Sastry, V. V. S. S.; and Reddy, T. S. R.: On the Adequacy of Modeling Dynamic Inflow for Helicopter Flap-Lag Stability. Paper No. 3.11, 8th European Rotorcraft Forum, Aix-en-Provence, France, 1982.*

163. Nagabhushanam, J.; and Gaonkar, G. H.: Rotorcraft Air Resonance in Forward Flight with Various Dynamic Inflow Models and Aeroelastic Couplings. Vertica, vol. 8, no. 4, 1984, pp. 373-394.*

164. Gaonkar, G. H.; and Peters, D. A.: Review of Dynamic Inflow Modeling for Rotorcraft Flight Dynamics, AIAA Paper 86-0845-CP, Proceedings of the AIAA/ASME/ASCE/AHS 27th SDM Conference, San Antonio, Tex., 1986.*

165. Nagabhushanam, J.; Gaonkar, G. H.; and Reddy, T. S. R.: Automatic Generation of Equations for Rotor-Body Systems with Dynamic Inflow for A Priori Ordering Schemes. Paper No. 37, Proceedings of the 7th European Rotorcraft Forum, Garmisch-Partenkirchen, Sept. 1981.*

166. Reddy, T. S. R.: Flap-Lag Damping of an Elastic Rotor Blade with Torsion and Dynamic Inflow in Hover from Symbolically Generated Equations. AIAA Paper 84-0989-CP, Palm Springs, Calif., 1984.

167. Reddy, T. S. R.; and Warmbrodt, W.: The Influence of Dynamic Inflow and Torsional Flexibility on Rotor Damping in Forward Flight from Symbolically Generated Equations. NASA CP-2400, 1984.

168. Reddy, T. S. R.: Symbolic Generation of Elastic Rotor Blade Equations Using a FORTRAN Processor and Numerical Study of Dynamic Inflow Effects on the Stability of Helicopter Rotors. NASA TM-86750, 1986.

169. Crespo da Silva, M. R. M.; and Hodges, D. H.: The Role of Computerized Symbolic Manipulation in Rotorcraft Dynamic Analysis. Computers and Mathematics with Applications, vol. 12A, no. 1, 1986, pp. 161-172.

170. Gaonkar, G. H.; Simha Prasad, D. S.; and Sastry, D.: On Computing Floquet Transition Matrices for Rotorcraft. J. Am. Helicopter Soc., vol. 26, no. 3, July 1981, pp. 56-61.*

171. Panda, B.; and Chopra, I.: Flap-Lag-Torsion Stability in Forward Flight. J. Am. Helicopter Soc., vol. 30, Oct. 1985, pp. 30-39.*

172. Schrage, Daniel P.; and Peters, David A.: Effect of Structural Coupling Parameters on the Flap-Lag Forced Response of a Rotor Blade in Forward Flight Using Floquet Theory. Vertica, vol. 3, no. 2, 1979, pp. 177-185.*

173. Friedmann, P.; and Shamie, J.: Aeroelastic Stability of Trimmed Helicopter Blades in Forward Flight. Vertica, vol. 1, no. 3, 1977, pp. 189-211.

174. Friedmann, P. P.; and Kottapalli, S. B. R.: Coupled Flap-Lag-Torsional Dynamics of Hingeless Rotors in Forward Flight. J. Am. Helicopter Soc., vol. 27, no. 4, Oct. 1982, pp. 28-36.

175. O'Malley, James A, III; Izadpanah, Amir P.; and Peters, D. A.: Comparisons of Three Numerical Trim Methods for Rotor Air Loads. Paper No. 58, Ninth European Rotorcraft Forum, Stresa, Italy, Sept. 1983.*

176. Friedmann, P. P.: Numerical Methods for Determining the Stability and Response of Periodic Systems with Application to Helicopter Rotor Dynamics and Aeroelasticity. Computers and Mathematics with Applications, vol. 12A, no. 1, 1986, pp. 131-148.*

177. Eipe, Abraham: Effect of Some Structural Parameters on Elastic Rotor Loads by an Iterative Harmonic Balance. Ph.D. Dissertation, Washington University, St. Louis, Mo., Dec. 1979.*

178. Wei, F.-S.; and Peters, D. A.: Lag Damping in Autorotation by a Perturbation Method. Paper No. 78-25, 34th Annual National Forum of the American Helicopter Society, Washington, D.C., 1978.*

179. Peters, D. A.; Kim, B. S.; and Chen, H. S.: Calculation of Trim Settings for a Helicopter Rotor by an Optimized Automatic Controller. J. Guidance, Control & Dynamics, vol. 7, no. 1, Jan.-Feb. 1984, pp. 85-91.*

180. Peters, David A.; and Izadpanah, Amir P.: Helicopter Trim by Periodic Shooting with Newton-Raphson Iteration. Proceedings of the 37th Annual National Forum of the American Helicopter Society, New Orleans, La., 1981, pp. 217-226.*

181. Hodges, Dewey H.: A Simplified Algorithm for Determining the Stability of Linear Systems. AIAA J., vol. 15, no. 3, Mar. 1977, pp. 424-425.

182. Peters, David A.; and Hohenemser, Kurt H.: Application of the Floquet Transition Matrix to Problems of Lifting Rotor Stability. J. Am. Helicopter Soc., vol. 16, no. 2, Apr. 1971, pp. 25-33.*

183. Friedmann, P.; and Silverthorn, L. J.: Aeroelastic Stability of Periodic Systems with Application to Rotor Blade Flutter. AIAA J., vol. 12, no. 11, Nov. 1974, pp. 1559-1565.

184. Friedmann, P.; Hammond, C. E.; and Woo, T.: Efficient Numerical Treatment of Periodic Systems with Application to Stability Problems. Int. J. Numerical Methods in Engineering, vol. 11, July 1977, pp. 1117-1136.

185. Peters, David A.: An Approximate Solution for the Free Vibrations of Rotating Uniform Cantilever Beams. NASA TM X-62,299, Sept. 1973.

186. Hodges, Dewey H.: An Approximate Formula for the Fundamental Frequency of Uniform Rotating Beams Clamped Off the Axis of Rotation. J. Sound and Vibration, vol. 77, no. 1, July 8, 1981, pp. 11-18.

187. Peters, D. A.; and Hodges, D. H.: In-Plane Vibration and Buckling of a Rotating Beam Clamped Off the Axis of Rotation. J. Appl. Mech., vol. 47, no. 2, June 1980, pp. 398-402.

188. Tong, Pin: The Nonlinear Instability in Flap-Lag of EE, PM Rotor Blades in Forward Flight. NASA CR-114524, 1971.

189. Friedmann, P.; and Tong, P.: Nonlinear Flap Lag Dynamics of Hingeless Helicopter Blades in Hover and in Forward Flight. J. Sound and Vibration, vol. 30, no. 1, 1973, pp. 9-31.

190. Johnson, Wayne: A Perturbation Solution of Helicopter Rotor Flapping Stability. NASA TM X-62,165, 1972.

191. Johnson, Wayne, A Perturbation Solution of Rotor Flapping Stability. Paper No. 72-955, AIAA 2nd Atmospheric Flight Mechanics Conference, Palo Alto, Calif., Sept. 1972.

192. Johnson, Wayne: A Perturbation Solution of Helicopter Rotor Flapping Stability. J. Aircraft, vol. 10, no. 5, May 1973, pp. 257-258.

193. Johnson, Wayne: Perturbation Solutions for the Influence of Forward Flight on Helicopter Rotor Flapping Stability. NASA TM X-62,361, 1974.

194. Yin, Sheng-Kuang; and Hohenemser, Kurt H.: The Method of Multiblade Coordinates in the Linear Analysis of Lifting Rotor Dynamic Stability and Gust Response at High Advanced Ratio. Paper No. 512, 27th Annual National V/STOL Forum of the American Helicopter Society, Washington, D.C., May 1971.

195. Hohenemser, K. H.; and Yin, S. K.: Analysis of Gust Alleviation Methods and Rotor Dynamics Stability. NASA CR-114387, 1971.

196. Hohenemser, Kurt H.; and Yin, S. K.: Effects of Blade Torsion, of Blade Flap Bending Flexibility and of Rotor Support Flexibility on Rotor Stability and Random Response. NASA CR-114480, 1972.

197. Biggers, J. C.: Some Approximations to the Flapping Stability of Helicopter Rotors. J. Am. Helicopter Soc., vol. 14, no. 4, Oct. 1974, pp. 24-33.

198. Young, M. I.: A Theory of Rotor Blade Motion Stability in Powered Flight. J. Am. Helicopter Soc., vol. 9, no. 3, July 1964.*

199. Hohenemser, K. H.; and Heaton, P. W.: Aeroelastic Instability of Torsionally Rigid Helicopter Blades. J. Am. Helicopter Soc., vol. 12, no. 2, Apr. 1967, pp. 1-13.*

200. Young, Maurice I., Dr.: A Simplified Theory of Hingeless Rotors with Application to Tandem Helicopters. Proceedings of the 18th Annual National Forum of the American Helicopter Society, Washington, D.C., May 1962.*

201. Curtiss, H. C., Jr.: Sensitivity of Hingeless Rotor Blade Flap-Lag Stability in Hover to Analytical Modeling Assumptions. AMS Report No. 1236, Princeton University, Princeton, N.J., 1975. (Also, NASA CR-137967, 1975.)

202. Ormiston, R. A.: Techniques for Improving the Stability of Soft-Inplane Hingeless Rotors. NASA TM X-62390, 1974.

203. Peters, David A.: An Approximate Closed-Form Solution for Lead-Lag Damping of Rotor Blades in Hover. NASA TM X-62,425, 1975.

204. Kaza, K. R. V.; and Kvaternik, R. G.: Examination of the Flap-Lag Stability of Rigid Articulated Rotor Blades. J. Aircraft, vol. 16, no. 12, Dec. 1979.

205. Tong, Pin: Nonlinear Instability of a Helicopter Blade. Paper No. 72-956, AIAA 2nd Atmospheric Flight Mechanics Conference, Palo Alto, Calif., Sept. 1972.

206. Friedmann, Peretz: Investigation of Some Parameters Affecting the Stability of a Hingeless Helicopter Blade in Hover. NASA CR-114525, 1972.

207. Friedmann, P.: Aeroelastic Instabilities of Hingeless Helicopter Blades. J. Aircraft, vol. 10, no. 10, Oct. 1973, pp. 623-631.

208. Friedmann, P.: Some Conclusions Regarding the Aeroelastic Stability of Hingeless Helicopter Blades in Hover and in Forward Flight. J. Am. Helicopter Soc., vol. 18, no. 4, Oct. 1973, pp. 13-23.

209. Ormiston, Robert A.; and Hodges, Dewey H.: Discussion of Some Conclusions Regarding the Aeroelastic Stability of Hingeless Helicopter Blades in Hover and Forward Flight. J. Am. Helicopter Soc., vol. 20, no. 3, July 1975, pp. 46-47.

210. White, William F., Jr.: Importance of Helicopter Dynamics to the Mathematical Model of the Helicopter. AGARD Flight Mechanics Panel, Specialists' Meeting, LARC, Nov. 1974.

211. Kunz, Donald L.: Effects of Unsteady Aerodynamics on Rotor Aeroelastic Stability. NASA TM-78,434, 1977.

212. Friedmann, P.; and Silverthorn, L. J.: Aeroelastic Stability of Coupled Flap-Lag Motion of Hingeless Helicopter Blades at Arbitrary Advance Ratios. NASA CR-132,431, 1974.

213. Friedmann, P.; and Silverthorn, L. J.: Flap-Lag Dynamics of Hingeless Helicopter Blades at Moderate and High Advance Ratios. Presented at AHS/NASA Ames Specialists' Meeting on Rotorcraft Dynamics, Feb. 13-15, 1974.

214. Friedmann, P.; and Silverthorn, L. J.: Aeroelastic Stability of Coupled Flap-Lag Motion of Hingeless Helicopter Blades at Arbitrary Advance Ratios. J. Sound and Vibration, vol. 39, no. 4, 1975, pp. 409-428.

215. Peters, D. A.: Flap-Lag Stability of Helicopter Rotor Blades in Forward Flight. J. Am. Helicopter Soc., vol. 20, no. 4, Oct. 1975, pp. 2-13.

216. Gaonkar, G. H.; and Peters, D. A.: Use of Multiblade SIU Coordinates for Helicopter Flap-Lag Stability with Dynamic Inflow. J. Aircraft, vol. 17, no. 2, Feb. 1980, pp. 112-118.*

217. Shamie, J.; and Friedmann, P.: Aeroelastic Stability of Complete Rotors with Application to a Teetering Rotor in Forward Flight. J. Sound and Vibration, vol. 53, no. 4, Aug. 1977, pp. 559-584.

218. Reddy, T. S. R.; and Warmbrodt, William: Forward Flight Aeroelastic Stability from Symbolically Generated Equations. J. Am. Helicopter Soc., vol. 31, no. 3, July 1986, pp. 35-54.

219. Ormiston, Robert A.; and Bousman, William G.: A Theoretical and Experimental Investigation of Flap-Lag Stability of Hingeless Helicopter Rotor Blades. Presented at the 8th Army Science Conference, West Point, N.Y., June 1972.

220. Ormiston, Robert A.; and Bousman, William G.: A Theoretical and Experimental Investigation of Flap-Lag Stability of Hingeless Helicopter Rotor Blades. NASA TM X-62,179, 1972.

221. Bousman, W. G.; Sharpe, D. L.; and Ormiston, R. A.: An Experimental Study of Techniques for Increasing the Lead-Lag Damping of Soft Inplane Hingeless Rotors. Paper No. 1035, 32nd Annual National V/STOL Forum of the American Helicopter Society, Washington, D.C., May 1976.

222. Curtiss, H. C., Jr.; and Putman, W. F.: An Experimental Investigation of the Flap-Lag Stability of a Hingeless Rotor with Comparable Levels of Hub and Blade Stiffness in Hovering Flight. NASA CR-151924, 1976.

223. Gaonkar, G. H.; McNulty, M. J.; and Nagabhushanam, J.: An Experimental and Analytical Investigation of Isolated Rotor Flap-Lag Stability in Forward Flight. Paper No. 66, 11th European Rotorcraft Forum, London, England, Sept. 1985.

224. Miller, R. H.; and Ellis, C. W.: Helicopter Blade Vibration and Flutter. J. Am. Helicopter Soc., vol. 1, no. 3, July 1956, pp. 19-38.*

225. Hodges, D. H.; and Ormiston, R. A.: Stability of Elastic Bending and Torsion of Uniform Cantilevered Rotor Blades in Hover. AIAA Paper 73-405, Proceedings of 14th AIAA/ASME/ASCE/AHS SDM Conference, Williamsburg, Va., Mar. 20-22, 1973.

226. Johnson, Wayne: Flap/Lag/Torsion Dynamics of a Uniform, Cantilever Rotor Blade in Hover. NASA TM 73,248, 1977.

227. Chopra, I.; and Johnson, W.: Flap-Lag-Torsion Aeroelastic Stability of Circulation-Controlled Rotors in Hover. J. Am. Helicopter Soc., vol. 24, no. 2, Apr. 1979.

228. Chopra, I.: Dynamic Analysis of Constant-Lift and Free Tip Rotor. J. Am. Helicopter Soc., vol. 28, Jan. 1983, pp. 24-33.

229. Pierce, G. Alvin; and White, William F., Jr.: Unsteady Rotor Aerodynamics at Low Inflow and Its Effects on Flutter. AIAA Paper 72-959, Palo Alto, Calif., 1972.

230. Sharpe, David L.: An Experimental Investigation of the Flap-Lag-Torsion Aeroelastic Stability of a Small-Scale Hingeless Helicopter Rotor in Hover. NASA TP-2546, 1986. (Also, AVSCOM TR 850A-9, Jan. 1986.)

231. Peterson, Randall L.; and Warmbrodt, William: Hover Test of a Full-Scale Hingeless Helicopter Rotor: Aeroelastic Stability, Peformance, and Loads Data. NASA TM-85892, 1984.

232. Warmbrodt, W.; and Peterson, R. L.: Hover Test of a Full-Scale Hingeless Rotor. NASA TM-85990, 1984.

233. Warmbrodt, William; and Peterson, Randall L.: Hover Test of a Full-Scale Hingeless Rotor. Paper No. 68, Tenth European Rotorcraft Forum, The Hague, Netherlands, Aug. 1984.

234. Astill, Clifford J.; and Niebanck, Charles F.: Prediction of Rotor Instability at High Forward Speeds. Vol. II Classical Flutter. USAAVLABS TR-68-18B, Feb. 1969.

235. Carta, Franklin O.; and Niebanck, Chares F.: Prediction of Rotor Instability at High Forward Speeds. Vol. III. Stall Flutter. USAAVLABS TR-68-18C, Feb. 1969.

236. Niebanck, Charles F.; and Elman, H. L.: Prediction of Rotor Instability at High Forward Speeds. Vol. IV. Torsional Divergence. USAAVLABS TR-68-18D, Feb. 1969.

237. Elman, H. L.; Niebanck, Charles F.; and Bain, Lawrence J.: Prediction of Rotor Instability at High Forward Speeds. Vol. V. Flapping and Flap-Lag Instability. USAAVLABS TR-68-18E, Feb. 1969.

238. Niebanck, Charles F.; and Bain, Lawrence J.: Rotor Aeroelastic Instability and Transient Characteristics. USAAVLABS TR-69-88, Feb. 1970.

239. Lytwyn, R. T.; and Miao, W.: Airborne and Ground Resonance of Hingeless Rotors. Paper No. 414, 26th Annual National Forum of the American Helicopter Society, Washington, D. C., 1970.*

240. Hohenemser, Kurt H.; and Yin, S. K.: The Effects of Some Rotor Feedback Systems on Rotor-Body Dynamics. NASA CR-114709, 1973.

241. Hohenemser, K. H.; and Yin, S. K.: On the Use of First Order Rotor Dynamics in Multiblade Coordinates. Paper No. 831, 30th Annual National Forum of the American Helicopter Society, Washington, D.C., 1974.

242. Hohenemser, K. H.; and Yin, S. K.: Methods Studies Toward Simplified Rotor-Body Dynamics. NASA CR-137570, 1974.

243. Ormiston, Robert A.: Concepts for Improving Hingeless Rotor Stability. Presented at the AHS Mideast Region Symposium on Rotor Technology, Essington, Pa., Aug. 1976.

244. Johnson, Wayne: Calculated Dynamic Characteristics of a Soft-Inplane Hingeless Rotor Helicopter. NASA TM-73,262, 1977.

245. Straub, F. K.; and Warmbrodt, W.: The Use of Active Controls to Augment Rotor/Fuselage Stability. J. Am. Helicopter Soc., vol. 30, July 1985, pp. 13-22.

246. Venkatesan, C.; and Friedmann, P.: Aeromechanical Stability Analysis of a Hybrid Heavy Lift Multirotor Vehicle in Hover. J. Aircraft, vol. 22, Nov. 1985, pp. 965-972.

247. Burkam, John E.; and Miao, Wen-Liu: Exploration of Aeroelastic Stability Boundaries with a Soft-in-Plane Hingeless-Rotor Model. Paper No. 610, 28th Annual National Forum of the American Helicopter Society, Washington, D.C., May 1972.*

248. Bousman, William G.: An Experimental Investigation of Hingeless Helicopter Rotor-Body Stability in Hover. NASA TM-78489, 1978. (Also, AVRADCOM TR 78-17 (AM), June 1978.)

249. Bousman, W. G.; and Hodges, D. H.: An Experimental Study of Coupled Rotor-Body Aeromechanical Instability of Hingeless Rotors in Hover. Vertica, vol. 3, no. 3/4, 1979, pp. 221-244.

250. Friedmann, P. P.; and Venkatesan, C.: Coupled Rotor/Body Aeromechanical Stability Comparison of Theoretical and Experimental Results. J. Aircraft, vol. 22, Feb. 1985, pp. 148-155.

251. Friedmann, P. P.; and Venkatesan, C.: Influence of Unsteady Aerodynamic Models on Aeromechanical Stability in Ground Resonance. J. Am. Helicopter Soc., vol. 31, Jan. 1986, pp. 65-74.

252. Yeager, W. T.; Hamouda, M. H.; and Mantay, W. R.: Aeromechanical Stability of a Hingeless Rotor in Hover and Forward Flight: Analysis and Wind Tunnel Tests. NASA TM-85653, 1983. (Also, AVRADCOM TR 83-B-5, Aug. 1983.)

253. Yeager, W. T. Jr.; Hamouda, M. H.; and Mantay, W. R.: Aeromechanical Stability of a Hingeless Rotor in Hover and Forward Flight: Analysis and Wind Tunnel Tests. Paper No. 54, Proceedings of the 9th European Rotorcraft Forum, Stresa, Italy, Sept. 1983.

254. Chen, C.; Staley, J. A.; Miao, W.: and Harris, F. D.: Aeroelastic Stability Test Results for a 1/5.86 Scale Model of a Bearingless Main Rotor System on the BO-105 Helicopter. Boeing Vertol Company Report D210-11245-1, July 1977.

255. Warmbrodt, W.; McCloud, J. L. III; Sheffler, M.; and Staley, J.: Full-Scale Wind-Tunnel Test of the Aeroelastic Stability of a Bearingless Main Rotor. Vertica, vol. 6, no. 3, 1982, pp. 165-180.

256. Dawson, S.: An Experimental Investigation of the Stability of a Bearingless Model Rotor in Hover. J. Am. Helicopter Soc., vol. 28, no. 4, Oct. 1983, pp. 29-34.

257. Bousman, W. G.; and Dawson, S.: Experimentally Determined Flutter from Two- and Three-Bladed Model Bearingless Rotors in Hover. J. Am. Helicopter Soc., vol. 31, July 1986, pp. 45-53.

258. Weller, William W.: Correlating Measured and Predicted Inplane Stability Characteristics for an Advanced Bearingless Rotor. NASA CR-166280, 1982.

259. Weller, W. H.: Correlation and Evaluation of Inplane Stability Characteristics for an Advanced Bearingless Main Rotor Model. NASA CR-166448, 1983.

260. Weller, W. H.; and Peterson, R. L.: Inplane Stability Characteristics for an Advanced Bearingless Main Rotor Model. J. Am. Helicopter Soc., vol. 29, no. 3, July 1984, pp. 45-53.

261. Mychalowycz, Evhen M.: Integrated Technology Rotor/Flight Research Rotor Preliminary Design. AVSCOM TR-86-D-8, Mar. 1987.

262. Reed, W. H., III; and Bland, S. R.: An Analytical Treatment of Aircraft Propeller Precession Instability. NASA TN D-659, 1961.

263. Houbolt, J. C.; and Reed, W. H., III: Propeller-Nacelle Whirl Flutter. J. Aeronaut. Sci., vol. 29, no. 3, Mar. 1962.

264. Reed, W. H., III: Review of Propeller-Rotor Whirl Flutter. NASA TR R-264, 1967.

265. Young, M. I.; and Lytwyn, R. T.: The Influence of Blade Flapping Restraint of the Dynamic Stability of Low Disk Loading Propeller-Rotors. J. Am. Helicopter Soc., vol. 12, no. 4, Oct. 1967.*

266. Hall, W. E., Jr.: Prop-Rotor Stability at High Advance Ratios. J. Am. Helicopter Soc., vol. 11, no. 2, Apr. 1966.*

267. Edenborough, H. K: Investigation of Tilt Rotor VTOL Aircraft Rotor-Pylon Stability. J. Aircraft, vol. 5, no. 6, Mar. 1968.*

268. Kvaternik, Raymond G.: Experimental and Analytical Studies in Tilt-Rotor Aeroelasticity. Presented at AHS/NASA Ames Research Center Specialists' Meeting on Rotorcraft Dynamics, Moffett Field, Calif., Feb. 1974.

269. Kvaternik, Raymond G.: A Review of Some Tilt-Rotor Aeroelastic Research at NASA-Langley. J. Aircraft, vol. 18, no. 5, May 1976, pp. 357-363.

270. Johnson, W.: Theory and Comparison with Tests of Two Full-Scale Prop-Rotors. NASA SP-352, 1974.

271. Johnson, W.: Analytical Modeling Requirements for Tilting Proprotor Aircraft Dynamics. NASA TN D-8013, 1975.

272. Johnson, W.: The Influence of Pitch-Lag Coupling on the Predicted Aeroelastic Stability of the XV-15 Tilting Proprotor Aircraft. NASA TM X-73213, Feb. 1977.

273. Alexander, H. R.; Hengen, L. M.; and Weiberg, J. A.: Aeroelastic Stability Characteristics of a V/STOL Tilt-Rotor Aircraft with Hingeless Blades: Correlation of Analysis and Test. J. Am. Helicopter Soc., vol. 20, no. 2, Apr. 1975.

274. Johnson, W.: Assessment of Aerodynamic and Dynamic Models in a Comprehensive Analysis for Rotorcraft. Computers and Mathematics, May 1985.

275. Research and Technology, 1985 Annual Report of the Langley Research Center. NASA TM-87623, 1985.

276. Popelka, D.; Sheffler, M.; and Bilger, J.: Correlation of Stability Test Results and Analysis for the 1/5-Scale V-22 Aeroelastic Model. J. Am. Helicopter Soc., vol. 32, no. 2, Apr. 1987.*

277. ITR Methodology Assessment Workshop. Proceedings of the U.S. Army Research & Technology Laboratory (AVRADCOM) and NASA Ames Research Center Conference, Moffett Field, Calif., June 1983 (to be published).

278. Donham, R. E.; and Cardinale, S. V.: Flight Test and Analytical Data for Dynamics and Loads in a Hingeless Rotor. U.S. Army Contract DAAJ01-73-C-0286, Lockheed Report LR 26215, Dec. 1973.

279. Johnston, J. F.; and Conner, F.: The Reactionless In-Plane Mode of Stiff-In-Plane Hingeless Rotors. LR 26214, Lockheed-California Company, Dec. 1973.

280. Johnston, J. F.; and Cook, J. R.: AH-56A Vehicle Development. Paper No. 574, 27th Annual National Forum of the American Helicopter Society, Washington, D.C., May 1971.*

281. Anderson, W. D.: Investigation of Reactionless Mode Stability Characteristics of a Stiff In-Plane Hingeless Rotor System. AHS Preprint No. 734, 29th Annual National Forum of the American Helicopter Society, Washington, D.C., 1973.*

282. Anderson, W. D.; and Johnston, J. F.: Comparison of Flight Data and Analysis for Hingeless Rotor Regressive Inplane Mode Stability. NASA SP-352, 1974.*

283. Hughes, Charles W.; and Wernicke, Rodney K.: Flight Test of a Hingeless Flexbeam Rotor System, USAAMRDL-TR-74-38, June 1974.

284. White, Bill; and Weller, William: The Flexhinge Rotor. American Helicopter Society Mideast Region Symposium on Rotor Technology, Essington, Pa., Aug. 1976.

285. Cresap, Wesley L.; Myers, Alan W.; and Viswanathan, Sathy P.: Design and Development Tests of a Four-Bladed Light Helicopter Rotor System. Paper No. 78-7, 34th Annual National Forum of the American Helicopter Society, Washington, D.C., May 1978.*

286. White, B. P.: Predesign Study of the Flexhinge Rotor for the Rotor Systems Research Aircraft. NASA CR-145162, July 1977.

287. Donham, R. E.; Cardinale, S. V.; and Sachs, I. B.: Ground and Air Resonance Characteristics of a Soft In-Plane Rigid Rotor System. J. Am. Helicopter Soc., vol. 14, no. 4, Oct. 1969.

288. Swindlehurst, Carl E., Jr.: Development of the Composite Bearingless Main Rotor System. Paper presented at the American Helicopter Society Mideast Regional Symposium on Rotor Technology, Essington, Pa., Aug. 1976.

289. Advanced System Design Study of a Composite Structures Rotor. NASA CR-145092, 1977.

290. Harris, Franklin D.; Cancro, Patrick A.; and Dixon, Peter G. C.: The Bearingless Main Rotor. Paper No. 4, 3rd European Rotorcraft and Powered-Lift Aircraft Forum, Aix-en-Provence, France, Sept. 1977.

291. Staley, James A.; and Reed, Donald A.: Aeroelastic Stability and Vibration Characteristics of a Bearingless Main Rotor. Boeing Vertol Document D210-11498-1, Vols. I,II, June 1979.

292. Sheffler, Marc; Staley, James; Hoover, James; Sovjak, Cheryl; and White, Fred: Full Scale Wind Tunnel Investigation of a Bearingless Main Helicopter Rotor Final Report. NASA CR-152373, 1980.

293. Warmbrodt, William; and McCloud, John L. III: A Full-Scale Wind Tunnel Investigation of a Helicopter Bearingless Main Rotor. NASA TM-81321, 1981.

294. Sheffler, M.; Warmbrodt, W.; and Staley, J.: Evaluation of the Effect of Elastomeric Damping Material on the Stability of a Bearingless Main Rotor System. American Helicopter Society Mideast Region Meeting on Rotor System Design, Philadelphia, Pa., Oct. 1980.

295. Bousman, William G.; Ormiston, Robert A.; and Mirick, Paul H.: Design Considerations for Bearingless Rotor Hubs. Paper No. A-83-39-62-1000, presented at the 39th Annual National Forum of the American Helicopter Society, St. Louis, Mo., 1983.

296. Carlson, Raymond G.; and Miao, Wen-Liu: Aeroelastic Analysis of the Elastic Gimbal Rotor. NASA CR-166287, 1981. (Also, USAAVRADCOM TR 82-A-3, May 1981.)

297. Gaffey, T. M.: The Effect of Positive Pitch-Flap Coupling (Negative w3) on Rotor Blade Motion Stability and Flapping. J. Am. Helicopter Soc., vol. 14, no. 2, Apr. 1969.*

298. Gaffey, T. M.; Yen, J. G.; and Kvaternik, R. G.: Analysis and Model Tests of the Proprotor Dynamics of a Tilt-Proprotor VTOL Aircraft. Air Force V/STOL Technology and Planning Conference, Las Vegas, Nev., Sept. 1969.

299. Johnson, W.: Predicted Dynamic Characteristics of the XV-15 Tilting Proprotor Aircraft in Flight and in the 40- by 80-Foot Wind Tunnel. NASA TM X-73158, 1976.

300. Marr, R. L.; Blackman, S.; Weiberg, J. A.; and Schroers, L. G.: Wind Tunnel and Flight Test of the XV-15 Tilt Rotor Research Aircraft. Paper No. 79-54, 35th Annual National Forum of the American Helicopter Society, Washington, D.C., 1979.

301. Bilger, J. M.; Marr, R. L.; and Zahedi, A.: Results of Structural Dynamic Testing of the XV-15 Tilt Rotor Research Aircraft. J. Am. Helicopter Soc., vol. 27, no. 2, Apr. 1982.*

302. Popelka, David; Sheffler, Marc; and Bilger, Jim: Correlation of Stability Test Results and Analysis for the 1/5 Scale V-22 Aeroelastic Model. Paper presented at the 41st Annual National Forum of the American Helicopter Society, Fort Worth, Tex., 1985.*

303. Johnson, W.; Lau, B. H.; and Bowles, J. V.: Calculated Performance, Stability, and Maneuverability of High-Speed Tilting Prop-Rotor Aircraft. NASA TM-88349, 1986.

304. Watts, G. A.; London, R. J.; and Snoddy, R. J.: Trim, Control, and Stability of a Gyro-Stabilized Hingeless Rotor at High Advance Ratio and Low Rotor Speed. NASA CR-114362, 1971.

305. Maloney, P. F.; and Porterfield, J. D.: Elastic Pitch Beam Tail Rotor. TR 76-35, U.S. Army Air Mobility R&D Lab, 1976.

306. Edwards, W. T.; and Miao, W.: Bearingless Tail Rotor Loads and Stability. Boeing Vertol Co. Report No. D210-11025-1 (USAAMRDL TR-76-16), 1976.

307. Full-Scale Wind Tunnel Investigation of the Advancing Blade Concept Rotor System. USAAVLABS Technical Report 7-25, U.S. Army Aviation Material Laboratories, Fort Eustis, Va., Aug. 1971.

308. Advancing Blade Concept (ABC) Technology Demonstrator. Applied Technology Laboratory, U.S. Army Research and Technology Laboratories (AVRADCOM), Fort Eustis, VA., Apr. 1977.

309. Chopra, Inderjit: Flap-Lag-Torsion Flutter Analysis of a Constant Lift Rotor. NASA CR-152244, Jan. 1979.

310. Chopra, I.: Dynamic Analysis of a Free-Tip Rotor. 1) Paper No. 81-0618-CP, presented at AIAA/ASME/ASCE/AHS 22nd SDM Conference, Atlanta, Ga., Apr. 6-10, 1981.

TABLE 1.- TECHNOLOGY BACKGROUND FOR ROTORCRAFT AEROELASTIC STABILITY: PRE-1970 PERIOD COMPARED WITH POST-1970

APPLICATIONS / TECHNOLOGY	PRE 1970	POST 1970
BLADE STABILITY	ARTICULATED/ TEETERING MODERATE SPEED BENDING-TORSION FLUTTER WAKE FLUTTER	HINGELESS/BEARINGLESS TILT ROTOR BENDING-TORSION FLUTTER WAKE FLUTTER FLAP-LAG TORSION FLOQUET THEORY
BEAM EQUATIONS	LINEAR ISOTROPIC MATERIALS	NONLINEAR MULTIPLE LOAD PATH STRUCTURES COMPOSITE MATERIALS
UNSTEADY AERODYNAMICS	2-D AERODYNAMICS THEODORSEN/LOEWY	2-D/3-D AERO THEODORSEN/LOEWY DYNAMIC INFLOW DYNAMIC STALL TRANSONIC AERO
GROUND RESONANCE AIR RESONANCE	CLASSICAL GROUND RESONANCE	COMPLEX/AEROMECHANICAL GROUND RESONANCE AIR RESONANCE HOVER, FORWARD FLIGHT

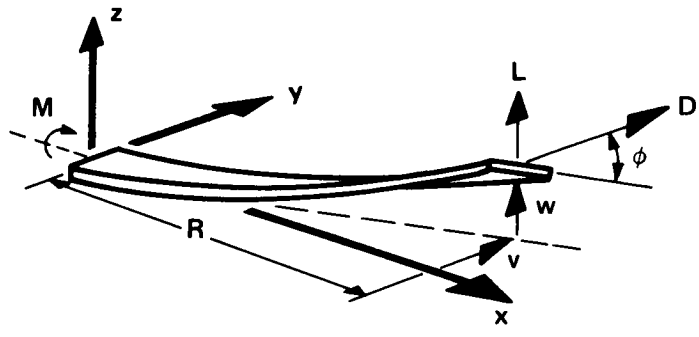

Figure 1.- Nonlinear torsion of an elastic cantilever beam resulting from simultaneous flapwise and chordwise bending.

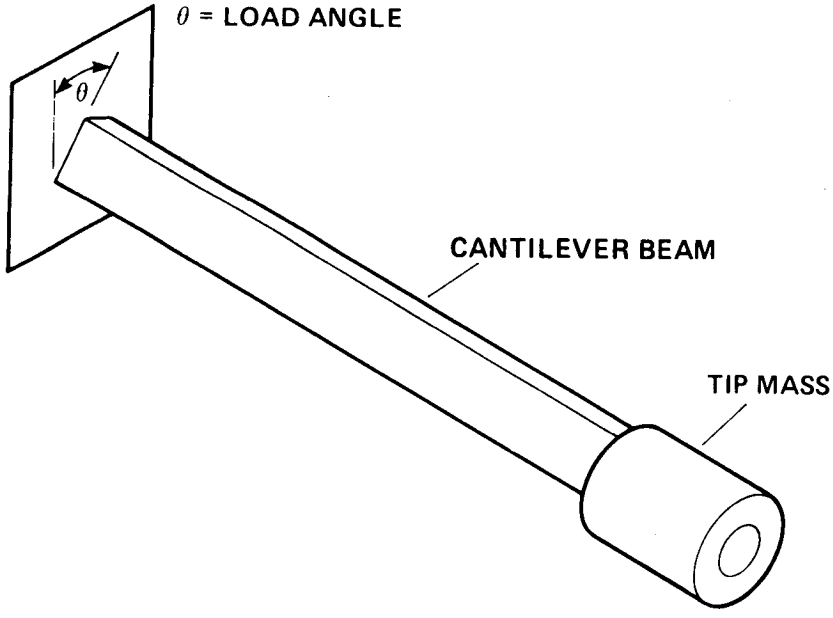

Figure 2.- Experimental arrangement for inducing nonlinear torsion by subjecting an elastic cantilever beam to combined flatwise and edgewise bending by varying load angle of tip-mass gravity force.

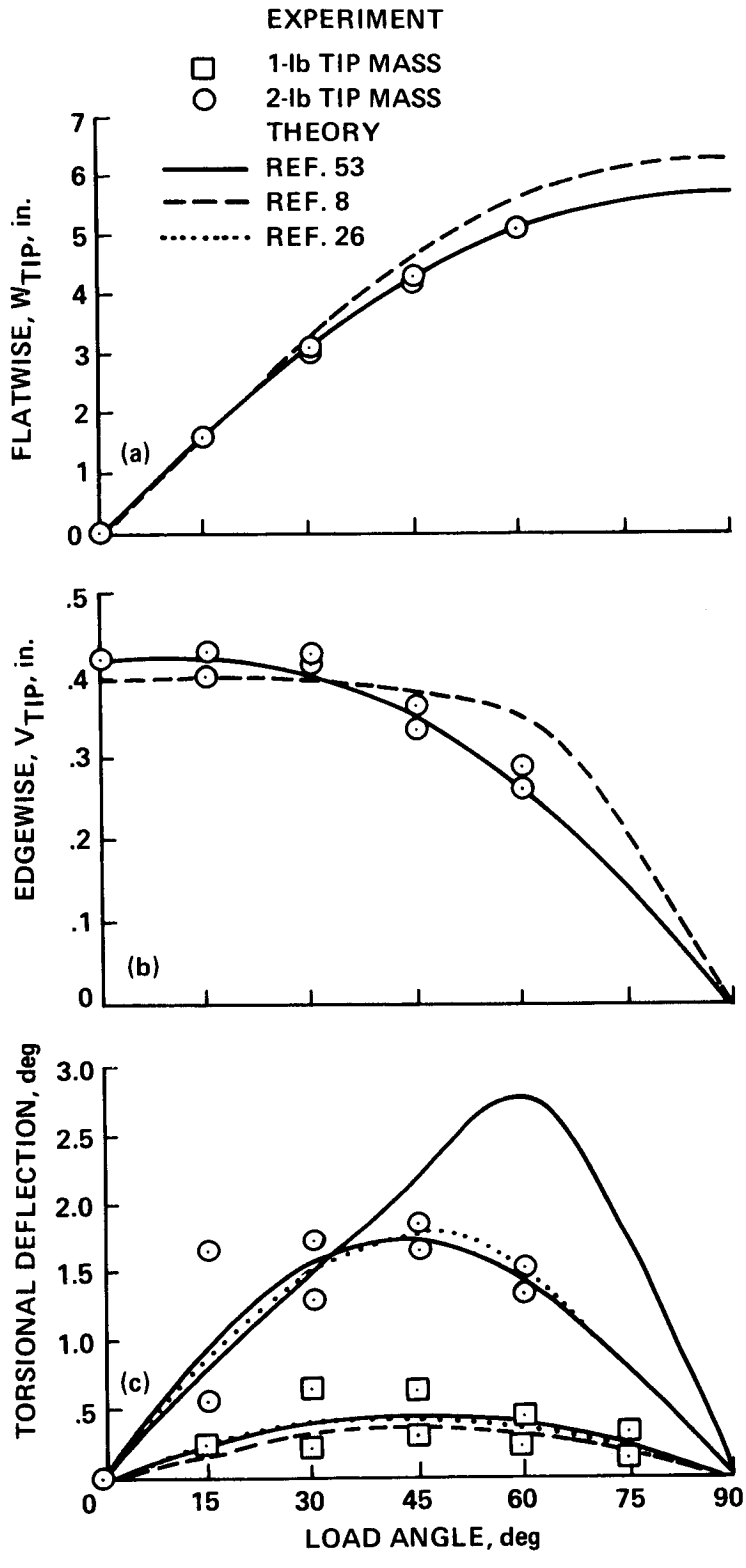

Figure 3.- Static deflections of Princeton beam compared with theoretical predictions. (a) Flatwise deflection. (b) Edgewise deflection. (c) Torsion deflection.

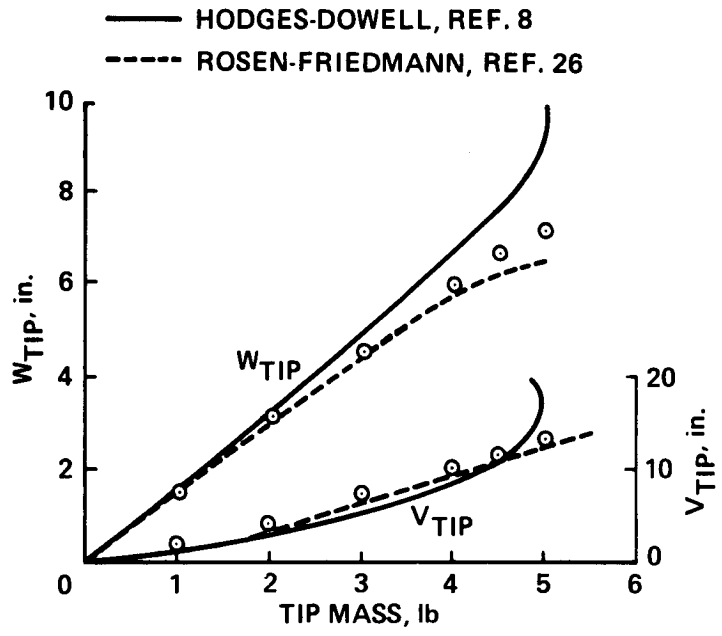

Figure 4.- Static flatwise and edgewise deflections of Princeton beam compared with theoretical predictions for 30° load angle.

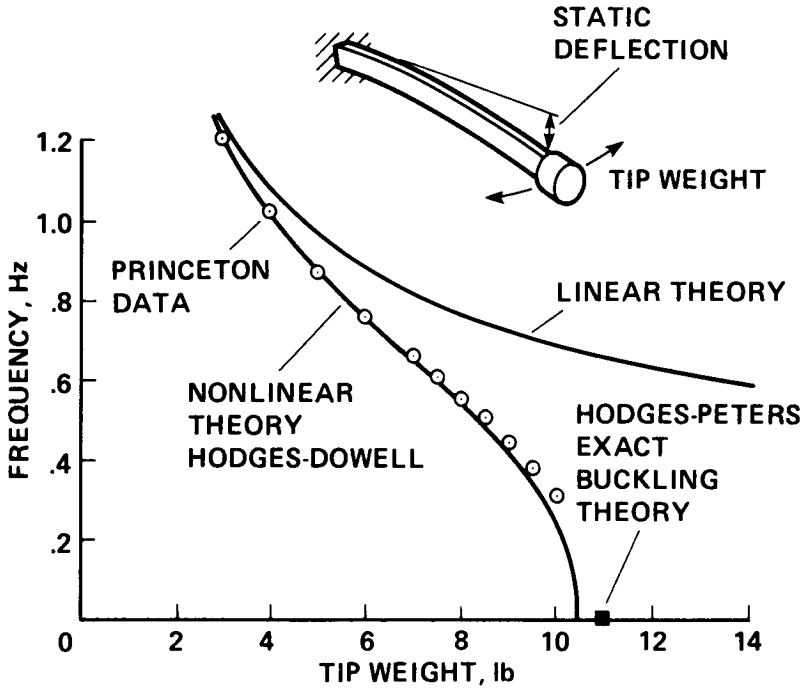

Figure 5.- Flatwise bending frequency of Princeton beam as a function of static edgewise loading together with nonlinear buckling.

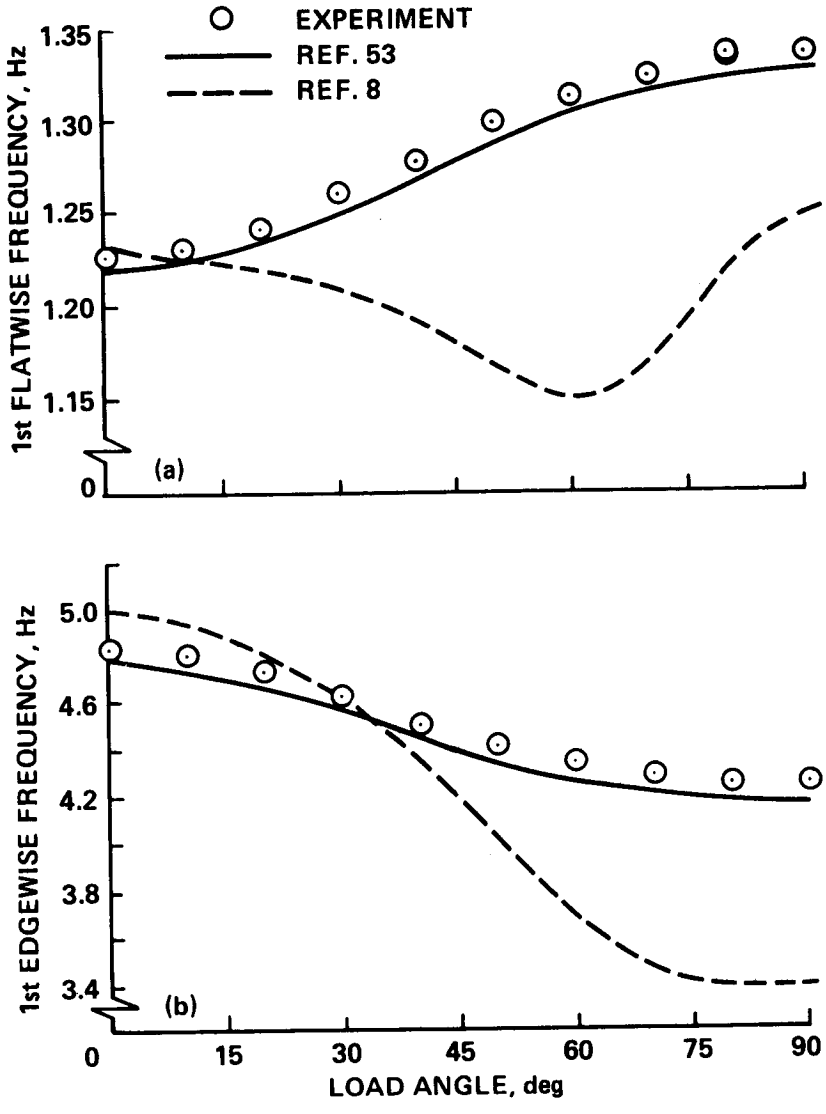

Figure 6.- Bending frequencies of Princeton beam as a function of load angle compared with theoretical predictions; 2-lb tip mass. (a) Flatwise frequency. (b) Edgewise frequency.

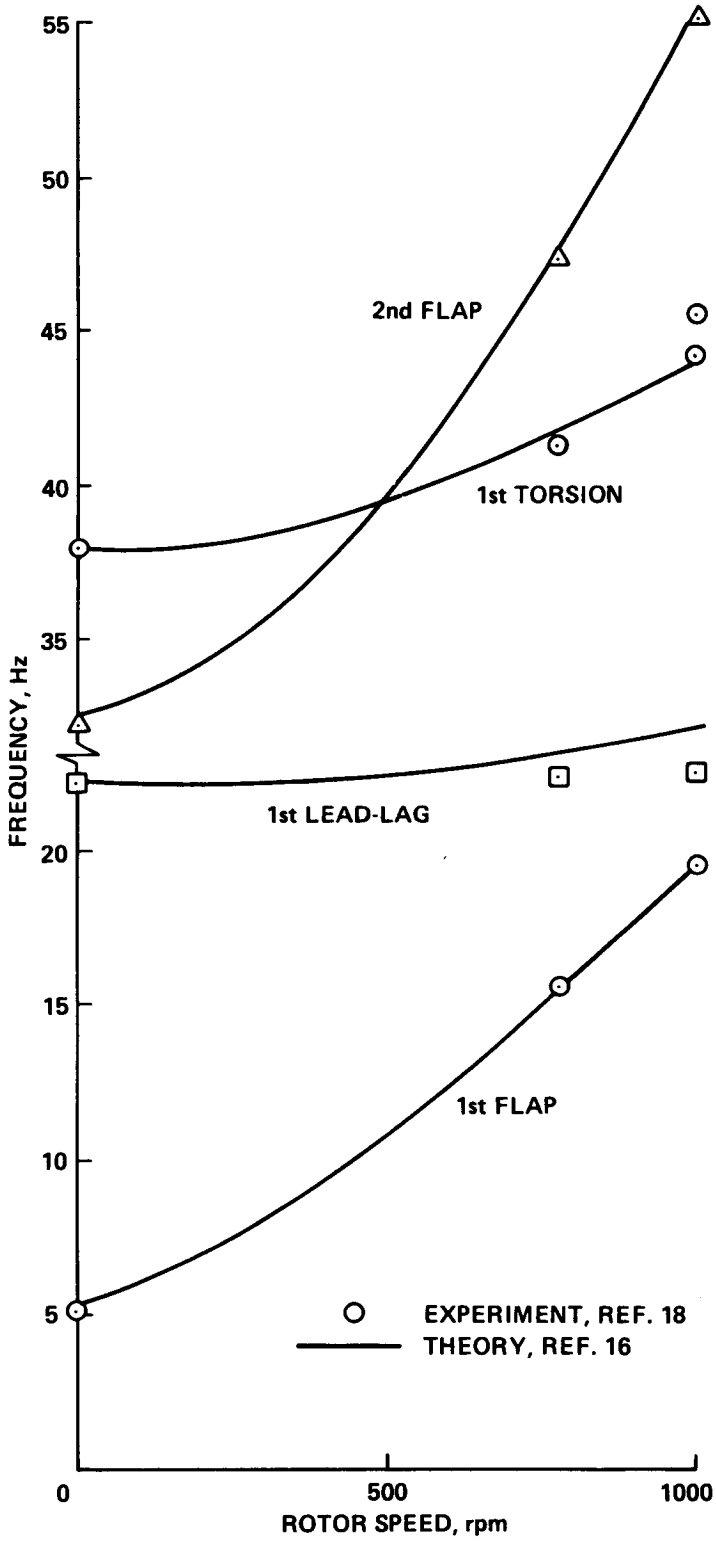

Figure 7.- Comparison of experimental and theoretical natural frequencies of a uniform cantilever elastic blade rotating in vacuum.

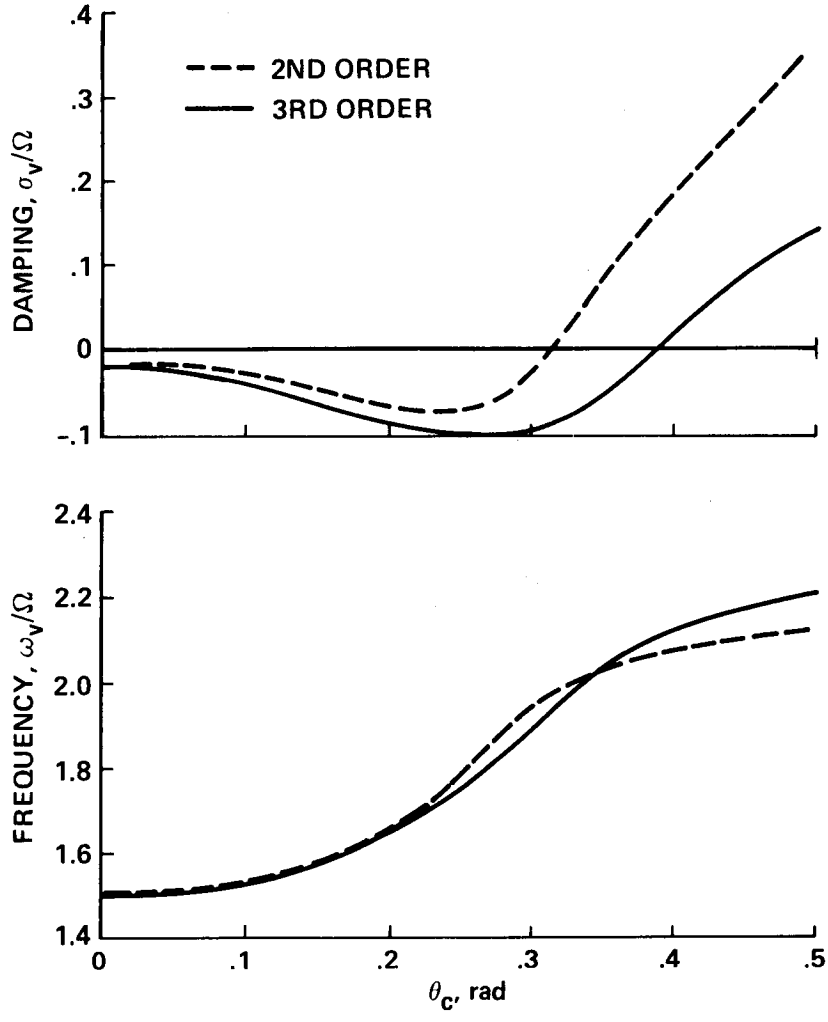

Figure 8.- Effect of third-order terms in elastic beam bending-torsion equations on predicted stiff-inplane rotor-blade lead-lag mode damping and frequency versus blade collective pitch, $\bar{\omega}_w = 1.15$, $\bar{\omega}_v = 1.5$, $\bar{\omega}_\phi = 2.5$.

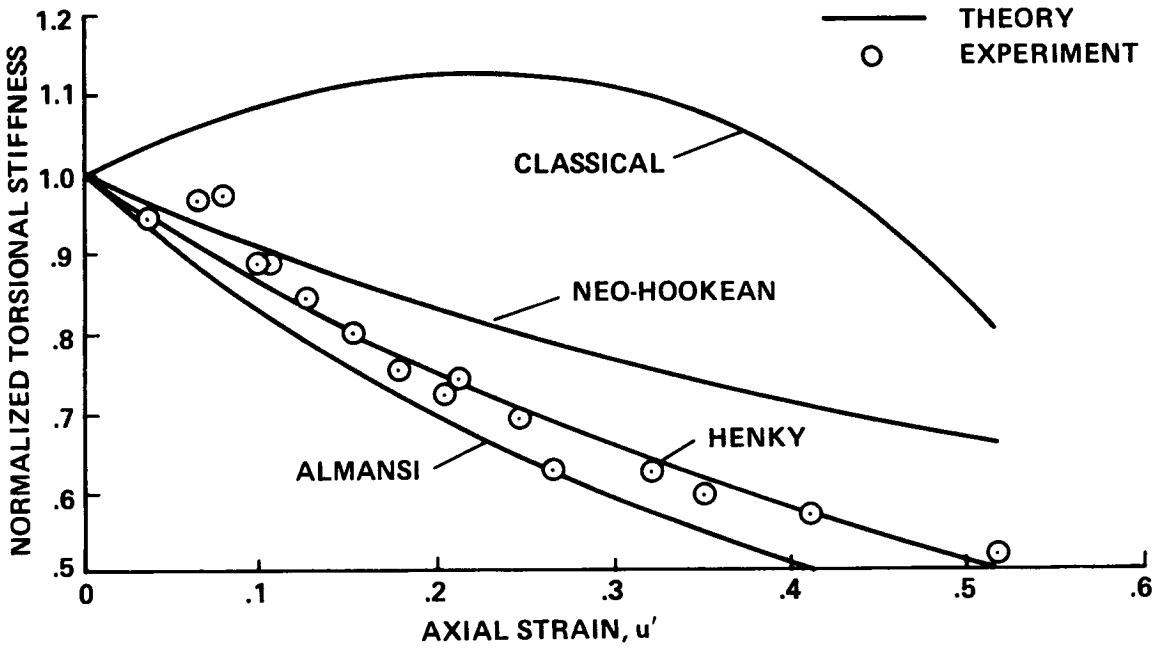

Figure 9.- The effect of axial strain on torsional stiffness for a beam of circular cross section.

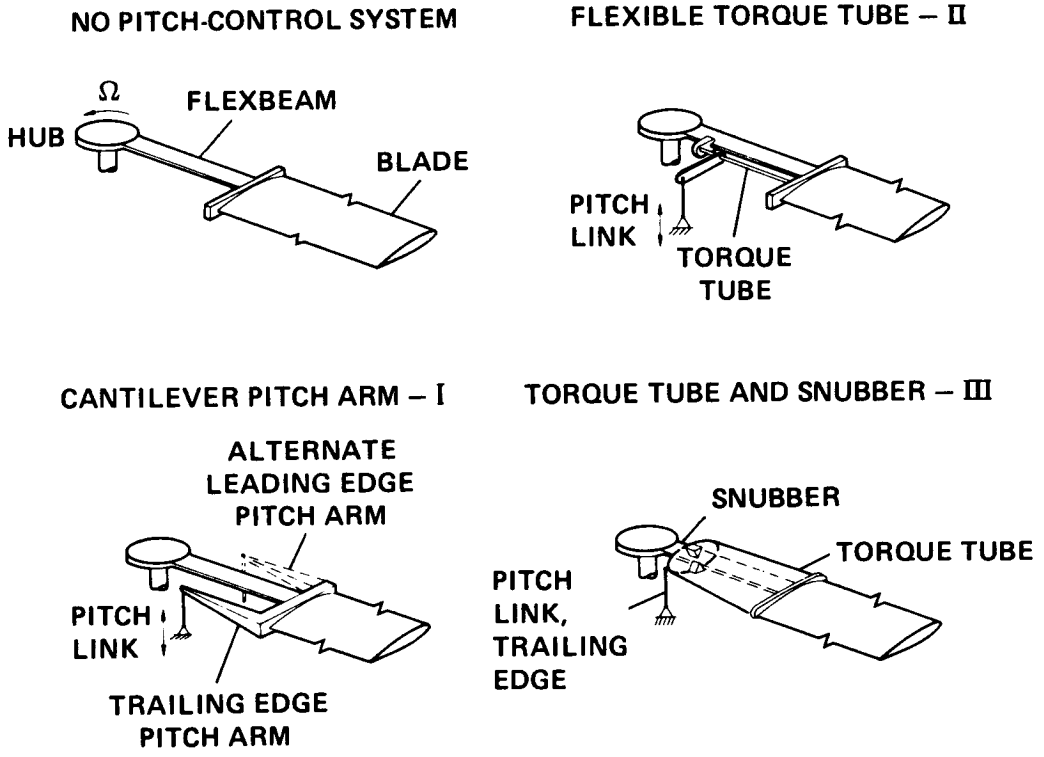

Figure 10.- Principal configurations for bearingless rotor blade pitch-control systems.

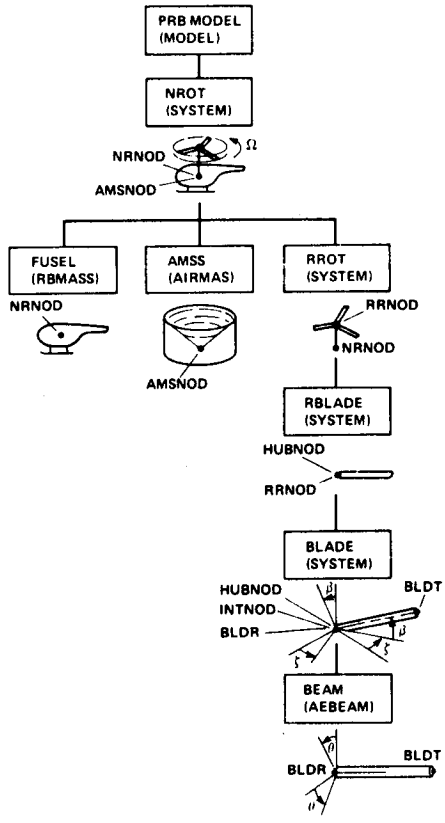

Figure 11.- Modeling a rotorcraft system with the elements and subsystems of GRASP.

Figure 12.- Lockheed 7.5-ft-diam hingeless rotor model installed in Aeroflightdynamics Directorate 7- by 10-ft wind tunnel.

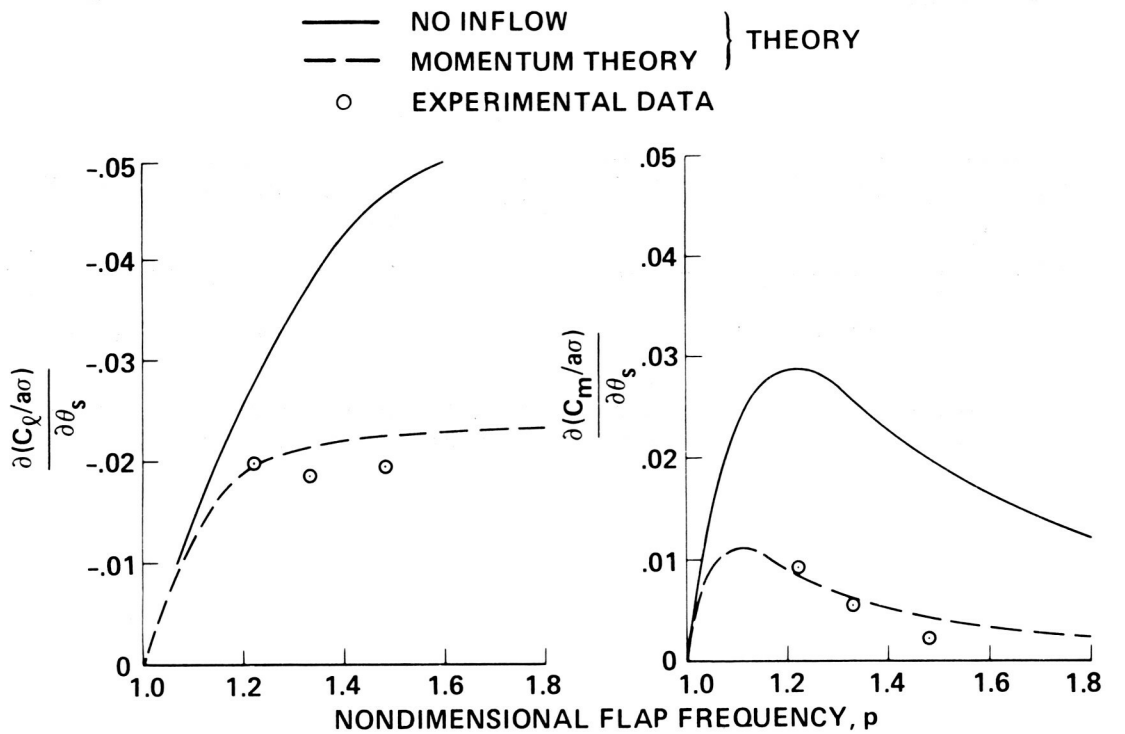

Figure 13.- Effect of dynamic inflow on static hub moment response derivatives of a hingeless rotor in hover at 4° collective pitch.

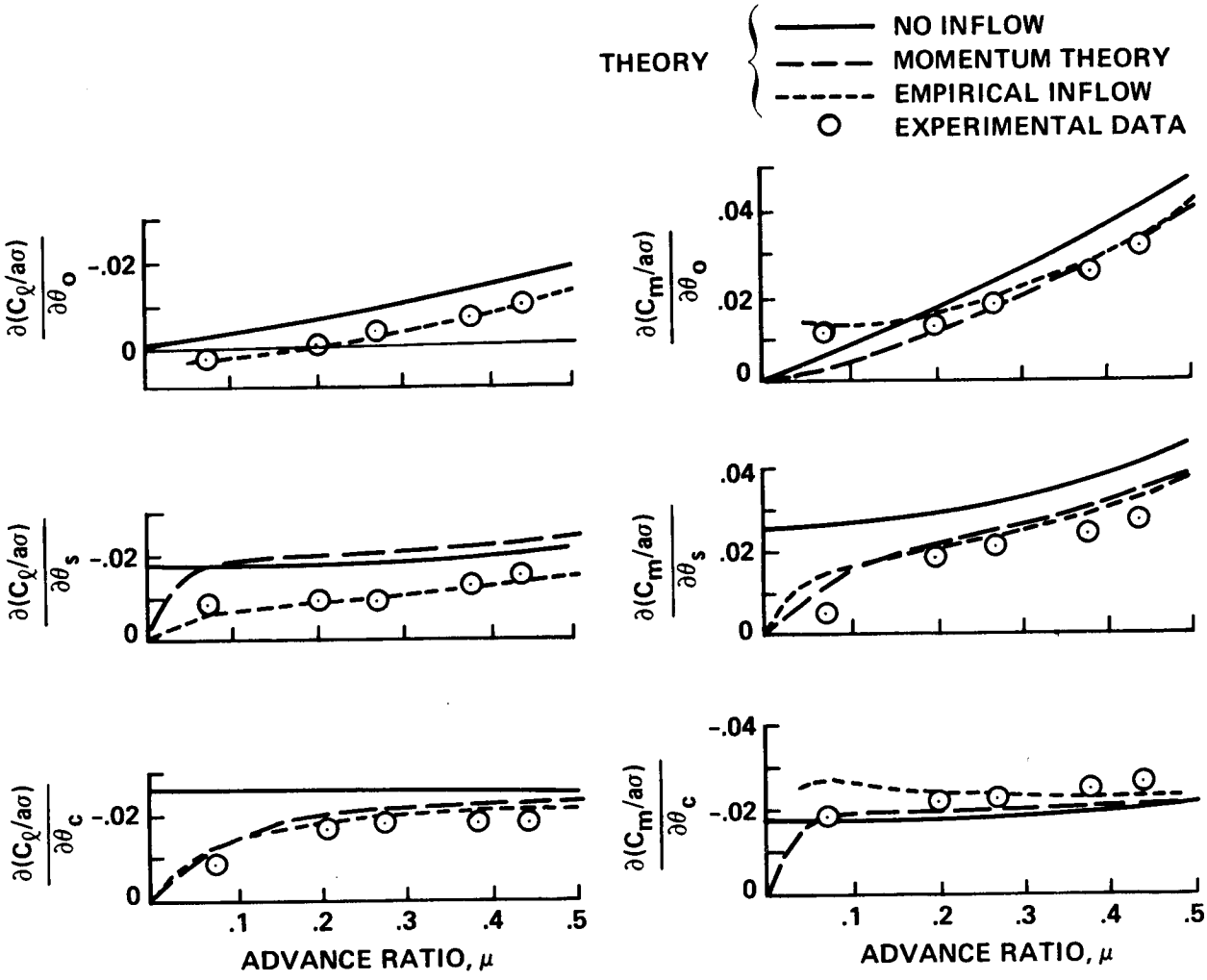

Figure 14.- Effect of dynamic inflow on static hub moment response derivatives of a hingeless rotor in forward flight at 0° collective pitch.

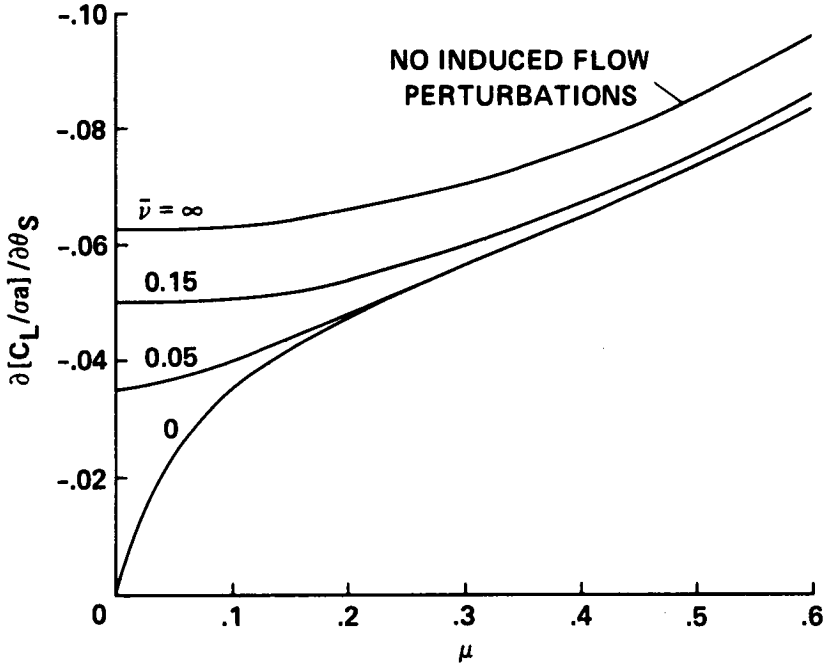

Figure 15.- Effect of mean inflow and advance ratio (contained within static inflow model) on a typical rotor hub moment response derivative.

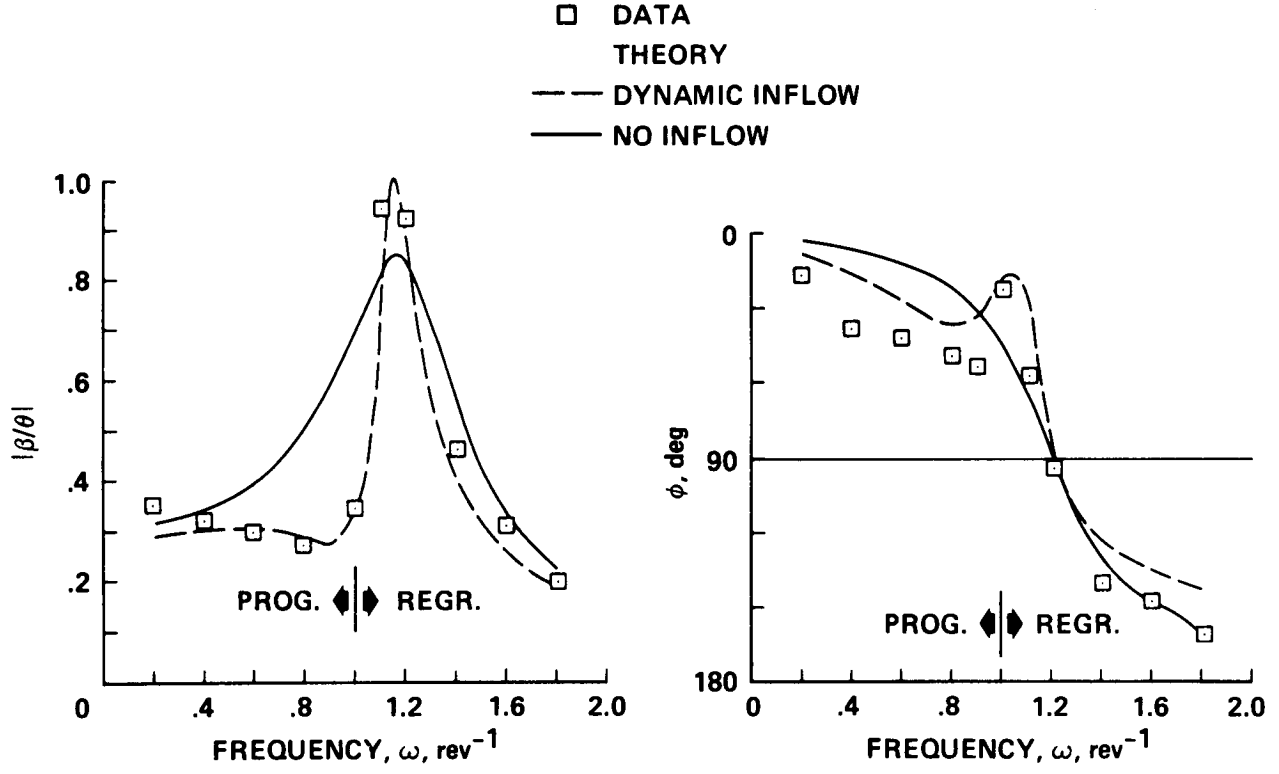

Figure 16.- Effect of dynamic inflow on frequency response of blade flapping to blade pitch excitation of a hovering rotor at 2° collective pitch.

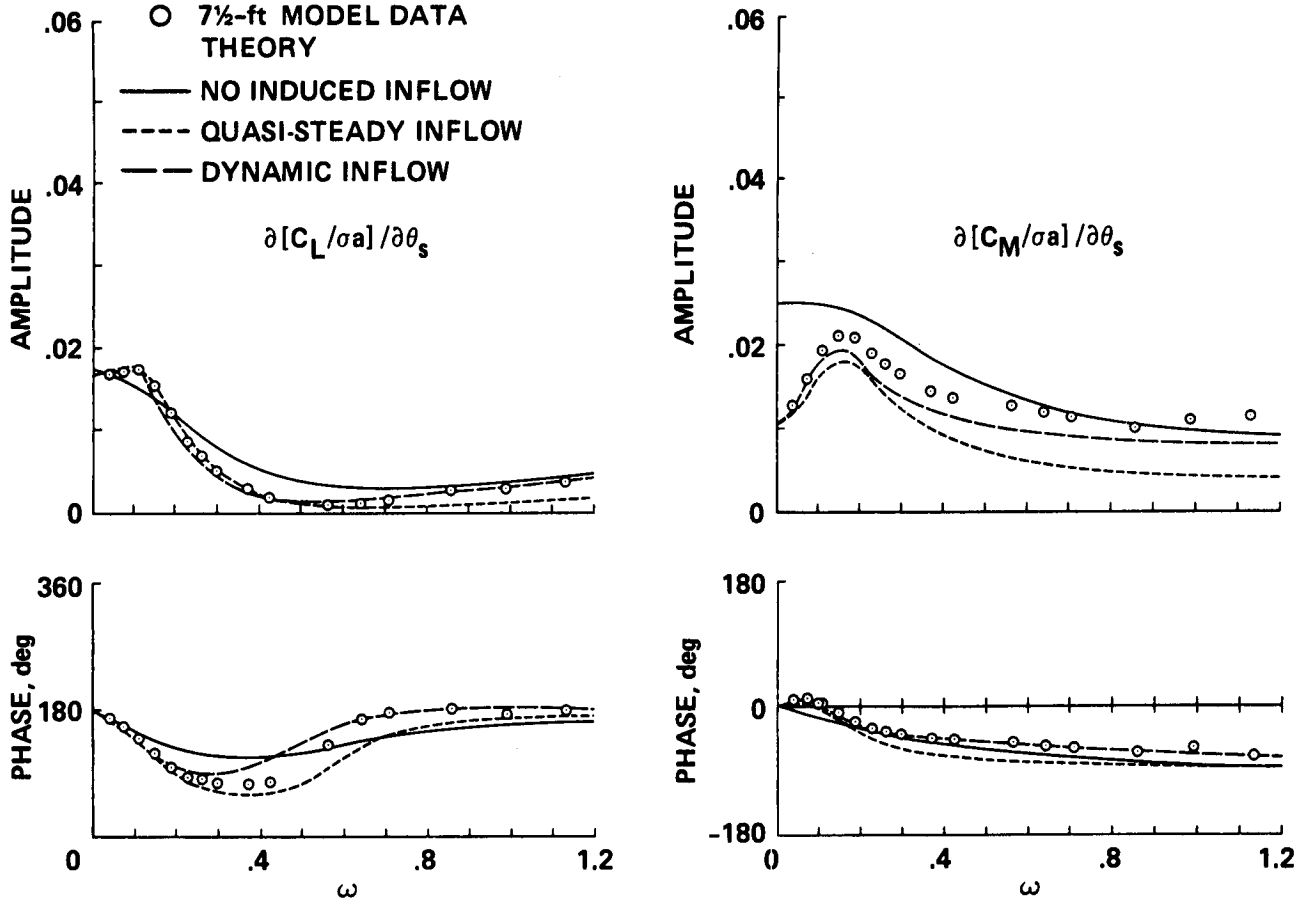

Figure 17.- Effect of momentum theory dynamic inflow on rotor-hub moment frequency response to cyclic pitch excitation for a hingeless rotor model in hover at 4° collective pitch.

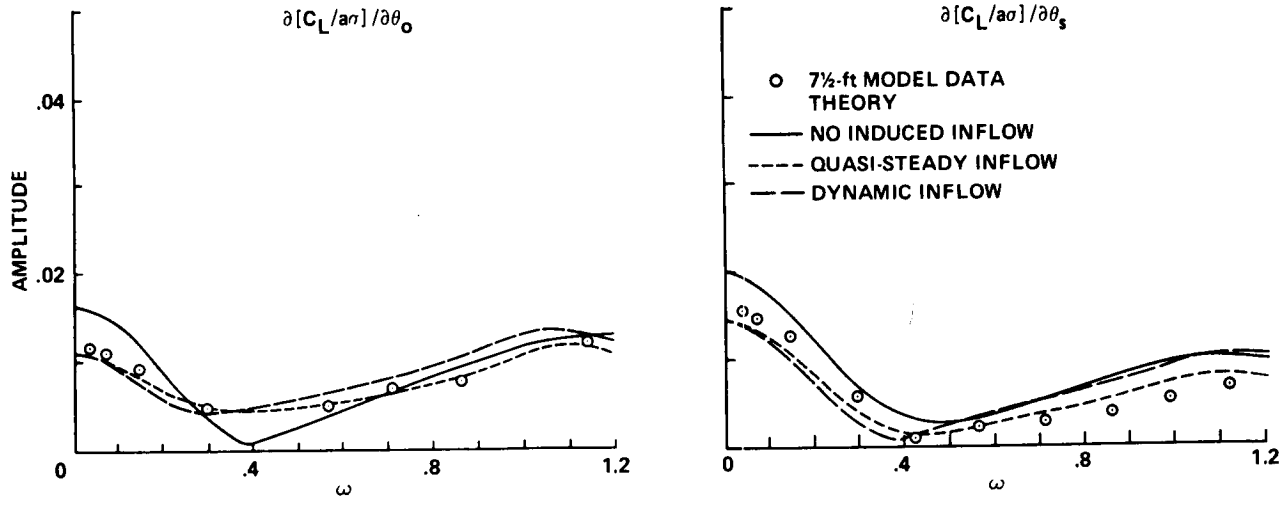

Figure 18.- Effect of empirical dynamic inflow model on rotor-hub moment frequency response to collective and cyclic pitch excitation for a hingeless rotor model in forward flight at 0.51 advance ratio and 0° collective pitch.

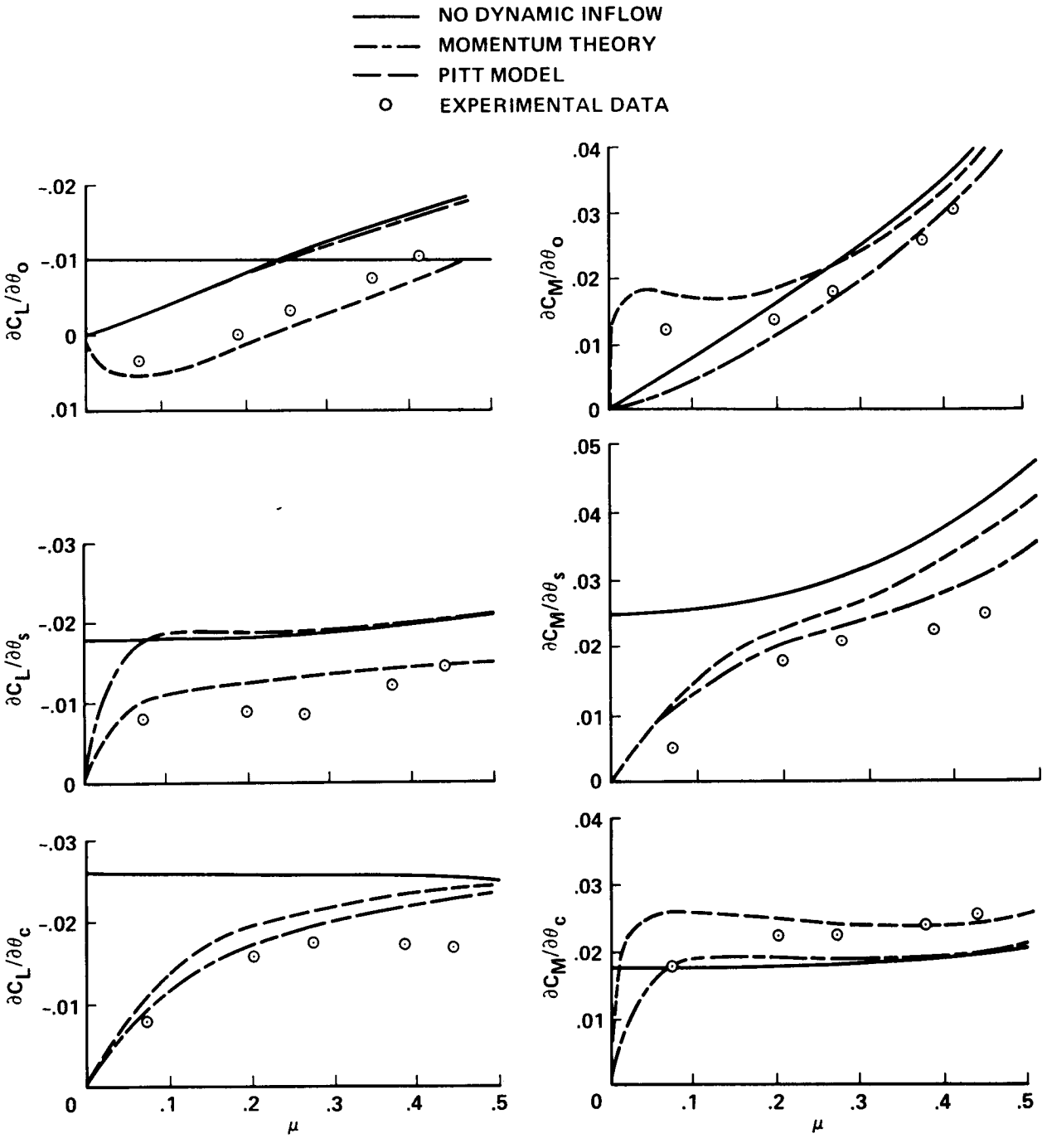

Figure 19.- Correlation of Pitt-Peters dynamic inflow theory with experimental data for static rotor-hub moment response derivatives in forward flight at 0° collective pitch.

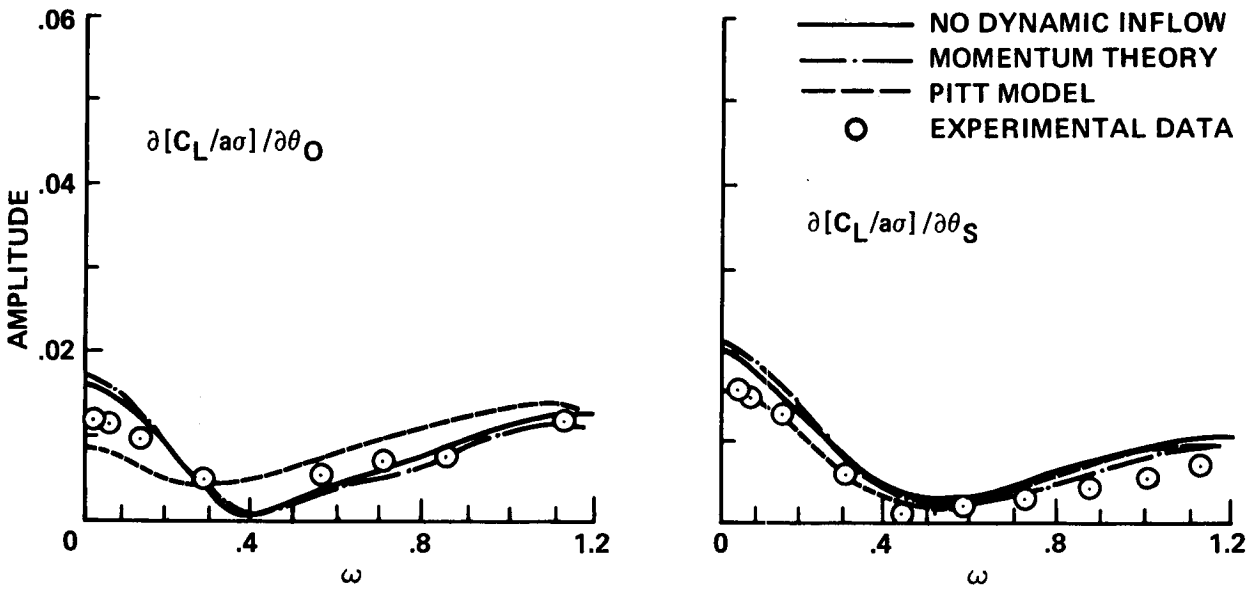

Figure 20.- Correlation of Pitt-Peters dynamic inflow theory with experimental data for rotor frequency response for a hingeless rotor in forward flight at 0.51 advance ratio at 0° collective pitch.

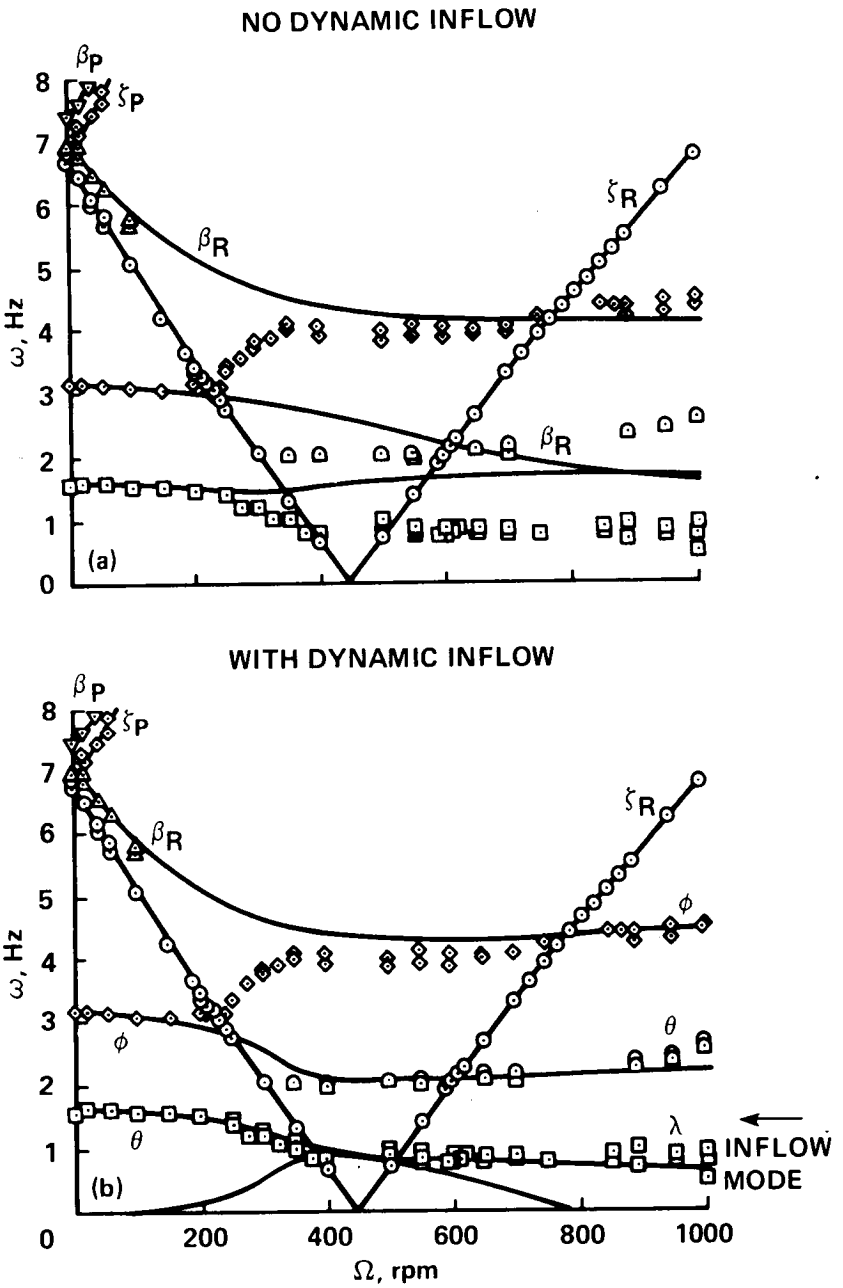

Figure 21.- Effects of dynamic inflow on the coupled rotor-body frequencies of a helicopter model in hover at 0° collective pitch. (a) Without dynamic inflow. (b) With dynamic inflow.

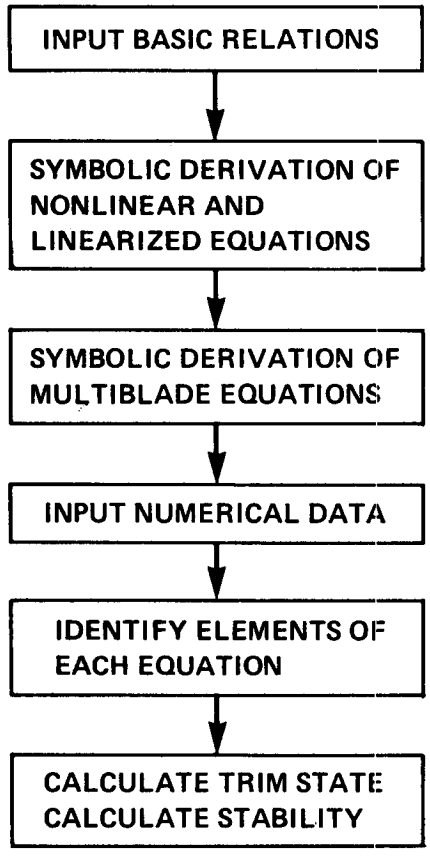

Figure 22.- Flowchart for derivation and solution of aeroelastic stability equations with an automatic symbolic manipulation program.

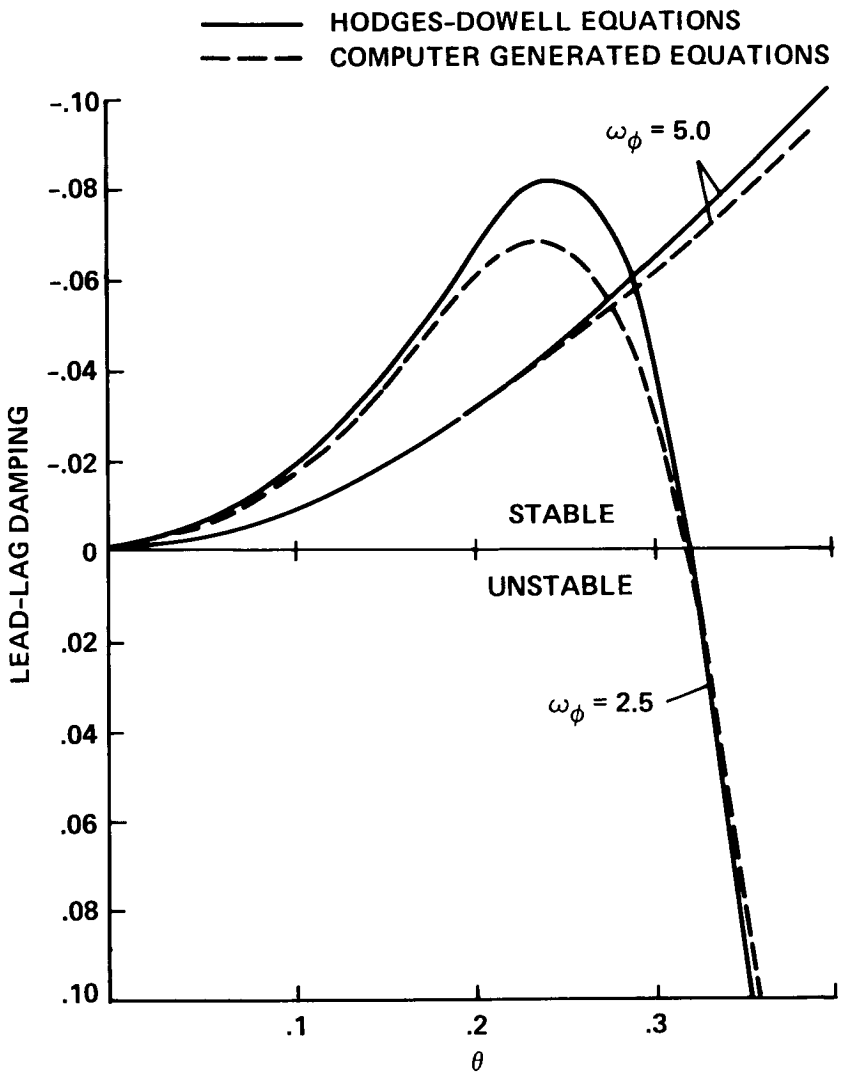

Figure 23.- Comparison of aeroelastic stability results obtained with conventional and computer-generated equations.

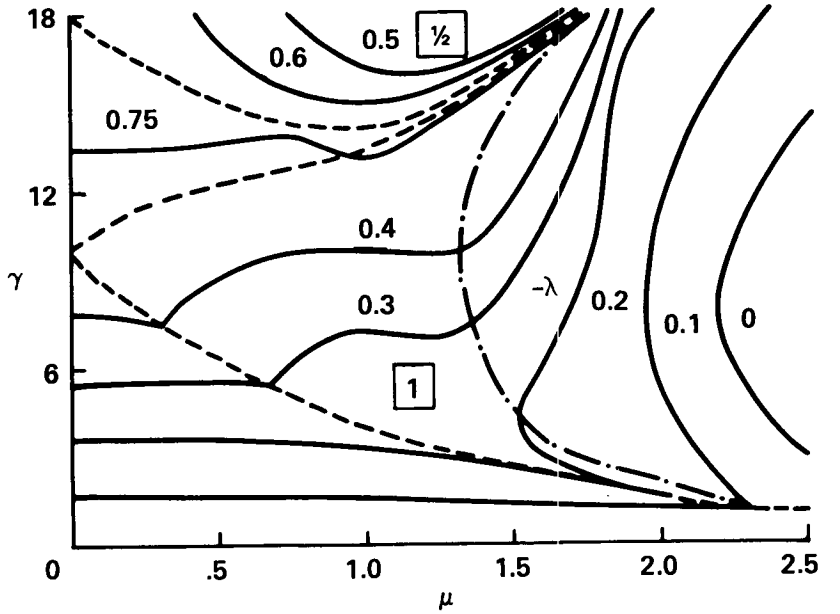

Figure 24.- Floquet theory results for contours of constant damping for spring restrained hinged-rigid blade in forward flight: p = 1.15.

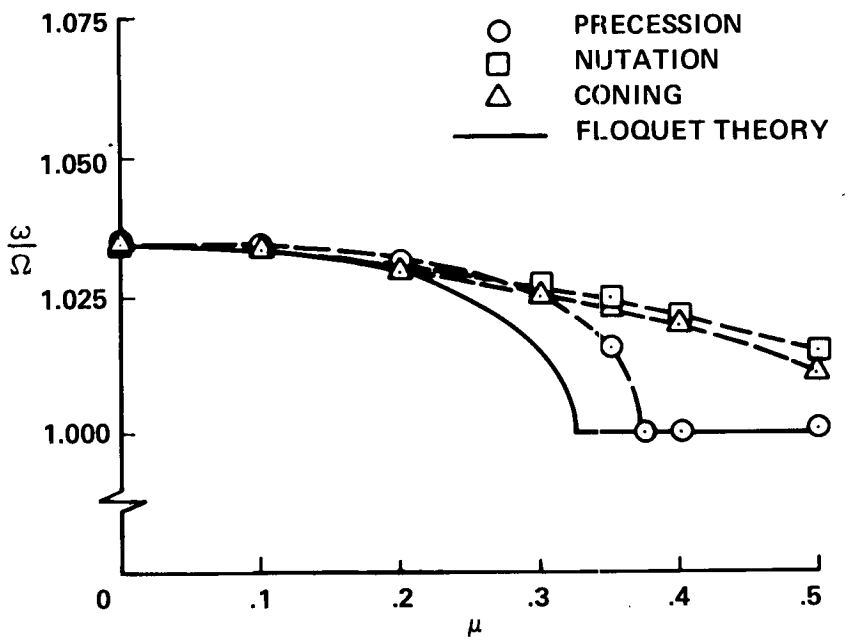

Figure 25.- Comparison of approximate constant coefficient multiblade equations and exact Floquet theory for frequency of hinged-rigid blade in forward flight: p = 1.1, γ = 6.

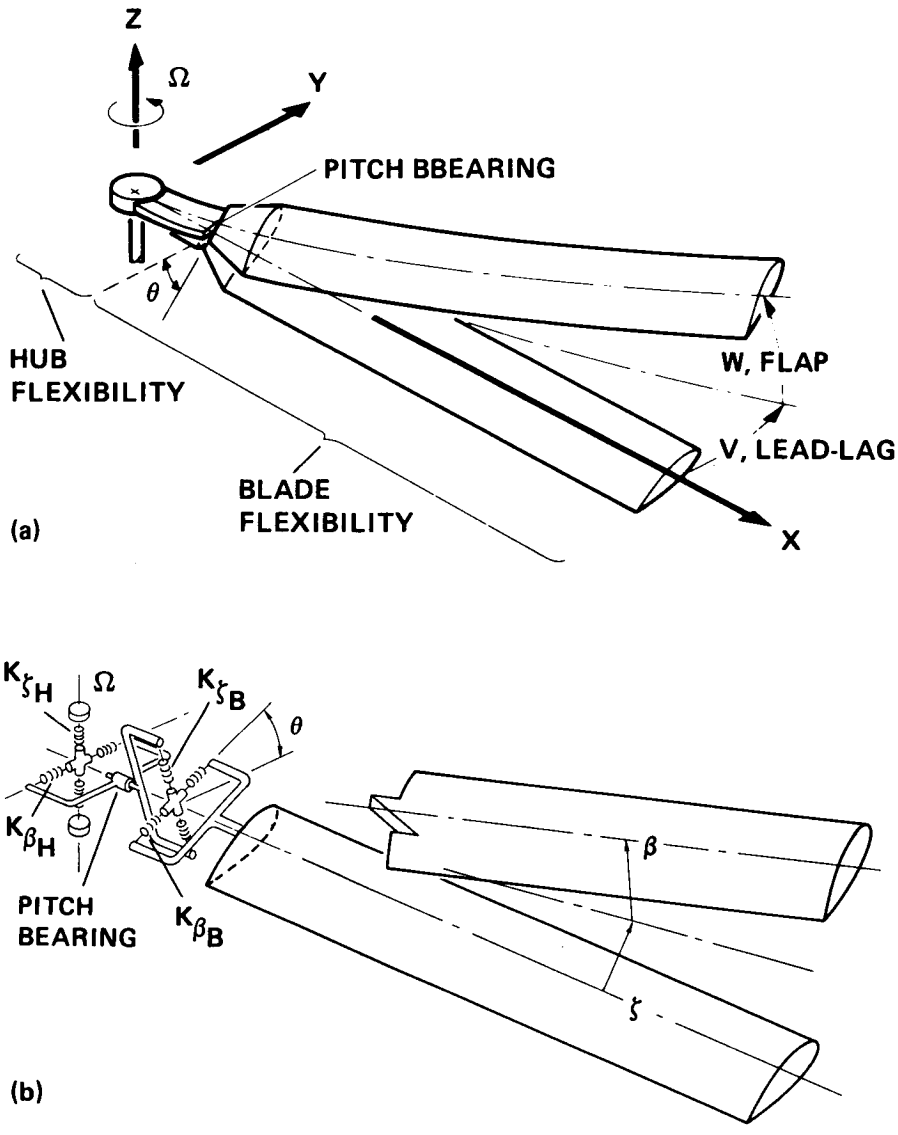

Figure 26.- Modeling of hingeless rotor blade for flap-lag stability analysis. (a) Hub and blade segments of elastic rotor blade. (b) Hinged-rigid blade representation with hub and blade flap-lag spring systems.

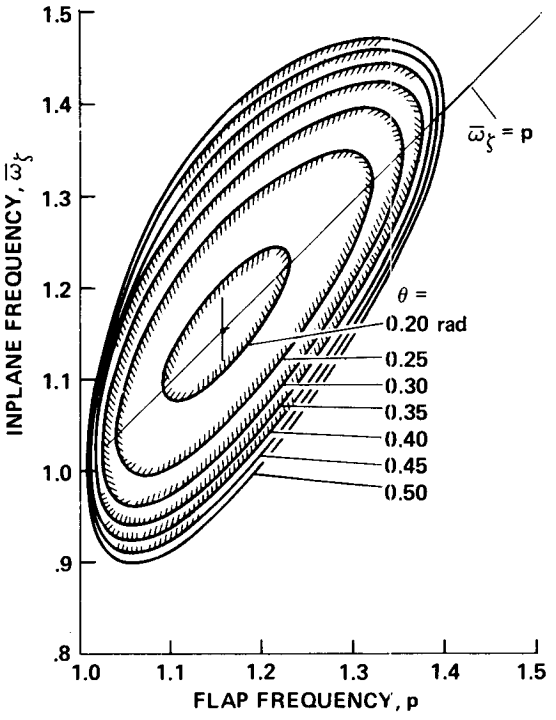

Figure 27.- Basic flap-lag stability boundaries for hinged-rigid blade in hover: R = 0, γ = 5.0, σ = 0.5.

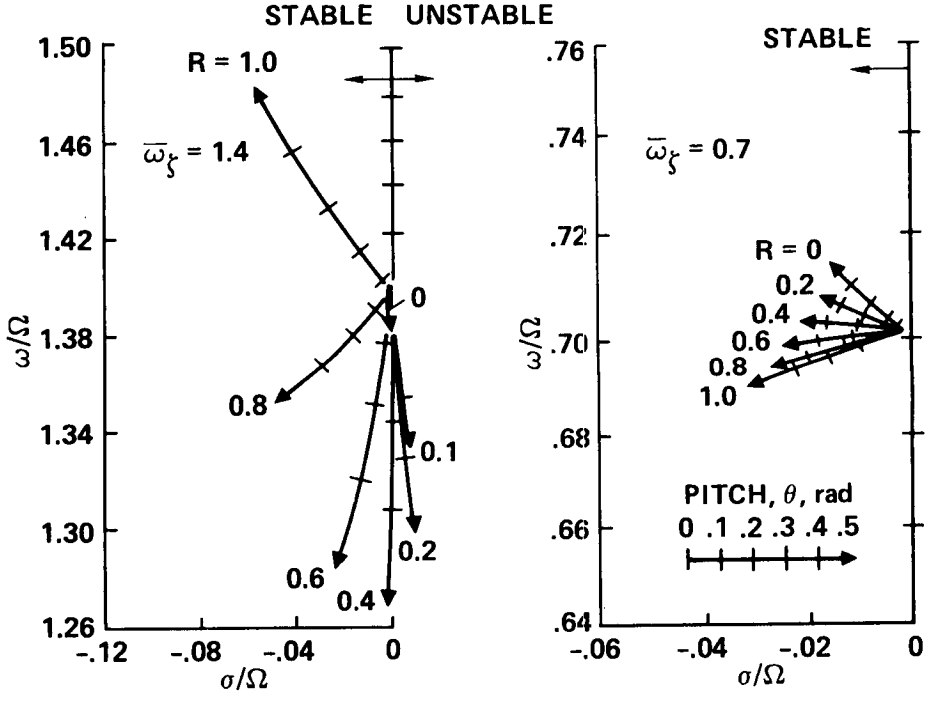

Figure 28.- Locus of lead-lag mode roots of hinged-rigid blade flap-lag system in hover for stiff- and soft-inplane configurations having variable flap-lag structural coupling: p = $\sqrt{4/3}$, γ = 5, σ = 0.05.

C-6

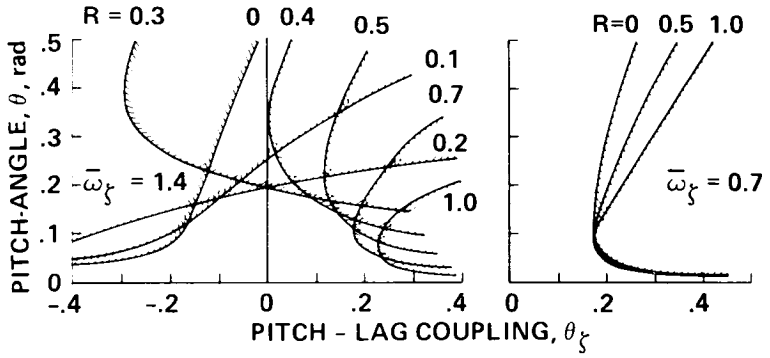

Figure 29.- Effect of pitch-lag coupling on flap-lag stability boundaries in hover of soft- and stiff-inplane hinged-rigid blades: $p = \sqrt{4/3}$, $\gamma = 5$, $\sigma = 0.05$.

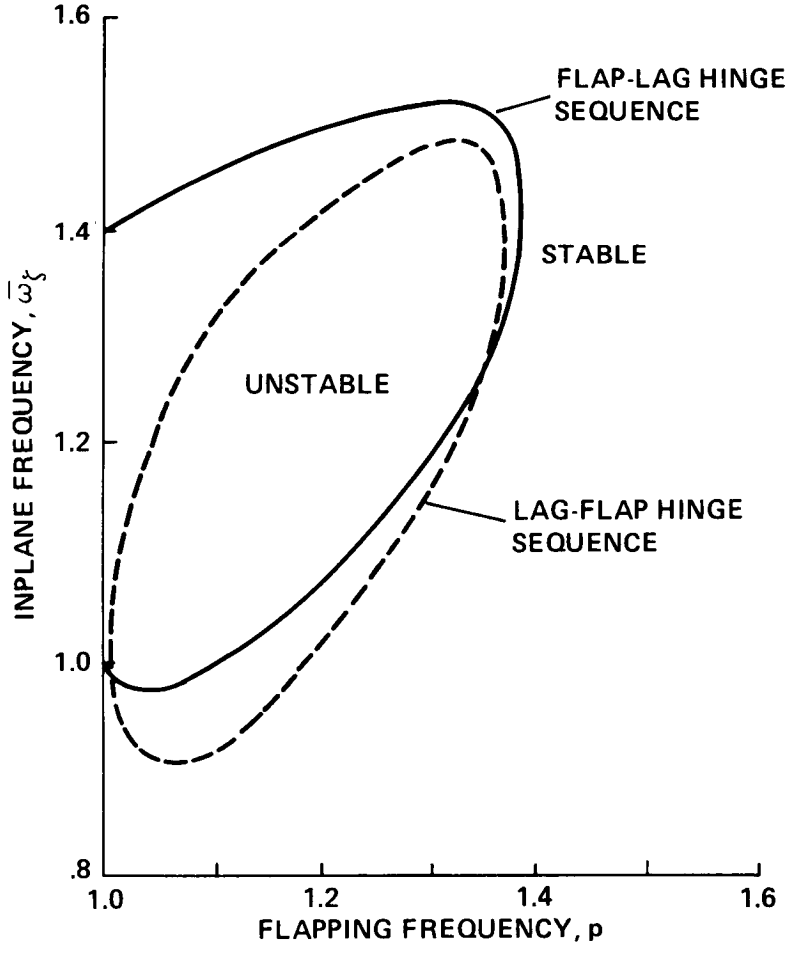

Figure 30.- Effect of hinge sequence on flap-lag stability of hinged-rigid blade in hover: $\theta = 0.4$ rad, $\gamma = 5$, $\sigma = 0.05$, $R = 0$.

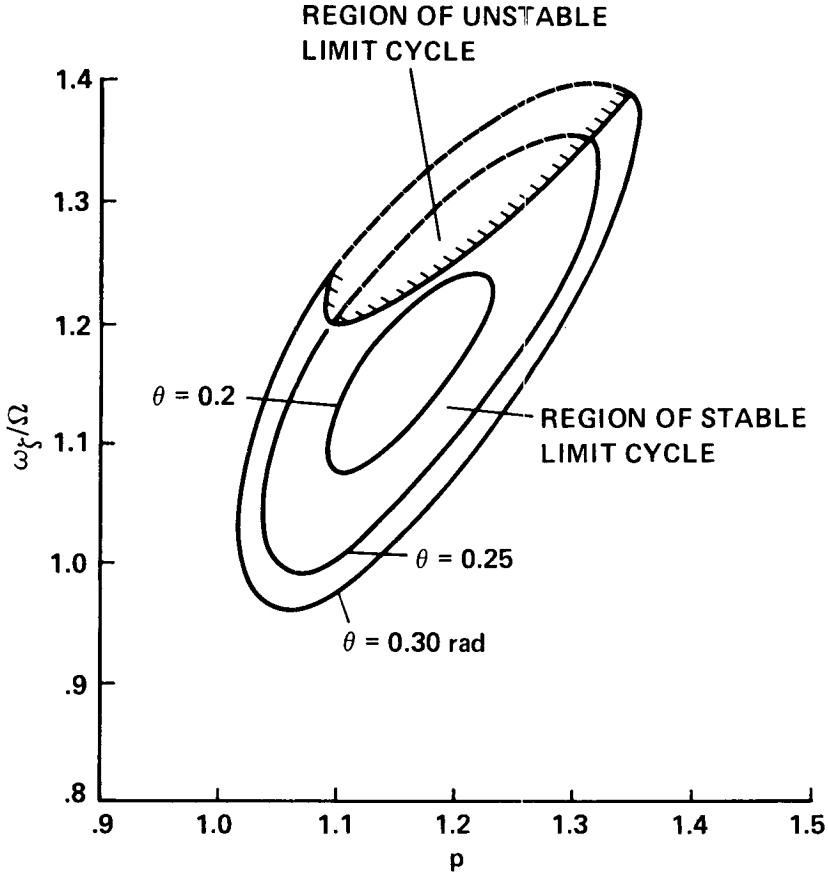

Figure 31.- Nonlinear flap-lag stability for hinged-rigid blade in hover: $\gamma = 5$, $\sigma = 0.05$.

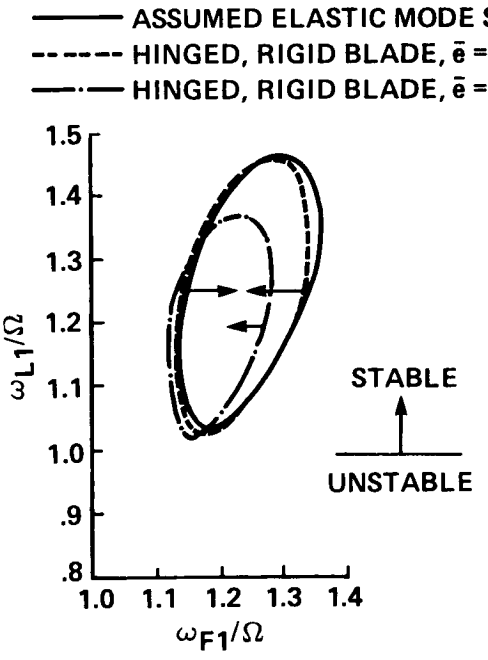

Figure 32.- Comparison of flap-lag instability for offset-hinged-rigid blade with elastic blade in hover: θ = 0.2 rad, γ = 10, σ = 0.05.

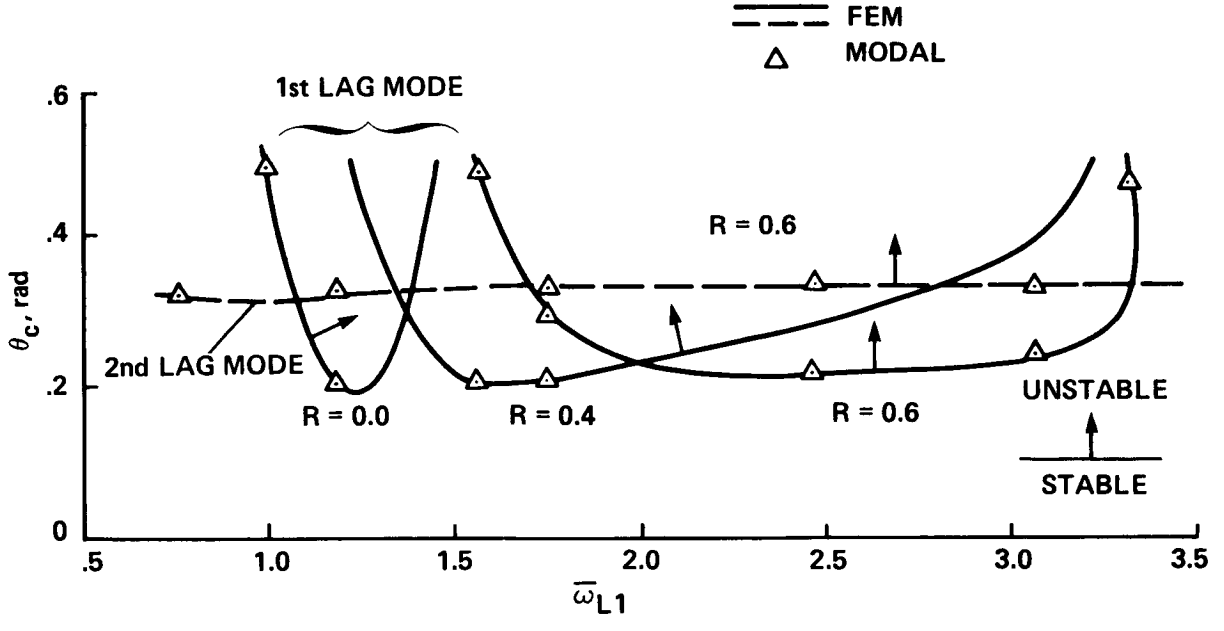

Figure 33.- Comparison of flap-lag stability boundaries of elastic blade in hover calculated with modal and finite-element methods: $\bar{\omega}_{F1}$ = 1.15, γ = 5, σ = 0.1.

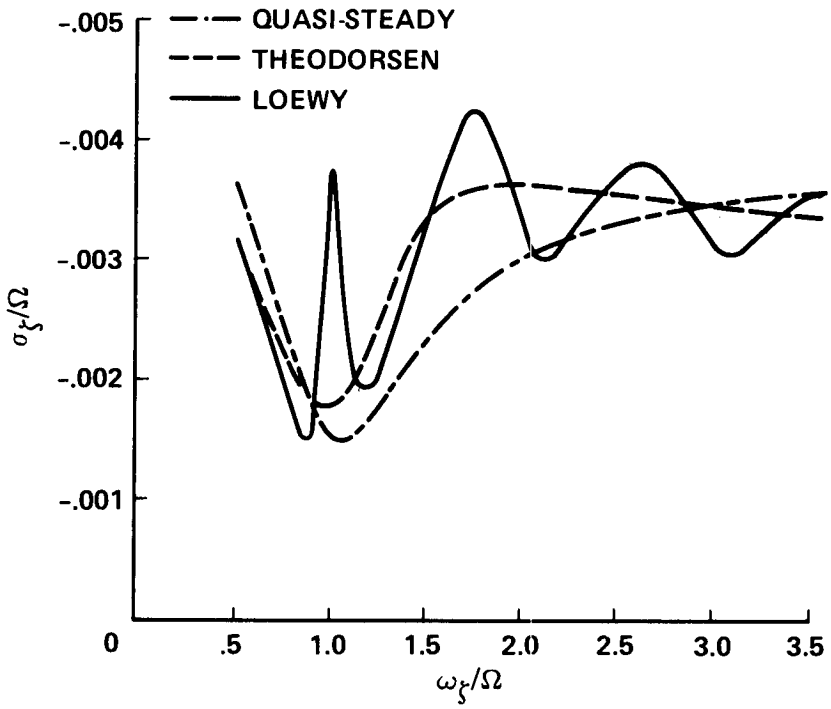

Figure 34.- Effects of unsteady aerodynamics on flap-lag stability of a hinged-rigid rotor blade in hover: $p = 1.1$, $\theta_o = 0.1$ rad, $\gamma = 8$, $\sigma = 0.05$, $R = 0$, $b = 1$.

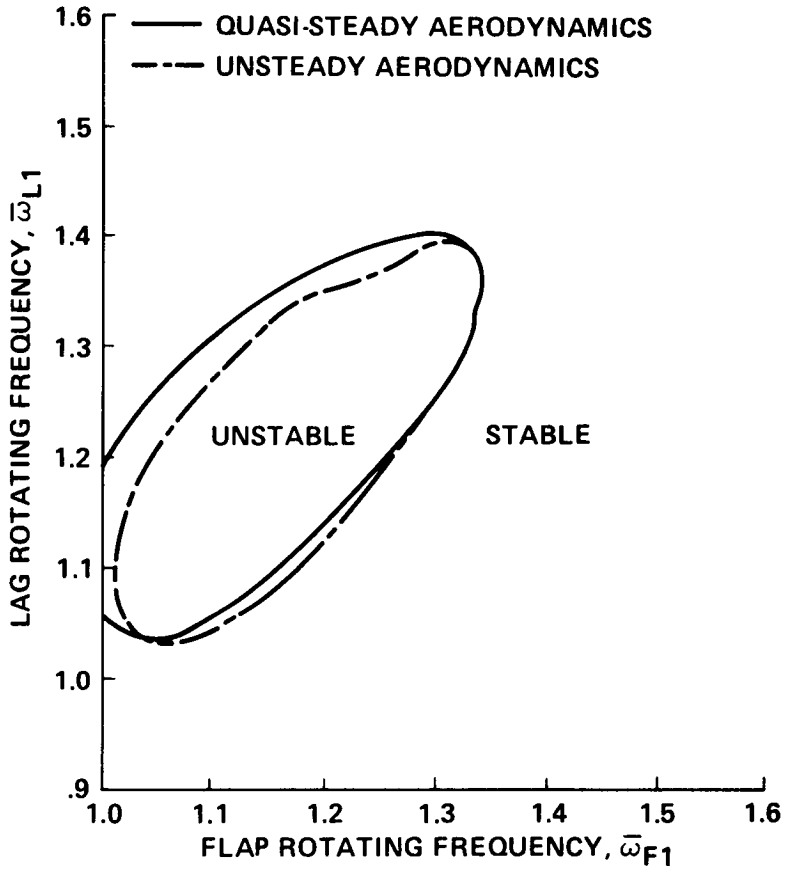

Figure 35.- Effects of finite-state model of Greenberg unsteady aerodynamic theory on flap-lag stability of hinged-rigid blade in hover: θ = 0.25 rad, γ = 5, σ = 0.05, R = 0, b = 4.

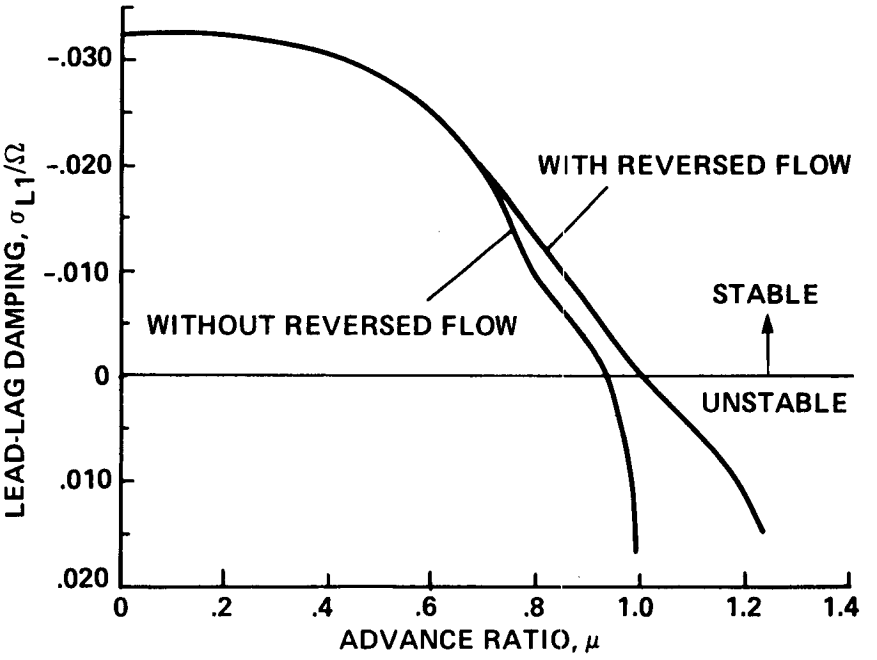

Figure 36.- Effects of reverse flow on lead-lag damping of elastic blade flap-lag analysis in forward flight: θ_o = 0.15 rad, $\bar{\omega}_{F1}$ = 1.175, $\bar{\omega}_{L1}$ = 1.283, γ = 10, σ = 0.05.

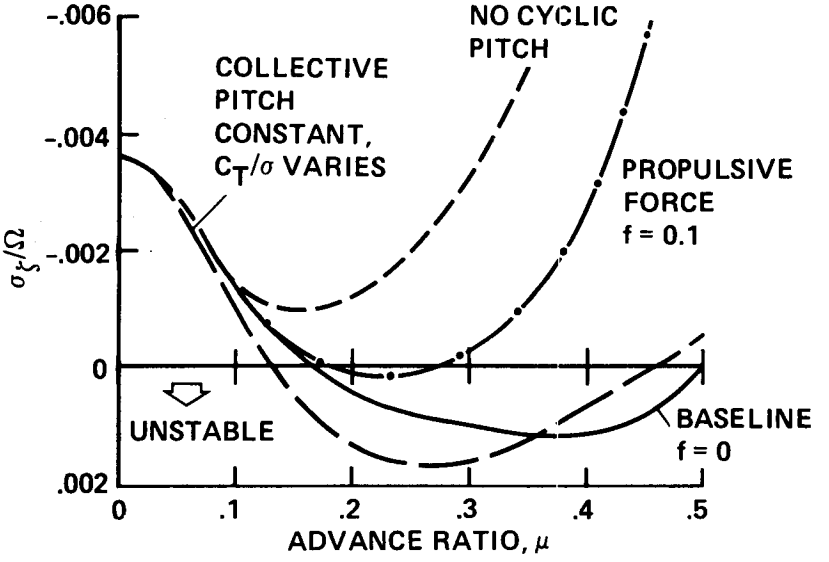

Figure 37.- Effects of trim condition on lead-lag damping of hinged-rigid blade flap-lag analysis in forward flight: p = 1.15, $\bar{\omega}_\zeta$ = 1.4, γ = 5, σ = 0.05, R = 0.

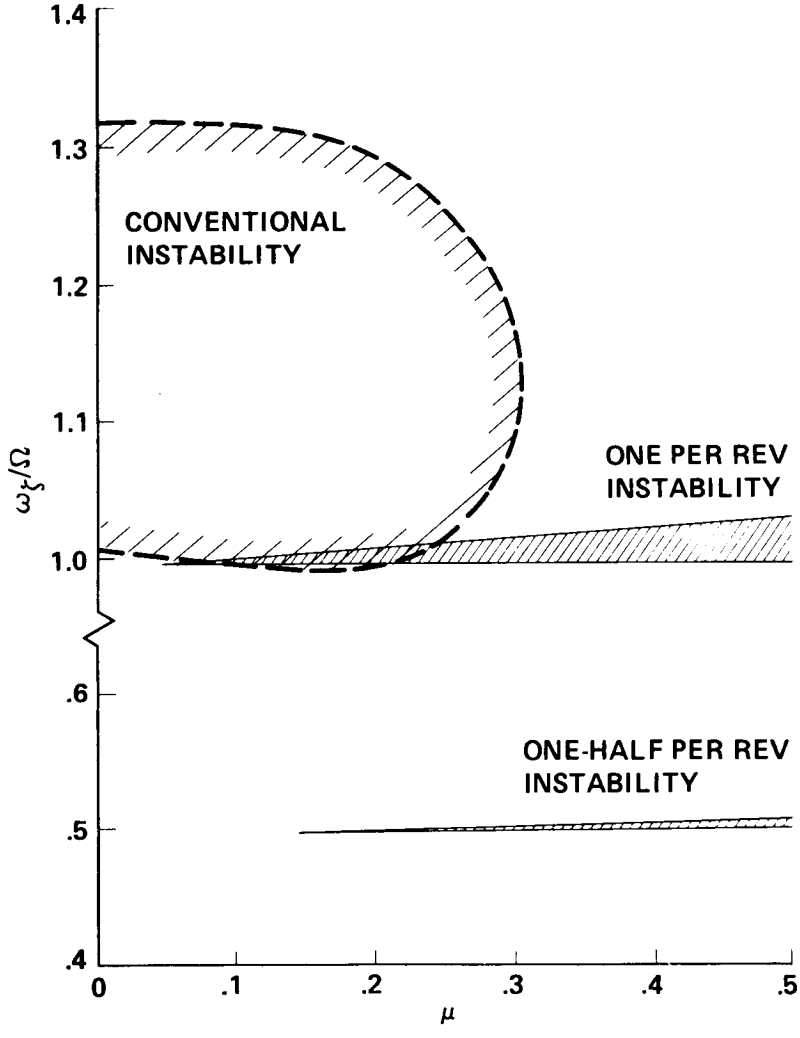

Figure 38.- Flap-lag stability boundaries in forward flight for hinged-rigid blade analysis illustrating conventional and parametric instability regions: $C_T/\sigma = 0.2$, $\gamma = 5$, $\sigma = 0.05$, $R = 0$.

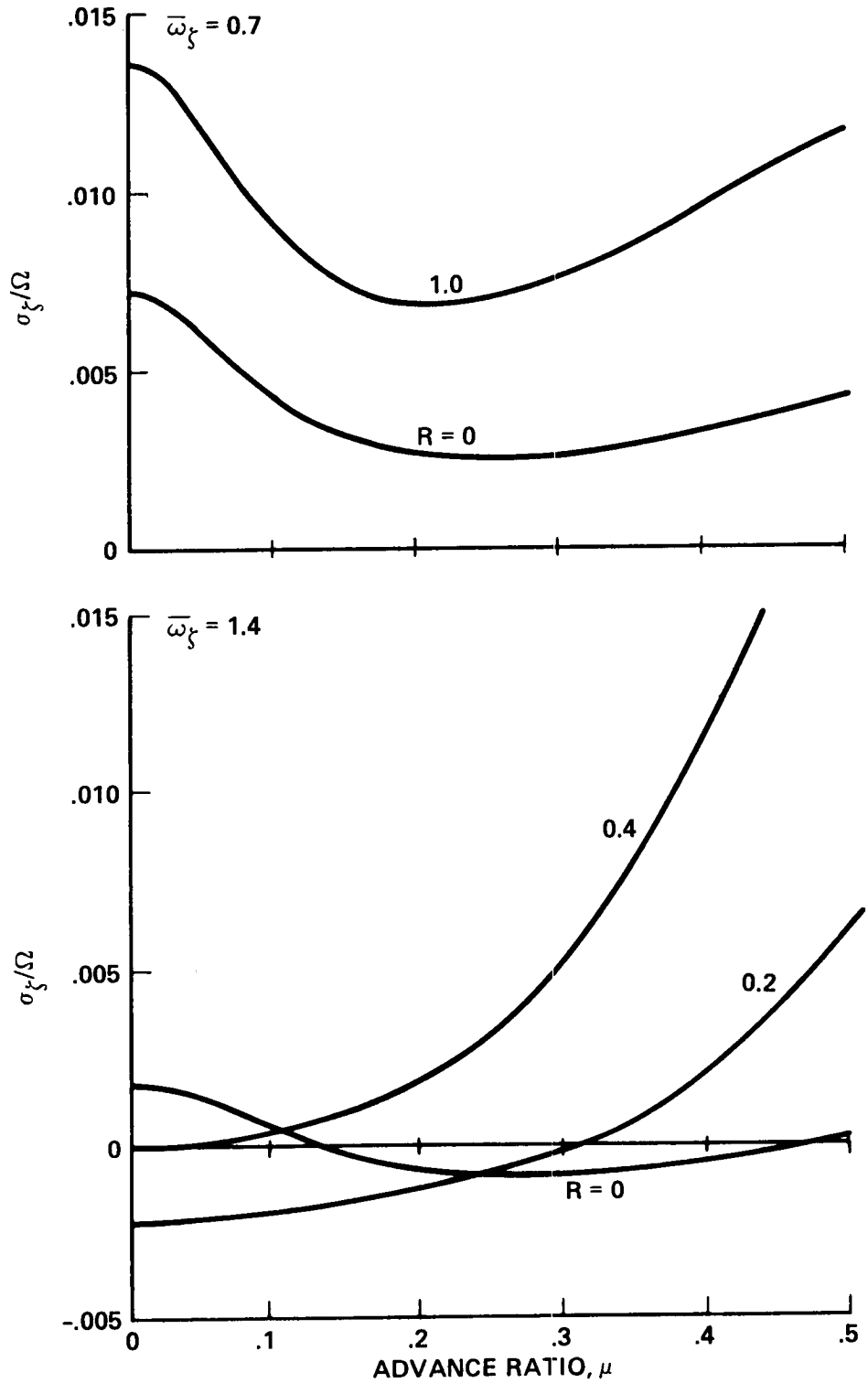

Figure 39.- Effects of flap-lag structural coupling on lead-lag damping of soft- and stiff-in-plane hinged-rigid blades in forward flight: p = 1.15, C_T/σ = 0.2, $\bar{f}$ = 0, γ = 5.

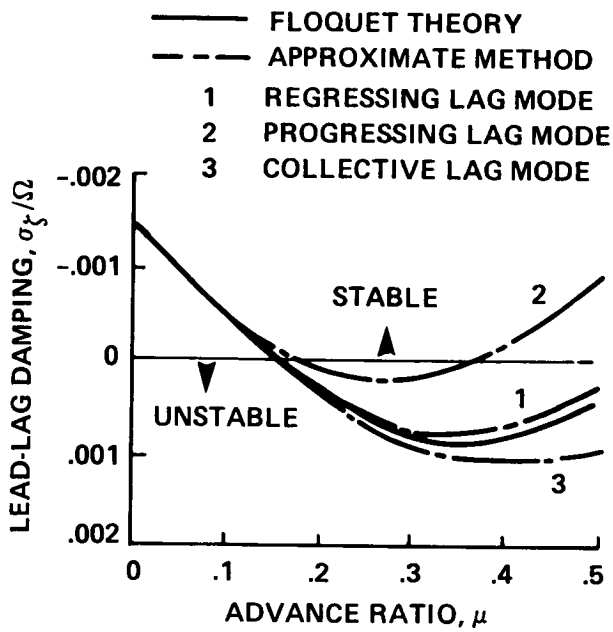

Figure 40.- Comparison of approximate constant coefficient multiblade equations with exact Floquet theory result for lead-lag damping of hinged-rigid blade flap-lag analysis in forward flight: $p = 1.15$, $\bar{\omega}_\zeta = 1.4$, $C_T/\sigma = 0.2$, $\bar{f} = 0$, $\gamma = 5$, $R = 0$.

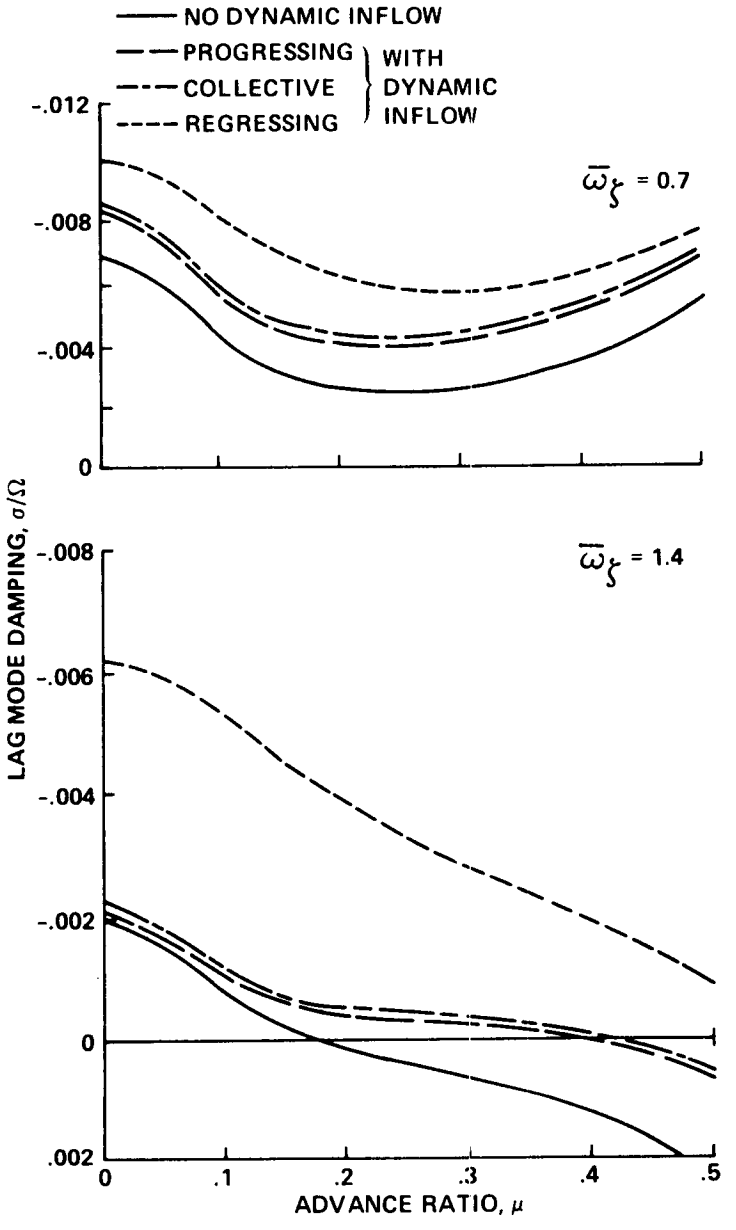

Figure 41.- Effects of dynamic inflow on lead-lag damping in forward flight for soft- and stiff-in-plane hinged-rigid blade flap-lag analysis: $p = 1.15$, $\gamma = 5$, $\sigma = 0.05$.

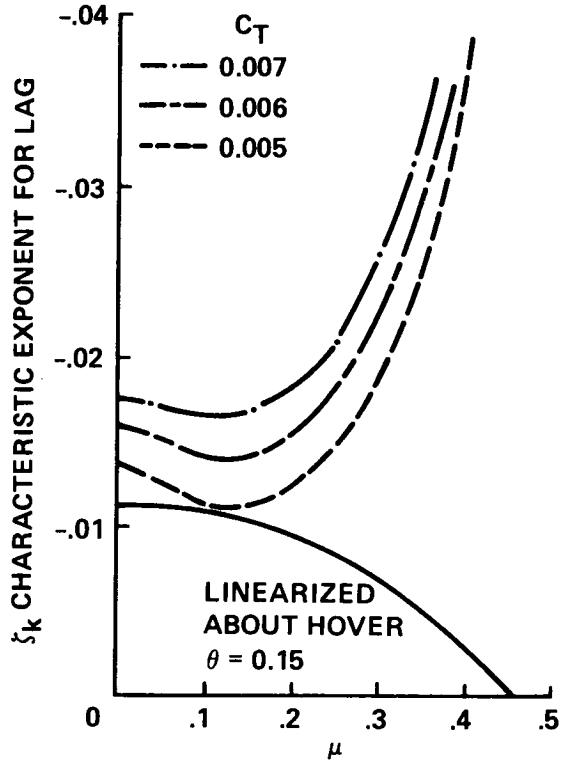

Figure 42.- Effects of trim condition on lead-lag damping of elastic blade flap-lag analysis in forward flight: θ_o = 0.15 rad, p = 1.175, $\bar{\omega}_\zeta$ = 1.28, γ = 10, σ = 0.05.

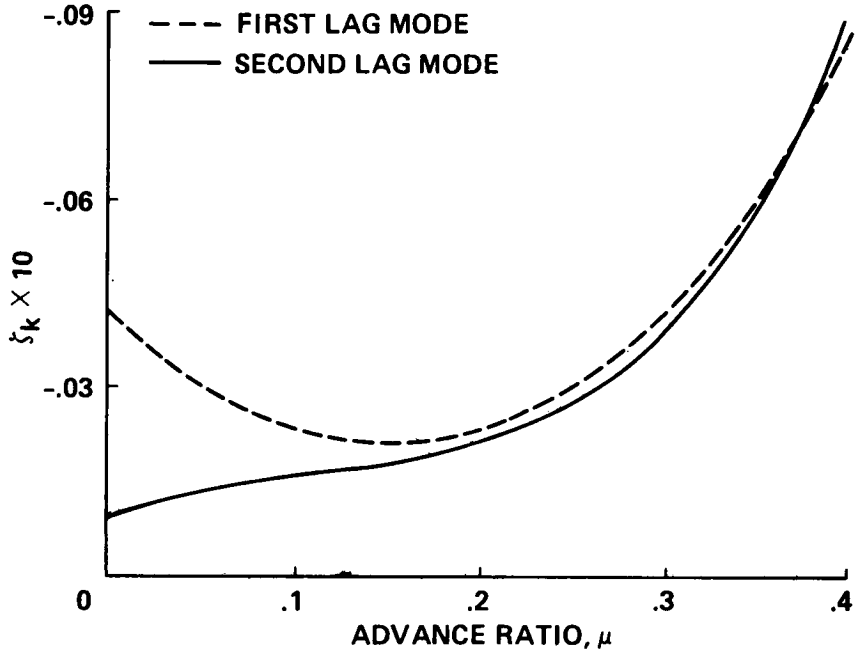

Figure 43.- Finite element calculation of lead-lag damping in forward flight for elastic blade flap-lag analysis: p = 1.125, $\bar{\omega}_\zeta$ = 0.732, C_W = 0.005, γ = 5.5, σ = 0.07, R = 0.6.

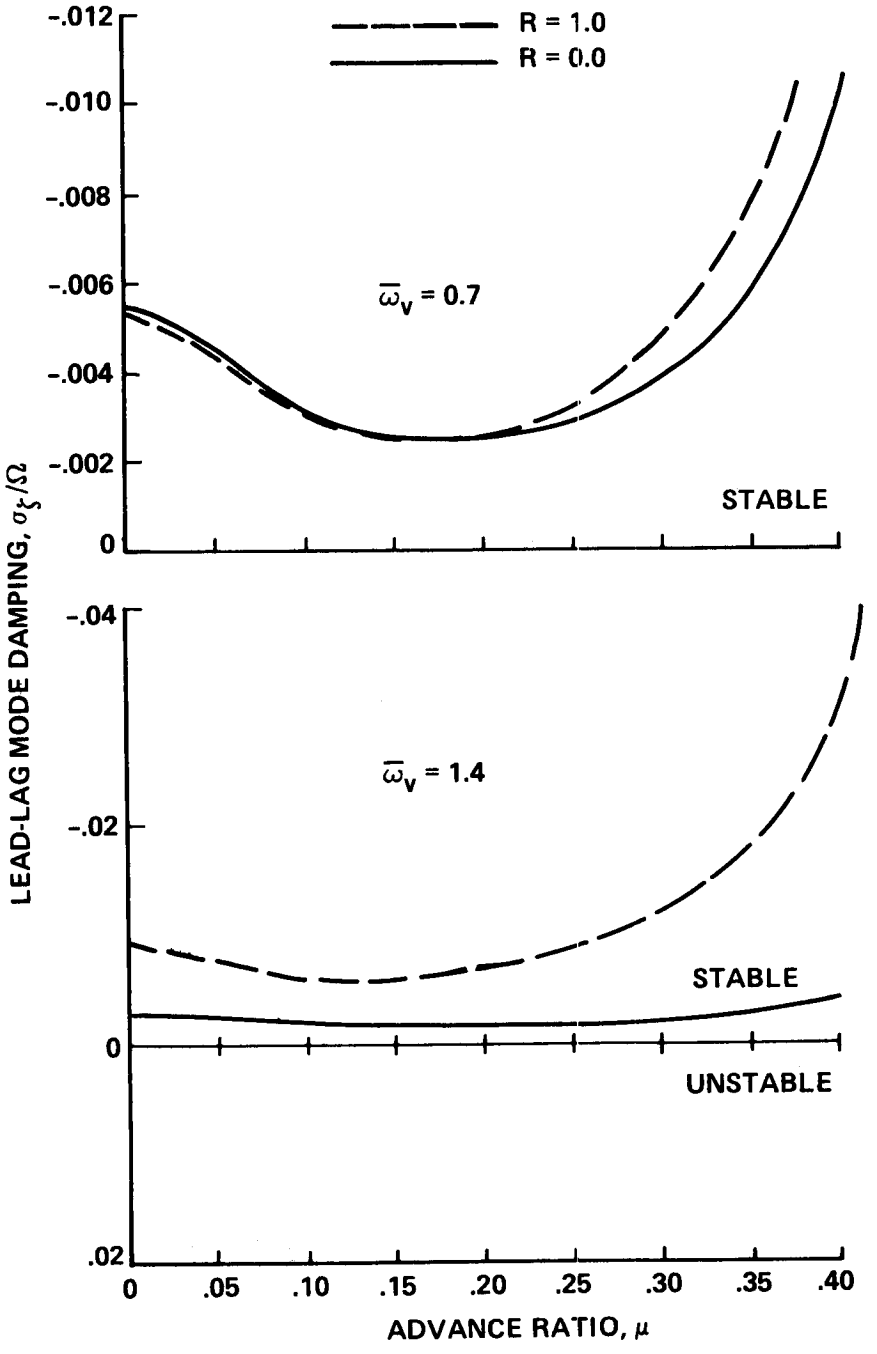

Figure 44.- Effects of flap-lag structural coupling on lead-lag damping of soft- and stiff-inplane elastic blade flap-lag analysis in forward flight: $p = 1.15$, $C_T/\sigma = 0.7$, $\bar{f} = 0.012$, $\gamma = 5$, $\sigma = 0.10$.

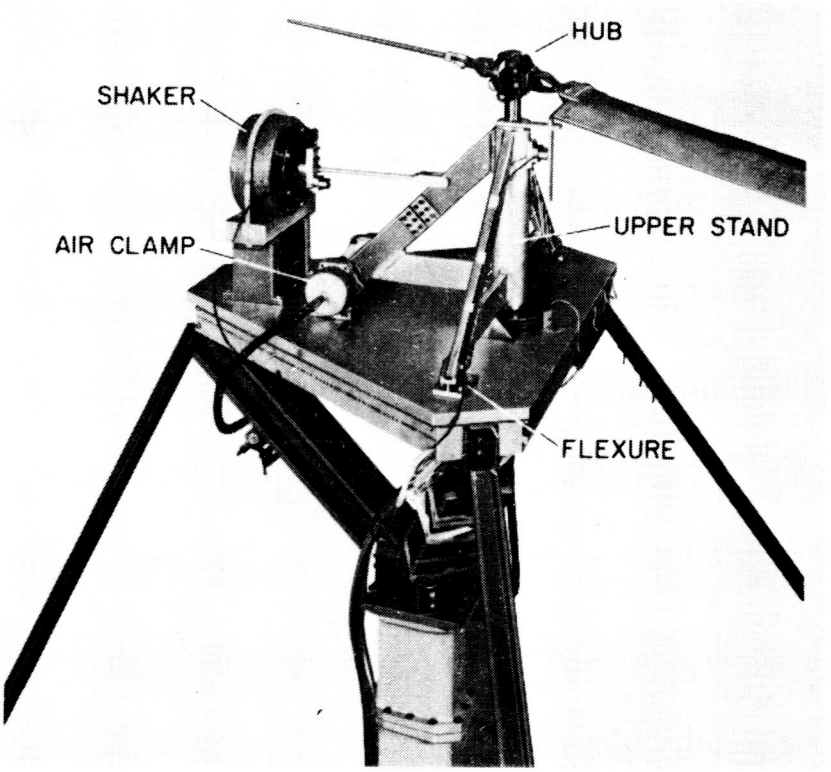

Figure 45.- Two-bladed 5.5-ft-diam flap-lag model rotor for hover experiments.

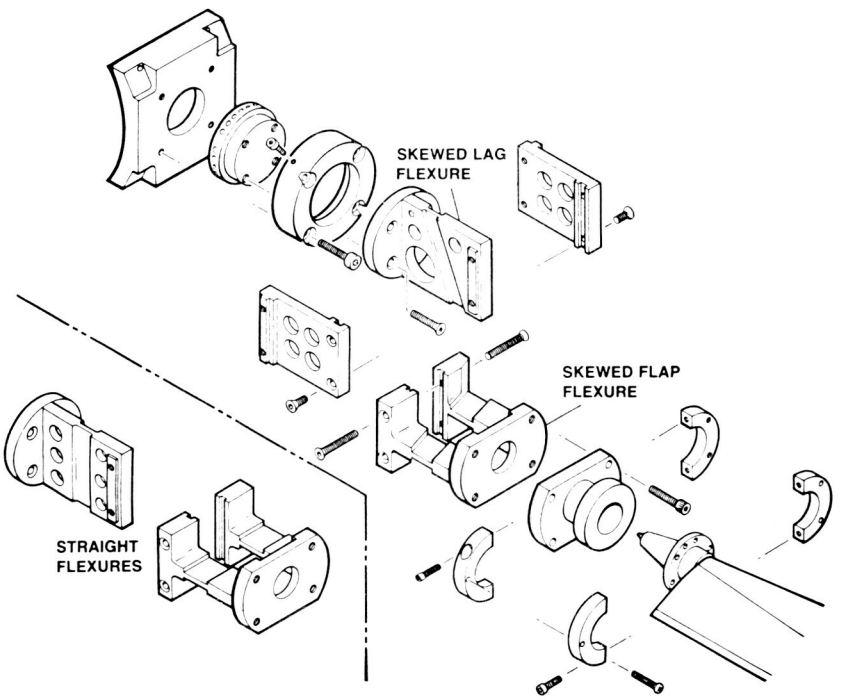

Figure 46.- Hub flexures to simulate spring restrained hinges for rigid blade flap-lag model rotor.

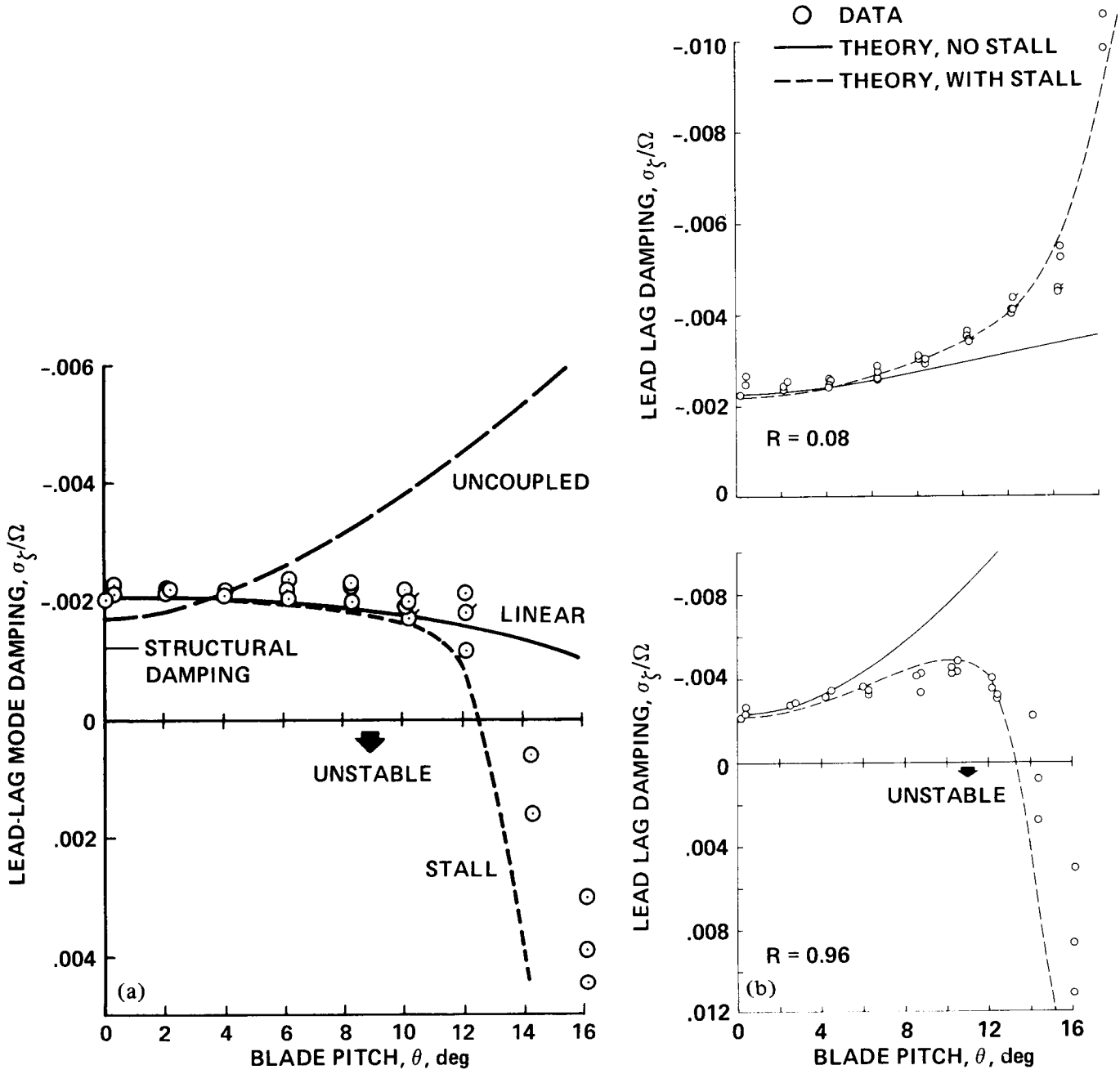

Figure 47.- Experimental lead-lag damping of flap-lag model in hover compared with theory with and without airfoil stall effects: γ = 2.84, σ = 0.0601, R = 0.08. (a) p = 1.17, $\bar{\omega}_\zeta$ = 1.21. (b) p = 1.28, $\bar{\omega}_\zeta$ = 1.62.

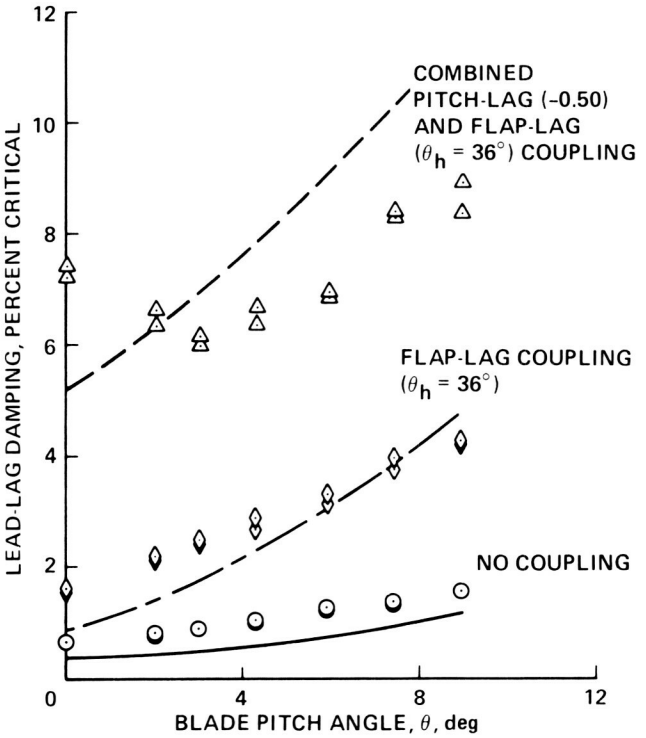

Figure 48.- Effects of aeroelastic couplings on experimental and theoretical lead-lag damping of flap-lag model in hover: $\bar{\omega}_\zeta = 0.7$, $\gamma = 7.99$, $\sigma = 0.033$.

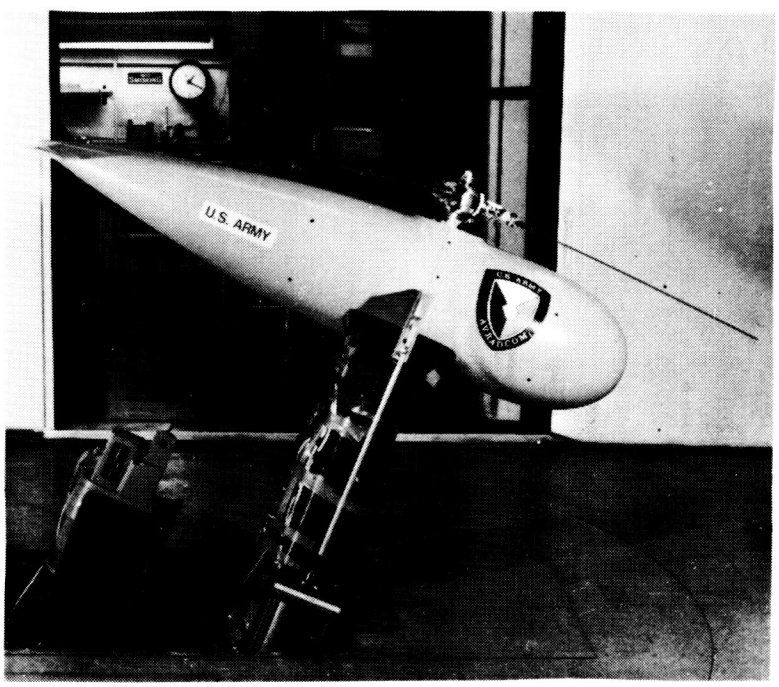

Figure 49.- Three-bladed flap-lag model rotor in 7- by 10-Foot Wind Tunnel.

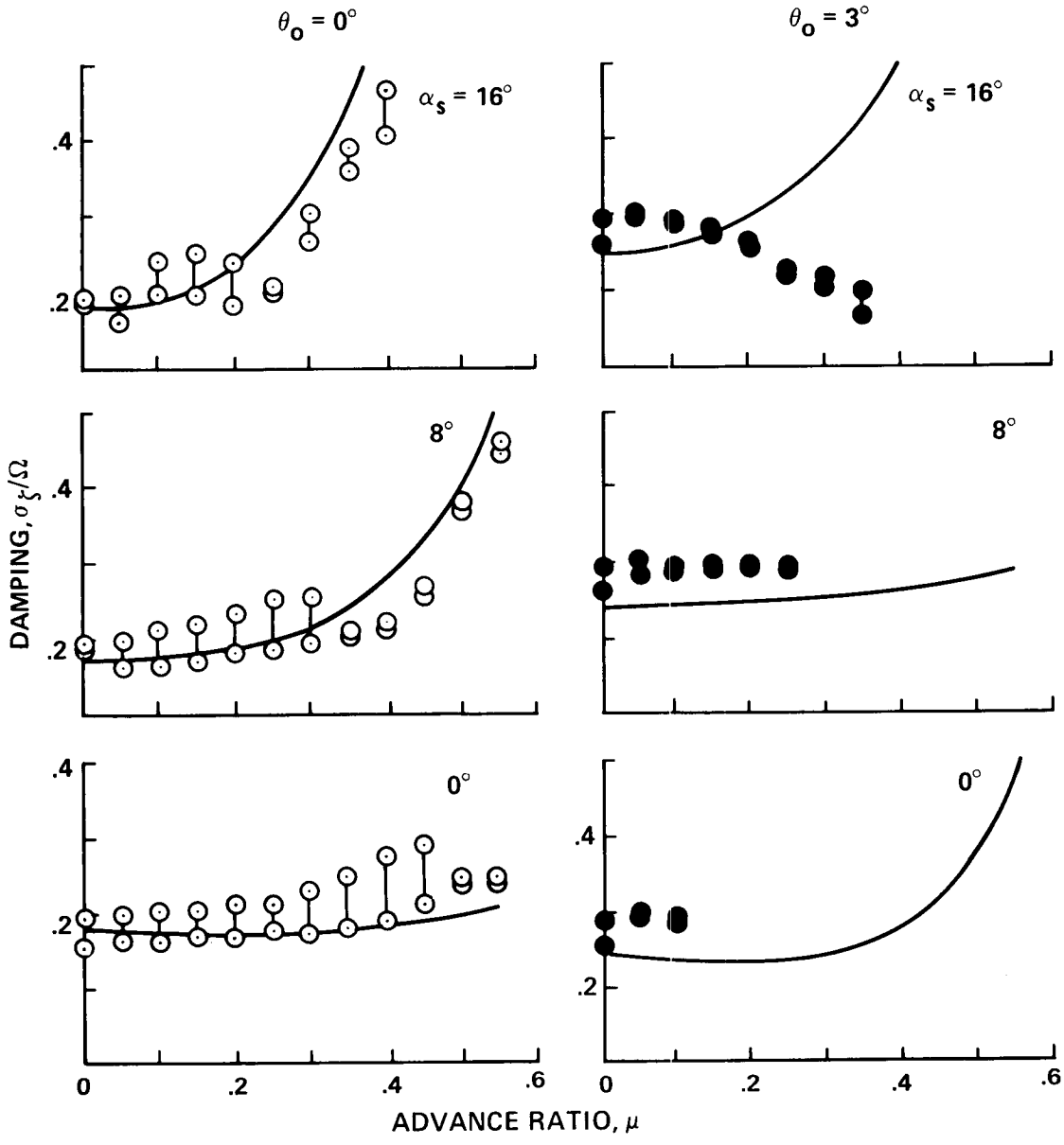

Figure 50.- Experimental lead-lag regressing mode damping of flap-lag model in forward flight compared with theory: Ω = 1000 rpm, γ = 7.54, σ = 0.0494, R = 0.

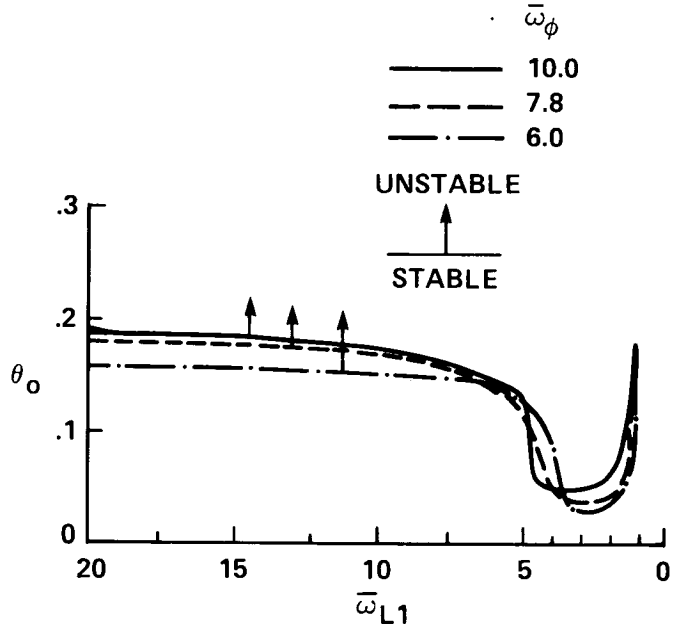

Figure 51.- Stability boundaries for rotor-blade elastic flap-lag bending and rigid-body root pitch in hover: $\bar{\omega}_{F1}$ = 1.2, γ = 8, σ = 0.08.

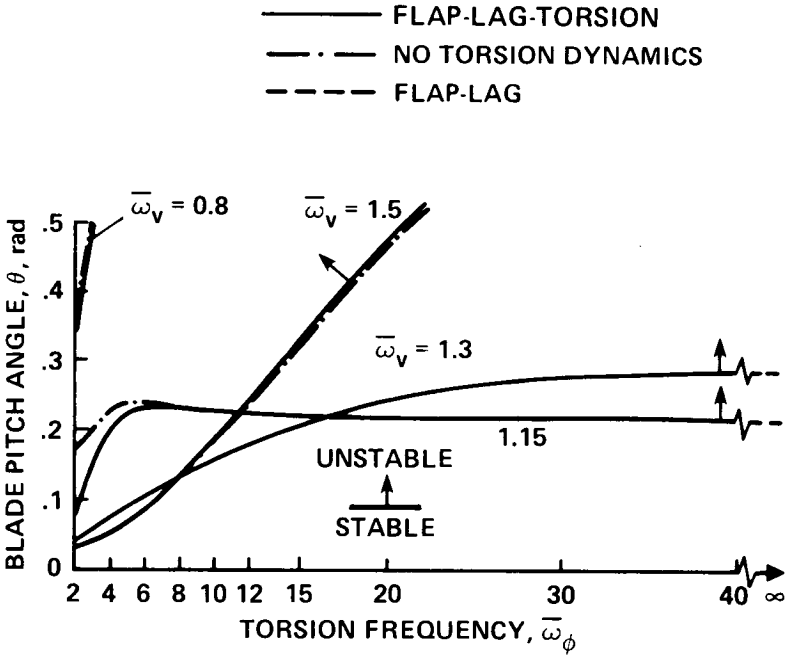

Figure 52.- Comparison of flap-lag-torsion stability boundaries for elastic blade in hover for different treatment of torsion motion: $\bar{\omega}_w$ = 1.15, γ = 5, σ = 0.1, R = 0.

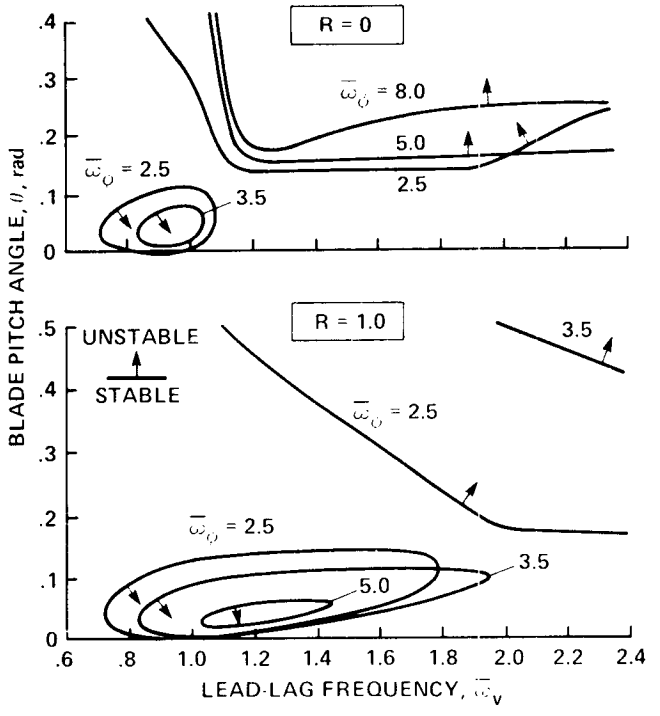

Figure 53.- Effects of flap-lag structural coupling and precone on elastic blade flap-lag-torsion stability boundaries in hover: $\bar{\omega}_w$ = 1.15, γ = 5, σ = 0.1, β_{pc} = 0.05 rad.

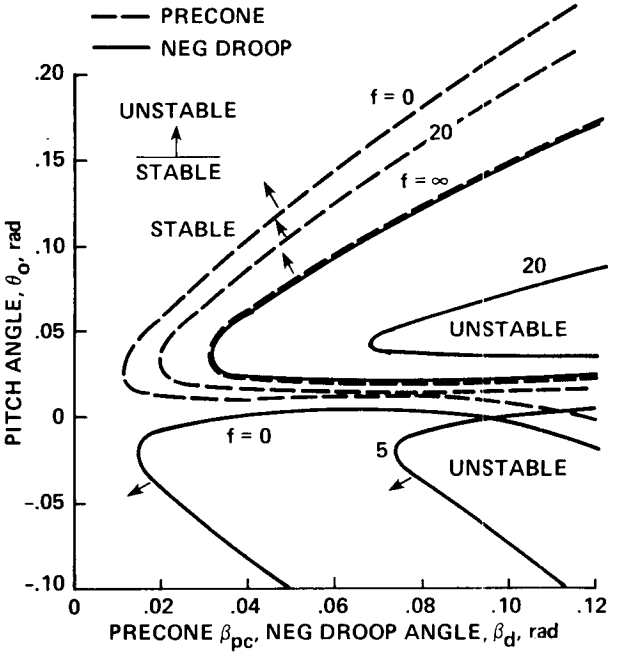

Figure 54.- Effects of precone, droop, and blade torsion-to-pitch link flexibility ratio on elastic blade flap-lag-torsion stability boundaries in hover: $\bar{\omega}_w$ = 1.15, $\bar{\omega}_v$ = 1.3, $\bar{\omega}_\phi$ = 4.0, γ = 5, σ = 0.1, R = 1.

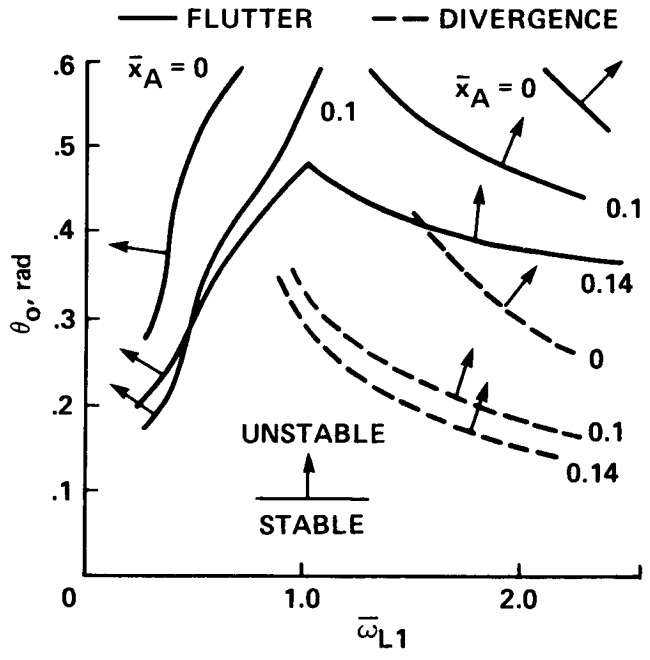

Figure 55.- Effects of chordwise aerodynamic center offsets on elastic blade flap-lag-torsion stability boundaries in hover: $\bar{\omega}_{F1} = 1.14$, $\bar{\omega}_{\phi} = 4.5$, $\gamma = 8$, $\sigma = 0.08$.

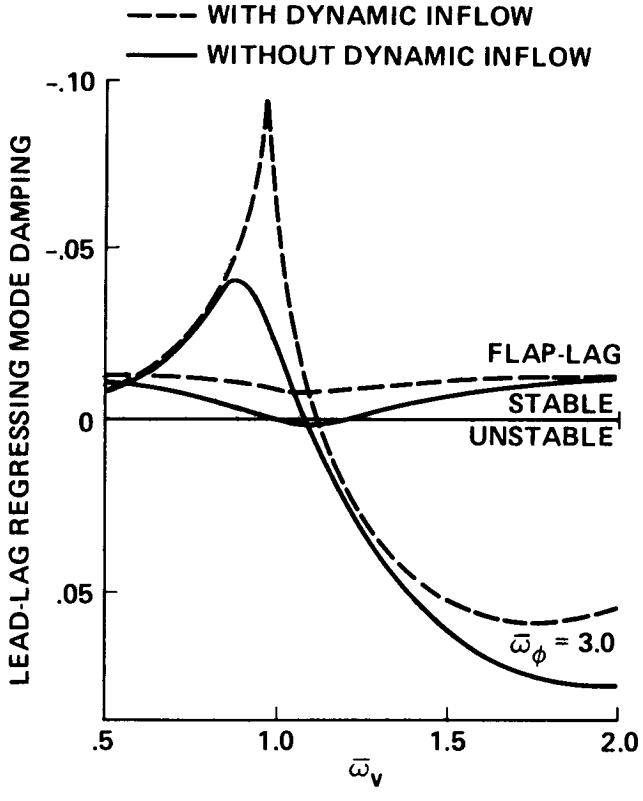

Figure 56.- Effects of dynamic inflow on regressing lead-lag mode damping of elastic blade flap-lag-torsion analysis in hover: $\theta = 0.3$ rad, $\bar{\omega}_w = 1.15$, $\bar{\omega}_{\phi} = 5$, $\gamma = 5$, $\sigma = 0.1$, $R = 0$.

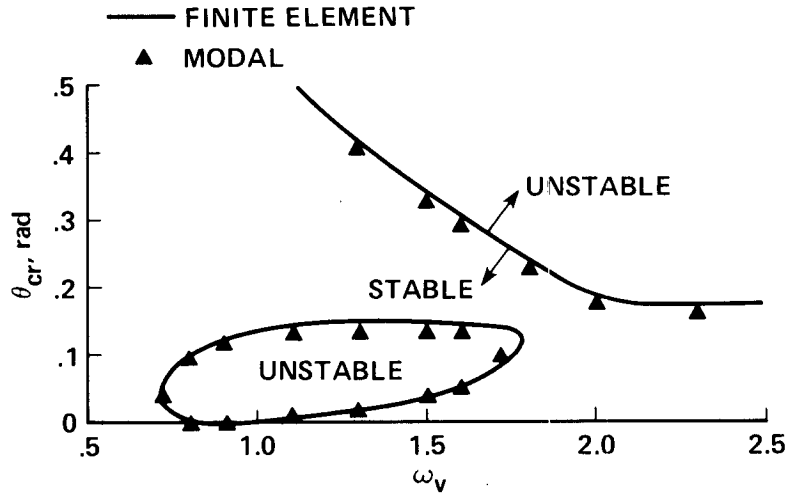

Figure 57.- Comparison of finite element and modal analysis results for flap-lag-torsion of elastic blade in hover: $\bar{\omega}_w = 1.15$, $\bar{\omega}_\phi = 2.5$, $\gamma = 5$, $\sigma = 0.1$, $R = 1$, $\beta_{pc} = 0.05$ rad.

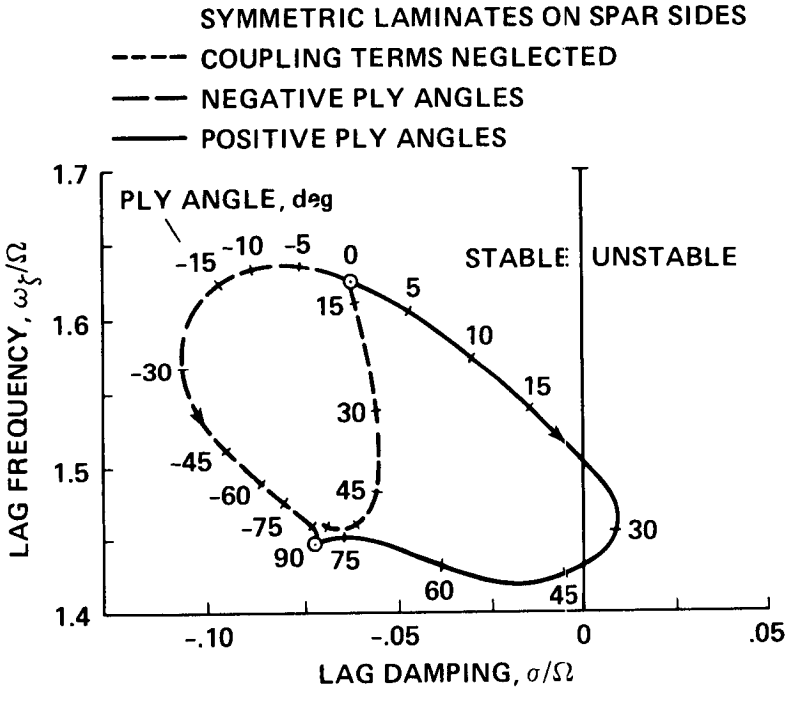

Figure 58.- Effects of composite material ply layup configuration on lead-lag frequency and damping of elastic blade flap-lag-torsion analysis in hover: $C_T/\sigma = 0.1$, $\gamma = 5$, $\sigma = 0.1$.

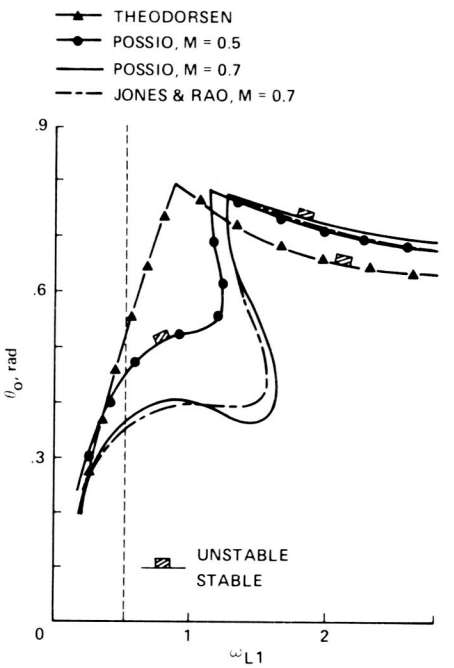

Figure 59.- Effects of unsteady aerodynamics and compressibility on elastic blade flap-lag-torsion stability boundaries in hover: $\bar{\omega}_{F1} = 1.142$, $\bar{\omega}_{T1} = 6.17$, $\gamma = 8$, $\sigma = 0.08$, $\bar{x}_A = 0.2$.

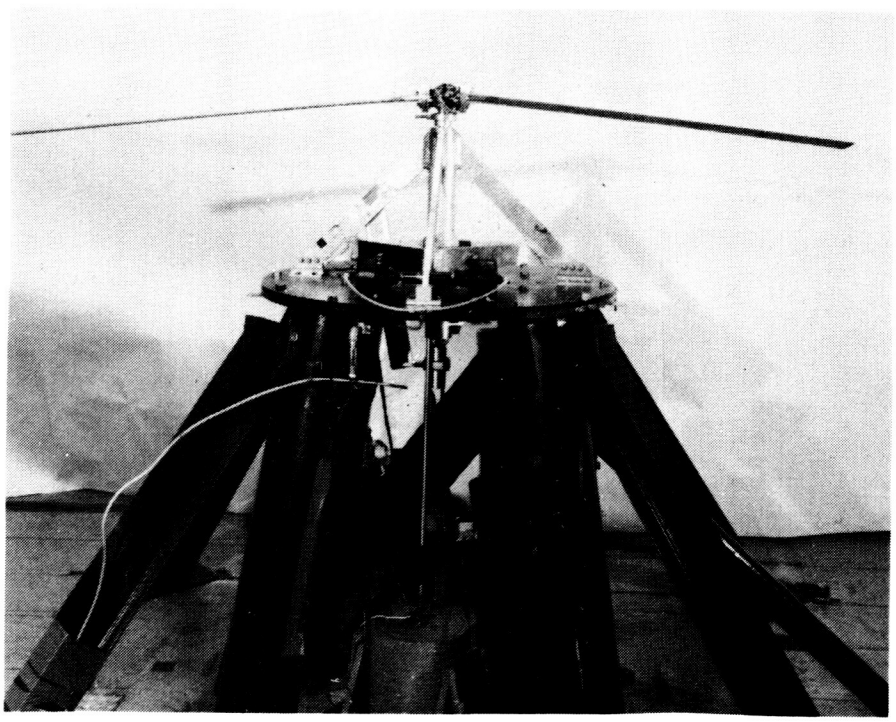

Figure 60.- Small scale 5.5-ft-diam elastic blade-rotor model for flap-lag torsion experiments in hover.

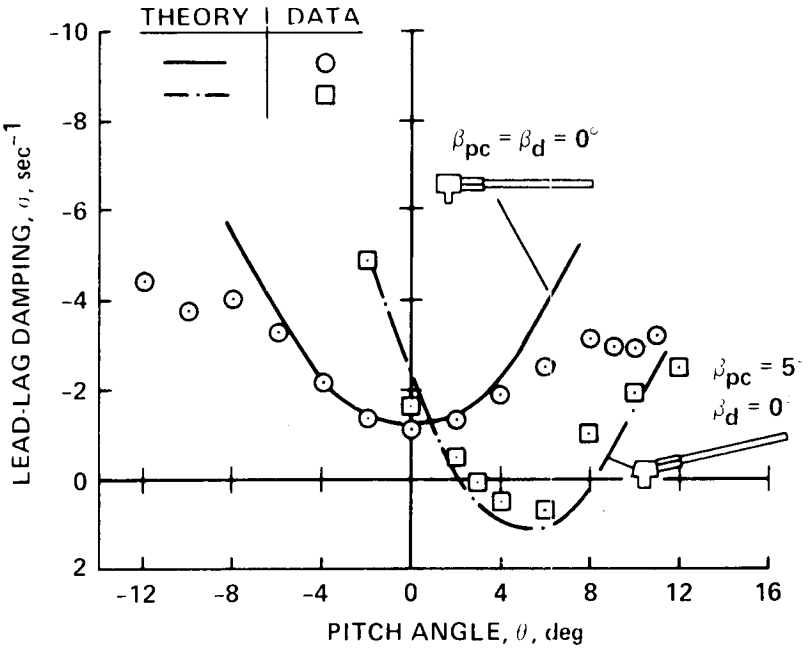

Figure 61.- Comparison of experimental and theoretical results for lead-lag mode damping of small-scale flap-lag-torsion model in hover with and without precone: $\bar{\omega}_w \cong 1.13$, $\bar{\omega}_v \cong 1.4$, $\bar{\omega}_\phi \cong 2.6$.

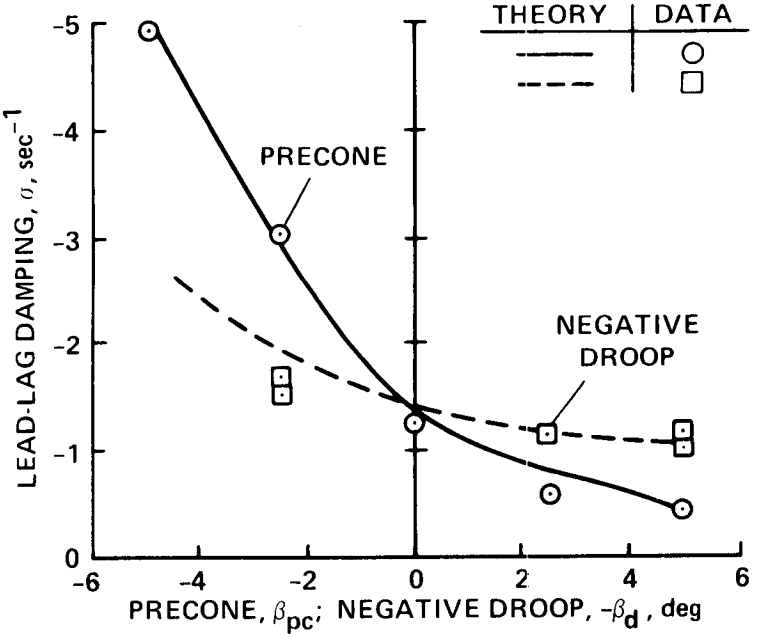

Figure 62.- Comparison of experimental and theoretical results for lead-lag mode damping of small-scale flap-lag-torsion model in hover as a function of precone and droop: $\theta_o = 2°$.

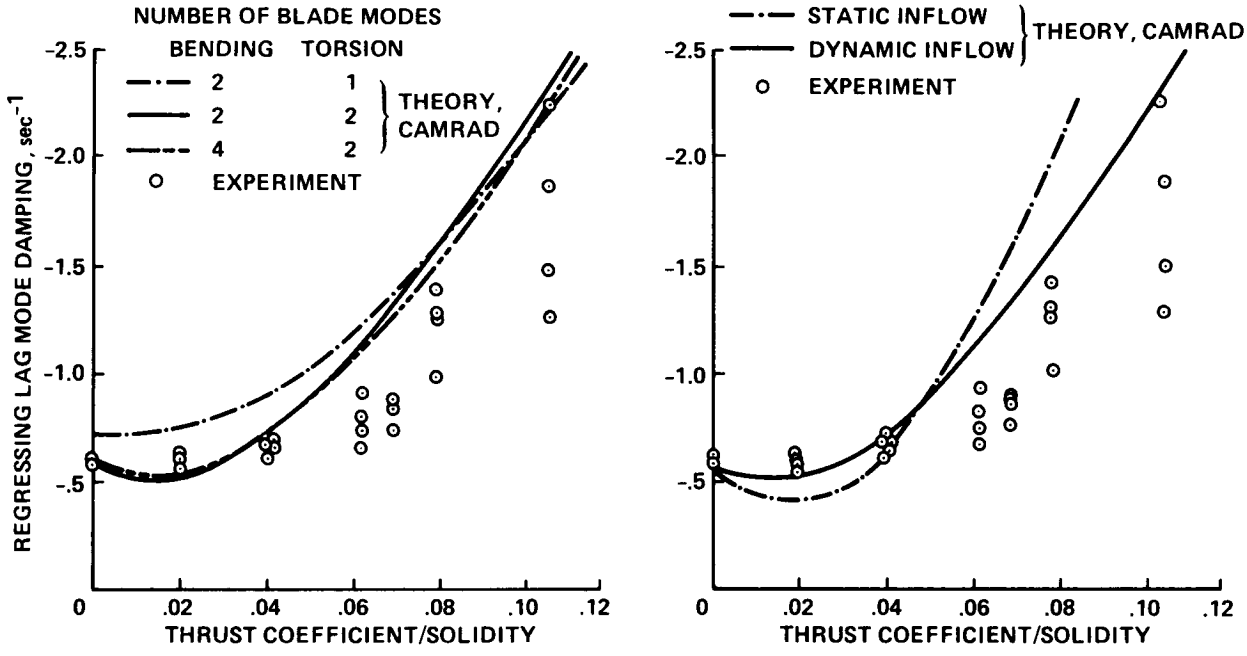

Figure 63.- Comparison with theory of experimental lead-lag mode damping of full-scale BO-105 rotor tested in 40- by 80-Foot Wind Tunnel.

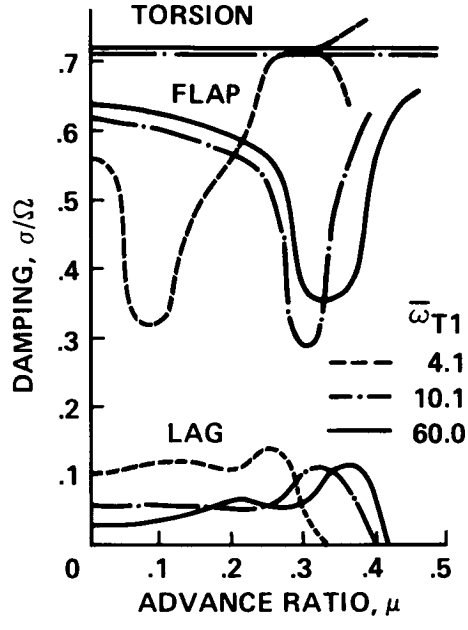

Figure 64.- Modal damping for elastic blade flap-lag-torsion analysis in forward flight: $\bar{\omega}_{F1} = 1.1$, $\bar{\omega}_{L1} = 0.902$, $\gamma = 10$, $\sigma = 0.05$, $C_W = 0.01$.

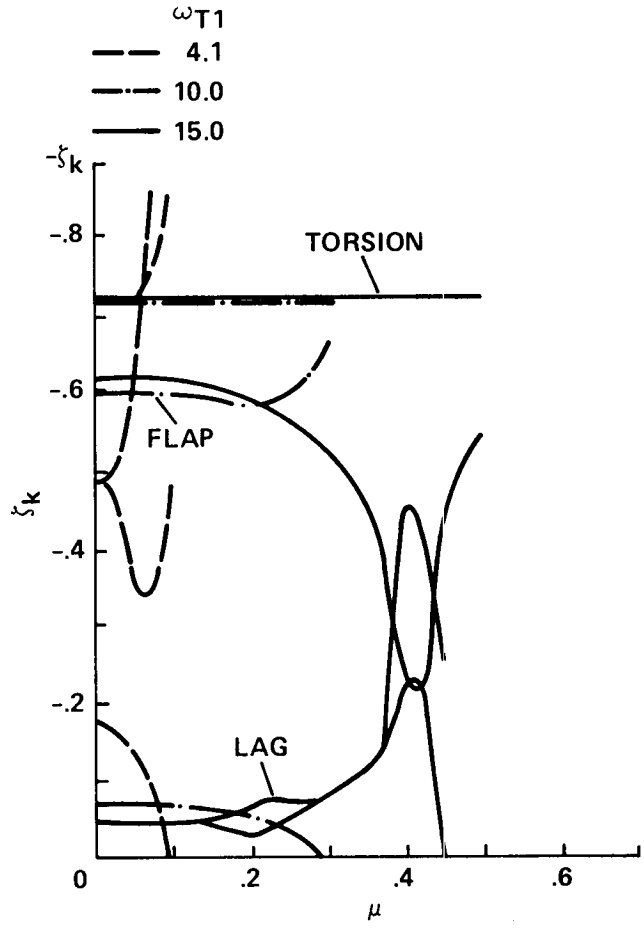

Figure 65.- Modal damping for elastic blade flap-lag-torsion analysis in forward flight with improved equations: $\bar{\omega}_{F1} = 1.1$, $\bar{\omega}_{L1} = 0.902$, $\gamma = 10$, $\sigma = 0.05$, $C_W = 0.01$.

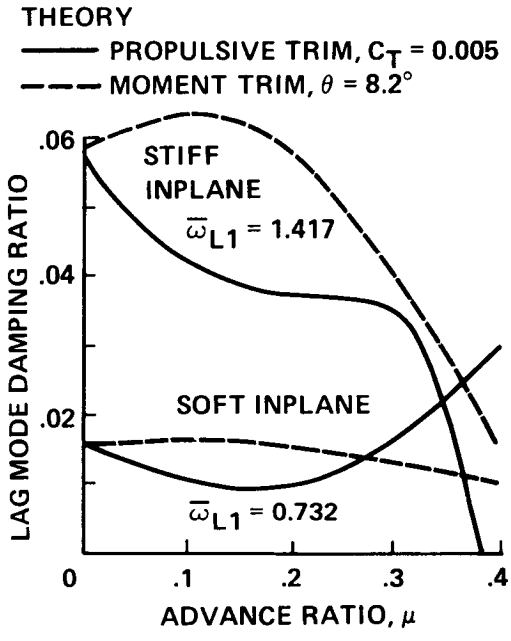

Figure 66.- Lead-lag mode damping for elastic blade flap-lag-torsion analysis in forward flight for two trim conditions: $\bar{\omega}_{F1} = 1.125$, $\bar{\omega}_{T1} = 3.176$, $\gamma = 5.5$, $\sigma = 0.07$, $R = 1$.

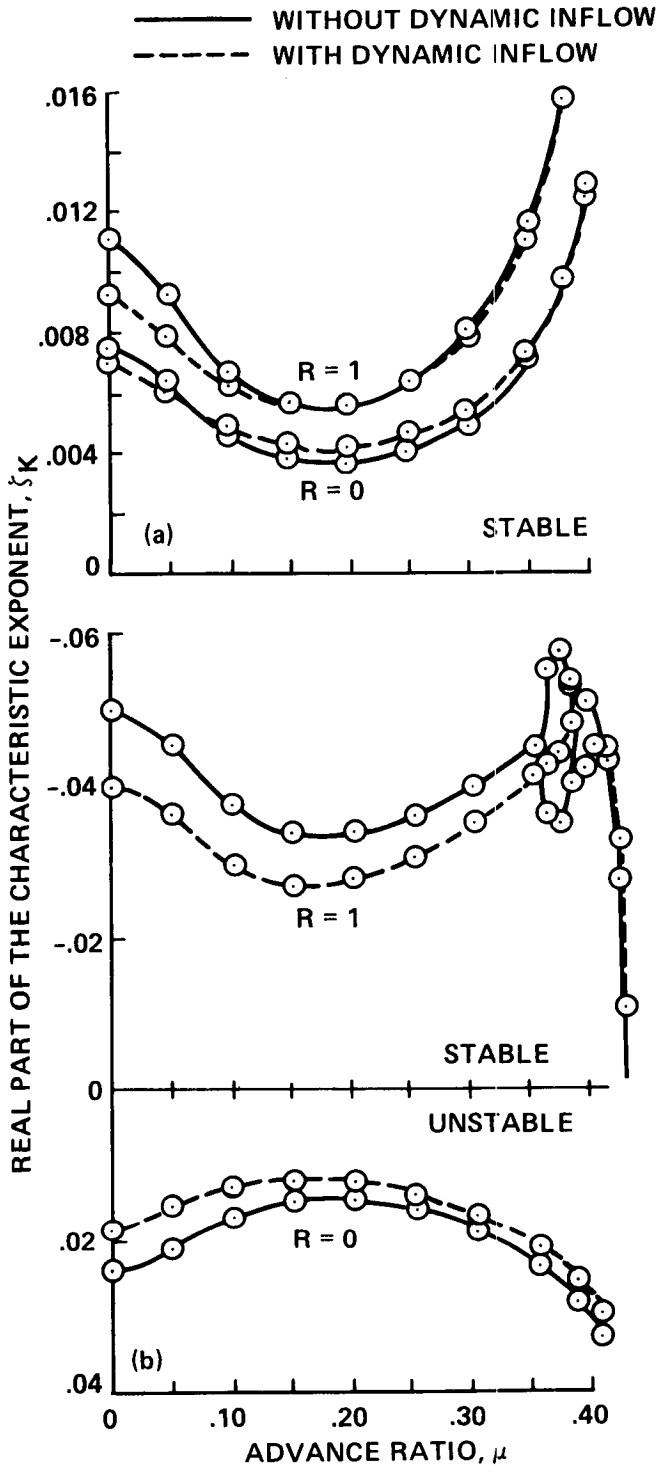

Figure 67.- Effects of dynamic inflow and flap-lag structural coupling on lead-lag regressing mode damping for elastic blade flap-lag-torsion analysis in forward flight: $\bar{\omega}_w = 1.15$, $\gamma = 5$, $\sigma = 0.1$. (a) Soft inplane: $\bar{\omega}_v = 0.7$. (b) Stiff inplane: $\bar{\omega}_v = 1.4$.

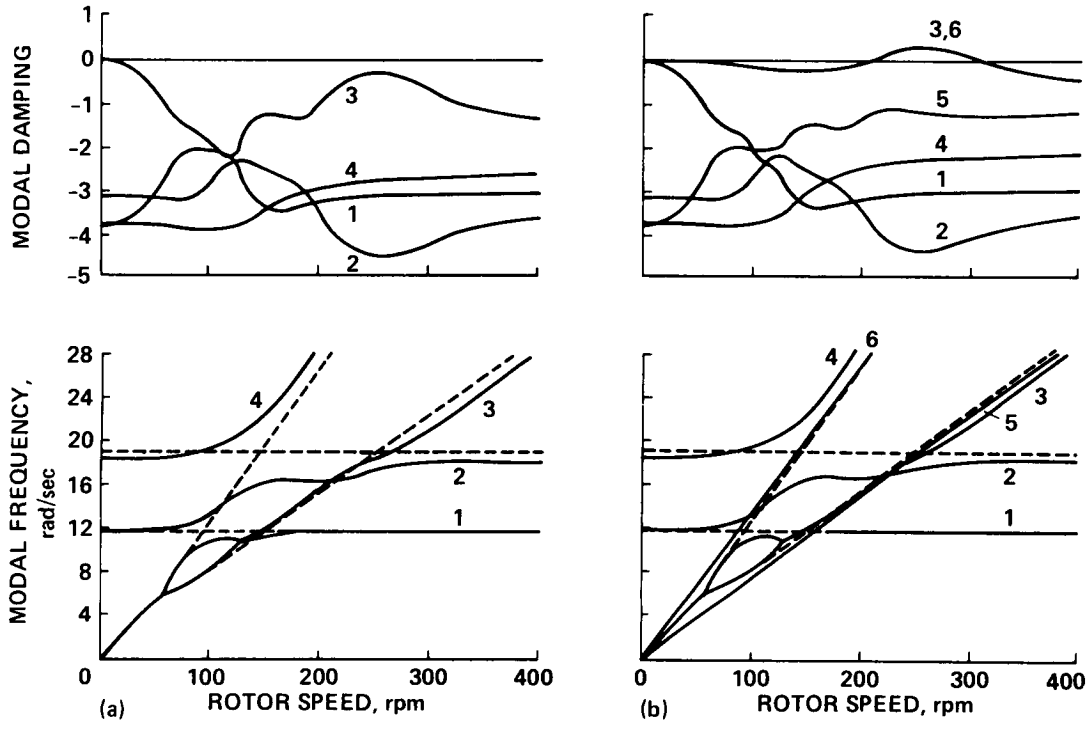

Figure 68.- Effects of blade dissimilarity on ground-resonance stability analysis of articulated rotor system. (a) All blade lead-lag dampers operative. (b) One damper inoperative.

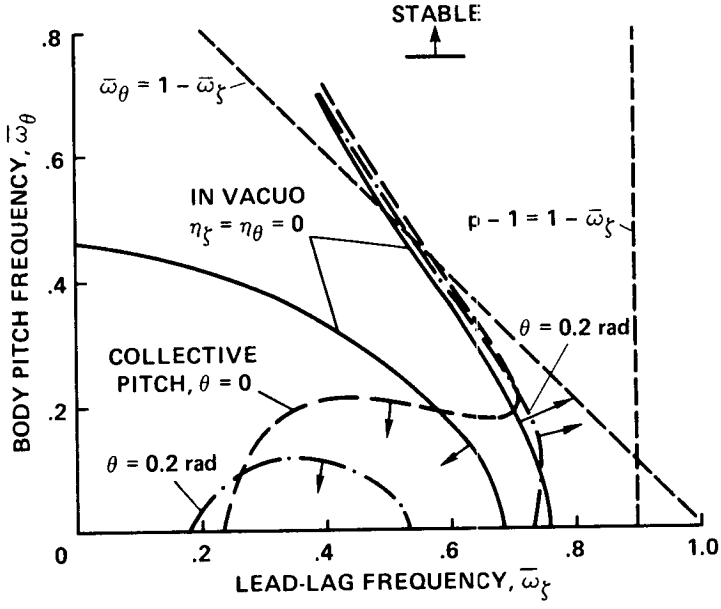

Figure 69.- Hingeless rotor ground-resonance stability boundaries with hinged-rigid blade flap, lead-lag, and body pitch degrees of freedom: $p = 1.1$, $\gamma = 5$, $\sigma = 0.05$, $R = 0$.

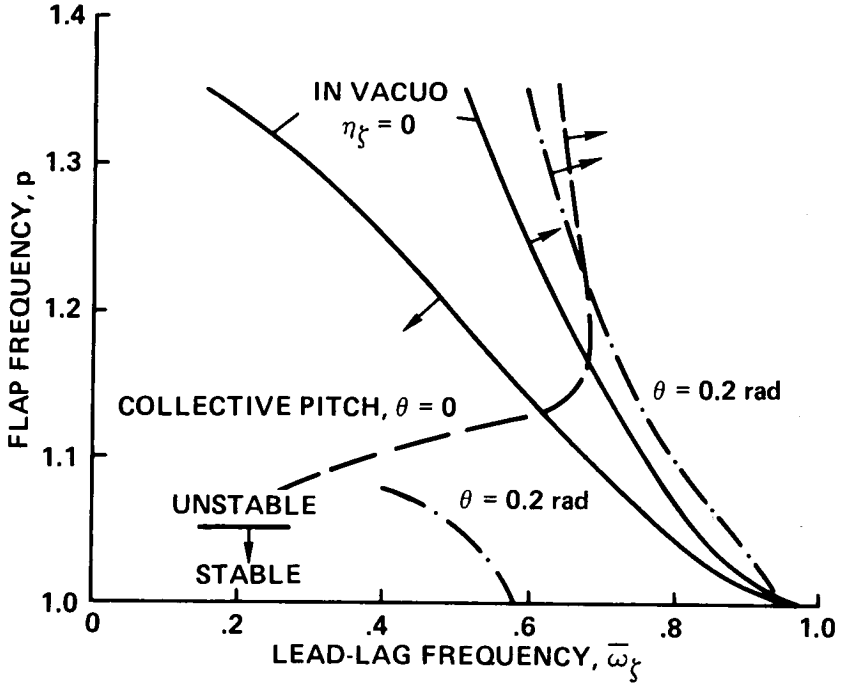

Figure 70.- Hingeless-rotor air-resonance stability boundaries with hinged-rigid blade flap, lead-lag, and body pitch degrees of freedom in hover: $\gamma = 5$, $\sigma = 0.05$.

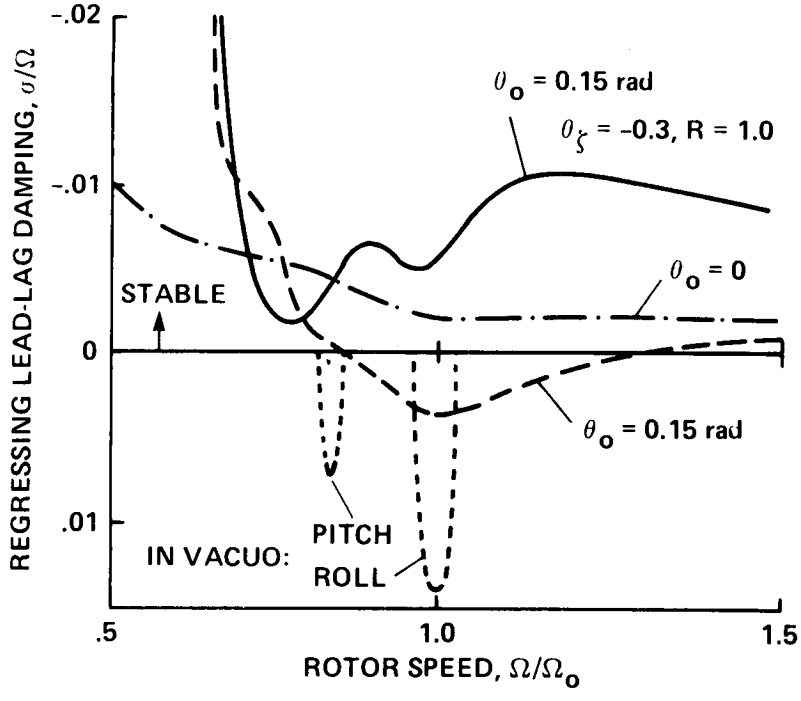

Figure 71.- The effects of aerodynamics, thrust, and aeroelastic couplings on hingeless-rotor air resonance in hover as a function of rotor speed: $p_o = 1.1$, $\bar{\omega}_{\zeta_o} = 0.7$, $\gamma = 5$, $\sigma = 0.05$.

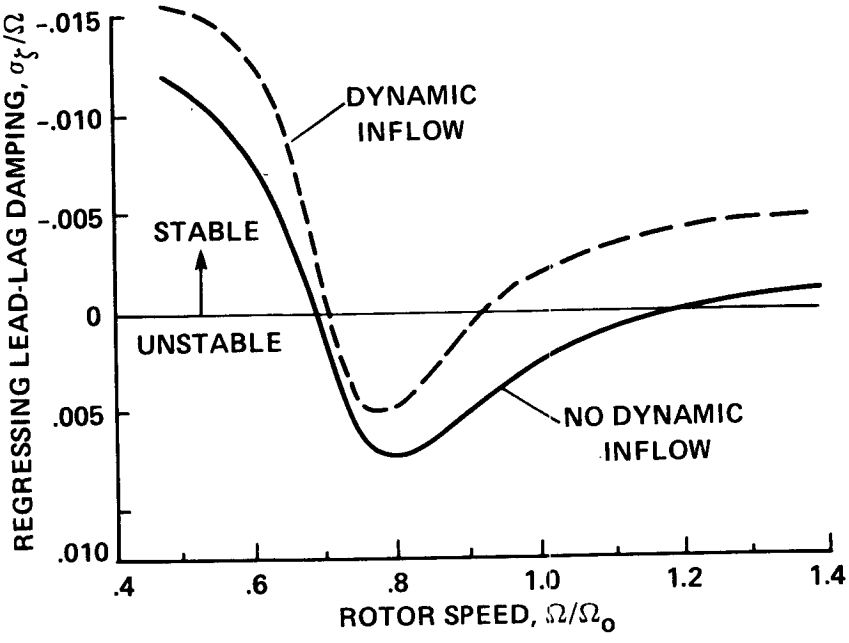

Figure 72.- Effect of dynamic inflow on hingeless-rotor air resonance for a matched stiffness configuration: θ_o = 0.3 rad, p_o = 1.1, $\bar{\omega}_{\zeta_o}$ = 0.458.

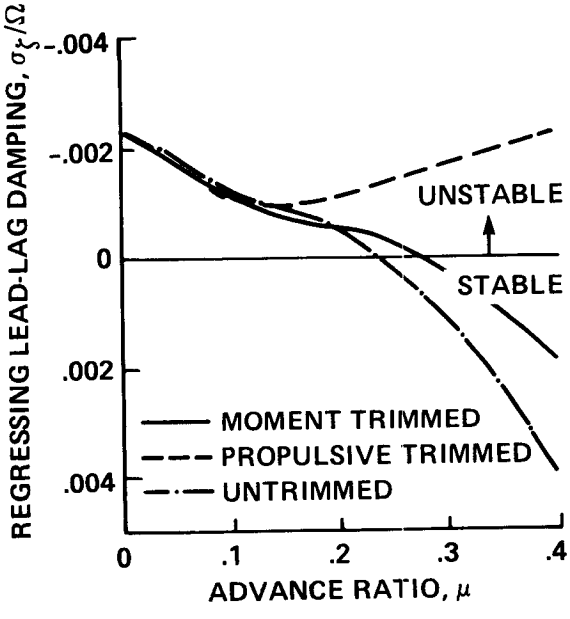

Figure 73.- Coupled rotor-body lead-lag regressing mode damping in forward flight for various trim conditions: p = 1.15, $\bar{\omega}_\zeta$ = 0.7, C_T/σ = 0.2.

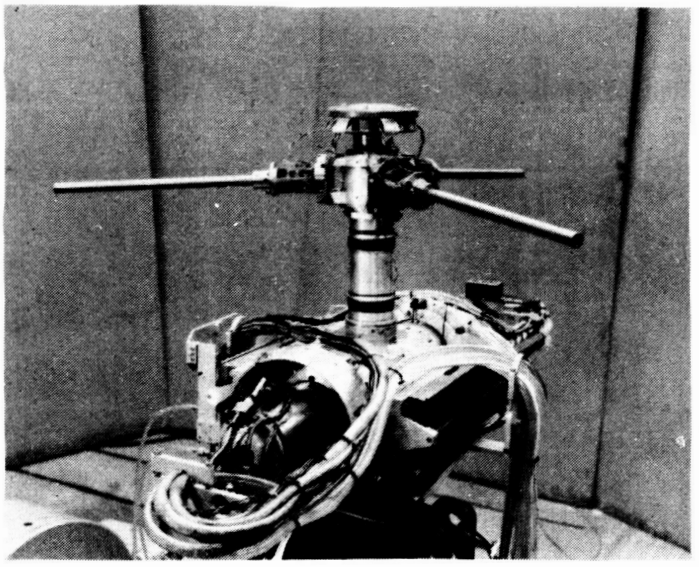

Figure 74.- Small-scale rotor model for coupled rotor-body stability experiments with non-airfoil blades to simulate in vacuum conditions.

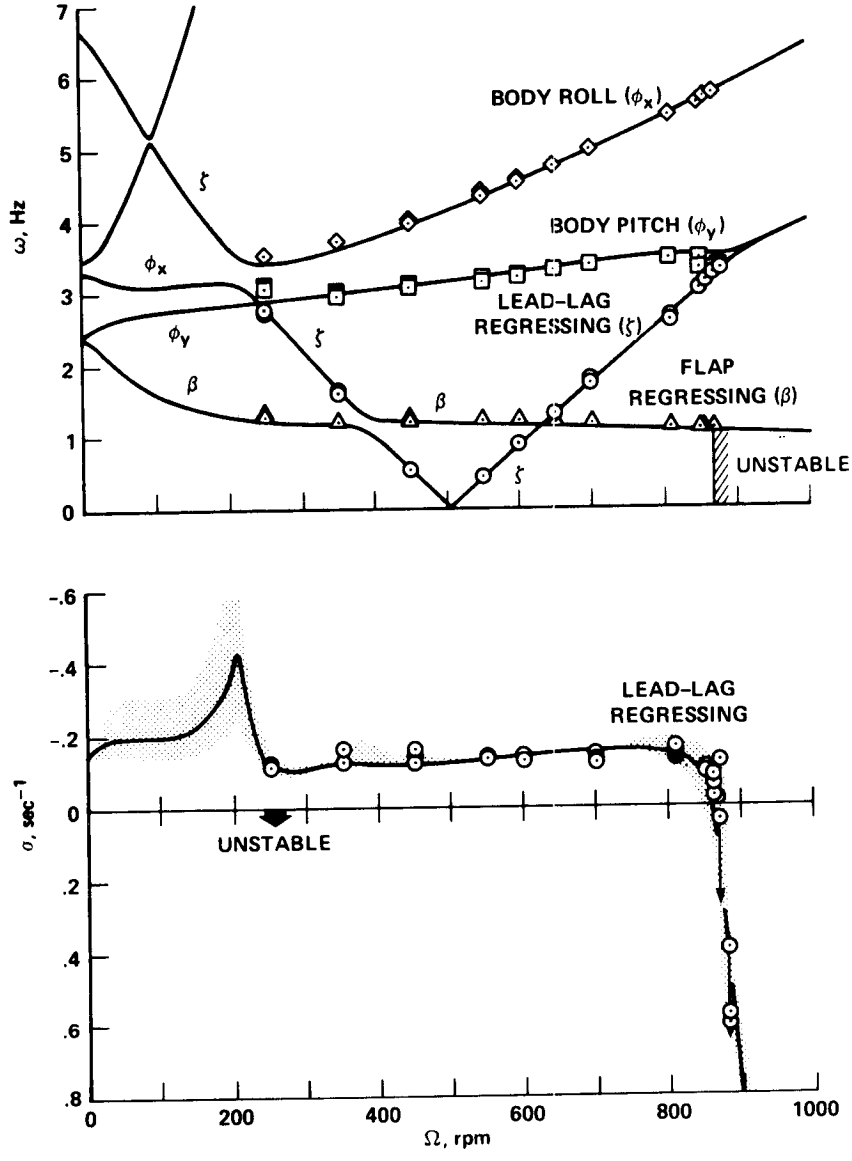

Figure 75.- Comparison of experimental and theoretical frequency and damping as a function of rotor speed for coupled rotor-body model with simulated in vacuum blades.

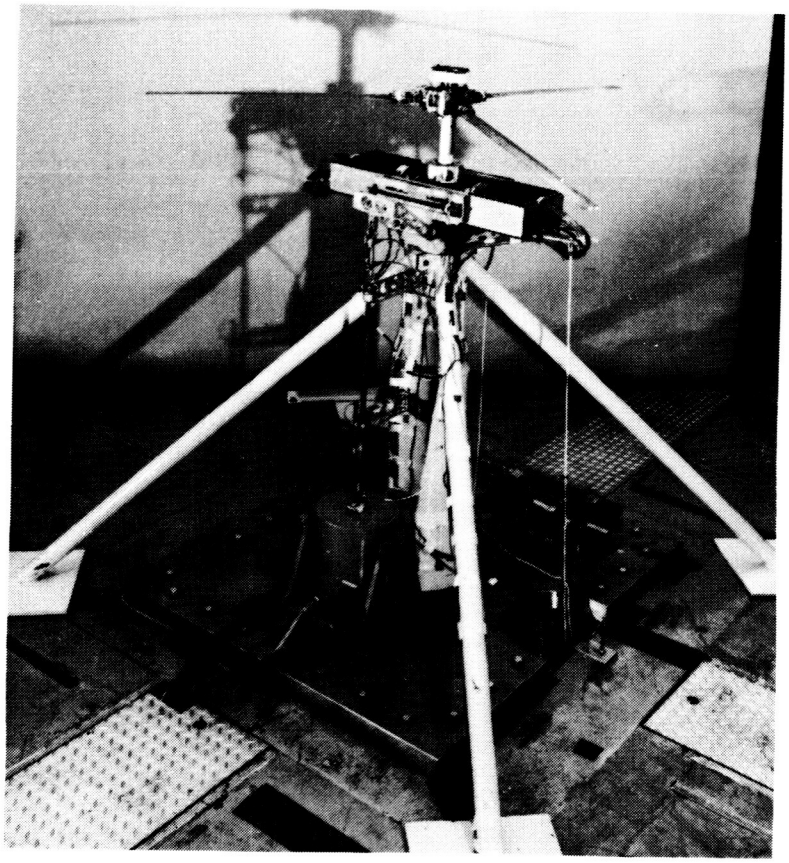

Figure 76.- Small-scale rotor model for coupled rotor-body hover stability experiments with 5.5-ft-diam three-bladed rotor.

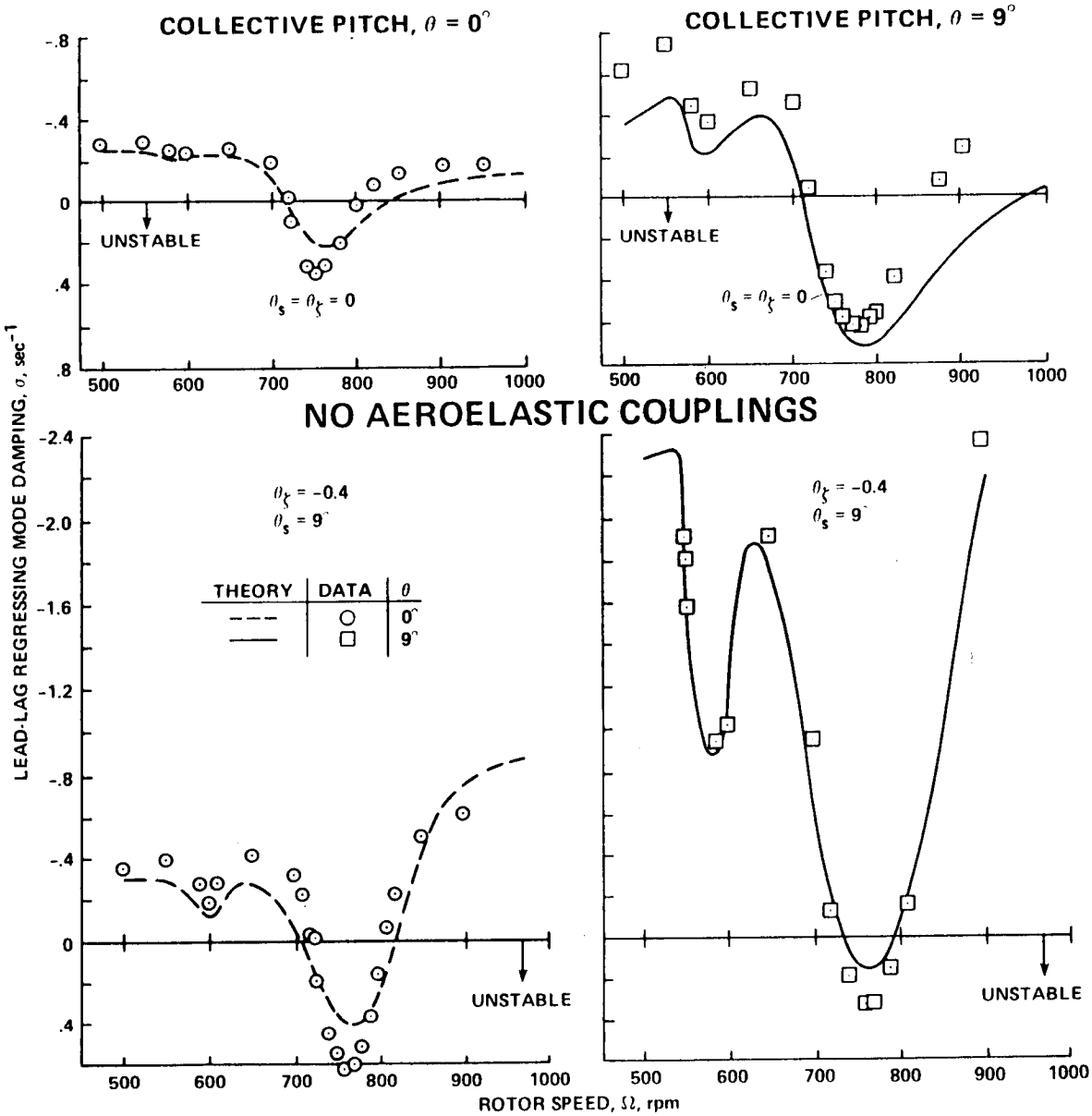

Figure 77.- Comparison of experimental and theoretical regressing lead-lag mode damping for coupled rotor-body model in hover including effects of aeroelastic coupling.

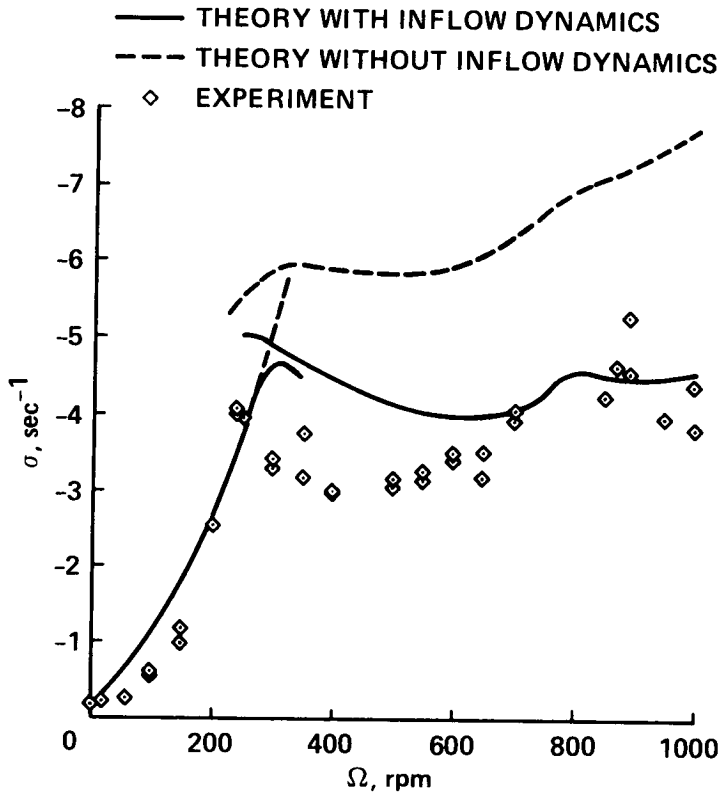

JOHNSON, 1982 (AFDD)

Figure 78.- Comparison of experimental and theoretical roll-mode damping for coupled rotor-body model in hover including effects of dynamic inflow.

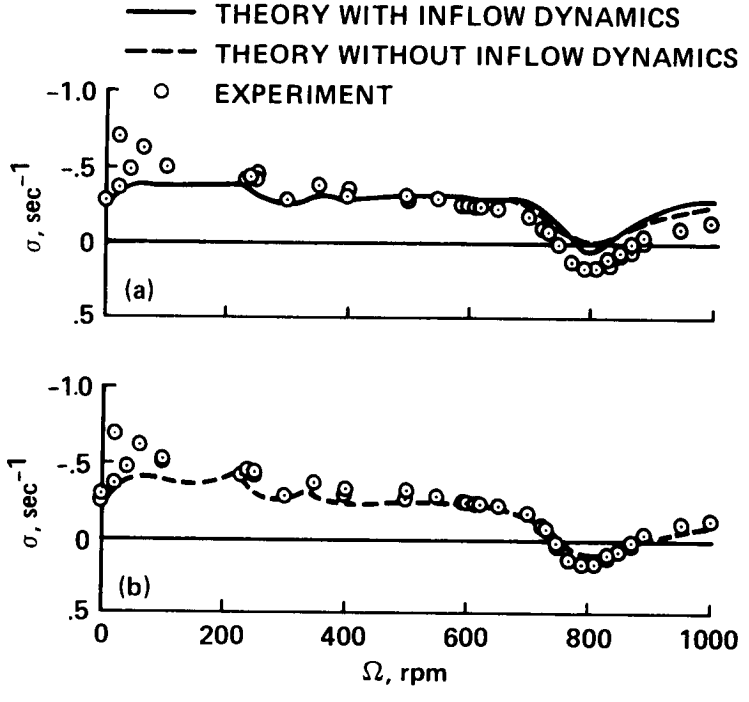

Figure 79.- Comparison of experimental and theoretical regressing lead-lag mode damping for coupled rotor-body model in hover. (a) Johnson's results including dynamic inflow. (b) Bousman's result without dynamic inflow.

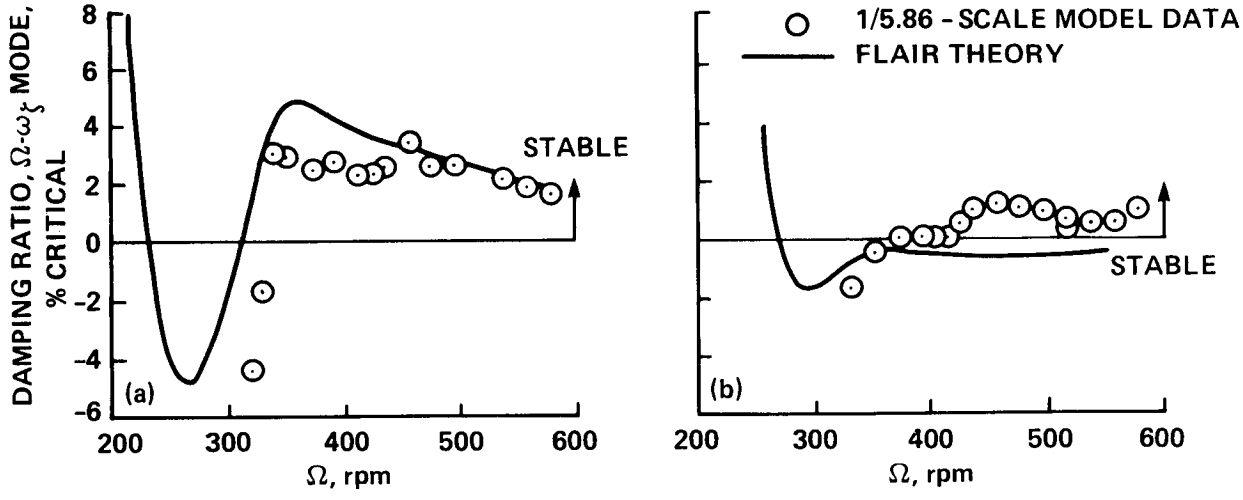

Figure 80.- Comparison of small-scale bearingless-rotor model experimental results for lead-lag regressing mode damping with FLAIR analysis, $\gamma = 3.64$, $\sigma = 0.07$. (a) $\theta_f = 6°$, $\beta_b = 2.5°$, $\theta_b = 1.95°$. (b) $\theta_f = 0°$, $\beta_f = 2.5°$, $\theta_b = 7.95°$.

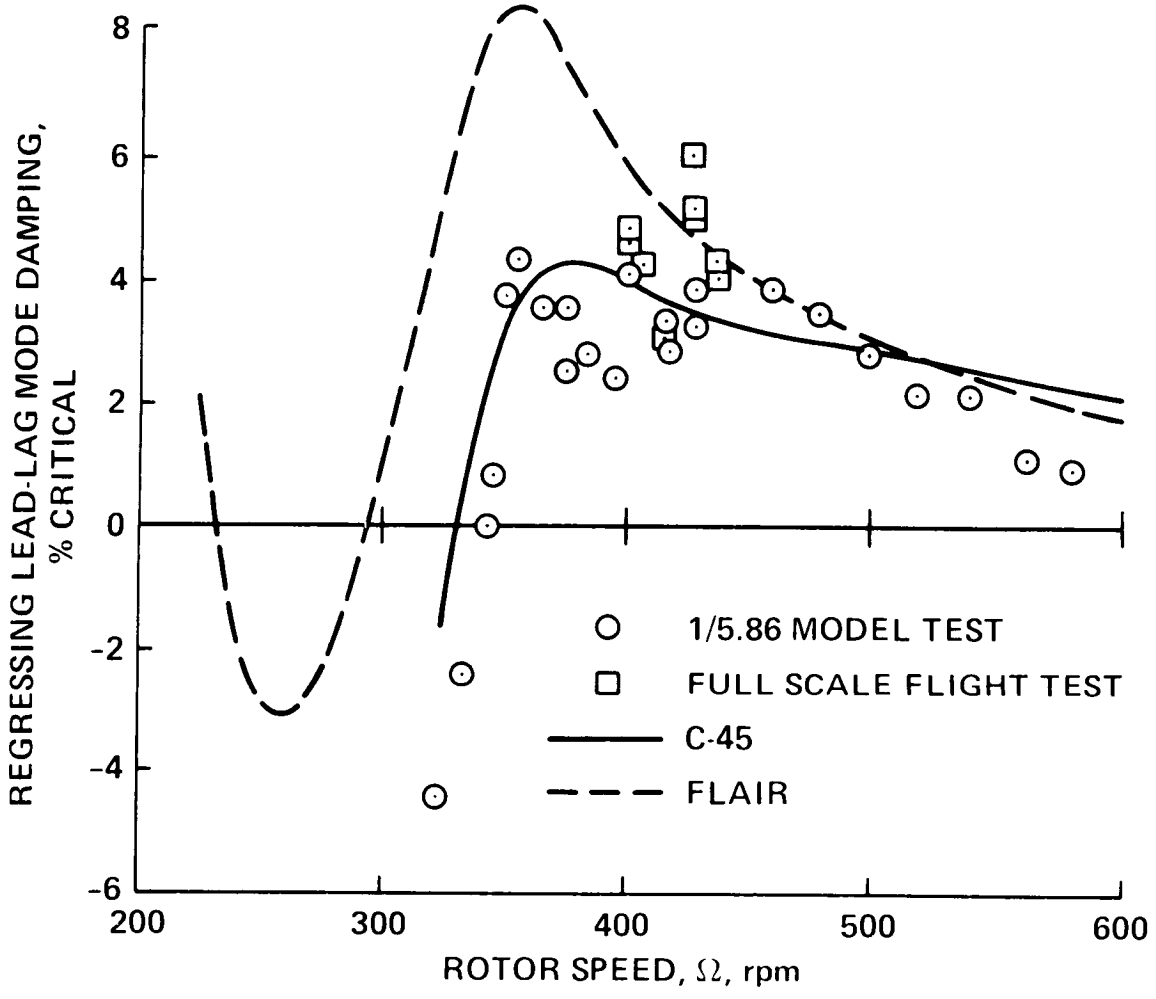

Figure 81.- Comparison of several experimental and theoretical results for hover air-resonance stability of Boeing Vertol BO-105 bearingless main rotor (BMR).

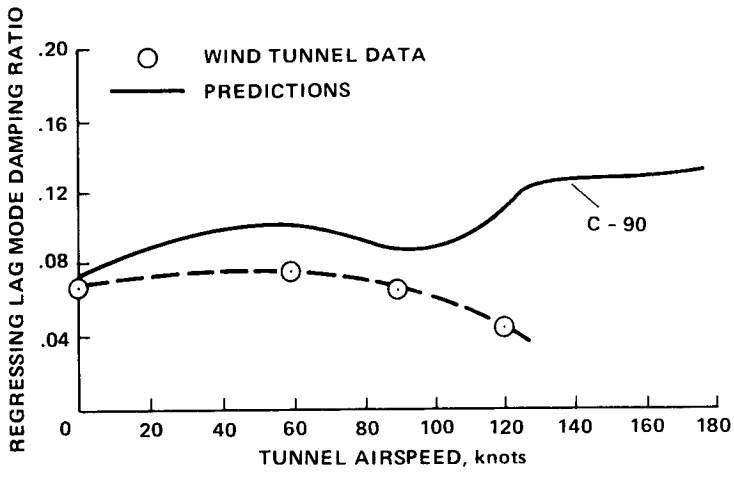

Figure 82.- Comparison of Boeing Vertol BMR 40- by 80-Foot Wind-Tunnel data with analysis for forward flight.

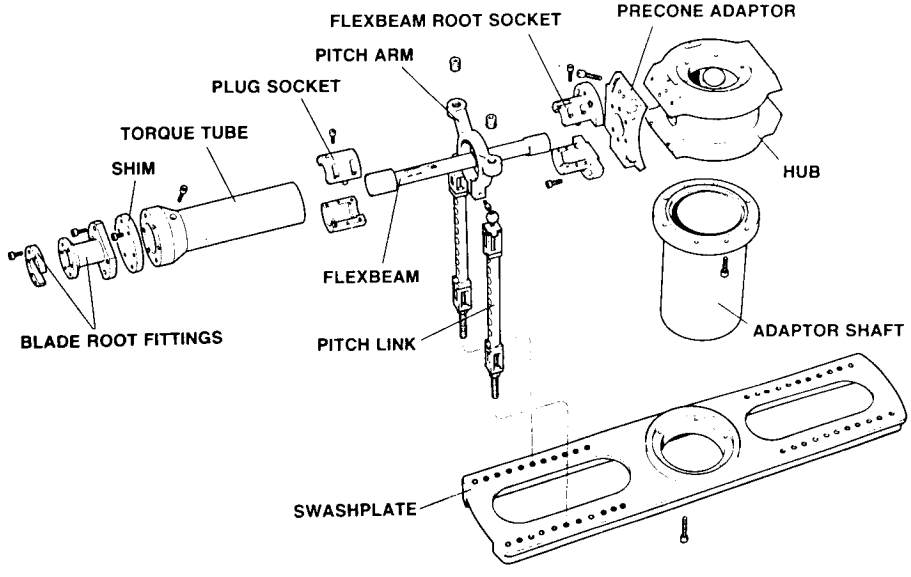

Figure 83.- Hub flexbeam and pitch-control system components of small-scale experimental bearingless rotor model.

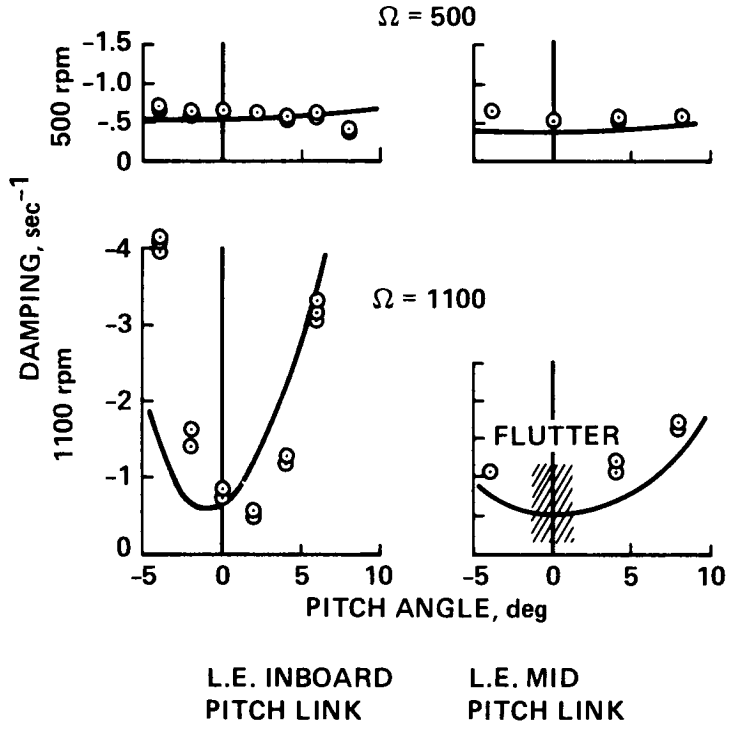

Figure 84.- Comparison of FLAIR theory with experimental measurements of lead-lag damping for small-scale, 2-blade bearingless-rotor model.

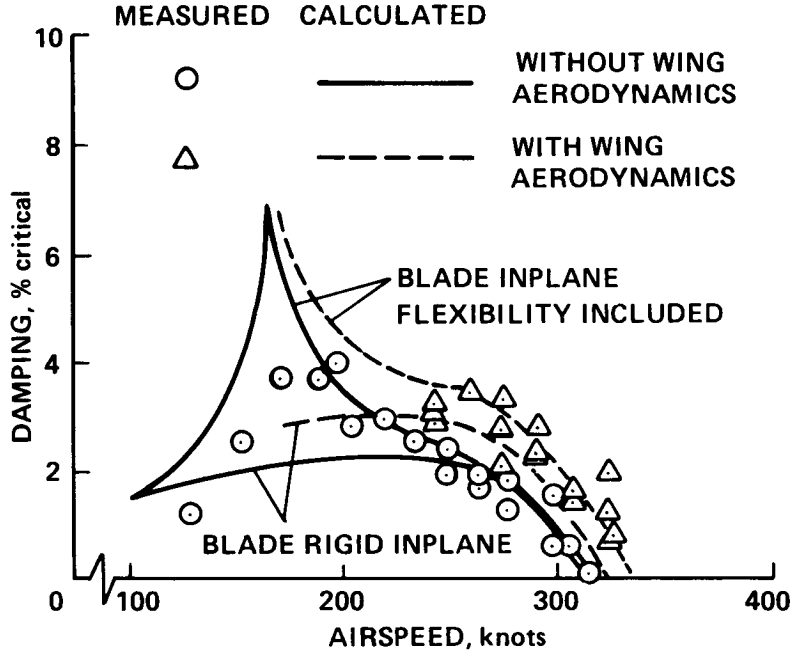

Figure 85.- Comparison of measured small-scale model wing beam mode damping with theory for Bell Model 266 tilt-rotor configuration.

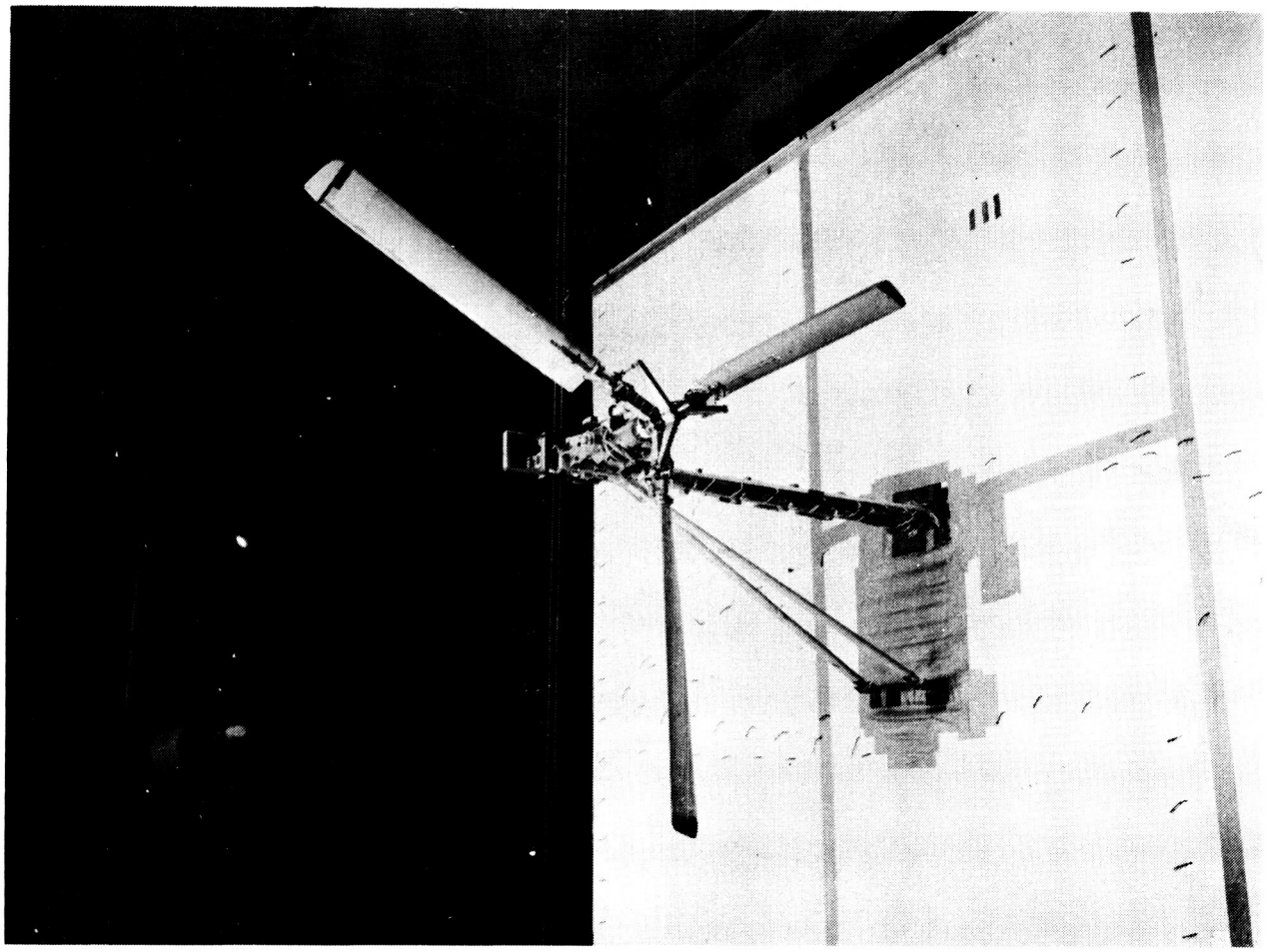

Figure 86.- Small-scale rotor, pylon, wing tilt-rotor research model installed in Langley Transonic Dynamics Tunnel.

Figure 87.- Full-scale semispan rotor-pylon-wing model installed in Ames 40- by 80-Foot Wind Tunnel.

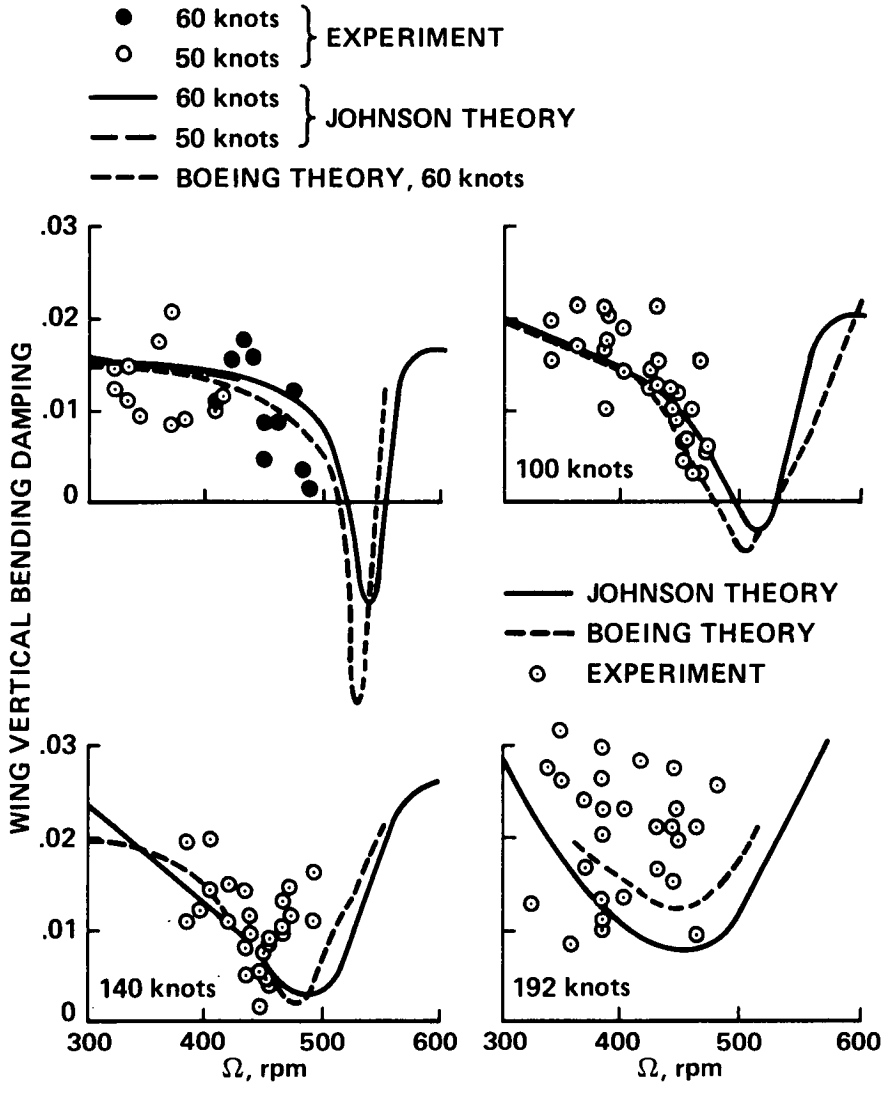

Figure 88.- Full-scale Boeing Vertol semispan rotor-pylon-wing model vertical wing bending mode experimental damping measurements compared with theory as a function of rotor speed for different tunnel velocities.

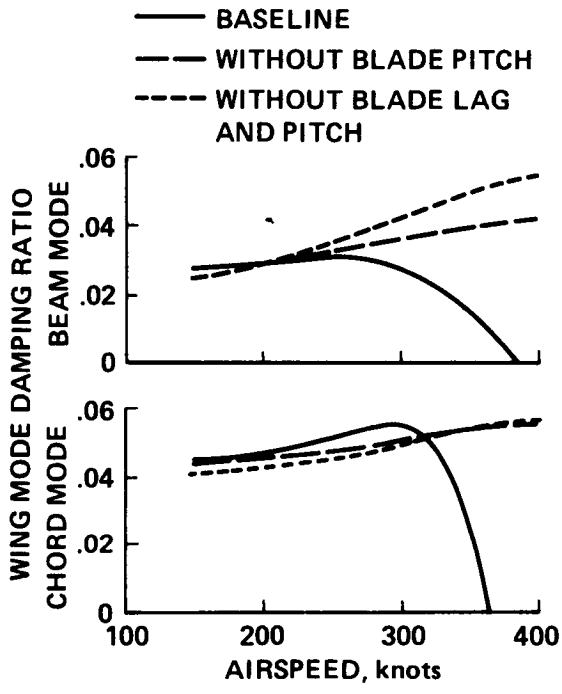

Figure 89.- Effects of rotor-blade pitch and lag motion on tilt-rotor wing bending mode damping in cruise flight.

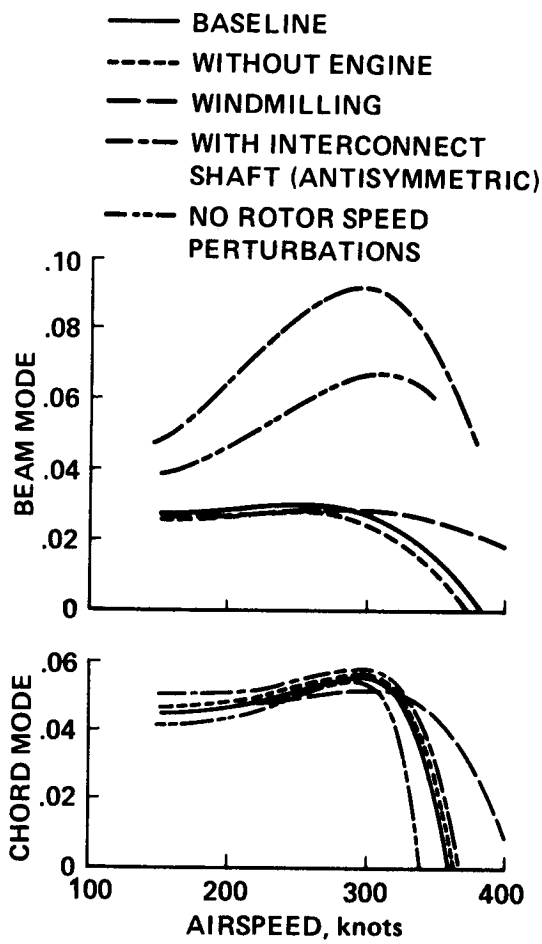

Figure 90.- Effects of rotor drive system dynamics and rotor-shaft interconnect on tilt-rotor wing bending-mode damping in cruise flight.

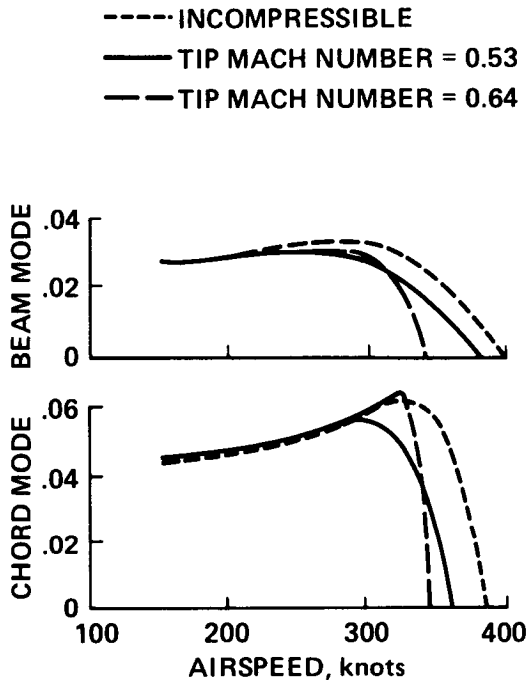

Figure 91.- Effects of compressible aerodynamics on tilt-rotor wing bending-mode damping in cruise flight.

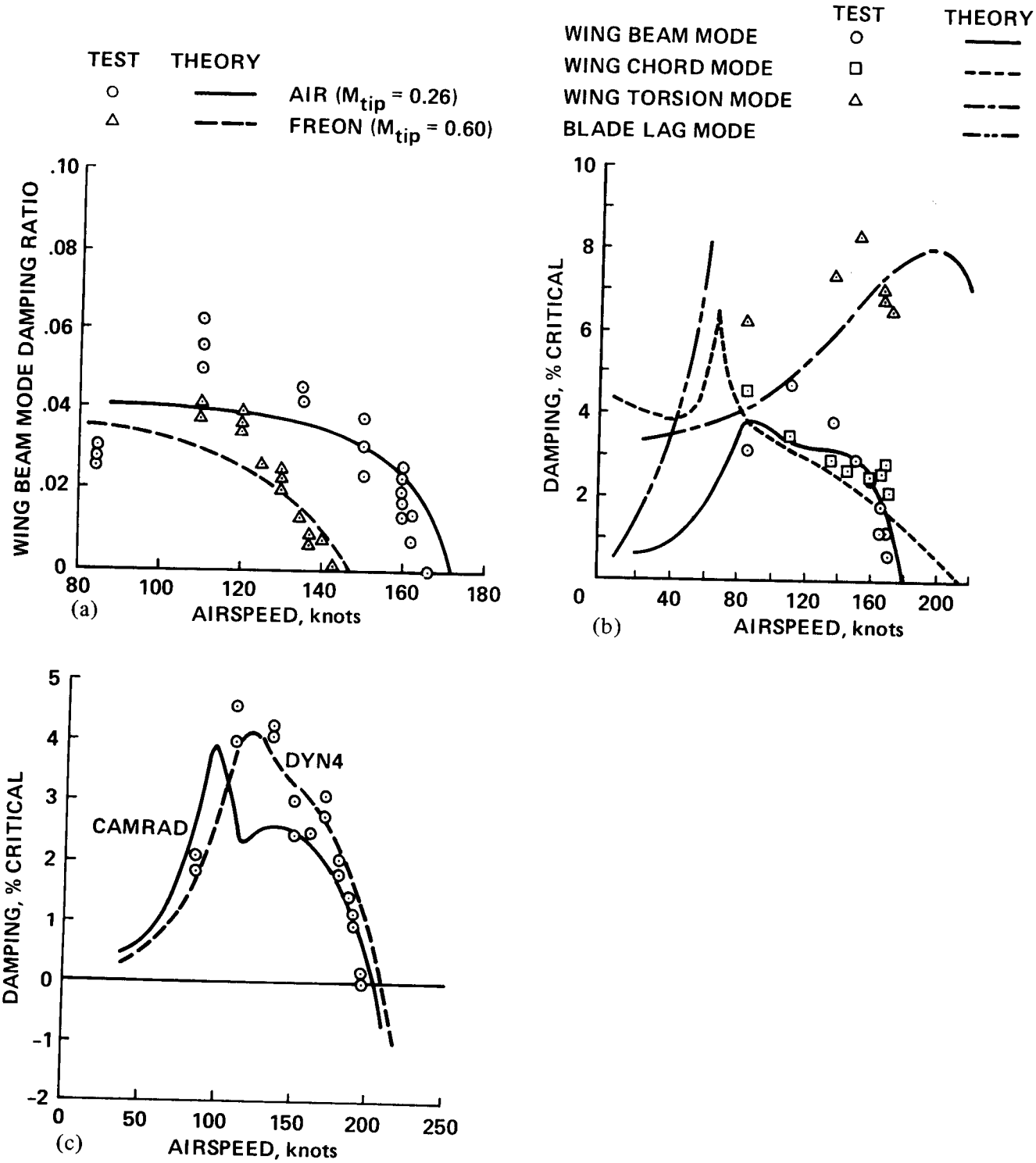

Figure 92.- Langley Transonic Dynamics Tunnel Model experimental stability measurements of small-scale V-22 tilt-rotor models compared with predictions of various theories. (a) CAMRAD. (b) PASTA. (c) CAMRAD and DYN4.

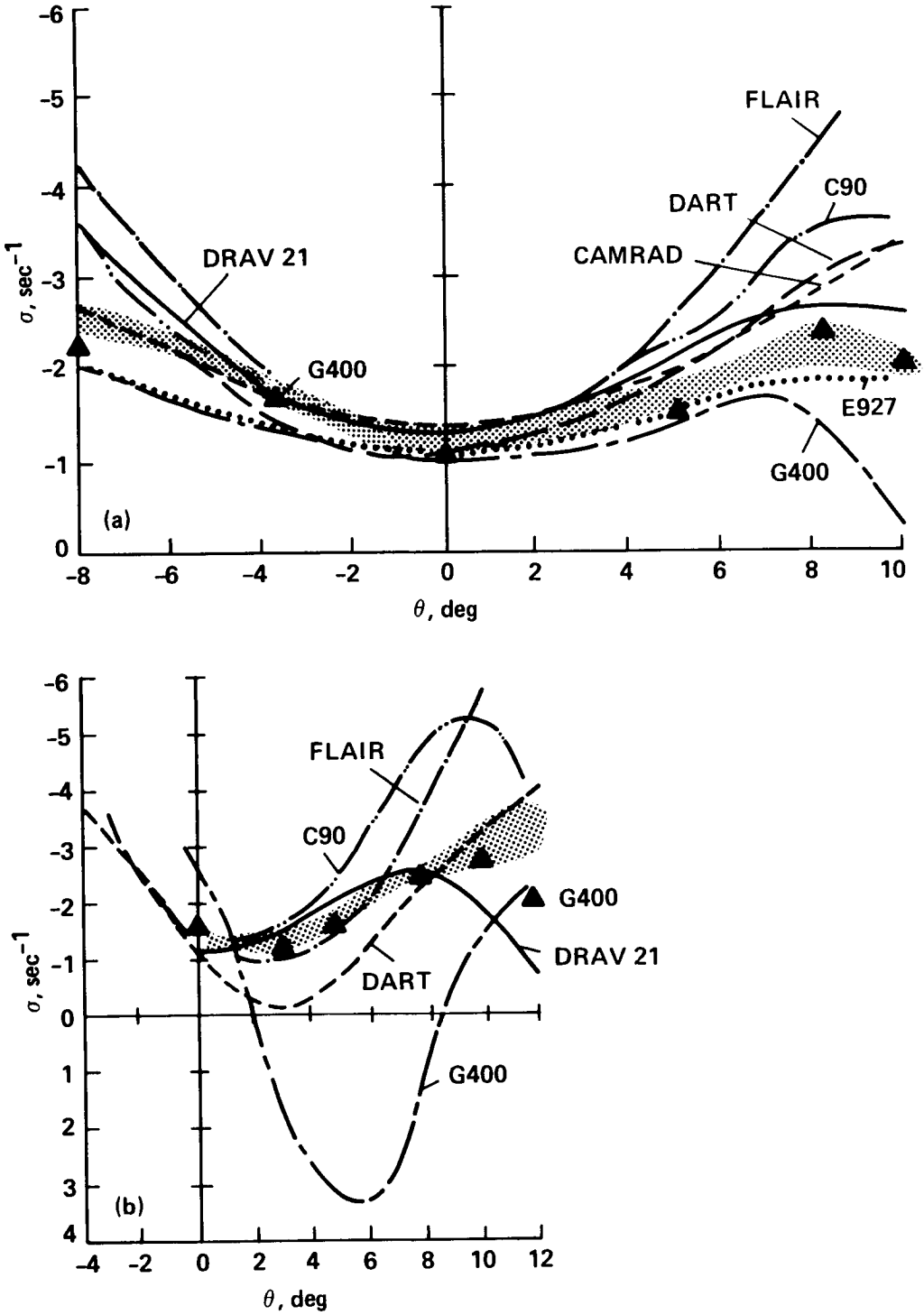

Figure 93.- Comparisons of lead-lag damping predicted by several aeroelastic stability analyses for a small-scale elastic blade flap-lag-torsion model in hover including experimental data; experimental data is shaded region. (a) No droop and stiff torsion flexure. (b) -5.0° droop and soft torsion flexure.

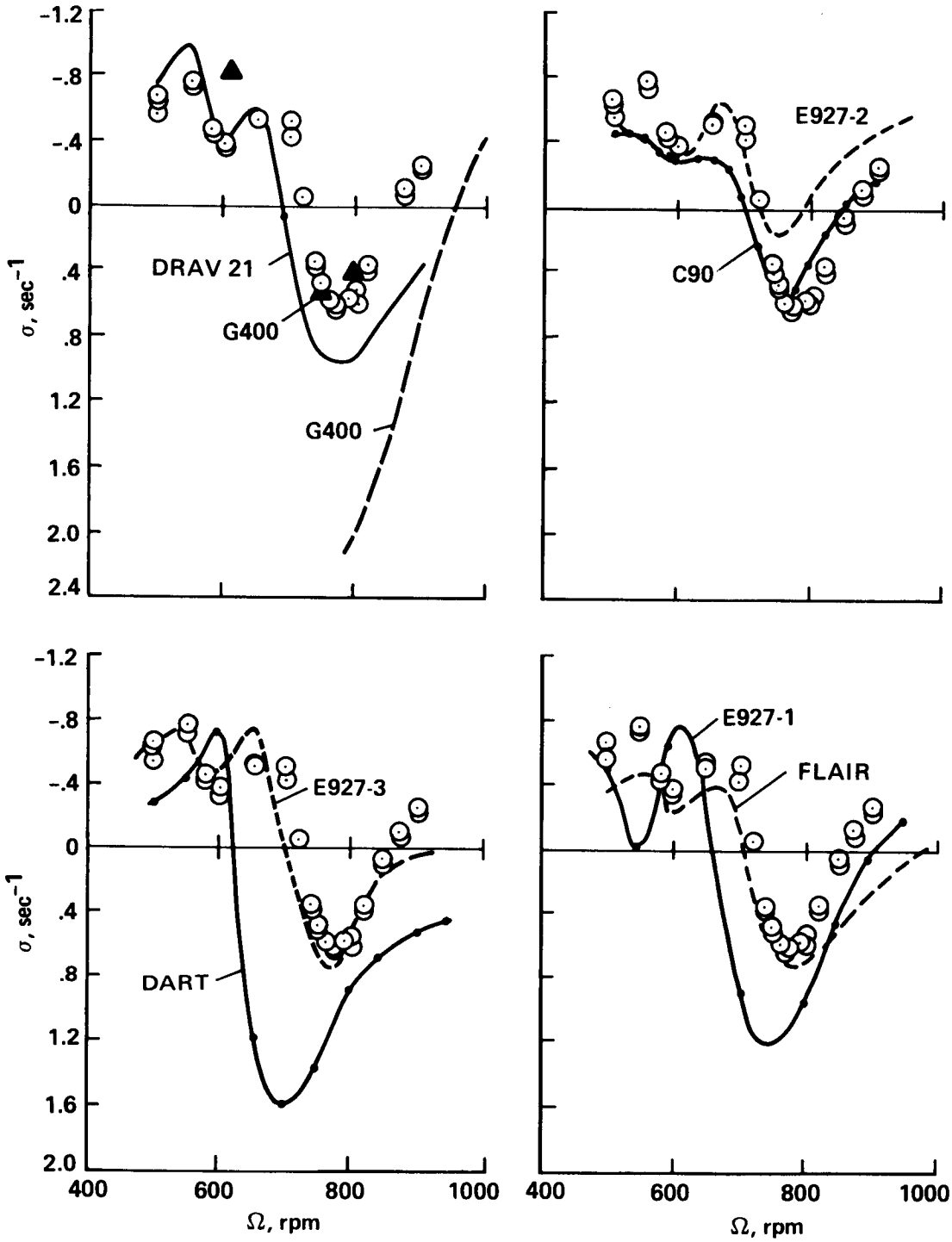

Figure 94.- Comparisons of regressing lead-lag damping predicted by several aeroelastic stability analyses for a coupled rotor-body model in hover including experimental data.

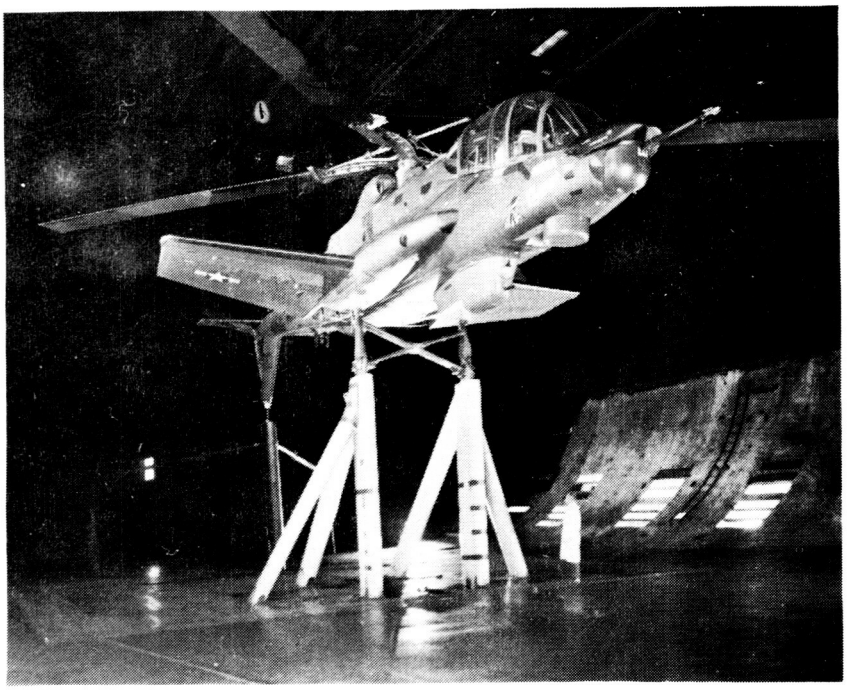

Figure 95.- Lockheed AH-56A Cheyenne installed in 40- by 80-Foot Wind Tunnel.

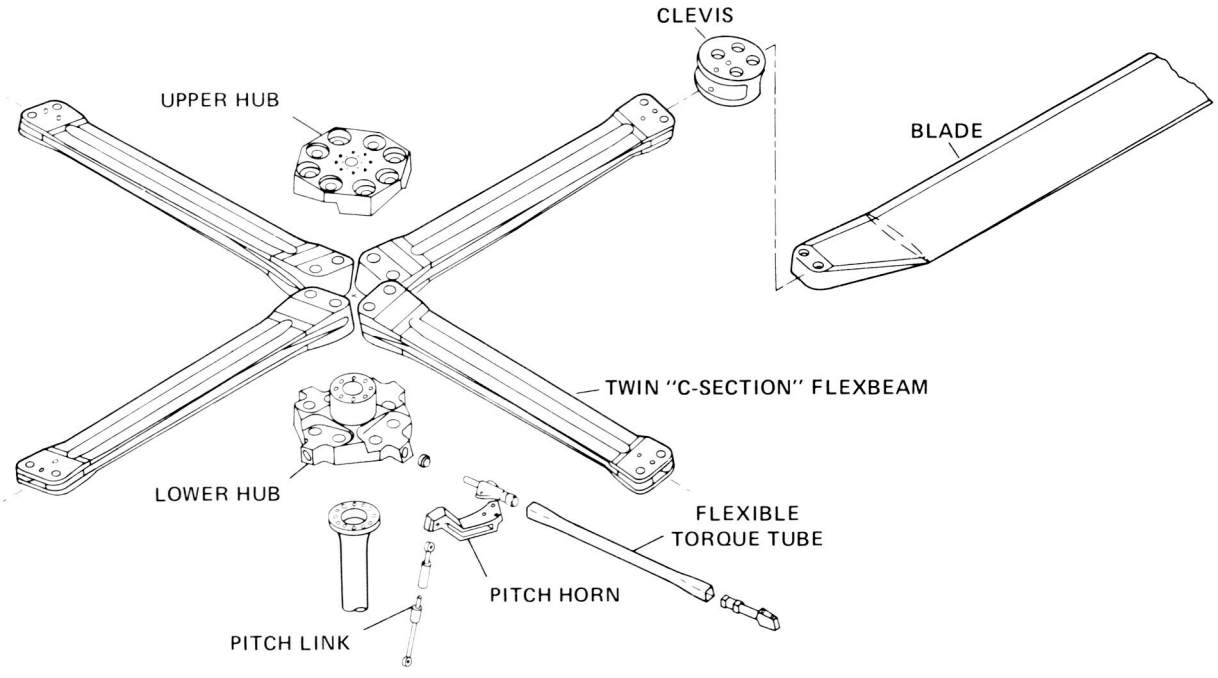

Figure 96.- Boeing Vertol bearingless main rotor (BMR).

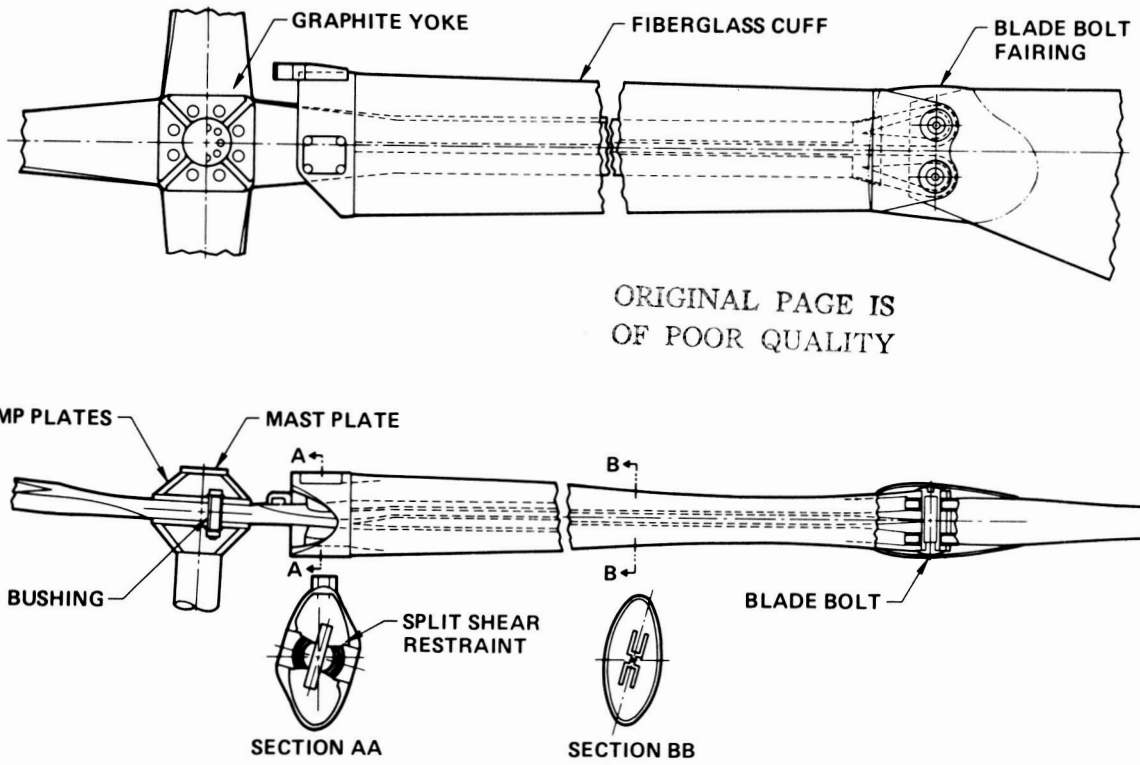

Figure 97.- A damperless bearingless-rotor hub design for the ITR/FRR rotor.

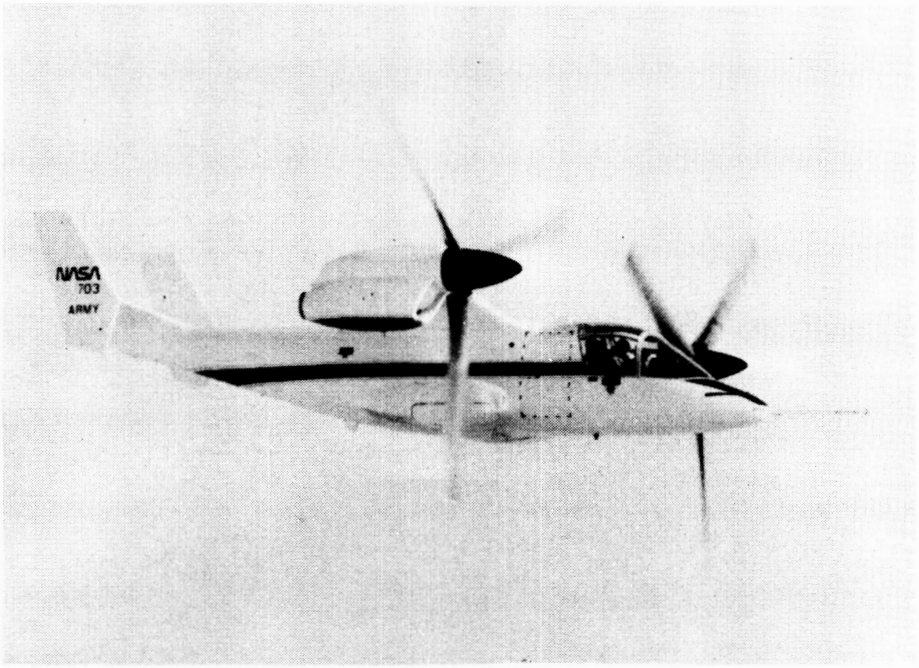

Figure 98.- Army/NASA-Bell XV-15 Tilt Rotor Research Aircraft in airplane configuration.